

Bootstrapping Universal Asymptotics of Conformal Field Theory via Thermal Effective Action

Thesis by
Jaeha Lee

In Partial Fulfillment of the Requirements for the
Degree of
Doctor of Philosophy

CALIFORNIA INSTITUTE OF TECHNOLOGY
Pasadena, California

2026
Defended September 16, 2025

© 2026

Jaeha Lee
ORCID: 0000-0001-9124-450X

All rights reserved except where otherwise noted

ACKNOWLEDGEMENTS

My years in Pasadena left me with the most important stories of my life. This period has been about both realizing and shaping myself. It has been possible only because of the people and environment around me, and in this acknowledgement, I want to express my gratitude to them all.

I want to begin these acknowledgments with the place where I belonged. Everything about studying abroad was exciting but new and challenging at the same time. I appreciate the PMA department and Caltech for offering me a great program including kind and helpful staff. I especially enjoyed the cozy fourth floor in the Downs-Lauritsen building. The well-designed common areas sparked many discussions I enjoyed throughout my PhD. Also, without our fourth floor's longtime secretary Carol, many things would not have been as smooth as they were.

I would next like to express my appreciation to my advisor, Hirosi, for his endless support. He has respected my freedom to explore many areas, but whenever I needed his help, he became supportive, showing me practical but also warm care. I feel fortunate to have been advised by him.

It was enjoyable to talk to professors at Caltech. My thesis committee chair David has also been an amazing collaborator. Collaboration with him was a fun and exciting experience. Without him, it would have been impossible to have a series of thermal effective action research papers. I also appreciate the Simons Collaboration on the Nonperturbative Bootstrap for funding and hosting bootstrap meetings. Tony and Sergei's interest in new technology for theoretical research aligned with my later PhD studies. It has been nice to talk with them and openly explore ideas about AI. I also want to show my gratitude to Cliff and Anton for serving as my committee members for my thesis and candidacy.

It was my pleasure to have discussions and collaborate with postdocs at Caltech. Nathan has been giving me great guidance on my physics research from the early days of my studies. Ning has always had many ideas and a genuine excitement for them. His passion for pursuing exciting things has motivated me. I also value my collaboration with Sridip; we worked on calculations together. Lastly, I am grateful to Temple and Yuya for the discussions we had.

My friends in the community will not be forgotten. There are many happy memories with my friends on the floor. Also, without them, I would have been more confused

and struggled with my research direction and decision-making. Important decisions in my life were made during my PhD. If it were not for Aike and Jerry, I would have been unable to face and be serious about my decisions. I also want to thank Aike for putting up with me as my officemate and for sharing her thoughtful perspective on the world. I wish all my friends every happiness.

Yoojung has been the one who has witnessed my struggles during my PhD closely. Even though she has had her own struggles during her PhD, she has been understanding. Also, it has been amazing to see how much she enjoys and loves doing research in astronomy. I am sure the purest devotion I have ever seen toward her research will take her much further, probably to points I cannot imagine.

I appreciate my friends from undergrad for being my most comfortable friends even though we cannot see each other often. Because of them, from time to time I could go back to my undergrad self without many worries or burdens. Also, because of these friends I could go through my most difficult times during my PhD.

My sister, my parents, and Yoojung's parents have shown warm interest in my studies. Even though I was bad at sharing my life abroad, their constant support and check-ins meant more than I showed.

To everyone mentioned here, thank you for making this journey possible.

ABSTRACT

This thesis explores the asymptotic behavior of Conformal Field Theory (CFT) data at high energies using thermal effective action methods. Well-established results from two dimensions like Cardy formula, OPE coefficient asymptotics, and spin-refined partition function are extended to higher-dimensional theories.

In the first part (Chapter 2), we study the asymptotic density of states formula to CFTs with continuous symmetries. Building on recent work that established the formula for finite groups, we derive universal results for compact Lie groups G . Together with checking on various theories, the formula is explained with thermal effective action.

In the second part (Chapter 3), we develop the systematic exploration of thermal effective action methods for Cardy formula for the general dimension. Additionally, by introducing the "hot spot hypothesis," shrinking circles in complex geometries act as local thermal circles, and we extends the applicability of thermal effective action from simple fibrated manifolds to diverse geometries with extreme focusing structures, opening new avenues for computing CFT observables.

In the third part (Chapter 4), we uncover a fractal-like structure in spin-refined partition functions in higher dimension using a cutting and gluing technique, decomposing the geometry into successive quotients and identifying Kaluza-Klein vortex defects. This reveals how thermal effective action methods remain robust even for discrete geometries and rational rotations.

Our methods are purely field-theoretic and apply to both holographic and non-holographic theories. The results have implications for understanding black hole microstates in AdS/CFT, the statistics of OPE coefficients, and potential extensions of bootstrap axioms beyond traditional crossing symmetry. The thermal effective action framework studied here provides a systematic approach to computing high-energy asymptotics in CFTs, opening new avenues for exploring the structure of conformal field theories in dimensions greater than two.

PUBLISHED CONTENT AND CONTRIBUTIONS

[1] Nathan Benjamin et al. “Angular fractals in thermal QFT”. In: *JHEP* 11 (2024), p. 134. doi: [10.1007/JHEP11\(2024\)134](https://doi.org/10.1007/JHEP11(2024)134). arXiv: [2405.17562](https://arxiv.org/abs/2405.17562) [hep-th].

Contributions

- Derived the form of the Kaluza-Klein vortex defects terms.
- Performed calculations for free theory examples.

[2] Nathan Benjamin et al. “Universal asymptotics for high energy CFT data”. In: *JHEP* 03 (2024), p. 115. doi: [10.1007/JHEP03\(2024\)115](https://doi.org/10.1007/JHEP03(2024)115). arXiv: [2306.08031](https://arxiv.org/abs/2306.08031) [hep-th].

Contributions

- Derived the exact form of the generalized Cardy formula.
- Performed calculations for all example theories for the generalized Cardy formula.
- Derived the regime of validity of the generalized Cardy formula.
- Derived subleading terms for the universal asymptotic formula for OPE coefficients.

[3] Monica Jinwoo Kang, Jaeha Lee, and Hirosi Ooguri. “Universal formula for the density of states with continuous symmetry”. In: *Phys. Rev. D* 107.2 (2023), p. 026021. doi: [10.1103/PhysRevD.107.026021](https://doi.org/10.1103/PhysRevD.107.026021). arXiv: [2206.14814](https://arxiv.org/abs/2206.14814) [hep-th].

Contributions

- Derived the exact form of the universal formula for asymptotic density of states in theories with symmetry of compact groups.
- Performed calculations for all example theories.

TABLE OF CONTENTS

Acknowledgements	iii
Abstract	v
Published Content and Contributions	vi
Table of Contents	vi
Chapter I: Introduction	1
Chapter II: Universal Formula for the Density of States with Continuous Symmetry	3
2.1 Introduction	3
2.2 Spurion analysis	6
2.3 Expansion in characters	8
2.4 Examples 1: $U(1)$ symmetry	9
2.5 Examples 2: non-abelian symmetry	16
2.6 Stability of black hole with non-abelian hair	21
Chapter III: Universal Asymptotics for High Energy CFT Data	25
3.1 Introduction	25
3.2 The thermal effective action	29
3.3 The density of high-dimension states	36
3.4 Density of states: examples	51
3.5 A "genus-2" partition function	56
3.6 Genus-2 global conformal blocks	72
3.7 OPE coefficients of heavy operators	86
3.8 Asymptotics of thermal 1-point functions	99
3.9 Discussion	102
Appendix A Thermal two-point function of momentum generators	109
Appendix B Scheme independence	114
Appendix C More on free theories	115
Appendix D Wilson coefficients for the 3D Ising model	125
Appendix E The shadow transform of a three-point function at large Δ	126
Appendix F Gluing factors	128
Appendix G Counting quantum numbers in the genus-2 block	132
Chapter IV: Angular Fractals in Thermal QFT	135
4.1 Introduction	135
4.2 Folding and unfolding the partition function	138
4.3 Kaluza-Klein vortex defects	150
4.4 Fermionic theories	159
4.5 Free theories	164
4.6 Topological terms: example in 2D CFT	174
4.7 Holographic theories	175
4.8 Journey to $\beta = 0$	179

4.9	Nonperturbative corrections	181
4.10	Discussion and future directions	183
Appendix A	Qualitative picture of the 3D Ising partition function	186
Appendix B	Review of plethystic sums	187
Appendix C	More examples for 4D and 6D CFTs	193
Appendix D	More on nonperturbative terms	195
Bibliography		207

Chapter 1

INTRODUCTION

Conformal Field Theory (CFT) is a special type of Quantum Field Theory that possesses strong symmetry, conformal symmetry. Because of this symmetry, we can write down all correlation functions once the "CFT data" are given: the scaling dimensions and charges of primary operators, and the OPE coefficients. Furthermore, checking consistency conditions of the theory imposes strong constraints on this data [194].

Crossing symmetry is a representative consistency condition concerning the associativity of the Operator Product Expansion (OPE). Although the concept is simple, the constraints it provides are deep and their constraining power has not been exhausted. As researchers overcome more technical difficulties in checking this consistency condition, it yields increasingly powerful constraints on CFT data, including that of the critical 3D Ising model [60, 87, 149].

Another famous consistency condition is modular invariance in 2D. The partition function of a CFT on the torus remains unchanged regardless of how we set the time direction. Modular invariance in 2D CFT fundamentally constrains local data. For example, it determines the spectrum of minimal models and provides bounds on physical quantities such as the Hellerman bound and HKS bound [146].

The S-transformation of modular invariance is particularly useful for obtaining high-energy asymptotic data like the Cardy formula and OPE coefficients in certain limits. This is because it can translate high-temperature conditions from a Laplace-transformed perspective to the domination of a single state or single Virasoro block. How to perform similar analyses for higher-dimensional ($d > 3$) CFTs has not been clearly understood, and my collaboration during graduate study was a journey to answer this question.

In Chapter 2, we further tested the high-energy asymptotic formula (2.1) conjectured in [102], which describes the density of states for given energy and charges under symmetry. We extended the conjecture to continuous symmetry as shown in equation (2.4), and we checked the formula on theories invariant under both $U(1)$ symmetry and non-abelian symmetry using free theory and holographic CFT. In this work, we first used the thermal effective action to explore asymptotic CFT data.

The concept of the thermal effective action was explained in [14, 127]. If a CFT does not have any protected gapless modes, we generically do not expect compactification of the CFT on a thermal circle to be gapless. The compactified theory typically has a nonzero mass gap $m_{\text{gap}} \propto T$ and a finite correlation length $\xi = 1/m_{\text{gap}}$.

On the other hand, when we couple a gapped quantum field theory to a background field, the partition function of the theory has an effective description using a local effective action of the background field. Through these two steps, we can approximate the partition function of a metric-coupled CFT in d dimensions with a thermal circle using a local effective action in $d - 1$ dimensions. We call this the thermal effective action. See also [192] and the introduction sections of Chapter 3 and Chapter 4 for details.

In Chapter 3, we calculate the partition function of CFTs on various manifolds using the thermal effective action, which gave us universal formulas for the asymptotics. We establish that the density of states follows the equation (3.74), with systematic corrections from higher-derivative terms. For heavy-heavy-heavy OPE coefficients, we construct a higher-dimensional analog of the genus-2 Riemann surface by gluing two three-punctured spheres S^d with cylinders. Through analysis of "hot spots" where thermal circles shrink, we derive asymptotic formulas for squared OPE coefficients, finding the equation (3.243). We also determine universal formulas for thermal one-point functions of heavy operators.

In Chapter 4, we develop a cutting and gluing technique to compute spin-refined partition functions, revealing an intricate fractal-like structure in the partition function $Z(\beta, \theta)$ as a function of angular fugacity. Near every rational angle $\theta = 2\pi p/q$, the partition function exhibits universal asymptotic behavior with the free energy scaling as f/q^{d-1} .

Chapter 2

UNIVERSAL FORMULA FOR THE DENSITY OF STATES WITH CONTINUOUS SYMMETRY

2.1 Introduction

In [102], a simple formula is derived for the density of black hole microstates in theory with finite group gauge symmetry G . The formula states that, if we pick a random state from a uniform distribution of all states of the black hole, the probability of it being in a unitary irreducible representation R of G is

$$P_R = \frac{(\dim R)^2}{|G|}, \quad (2.1)$$

where $|G|$ is the number of elements in G so that

$$\sum_R P_R = 1. \quad (2.2)$$

It was also conjectured in the paper that the formula applies to any conformal field theory (CFT) on a sphere with finite group global symmetry G . This generalizes the result of [174] from two dimensions to arbitrary dimensions. The conjecture is verified in the context of free field theories and weakly coupled theories in [42], and a general derivation is presented in [160] using the result of [54]. See also [66] for earlier results on black holes with discrete gauge charges in specific models.

In this paper, we generalize this result to the case where G is a compact Lie group. Since $|G|$ is infinite and G has infinitely many unitary irreducible representations, equation (2.1) needs modifications. We show that, at high temperature and on a compact Cauchy surface, the probability P_R for a random state to be in a representation R of G is given by

$$P_R = (\dim R)^2 \left(\frac{4\pi}{b T^{d-1}} \right)^{\dim G/2} \exp \left[-\frac{c_2(R)}{b T^{d-1}} + \dots \right], \quad (2.3)$$

where T is the temperature, d is the dimensions of the spacetime of the CFT, $c_2(R)$ is the second Casimir of R , and \dots represents terms subleading in $1/T$. An important point is that b is a positive constant independent of R and T . For small representations, where $c_2(R) \ll T^{d-1}$, the R -dependence of P_R is captured by the $(\dim R)^2$ factor as in the finite group case (2.1). For large representations where $c_2(R) \gg T^{d-1}$, P_R decays exponentially.

We derive equation (2.3) by calculating the twisted partition function,

$$Z(T, g) = \text{Tr} \left[U(g) e^{-\beta \hat{H}} \right], \quad (2.4)$$

where the trace is taken over the CFT Hilbert space, $U(g)$ is the action of $g \in G$ on the Hilbert space, $\beta = 1/T$, and \hat{H} is the Hamiltonian. When $g = 1$, it is the standard partition function with the universal large T behavior,

$$Z(T, g = 1) = \exp \left(a T^{d-1} + \dots \right), \quad (2.5)$$

for some constant a . In two dimensions, it is related to the Cardy formula with

$$a = \pi^2 (c_L + c_R)/6, \quad (2.6)$$

where c_L and c_R are the central charges in the left and right movers.

We employ the spurion analysis for the theory obtained by dimensional reduction of the CFT on the thermal circle and show that the g dependence of $Z(T, g)$ is of the form

$$Z(T, g = e^{i\phi}) = \exp \left(a T^{d-1} - \frac{b}{4} T^{d-1} \langle \phi, \phi \rangle + \dots \right), \quad (2.7)$$

where the inner product $\langle \phi, \phi \rangle$ is given by the Killing form. In this description, the constant b is related to the tension of the domain wall which generates the g -twisted sector and therefore is positive. We also verify this formula by calculating b for free field theories and for holographic conformal field theories. Since the twisted partition function $Z(T, g)$ is a class function of g , *i.e.*, invariant under the conjugation $g \rightarrow hgh^{-1}$ for any $h \in G$, we can expand $Z(T, g)$ in characters $\chi_R(g)$ of unitary irreducible representations of G . We calculate the coefficients for the expansion of equation (2.7) and obtain

$$Z(T, g)/Z(T, 1) = \left(\frac{4\pi}{b T^{d-1}} \right)^{\dim G/2} \sum_R \dim R \cdot \chi_R(g) \exp \left(-\frac{c_2(R)}{b T^{d-1}} + \dots \right). \quad (2.8)$$

Our main result (2.3) then follows.

For $d = 1$, equation (2.3) is derived for BF gauge theory coupled to Jackiw–Teitelboim gravity [129]. For $d = 2$, the formula for $G = U(1)$ is derived using the modular invariance of 2D CFTs [174]. Our results generalize this to $d \geq 3$ and to non-abelian G . The exponential suppression factor in equation (2.7) is also mentioned for free field theories in a note added to [42]. We note that the right-hand side of equation (2.8) is in the same form as that of the partition function of the

two-dimensional Yang–Mills theory with gauge group G and the coupling constant proportional to $1/T^{(d-1)/2}$ [30, 90, 166, 184, 205]. There may also be a connection between our results and the recent study of the entanglement entropy in the presence of a global symmetry [53].

In the holographic derivation of equation (2.8), we use the Einstein gravity coupled to the Yang–Mills theory with gauge group G and a finite number of matter fields in anti-de Sitter space (AdS). When G is non-abelian, there are two types of relevant bulk geometries besides the thermal AdS: black holes with and without non-abelian hair. Both bulk geometries obey the same boundary condition at the infinity of AdS. However, the former has genuinely non-abelian configurations of the gauge field, while the gauge field in the latter is commutative. There is extensive literature on such solutions (see [202, 204] for some reviews). One of the outstanding questions in this area has been whether solutions with non-abelian hair are thermodynamically stable. As we will show in this paper, the two types of solutions, with and without non-abelian hair, converge in the high temperature limit $T \rightarrow \infty$. We compute the $1/T$ corrections to their thermodynamical quantities for purely electric solutions and show that the black holes with non-abelian hair have lower free energies. This determines that the black holes with non-abelian hair are thermodynamically more stable.

The coefficients a and b computed for free field theories and holographic CFTs are summarized in Table 2.1 below. When we have N free scalars or N free fermions, both a and b are proportional to N . In holographic CFTs, both a and b are proportional to ℓ^{d-1}/G_N assuming $G_N \sim e^2$, where G_N is the Newton’s constant, e is the gauge coupling constant, and ℓ is the curvature radius of AdS. Thus, in both the free field theories and holographic CFTs, a and b are proportional to the number of degrees of freedom of the system.

	a	b
A free scalar with $G = U(1)$	$2\zeta(d)$	$4\zeta(d-2)$
A free scalar in a representation ρ of G	$2\zeta(d) \dim \rho$	$4\zeta(d-2) c_2(\rho) \frac{\dim \rho}{\dim G}$
A free spinor with $G = U(1)$	$d=2 : \zeta(2) = \pi^2/6$ $d=3 : \frac{3\zeta(3)}{16 \log 2}$	1
Holographic CFT	$\left(\frac{4\pi}{d}\right)^{d-1} \frac{w_{d-1} \ell^{d-1}}{4dG_N}$	$\left(\frac{4\pi}{d}\right)^{d-2} \frac{4(d-2)w_{d-1} \ell^{d-1}}{e^2}$

Table 2.1: The coefficients a and b in equation (2.5) for a variety of CFTs. For the free scalar, the results are for $d > 3$. w_{d-1} is the area of the unit $(d-1)$ -sphere.

The organization of this paper is as follows. In Section 2.2, we give a general argument for the large T behavior in equation (2.7) using the spurion analysis for the theory obtained by dimensional reduction of the CFT on the thermal circle. In Section 2.4, we derive the large T behavior when $G = U(1)$ for free field theories and holographic CFTs. In Section 2.5, we generalize these results to a non-abelian group G . The holographic dual in this case involves the Yang–Mills theory with gauge group G , and we need to consider two types of black hole solutions: those with and without non-abelian hair. We show that the two solutions converge at high temperature and reproduce the behavior in equation (2.8). In Section 2.6, we discuss the thermodynamical stability of the black hole with non-abelian hair.

2.2 Spurion analysis

Consider a d -dimensional CFT on a $(d-1)$ -dimensional compact Cauchy surface Σ_{d-1} times the thermal circle S_β^1 at temperature $T = 1/\beta$. We assume that the CFT is invariant under a compact Lie group G . To calculate the twisted partition function (2.4), we use the approach of [14, 75, 126] and couple the CFT to a background gauge field A with gauge group G .¹ Upon dimensional reduction on S_β^1 , dynamical degrees of freedom acquire thermal masses. The low energy theory on Σ_{d-1} is then described by a gauge field $a = A|_{\Sigma_{d-1}}$ coupled to a scalar field ϕ in the adjoint representation of G , which is related to the holonomy of the gauge field around the

¹We thank David Simmons-Duffin for discussion on this approach.

thermal circle as

$$g = \exp \left(i \oint_{S_\beta^1} A \right) \equiv e^{i\phi}. \quad (2.9)$$

The low energy effective Lagrangian in $(d - 1)$ dimensions has the derivative expansion,

$$\mathcal{L} = \text{tr}_{\text{Adj}} \left[T^{d-1} V(e^{i\phi}) + c T^{d-3} (\mathcal{D}\phi)^2 + g_{YM}^{-2} F^2 + \dots \right], \quad (2.10)$$

where the trace is taken over the adjoint representation, the scalar potential $\text{Tr}V(g)$ is a class function of g as required by gauge invariance in d dimensions, \mathcal{D} is the covariant derivative, $F = da + a^2$, and \dots are terms suppressed by $1/T$. The twisted partition function $Z(T, g)$ is obtained by setting $g = e^{i\phi}$ to be constant and $a = 0$. Therefore, its g -dependence is captured by the potential term $\text{Tr}V(g)$ in the effective Lagrangian as

$$Z(T, g)/Z(T, 1) = \exp \left(-\text{tr}_{\text{Adj}} \left[T^{d-1} V(g) \text{vol}(\Sigma_{d-1}) \right] + \dots \right). \quad (2.11)$$

Now, we relate the potential $\text{Tr}V(g)$ to the tension of the domain wall which generates the g -twisted sector in the CFT Hilbert space. To do so, we note that the Lagrangian density (2.10) is of the same form for any smooth compact manifold Σ_{d-1} , provided we use the metric of Σ_{d-1} to write \mathcal{L} in a diffeomorphism invariant way. In particular, we can choose $\Sigma_{d-1} = \tilde{S}^1 \times \Sigma_{d-2}$, with \tilde{S}^1 having unit circumference and the thermal boundary condition, and compute $V(g)$ for this geometry. By exchanging the thermal circle S_β^1 with \tilde{S}^1 , we can interpret the twisted partition function $Z(T, g)$ as the untwisted partition function in the g -twisted sector on $S_\beta^1 \times \Sigma_{d-2}$ with the twist along the S_β^1 direction [189]. Since we are computing the partition function of the CFT, we can rescale the spacetime so that the thermal circle S_β^1 has unit circumference and the volume of $\tilde{S}^1 \times \Sigma_{d-2}$ is proportional to T^{d-1} . In the limit of $T \rightarrow \infty$, the exponent $\text{Tr} \left[T^{d-1} V(g) \text{vol}(\Sigma_{d-1}) \right] + \dots$ of equation (2.11) can be interpreted as the ground state energy of the g -twisted sector on $S_\beta^1 \times \Sigma_{d-2}$ times the circumference T of the rescaled \tilde{S}^1 .

Since we expect that the ground state energy of the g -twisted sector with $g \neq 1$ is higher than that of the untwisted ground state, $\text{Tr}V(g)$ should have the global minimum at $g = 1$. Therefore, in the high temperature limit,

$$Z(T, g)/Z(T, 1) \rightarrow C(T) \delta(g, 1), \quad T \rightarrow \infty, \quad (2.12)$$

for some $C(T)$, where $\delta(g, 1)$ is the delta-function on the group manifold G localized at $g = 1$. Since the delta-function can be expanded in terms of characters as

$$\delta(g, 1) = \sum_R \dim R \cdot \chi_R(g), \quad (2.13)$$

where the sum is over unitary irreducible representations of G and we normalized the volume of G to be 1, we conclude that the probability P_R for a random state to be in the representation R is proportional to $(\dim R)^2$, for fixed R in the limit of $T \rightarrow \infty$. This explains the $(\dim R)^2$ factor in equation (2.3).

To reproduce the $\exp[-c_2(R)/(b T^{d-1})]$ factor in equation (2.3), we expand the potential $\text{Tr}V(g)$ around $g = 1$. Since it is a class function of g , the expansion should take the form,

$$\text{tr}_{\text{Adj}} [T^{d-1} V(g = e^{i\phi}) \text{vol}(\Sigma_{d-1})] = \text{constant} + \frac{b}{4} T^{d-1} \langle \phi, \phi \rangle + \dots \quad (2.14)$$

The coefficient b must be non-negative since the minimum of $\text{Tr}V(g)$ is at $g = 1$. This reproduces equation (2.7). As we will show in Section 4.4, this is equivalent to equation (2.8) and therefore to equation (2.3).

2.3 Expansion in characters

We have shown that the twisted partition function has the universal high temperature behavior,

$$Z(T, g = e^{i\phi})/Z(T, 1) = \exp \left[-\frac{b}{4} T^{d-1} \langle \phi, \phi \rangle + \dots \right]. \quad (2.15)$$

Since it is a class function of g , we can expand it in characters $\chi_R(g)$. The purpose of this section is to find the expansion coefficients and derive equation (2.8).

To do so, we use the fact that the left-hand side of (2.15) approximately solves the heat equation for $T \gg 1$ as

$$\left(\frac{b T^d}{d-1} \frac{\partial}{\partial T} + \Delta \right) \left[\left(\frac{b T^{d-1}}{4\pi} \right)^{\dim G/2} \frac{Z(T, g)}{Z(T, 1)} \right] \simeq 0, \quad (2.16)$$

and obeys the initial condition,

$$\left. \left(\frac{b T^{d-1}}{4\pi} \right)^{\dim G/2} \frac{Z(T, g)}{Z(T, 1)} \right|_{T=\infty} = \delta(g, 1). \quad (2.17)$$

Here Δ is the Laplace operator on the group manifold G . Since each character is an eigenstate of the Laplace operator,

$$\Delta \chi_R(g) = -c_2(R) \chi_R(g), \quad (2.18)$$

and since characters make an orthonormal basis of class functions, $\{\chi_R(g)e^{-c_2(R)/(bT^{d-1})}\}_R$ gives the complete set of solutions to the heat equation. Therefore, we can expand,

$$\left(\frac{bT^{d-1}}{4\pi}\right)^{\dim G/2} \frac{Z(T, g)}{Z(T, 1)} \simeq \sum_R d_R \chi_R(g) \exp\left(-\frac{c_2(R)}{bT^{d-1}}\right). \quad (2.19)$$

To determine the expansion coefficient d_R , we use the initial condition (2.17), which can be written as

$$\sum_R d_R \chi_R(g) = \delta(g, 1). \quad (2.20)$$

Since $\delta(g, 1) = \sum_R \dim R \cdot \chi_R(g)$, the expansion coefficients are determined as

$$d_R = \dim R, \quad (2.21)$$

and we obtain

$$Z(T, g)/Z(T, 1) = \left(\frac{4\pi}{bT^{d-1}}\right)^{\dim G/2} \sum_R \dim R \cdot \chi_R(g) \exp\left(-\frac{c_2(R)}{bT^{d-1}} + \dots\right). \quad (2.22)$$

2.4 Examples 1: $U(1)$ symmetry

In the remainder of the paper, we will study free field theories and holographic CFTs on $S_\beta^1 \times S^{d-1}$ and calculate the coefficient b explicitly. The circumference of the thermal circle S_β^1 is β , and the radius of the Cauchy surface S^{d-1} is normalized to be 1.

We begin by studying CFTs with $G = U(1)$. Each state in the Hilbert space can be labeled by a charge Q , and the conjectured formula takes the form,

$$P_Q = \sqrt{\frac{4\pi b}{T^{d-1}}} \exp\left[-\frac{Q^2}{bT^{d-1}} \left(1 + O\left(\frac{1}{T}, \frac{Q^2}{T^{2d-4}}\right)\right)\right]. \quad (2.23)$$

We verify this by calculating the grand canonical partition function with an imaginary chemical potential $\mu = iT\theta$,

$$Z(T, \mu = iT\theta) = \text{Tr} \left[e^{-\beta \hat{H} + i\theta \hat{Q}} \right]. \quad (2.24)$$

We assume that \hat{Q} is quantized in such a way that the field with the smallest non-zero $U(1)$ charge has charge 1. In the limit of large T and small μ , we show

$$Z(T, \mu) = \exp \left[aT^{d-1} \left(1 + O\left(\frac{1}{T}\right)\right) + \frac{b}{4} T^{d-3} \mu^2 \left(1 + O\left(\mu^2, \frac{1}{T}\right)\right) \right], \quad (2.25)$$

for some constants a and b . The Fourier transformation of this formula with respect to $\theta = -i\beta\mu$ gives the canonical partition function, which leads to equation (2.23).

Free field theory

Free scalar theories:

Consider a massless complex free scalar field ϕ in d spacetime dimensions.² We normalize the $U(1)$ generator \hat{Q} such that ϕ has charge 1. For such a theory on $\mathbb{R} \times S^{d-1}$, the grand canonical partition function with an imaginary chemical potential is given by [165],

$$Z_{\text{scalar}}(T, \mu = iT\theta) = \exp \left[\sum_{n=1}^{\infty} \frac{e^{-n\beta \frac{d-2}{2}}}{n} \cos(n\theta) \frac{(1 - e^{-2n\beta})}{(1 - e^{-n\beta})^d} \right]. \quad (2.26)$$

As we are interested in the high temperature limit, that is, when $\theta = -i\beta\mu$ is small, we first expand the exponent in powers of θ as

$$Z_{\text{scalar}}(T, \mu) = \exp \left[\sum_{k=0}^{\infty} C_k \theta^{2k} \right], \quad (2.27)$$

where the coefficient C_k is given by

$$C_k = \frac{(-1)^k}{(2k)!} \sum_{n=1}^{\infty} n^{2k-1} e^{-\frac{(d-2)}{2}n\beta} \frac{(1 - e^{-2n\beta})}{(1 - e^{-n\beta})^d}. \quad (2.28)$$

At high temperature, one might think that the sum over n in equation (2.28) can be approximated by an integral over $x = n\beta$ as

$$C_k \approx \frac{(-1)^k}{(2k)!} T^{2k} \int_0^{\infty} f(x) dx, \quad f(x) = x^{2k-1} e^{-\frac{d-2}{2}x} \frac{(1 - e^{-2x})}{(1 - e^{-x})^d}. \quad (2.29)$$

However, we need to be careful when $2k \leq d-1$ as $f(x)$ is singular at $x = 0$ and the integral approximation will fail when x is small. To take this into account, we introduce a cutoff at some small value x_0 and use the integral approximation only for $x > x_0$. The terms in the summation in equation (2.28) are not converted to integral form when n is such that $n\beta < x_0$. Taking this singular behavior into account, the correct approximation is

$$C_k \approx \frac{(-1)^k}{(2k)!} \left(2T^{d-1} \sum_{n=1}^{x_0 T} n^{2k-d} + T^{2k} \int_{x_0}^{\infty} dx f(x) \right). \quad (2.30)$$

²We generally assume that $d > 3$ due to certain subtleties with massless scalar fields in two and three dimensions which we discuss later.

It is straightforward to show that equation (2.30) is independent of x_0 for large values of T . In this way, we find that the coefficients C_k can be approximated as

$$C_k \approx \begin{cases} \frac{(-1)^k}{(2k)!} \left(\int_0^\infty dx x^{2k-1} e^{-\frac{d-2}{2}x} \frac{(1-e^{-2x})}{(1-e^{-x})^d} \right) T^{2k} & 2k \geq d, \end{cases} \quad (2.31a)$$

$$\begin{cases} \frac{(-1)^k}{(2k)!} \left(2 \log T + 2\gamma + 2 \log x_0 \right. \\ \left. + \int_{x_0}^\infty dx x^{2k-1} e^{-\frac{d-2}{2}x} \frac{(1-e^{-2x})}{(1-e^{-x})^d} \right) T^{d-1} & 2k = d-1, \end{cases} \quad (2.31b)$$

$$\begin{cases} \frac{(-1)^k}{(2k)!} 2\zeta(d-2k) T^{d-1} \\ - \frac{(-1)^k}{(2k)!} T^{2k} \left(\frac{2x_0^{2k-d+1}}{d-2k-1} + \int_{x_0}^\infty dx x^{2k-1} e^{-\frac{d-2}{2}x} \frac{(1-e^{-2x})}{(1-e^{-x})^d} \right) & 2k < d-1. \end{cases} \quad (2.31c)$$

The constant γ appearing in equation (2.31b) is the Euler–Mascheroni constant. At $\theta = 0$, the partition function is $Z_{\text{scalar}}(T, 0) = e^{C_0}$. Since equation (2.31c) gives $C_0 = 2\zeta(d) T^{d-1}$, the coefficient a in equation (2.5) is given by $a = 2\zeta(d)$ for the massless free scalar.

For $d > 3$, equation (2.31c) gives

$$C_1 \approx \zeta(d-2) T^{d-1}, \quad (2.32)$$

where we ignore the second term of equation (2.31c), since it is subleading in $1/T$. Thus we find that the grand canonical partition function is

$$Z_{\text{scalar}}(T, \mu) \approx \exp \left[\zeta(d-2) T^{d-3} \mu^2 (1 + O(\mu^2, 1/T)) \right] Z_{\text{scalar}}(T, 0). \quad (2.33)$$

In summary, the grand canonical partition function of the massless free complex scalar field theory in $d > 3$ demonstrates the universal behavior at high temperature as in equation (2.25), with constants

$$a = 2\zeta(d), \quad b = 4\zeta(d-2). \quad (2.34)$$

When $d = 3$, we use equation (2.31b) to obtain

$$Z_{\text{scalar}}(T, \mu) \approx \exp \left[(\log T + 2.96351...) \mu^2 (1 + O(\mu^2, 1/T)) \right] Z_{\text{scalar}}(T, 0). \quad (2.35)$$

However, the massless scalar field at $d = 3$ does not make sense at finite temperature since it has the same infrared issue as that of the massless scalar field at $d = 2$. We believe that the appearance of the $\log T$ singularity is a reflection of the infrared pathology in this case.

Free spinor theories:

For the massless scalar field, we cannot consider theories in $d = 2, 3$ due to the infrared problem. As it is good to also have an example in these dimensions, we consider the theory of a free spinor field.

In two dimensions, the grand canonical partition function of a free complex Weyl spinor is given by

$$Z_{\text{spinor}}(T, \mu = iT\theta) = \prod_{n=1}^{\infty} (1 + e^{-\beta(n-\frac{1}{2})} e^{i\theta})(1 + e^{-\beta(n-\frac{1}{2})} e^{-i\theta}). \quad (2.36)$$

We can transform this into the plethystic form as

$$\begin{aligned} Z_{\text{spinor}}(T, \mu = iT\theta) &= \exp \left[\sum_{n=1}^{\infty} \left(\log(1 + e^{-\beta(n-\frac{1}{2})} e^{i\theta}) + \log(1 + e^{-\beta(n-\frac{1}{2})} e^{-i\theta}) \right) \right] \\ &= \exp \left[- \sum_{n,m=1}^{\infty} \frac{(-1)^m}{m} \left(e^{-\beta m(n-\frac{1}{2})} e^{im\theta} + e^{-\beta m(n-\frac{1}{2})} e^{-im\theta} \right) \right] \\ &= \exp \left[- \sum_{m=1}^{\infty} \frac{(-1)^m}{m} \frac{\cos(m\theta)}{\sinh \frac{m\beta}{2}} \right]. \end{aligned} \quad (2.37)$$

As in the free scalar case, we expand the exponent of the partition function in θ as

$$Z_{\text{spinor}}(T, i\mu) = \exp \left[\sum_{k=0}^{\infty} D_k \theta^{2k} \right], \quad (2.38)$$

for some coefficients D_k . We find that

$$D_1 = -\frac{1}{2} \sum_{m=1}^{\infty} (-1)^m \frac{m}{\sinh \frac{m\beta}{2}} = -\frac{1}{2} \sum_{n=1}^{\infty} \left(\frac{2n}{\sinh(n\beta)} - \frac{2n-1}{\sinh\left(\frac{2n-1}{2}\beta\right)} \right), \quad (2.39)$$

where we split the series into $m = 2n$ and $m = 2n - 1$ terms and sum them as pairs, which is valid as D_1 converges due to the hyperbolic sine function in the denominator. At high temperature, we can approximate the summation as an integration over $x = n\beta$:

$$D_1 \approx -\frac{T^2}{4} \int_0^{\infty} dx (f(x+\beta) - f(x)) \approx -\frac{T^2}{4} \int_0^{\infty} dx f'(x) \beta \approx \frac{T}{4}, \quad f(x) = \frac{x}{\sinh x}. \quad (2.40)$$

Similarly,

$$D_0 = - \sum_{m=1}^{\infty} \frac{(-1)^m}{m \sinh \frac{m\beta}{2}}. \quad (2.41)$$

In this case, we need the cutoff x_0 to convert the sum into an integral as

$$D_0 \approx -2T \sum_{m=1}^{x_0 T} \frac{(-1)^m}{m^2} - \frac{T}{2} \int_{x_0}^{\infty} dx g'(x) \approx \zeta(2)T, \quad g(x) = \frac{1}{x \sinh \frac{x}{2}}, \quad (2.42)$$

where we used the zeta function identity $-\sum_{m=1}^{\infty} \frac{(-1)^m}{m^2} = \frac{\zeta(2)}{2}$.

Let us turn to $d = 3$, where the grand canonical partition function of the free spinor theory is

$$Z_{\text{spinor}}(T, \mu = iT\theta) = \prod_{n=0}^{\infty} (1 + e^{-\beta(n+1)} e^{i\theta})^{2n+1} (1 + e^{-\beta(n+1)} e^{-i\theta})^{2n+1} \quad (2.43)$$

$$= \exp \left[- \sum_{m=1}^{\infty} \frac{(-1)^m}{m} e^{-\frac{m\beta}{2}} \frac{\coth \frac{m\beta}{2}}{\sinh \frac{m\beta}{2}} \cos(m\theta) \right]. \quad (2.44)$$

Expanding the exponent in powers of θ , we find the coefficients to be

$$\begin{aligned} D_0 &\approx - \sum_{m=1}^{x_0 T} (-1)^m \frac{4}{m^3 \beta^2} + \frac{T}{2} \int_{x_0}^{\infty} dx f'(x) \approx 3\zeta(3), \quad f(x) = \frac{1}{x} e^{-\frac{x}{2}} \frac{\coth \frac{x}{2}}{\sinh \frac{x}{2}}, \\ D_1 &\approx - \sum_{m=1}^{x_0 T} (-1)^m \frac{4}{m \beta^2} + \frac{T}{2} \int_{x_0}^{\infty} dx g'(x) \approx 4T^2 \log 2, \quad g(x) = x e^{-\frac{x}{2}} \frac{\coth \frac{x}{2}}{\sinh \frac{x}{2}}, \end{aligned} \quad (2.45)$$

where we used zeta function identities $\sum_{m=1}^{\infty} \frac{(-1)^m}{m} = \log 2$ and $\sum_{m=1}^{\infty} \frac{(-1)^m}{m^3} = -\frac{3}{4}\zeta(3)$.

Combining these results, we find

$$Z_{\text{spinor}}(T, \mu) \approx \begin{cases} \exp \left[\frac{1}{4T} \mu^2 (1 + O(\mu^2, 1/T)) \right] Z_{\text{spinor}}(T, 0) & d = 2, \\ \exp \left[4 \log 2 \mu^2 (1 + O(\mu^2, 1/T)) \right] Z_{\text{spinor}}(T, 0) & d = 3, \end{cases} \quad (2.46a)$$

$$Z_{\text{spinor}}(T, 0) \approx \begin{cases} e^{\zeta(2)T} & d = 2, \\ e^{3\zeta(3)T^2} & d = 3. \end{cases} \quad (2.46b)$$

where the partition functions at $\beta\mu = 0$ for both dimensions are given by

$$Z_{\text{spinor}}(T) = Z_{\text{spinor}}(T, 0) \approx \begin{cases} e^{\zeta(2)T} & d = 2, \\ e^{3\zeta(3)T^2} & d = 3. \end{cases} \quad (2.46c)$$

$$(2.46d)$$

Equations (2.46c) and (2.46d) show that the free Weyl spinor theory also demonstrates the universal behavior in equation (2.25) at high temperature with the coefficients

$$a = \zeta(2) = \frac{\pi^2}{6}, \quad b = 1, \quad (2.47)$$

for $d = 2$, and

$$a = 3\zeta(3), \quad b = 16\log 2, \quad (2.48)$$

for $d = 3$. For $d = 2$, the Cardy formula gives $a = \pi^2(c_L + c_R)/6$, and the above value of a is consistent with $(c_L, c_R) = (1, 0)$ for the complex Weyl spinor. As expected, the result at $d = 3$ is free from the $\log T$ singularity we saw for the free scalar field in equation (2.35).

Holographic CFT

We now consider a holographic CFT, whose bulk theory is described at low energy in terms of the Einstein gravity coupled to the Maxwell field and a finite number of matter fields in AdS_{d+1} . The action of the theory is given by

$$I = \int d^{d+1}x \sqrt{-g} \left[\frac{1}{16\pi G_N} \left(R + \frac{d(d-1)}{\ell^2} \right) - \frac{1}{4e^2} F^2 + \dots \right], \quad (2.49)$$

where \dots represents matter field terms. The curvature radius ℓ is related to the cosmological constant as $\Lambda = -d(d-1)/2\ell^2$. To calculate the grand canonical partition function, we impose the boundary condition that the boundary geometry is $S_\beta^1 \times S^{d-1}$ and the gauge field A has the holonomy around the thermal circle S_β^1 at the boundary given by

$$\exp \left(i \oint_{S_\beta^1} A_\tau \right) = e^{\beta\mu}, \quad (2.50)$$

where μ is identified with the chemical potential of the boundary CFT. We solve the Einstein and Maxwell equations assuming the spherical symmetry on S^{d-1} and setting all other matter fields to zero.

There are two classical solutions under these conditions; one is the thermal AdS and the other is the AdS Reissner–Nordstrom (RN) black hole. At high temperature, the RN solution is dominant [56, 57]. The RN solution can be written in static coordinates as

$$ds^2 = V(r) d\tau^2 + \frac{dr^2}{V(r)} + r^2 d\Omega_{d-1}^2, \quad V(r) = 1 - \frac{m}{r^{d-2}} + \frac{vq^2}{r^{2d-4}} + \frac{r^2}{\ell^2}, \quad (2.51a)$$

$$A = -i \sqrt{\frac{d-1}{2(d-2)}} \left(\frac{q}{r_H^{d-2}} - \frac{q}{r^{d-2}} \right) d\tau, \quad v = \frac{4\pi G_N}{e^2}, \quad (2.51b)$$

where m and q are related to the ADM mass and the charge of the black hole [56, 155, 183]. This solution has its ADM mass, charge, temperature, and entropy given

by

$$M = \frac{(d-1)w_{d-1}}{16\pi G_N} r_H^{d-2} \left(1 + \frac{vq^2}{r_H^{2d-4}} + \frac{r_H^2}{l^2} \right), \quad (2.52a)$$

$$Q = \sqrt{2(d-1)(d-2)} \left(\frac{w_{d-1}}{8\pi G_N} \right) vq, \quad (2.52b)$$

$$T = \frac{d-2}{4\pi r_H} \left(1 - \frac{vq^2}{r_H^{2d-4}} \right) + \frac{r_H d}{4\pi l^2}, \quad (2.52c)$$

$$S = \frac{w_{d-1}}{4G_N} r_H^{d-1}, \quad (2.52d)$$

where w_{d-1} is the surface area of the unit $(d-1)$ -sphere, and the horizon radius r_H is the largest real positive root of $V(r)$ [1, 11, 57, 106]. The chemical potential of the black hole system is related to the charge Q as

$$\mu = \sqrt{\frac{d-1}{2(d-2)}} \frac{q}{r_H^{d-2}} = \frac{e^2}{(d-2)w_{d-1}} \frac{Q}{r_H^{d-2}}. \quad (2.53)$$

By the AdS/CFT correspondence, the grand canonical partition function of the CFT can be calculated using the Euclidean action for this solution.

At high temperature, the horizon radius r_H of the stable black hole grows linearly in the temperature as

$$T \approx \frac{r_H d}{4\pi l^2} (1 - X), \quad X = \frac{d-2}{d} \frac{vq^2 l^2}{r_H^{2d-2}}, \quad (2.54)$$

where we keep X as small which is equivalent to small $|\mu|$ approximation in free field calculation. The grand potential $\Phi(T, \mu)$ is related to the grand canonical partition function as

$$Z_{AdS}(T, \mu) = e^{-\beta\Phi(T, \mu)}, \quad (2.55)$$

and is given by the Euclidean action of the RN solution,

$$\Phi(T, \mu) = M - TS - \mu Q \approx -\frac{w_{d-1} r_H^d}{16\pi G_N l^2} \left(1 + \frac{d}{d-2} X \right). \quad (2.56)$$

Using

$$r_H = \frac{4\pi l^2}{d} \frac{T}{1-X}, \quad X = \frac{d(d-2)^2}{8\pi^2 l^2 (d-1)} \frac{v\mu^2}{T^2} + O(X^2), \quad (2.57)$$

we find

$$-\beta\Phi(T, \mu) \approx \frac{w_{d-1} (4\pi l^2/d)^d}{16\pi G_N l^2} T^{d-1} + \frac{w_{d-1} (d-2)}{e^2} \left(\frac{4\pi l^2}{d} \right)^{d-2} \mu^2 T^{d-3}. \quad (2.58)$$

Rescaling the temperature as $\ell T \rightarrow T$, the grand canonical partition function of the dual CFT on the sphere with unit radius is given by

$$Z_{CFT}(T, \mu) \approx \exp \left[w_{d-1} \left(\frac{4\pi}{d} \right)^{d-1} \left(\frac{\ell^{d-1}}{4dG_N} T^{d-1} + \frac{d(d-2)\ell^{d-1}}{4\pi e^2} \mu^2 T^{d-3} \right) \right]. \quad (2.59)$$

This determines the coefficients a and b of equation (2.25) in this case as

$$a = \left(\frac{4\pi}{d} \right)^{d-1} \frac{w_{d-1} \ell^{d-1}}{4dG_N}, \quad b = \left(\frac{4\pi}{d} \right)^{d-2} \frac{4(d-2)w_{d-1} \ell^{d-1}}{e^2}. \quad (2.60)$$

2.5 Examples 2: non-abelian symmetry

When G is non-abelian, we utilize the fact that the twisted partition function $Z(T, g)$ is a class function invariant under the conjugation $g \rightarrow hgh^{-1}$ for any h . This allows us to restrict g to the maximum torus of G and simplify our calculation. In both free field theories and holographic CFTs, we find

$$Z(T, g = e^{i\phi}) = \exp \left[-\frac{b}{4} T^{d-1} \langle \phi, \phi \rangle + \dots \right] Z(T, g = 1), \quad (2.61)$$

where $g = e^H$ and the constant b depends on the theory but not on g or T . In particular, the partition function $Z(T, g)$ is peaked at $g = 1$. In fact, it is related to a solution to the heat equation on the group manifold G with the diffusion time related to $1/T^{d-1}$. This will enable us to expand the partition function in characters of G to obtain equation (2.8).

Massless free scalar

Suppose a compact Lie group G has a faithful unitary representation ρ with $\dim \rho = n$. Consider n massless scalar fields in d dimensions. Though the theory has a larger symmetry of $O(n)$, we focus on its G subgroup. We would like to calculate the finite temperature partition function of this theory with an insertion of $g \in G$ as

$$Z(T, g) = \text{Tr} \left[U(g) e^{-\beta \hat{H}} \right]. \quad (2.62)$$

Since $Z(T, g)$ is a class function of g , without loss of generality, g can be restricted to the maxim torus of G . In this case, $U(g)$ acts as a multiplication of a phase factor on each of the scalar fields. We can then apply equation (2.26) for $G = U(1)$ to each scalar field and assemble the results to obtain

$$Z_{\text{scalar}}(T, g) = \exp \left[\sum_{n=1}^{\infty} \frac{e^{-\frac{d-2}{2}n\beta}}{n} \frac{\chi_{\rho}(g^n) + \chi_{\rho}^*(g^n)}{2} \frac{(1 - e^{-2n\beta})}{(1 - e^{-n\beta})^d} \right], \quad (2.63)$$

where χ_ρ is the character of the representation ρ and χ_ρ^* is that for its conjugate. Writing $g = e^{i\phi}$ and expanding in powers of ϕ ,

$$\begin{aligned} \frac{\chi_\rho(g^n) + \chi_\rho^*(g^n)}{2} &= \text{tr}_\rho \left(1 - n^2 \phi^2 + \dots \right) \\ &= \dim \rho - \frac{\dim \rho}{\dim G} c_2(\rho) \langle \phi, \phi \rangle n^2 + \dots, \end{aligned} \quad (2.64)$$

where tr_ρ is the trace over the representation ρ and $\langle \phi, \phi \rangle = \text{tr}_{\text{Adj}} \phi^2$. We can repeat the calculation of $G = U(1)$ in Section 2.4 to obtain

$$Z_{\text{scalar}}(T, e^{i\phi}) \approx \exp \left[-\zeta(d-2) T^{d-1} \frac{\dim \rho}{\dim G} c_2(\rho) \langle \phi, \phi \rangle + \dots \right] Z_{\text{scalar}}(T, g=1), \quad (2.65)$$

where we assumed $d > 3$.

Holographic CFT

Consider a holographic CFT in d dimensions, whose bulk theory is described in low energy in terms of the Einstein gravity coupled to the Yang–Mills field with gauge group G and a finite number of matter fields in AdS_{d+1} . The action of the theory is given by

$$I = \int d^{d+1}x \sqrt{-g} \left[\frac{1}{16\pi G_N} \left(R + \frac{d(d-1)}{l^2} \right) - \frac{1}{4e^2} \langle F, F \rangle + \dots \right], \quad (2.66)$$

where F is in the Lie algebra of gauge group G and \dots represents matter field terms. To calculate the grand canonical partition function, we impose the boundary condition that the boundary geometry is $S_\beta^1 \times S^{d-1}$ and the gauge field A_μ has the holonomy around the thermal circle S_β^1 as

$$\mathcal{P} \exp \left(i \oint_{S_\beta^1} A \right) = e^{\beta \mu} = g. \quad (2.67)$$

We assume that the solution is spherically symmetric on S^{d-1} , and all the other matter fields are set to zero. We calculate the field strength and the stress-energy tensor as

$$F_{\mu\nu} = \partial_\mu A_\nu - \partial_\nu A_\mu - i [A_\mu, A_\nu], \quad T_{\mu\nu} = \frac{1}{e^2} \left(\langle F_{\mu\alpha}, F_\nu^\alpha \rangle - \frac{1}{4} g_{\mu\nu} \langle F_{\alpha\beta}, F^{\alpha\beta} \rangle \right). \quad (2.68)$$

There are three classical solutions under these conditions. The first is the thermal AdS,

$$ds^2 = \left(1 - \frac{\Lambda r^2}{3} \right) d\tau^2 + \frac{dr^2}{1 - \frac{\Lambda r^2}{3}} + r^2 d\Omega_{d-1}^2, \quad A = -i\mu d\tau. \quad (2.69)$$

The second makes use of the $U(1)$ RN solution (2.49), $ds_{U(1)}^2$ and a_μ with the chemical potential $\mu_{U(1)}$, by the substitution,

$$ds^2 = ds_{U(1)}^2, \quad A_\mu = \frac{\phi}{\langle \phi, \phi \rangle^{1/2}} a_\mu, \quad \mu = \frac{\phi}{\langle \phi, \phi \rangle^{1/2}} \mu_{U(1)}. \quad (2.70)$$

Since H commutes with itself, the Yang–Mills equation for A_μ reduces to the Maxwell equations for a_μ . The rescaling by $\langle \phi, \phi \rangle^{-1/2}$ is needed to match the stress energy tensors of both systems.

The third is a genuinely non-abelian solution. A dyonic black hole solution with $SU(N)$ hair is known in AdS_4 [191]. Here, we construct a purely electric black hole solution with $SU(2)$ hair with the following ansatz [28]

$$\begin{aligned} ds^2 &= -\mu(r)\sigma(r)^2 dt^2 + \frac{dr^2}{\mu(r)} + r^2 d\theta^2 + r^2 \sin^2\theta d\phi^2, \\ \mu(r) &= 1 - \frac{2m(r)}{r} - \frac{\Lambda r^2}{3}, \\ A_\mu &= h(r) \frac{\tau_3}{2} dt + w(r) \frac{\tau_1}{2} d\theta + \left(\cot\theta \frac{\tau_3}{2} + w(r) \frac{\tau_2}{2} \right) \sin\theta d\phi, \end{aligned} \quad (2.71)$$

where we use Pauli matrices $\tau_{1,2,3}$ as generators of the Lie algebra of $SU(2)$ and the inner product is defined as twice the trace of two elements' multiplication. The AdS boundary condition requires $\sigma(r \rightarrow \infty) = 1$. The functions, $\sigma(r)$, $m(r)$, $h(r)$, and $w(r)$, are determined by numerically solving the Einstein Yang–Mills equations, which take the form [28],

$$h'' = h' \left(\frac{\sigma'}{\sigma} - \frac{2}{r} \right) + \frac{2w^2}{\mu r^2} h, \quad (2.72a)$$

$$w'' + w' \left(\frac{\sigma'}{\sigma} + \frac{\mu'}{\mu} \right) + \frac{wh^2}{\sigma^2 \mu^2} + \frac{w(1-w^2)}{\mu r^2} = 0 \quad (2.72b)$$

$$m' = v \left(\frac{r^2 h'^2}{2\sigma^2} + \frac{w^2 h^2}{\sigma^2 \mu} + \mu w'^2 + \frac{1}{2r^2} (1-w^2)^2 \right), \quad (2.72c)$$

$$\sigma' = v \left(\frac{2\sigma w'^2}{r} + \frac{2w^2 h^2}{\sigma \mu^2 r} \right), \quad (2.72d)$$

where the prime denotes differentiation with respect to r . The horizon radius r_H is defined as the largest solution to $\mu(r) = 0$ and $v = 4\pi G_N/e^2$.

Since we have the three possible solutions, we should determine which one gives the dominant contribution to the partition function. Above the Hawking–Page temperature, we should consider either the second or the third solution. It turns out that the two solutions converge at high temperature. This is because, as the

temperature rises, the horizon grows and approaches the AdS boundary, where the interaction terms in the bulk equations of motion are suppressed. This expectation will be confirmed by the numerical computation below.

In the asymptotically *AdS* case, there are stable hairy black hole solutions, and those with $SU(N)$ hair have been extensively studied [28, 191, 201–203]. In particular, Bjaraker and Hosotani in [28] discussed the existence of a purely electric $SU(2)$ charged black hole in AdS_4 , which is of our interest, but it has not been constructed explicitly.

Let us construct the genuinely non-abelian solution with $SU(2)$ purely electric hair in AdS_4 at high temperature. We determine $\sigma(r)$, $m(r)$, $h(r)$, and $w(r)$ by integrating equations (2.72) from the horizon to the infinity. Since a thermodynamically stable black hole has a large horizon at high temperature, we can expand them in the inverse powers of r_H as

$$\begin{aligned} h(r) &= r_H \tilde{h}_0(\tilde{r}) + r_H^{-1} \tilde{h}_1(\tilde{r}) + O(r_H^{-2}), & m(r) &= r_H^3 \tilde{m}_0(\tilde{r}) + r_H \tilde{m}_1(\tilde{r}) + O(1), \\ \sigma(r) &= 1 + r_H^{-2} \tilde{\sigma}_1(\tilde{r}) + O(r_H^{-3}), & w(r) &= \tilde{w}_0(\tilde{r}) + r_H^{-2} \tilde{w}_1(\tilde{r}) + O(r_H^{-3}), \\ \mu(r) &= r_H^2 \tilde{\mu}_0 + \tilde{\mu}_1 + O(r_H^{-1}), \end{aligned} \tag{2.73}$$

where $\tilde{r} = r/r_H$. Once we substitute this expansion into Einstein Yang–Mills equations (2.72), and solve the leading order equations, we get leading value of the functions:

$$\tilde{h}_0(\tilde{r}) = h'_H \left(1 - \frac{1}{\tilde{r}}\right), \quad \tilde{m}_0(\tilde{r}) = \left(\frac{-\Lambda + 3vh'_H^2}{6} - \frac{vh'_H^2}{2\tilde{r}}\right), \quad \tilde{\sigma}_0(\tilde{r}) = 1, \tag{2.74}$$

and \tilde{w}_0 is the solution of

$$0 = \tilde{w}_0 + \frac{3vh'_H^2(\tilde{r}-2) - \Lambda\tilde{r}(1+2\tilde{r}^3)}{\tilde{r}(\tilde{r}-1)(-3vh'_H^2 - \Lambda(\tilde{r}+\tilde{r}^2+\tilde{r}^3))} \dot{\tilde{w}}_0 + \frac{9h'_H^2\tilde{r}^2}{(3vh'_H^2 + \Lambda(\tilde{r}+\tilde{r}^2+\tilde{r}^3))^2} \tilde{w}_0. \tag{2.75}$$

Here, $h'_H = \frac{dh(r)}{dr}|_{r=r_H} \sim \frac{d\tilde{h}_0(\tilde{r})}{d\tilde{r}}|_{\tilde{r}=1}$. Then, the leading thermodynamic quantities of

the black hole with non-abelian hair are given by [28],

$$Q_E = \frac{4\pi}{e^2} h'(r) r^2 \frac{\tau_3}{2} \Big|_{r \rightarrow \infty} \xrightarrow{r_H \rightarrow \infty} \frac{4\pi}{e^2} r_H^2 h'_H \frac{\tau_3}{2}, \quad (2.76a)$$

$$Q_M = \frac{4\pi}{e^2} (1 - w(r)^2) \frac{\tau_3}{2} \Big|_{r \rightarrow \infty} \xrightarrow{r_H \rightarrow \infty} \frac{4\pi}{e^2} \left(1 - \tilde{w}_0(\tilde{r})^2\right) \frac{\tau_3}{2}, \quad (2.76b)$$

$$M = \frac{m(r)}{G_N} \Big|_{r \rightarrow \infty} \xrightarrow{r_H \rightarrow \infty} \frac{-\Lambda + 3v h'_H^2}{6G_N} r_H^3, \quad (2.76c)$$

$$T = \frac{1}{4\pi} \sigma(r_H) \mu'(r_H) \xrightarrow{r_H \rightarrow \infty} \frac{r_H}{4\pi} (-\Lambda - v h'_H^2), \quad (2.76d)$$

$$S = \frac{\pi r_H^2}{G_N}. \quad (2.76e)$$

The AdS boundary condition implies $\tilde{w}_0(\tilde{r} \rightarrow \infty) = 1$. Since it is known that the black hole is unstable if $w(r)$ has a node (a nontrivial solution to $w(r) = 0$) [29, 200], we require $\tilde{w}_0(\tilde{r})$ be positive everywhere. Under these conditions, we find a unique solution for \tilde{w}_0 when Λ , v and h'_H are given. This establishes the existence of a stable (nodeless) solution in leading order for given values of r_H , Λ , v , and h'_H , provided $h'_H^2, v h'_H^2 < -\Lambda$, which are always satisfied for large enough T .

As expected, at high temperature, the thermodynamic quantities of the solution converge to those of the embedded $U(1)$ RN black hole as

$$\begin{aligned} M &= \frac{r_H}{2G_N} \left(-\frac{\Lambda r_H^2}{3} + \frac{e^2 G_N Q^2}{4\pi r_H^2} \right), & Q_E &= Q \frac{\tau_3}{2}, \\ T &= \frac{1}{4\pi r_H} \left(-\Lambda r_H^2 - \frac{e^2 G_N Q^2}{4\pi r_H^2} \right), & S &= \frac{\pi r_H^2}{G_N}. \end{aligned} \quad (2.77)$$

In Figure 2.1, we show the Helmholtz free energies of the two solutions as functions of T , with Q , v and Λ fixed as

$$\sqrt{-\Lambda} G_N Q = 100, \quad v = 1, \quad \Lambda = -1. \quad (2.78)$$

We observe that Helmholtz free energies of the two solutions converge at high temperature. We also note that, if we look at smaller temperature, the free energy of the $U(1)$ RN black hole (in the orange curve) becomes larger than that of the genuinely non-abelian solution (in the dotted red curve). We will discuss more about it in Section 2.6.

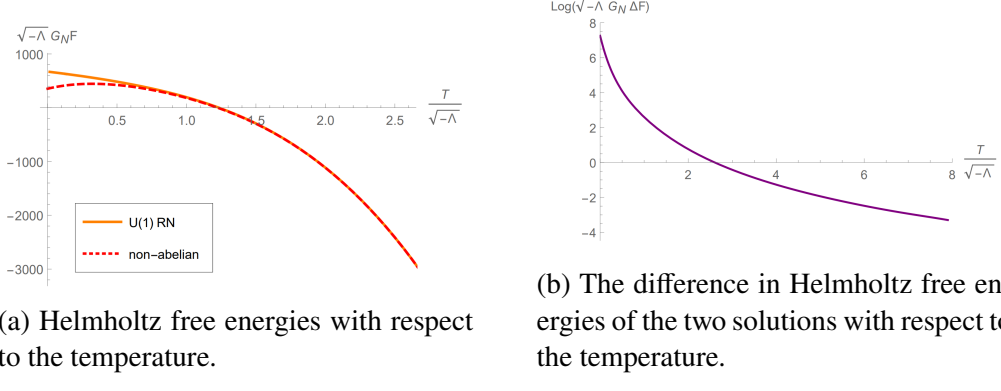


Figure 2.1: They are plotted at a fixed value of $\Lambda = -1$, $v = 1$ and $\sqrt{-\Lambda} G_N Q = 100$.

Having our expectation confirmed, we can utilize the $U(1)$ RN solution to estimate the high temperature behavior of the holographic CFT with non-Abelian global symmetry G in any dimensions. In particular,

$$Z_G \left(T, \mu = \frac{\phi}{\langle \phi, \phi \rangle^{1/2}} \mu_{U(1)} \right) \sim Z_{U(1)} (T, \mu_{U(1)}), \quad T \gg \frac{1}{\ell}, \quad (2.79)$$

where Z_G denotes the grand canonical partition function for the Einstein Yang–Mills system in AdS_{d+1} with gauge group G and $Z_{U(1)}$ is that for the Einstein Maxwell system. By using equation (2.59), we obtain

$$\begin{aligned} Z_G(T, \mu) &= \exp \left[a T^{d-1} + \frac{b}{4} T^{d-3} \langle \mu, \mu \rangle + \dots \right] \\ &= \exp \left[a T^{d-1} - \frac{b}{4} T^{d-1} \langle \phi, \phi \rangle + \dots \right], \end{aligned} \quad (2.80)$$

where $\beta \mu = i \phi$.

2.6 Stability of black hole with non-abelian hair

In the holographic CFT with non-abelian gauge symmetry, there are two types of black holes solutions, with and without non-abelian hair. In the previous section, we showed that the two solutions converge at high temperature. Since the two solutions differ at lower temperature, it is interesting to find out which solution is preferred thermodynamically. In this section, we calculate $1/T$ corrections to the Helmholtz free energies of the two solutions at the same temperature and charge. We find that the black hole with non-abelian hair has a lower free energy and is more stable. To be specific, we consider $G = SU(2)$ though we believe the results apply to any compact Lie group.

Since we know the exact solution without non-abelian hair, we focus on evaluating $1/T$ corrections to the solution with hair. We start with the equations,

$$\begin{aligned}\ddot{\tilde{h}}_1 &= -\frac{2\dot{\tilde{h}}_1}{\tilde{r}} + \tilde{\delta}_h, & \tilde{\delta}_h &= \dot{\tilde{\sigma}}_1 \dot{\tilde{h}}_0 + \frac{2\tilde{w}_0^2}{\tilde{\mu}_0 \tilde{r}^2} \tilde{h}_0, \\ \dot{\tilde{m}}_1 &= v \left(\tilde{r}^2 \dot{\tilde{h}}_0 \dot{\tilde{h}}_1 - \tilde{r}^2 \dot{\tilde{h}}_0^2 \tilde{\sigma}_1 + \tilde{\delta}_m \right), & \tilde{\delta}_m &= \frac{\tilde{w}_0^2 \tilde{h}_0^2}{\tilde{\mu}_0} + \tilde{\mu}_0 \dot{\tilde{w}}_0^2, \\ \dot{\tilde{\sigma}}_1 &= v \left(\frac{2\dot{\tilde{w}}_0^2}{\tilde{r}} + \frac{2\tilde{w}_0^2 \tilde{h}_0^2}{\tilde{\mu}_0^2 \tilde{r}} \right),\end{aligned}\quad (2.81)$$

which are subleading order terms of equation (2.72) with respect to the expansion taken in equation (2.73). These differential equations depend on the zeroth order quantities; we note that $\tilde{\sigma}_0$, \tilde{h}_0 and \tilde{m}_0 are directly calculated to be equation (2.74), whereas \tilde{w}_0 is solved numerically, when Λ and h'_H are given, using the differential equation in equation (2.75). Hence, we know all zeroth-order quantities, and we can decide \tilde{h}_1 , \tilde{m}_1 , \tilde{w}_1 , and $\tilde{\sigma}_1$ from equation (2.81). We first find $\dot{\tilde{h}}_1$ as

$$\dot{\tilde{h}}_1(\tilde{r}) = \frac{1}{\tilde{r}^2} \int_1^{\tilde{r}} d\tilde{r}' \tilde{r}'^2 \tilde{\delta}_h(\tilde{r}'). \quad (2.82)$$

Since $\sigma(r)$ goes to one when $\tilde{r} \rightarrow \infty$, $\tilde{\sigma}_1$ goes to zero as $\tilde{r} \rightarrow \infty$, and

$$\tilde{\sigma}_1(\tilde{r}) = -\Delta \tilde{\sigma} + \int_1^{\tilde{r}} d\tilde{r}' \dot{\tilde{\sigma}}_1(\tilde{r}'), \quad \Delta \tilde{\sigma} := \int_1^\infty d\tilde{r} \dot{\tilde{\sigma}}_1(\tilde{r}). \quad (2.83)$$

Then, by taking the quantities $\dot{\tilde{h}}_1$ and $\tilde{\sigma}_1$, given by equations (2.82) and (2.83), we can solve \tilde{m}_1 in equation (2.81) as

$$\frac{\tilde{m}_1(\tilde{r})}{v} = \frac{1}{2v} + \int_1^{\tilde{r}} d\tilde{r}' \frac{h'_H}{\tilde{r}'} \int_1^{\tilde{r}'} d\tilde{r}'' \tilde{r}''^2 \tilde{\delta}_h(\tilde{r}'') + \int_1^{\tilde{r}} d\tilde{r}' \frac{h_H^2}{\tilde{r}'} \left(\Delta \tilde{\sigma} - \int_1^{\tilde{r}'} d\tilde{r}'' \dot{\tilde{\sigma}}_1(\tilde{r}'') \right) + \int_1^{\tilde{r}} d\tilde{r}' \tilde{\delta}_m(\tilde{r}'). \quad (2.84)$$

We are interested in $\tilde{m}_1(\tilde{r} \rightarrow \infty)$ because it corresponds to the mass of the black hole. The subleading contribution to the mass of the non-abelian black hole is expressed as

$$\tilde{m}_1(\tilde{r} \rightarrow \infty) = \frac{1}{2} + \int_1^\infty d\tilde{r} v \left(h'_H \tilde{r} \tilde{\delta}_h(\tilde{r}) + h_H^2 \left(1 - \frac{1}{\tilde{r}} \right) \dot{\tilde{\sigma}}_1(\tilde{r}) + \tilde{\delta}_m(\tilde{r}) \right). \quad (2.85)$$

Now that we have computed \tilde{h}_1 , \tilde{m}_1 , and $\tilde{\sigma}_1$, we can estimate the thermodynamic

quantities of the black hole as

$$\begin{aligned} Q &\approx \frac{v}{G_N} \left(r_H^2 h'_H + \int_1^\infty d\tilde{r} \tilde{r}^2 \tilde{\delta}_h(\tilde{r}) \right) \frac{\tau_3}{2}, \\ T &\approx \frac{r_H}{4\pi G_N} \dot{\tilde{\mu}}_0 \Big|_{\tilde{r}=1} + \frac{1}{4\pi G_N r_H} \left(\dot{\tilde{\mu}}_1 - \dot{\tilde{\mu}}_0 \Delta \tilde{\sigma} \right) \Big|_{\tilde{r}=1}, \\ M &\approx \frac{-\Lambda + 3vh'_H^2}{6G_N} r_H^3 + \frac{\tilde{m}_1(\tilde{r} \rightarrow \infty)}{G_N} r_H, \end{aligned} \quad (2.86)$$

where $\tilde{r} = r/r_H$ and the mass M is evaluated in the infinite radius limit, provided from the value of $m(r)$ at $r \rightarrow \infty$. Finally, the Helmholtz free energy of black hole with non-abelian hair is given by,

$$\begin{aligned} F &= M - TS \\ &= r_H^3 \tilde{F}_0 + \frac{r_H}{G_N} \left(\frac{1}{4} + v \int_1^\infty d\tilde{r} \Delta \tilde{m}(\tilde{r}) + \frac{1}{4} (-\Lambda + vh'_H^2) \Delta \tilde{\sigma} \right), \end{aligned} \quad (2.87)$$

where $v\Delta \tilde{m}$ is the integrand of the equation (2.85) and

$$\tilde{F}_0 = \frac{1}{G_N} \left(\frac{1}{12} \Lambda + \frac{3}{4} vh'_H^2 \right). \quad (2.88)$$

Let us compare this with the free energy of the $U(1)$ RN black hole. For the solution to have the same temperature and charge, the radius of the horizon of the RN black hole must be

$$r_{H,RN} = r_H + \frac{\Delta \tilde{r}}{r_H}, \quad \Delta \tilde{r} = \frac{-(-\Lambda + vh'_H^2) \Delta \tilde{\sigma} + 2vh'_H \int_1^\infty d\tilde{r} \tilde{r}^2 \tilde{\delta}_h(\tilde{r})}{-\Lambda + 3vh'_H^2}. \quad (2.89)$$

The free energy is then

$$F_{RN} = r_H^3 \tilde{F}_0 + \frac{r_H}{G_N} \left(\frac{1}{4} + vh'_H \int_1^\infty d\tilde{r} \tilde{r}^2 \tilde{\delta}_h(\tilde{r}) + \frac{1}{4} (-\Lambda + vh'_H^2) \Delta \tilde{\sigma} \right). \quad (2.90)$$

We remark again that the two free energies in equations (2.87) and (2.90) have same leading behavior. By taking the difference of the two free energies, we obtain

$$F_{RN} - F = \frac{v r_H}{G_N} \left(h'_H \int_1^\infty d\tilde{r} \tilde{r}^2 \tilde{\delta}_h(\tilde{r}) - \int_1^\infty d\tilde{r} \Delta \tilde{m}(\tilde{r}) \right), \quad (2.91)$$

which comes from the $1/T$ correction. When we numerically calculate this difference, it has strictly positive value as shown in Figure 2.2. Therefore, the black hole with non-abelian hair has a smaller free energy and is thermodynamically preferred over the $U(1)$ RN black hole at finite temperature.

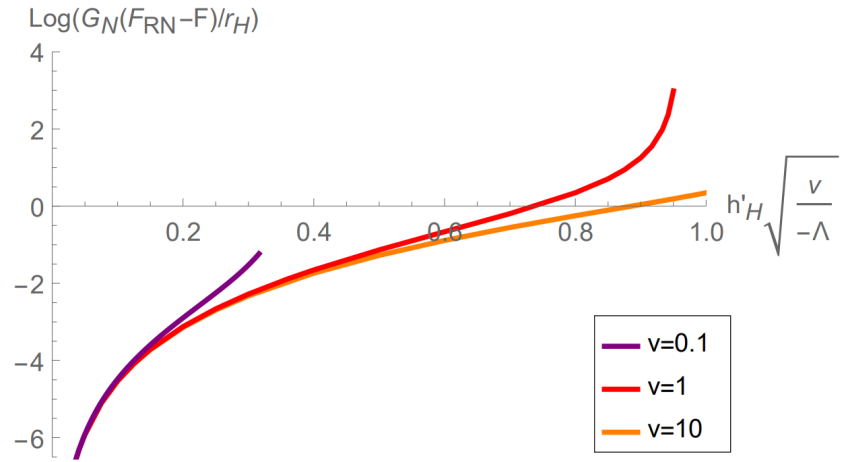


Figure 2.2: $\log [G_N(F_{RN} - F)/r_H]$ as a function of $h'_H \sqrt{v/-\Lambda}$ when $\Lambda = -1$.

UNIVERSAL ASYMPTOTICS FOR HIGH ENERGY CFT DATA

3.1 Introduction

What is the behavior of conformal field theory (CFT) data at high energies? This question is well-studied in two dimensions. For instance, the density of states of any 2D CFT at high energies takes the following universal form, known as the Cardy formula [46]:

$$\rho^{d=2}(\Delta, J) \sim \exp \left[\sqrt{\frac{c}{3}} \pi \left(\sqrt{\Delta + J - \frac{c}{12}} + \sqrt{\Delta - J - \frac{c}{12}} \right) \right], \quad \Delta - |J| \gg c. \quad (3.1)$$

Here, $\rho^{d=2}(\Delta, J)$ is the density of local operators (equivalently states on S^1) with scaling dimension Δ and spin J . The entropy at high energies is controlled by a single theory-dependent number: the central charge c . The Cardy formula follows from modular invariance of the genus one partition function.

Though (3.1) is valid for all 2D CFTs, it has a particularly nice interpretation for CFTs dual to quantum gravity in weakly-curved AdS_3 . In such theories, the entropy $\log \rho^{d=2}(\Delta, J)$ is interpreted as the area of a BTZ black hole with spin J and mass M given by [197]

$$M = \frac{1}{\ell_{\text{AdS}}} \left(\Delta - \frac{c}{12} \right), \quad (3.2)$$

in an AdS_3 space with [38]

$$c = \frac{3\ell_{\text{AdS}}}{2G_N}. \quad (3.3)$$

The Cardy formula then becomes a statement of universality of black hole entropy, regardless of the microscopic details of the quantum gravity theory.

OPE coefficients of heavy operators in 2D CFTs obey similar, though perhaps less well-known, universal formulas. In [44], a formula for average squared OPE coefficients of three heavy Virasoro primaries was derived using modular invariance of the genus two partition function. For example, when all three operators have roughly equal dimensions $\Delta_i = \Delta \gg c$, it takes the form

$$(C_{\text{HHH}}^{d=2})^2 \sim \left(\frac{27}{16} \right)^{3\Delta} e^{-6\pi\sqrt{\frac{c-1}{24}\Delta}} \Delta^{\frac{5c-11}{36}}, \quad \Delta \gg c. \quad (3.4)$$

Similar formulas were derived for OPE coefficients with one or two heavy operator(s) (see e.g. [141]). These formulas were subsequently unified in [67], with interesting connections to the DOZZ formula. In holographic theories, the formula for $(C_{\text{HHH}}^{d=2})^2$ matches the contribution of a two-sided wormhole connecting a pair of boundary three-point functions [58].

In this paper, we explore whether similar universal formulas exist for higher dimensional CFTs. We will use purely field-theoretic methods, so our results will be applicable to both holographic and non-holographic theories. An immediate puzzle is that there is no simple analog of modular invariance in higher dimensional geometries like $S^1 \times S^{d-1}$ ($d \geq 3$). (See [18, 21, 116, 156, 189, 190] for some discussion and progress on modular invariance in higher dimensions.) However, we can instead use a beautiful idea from [14, 27, 127], which was used to count the density of states in higher dimensional CFTs in [27, 188]. (Similar ideas were used for studying supersymmetric indices in [75].) The key point is that finding the leading asymptotics of CFT data doesn't require full modular invariance — we just need a sufficiently powerful effective theory for a CFT dimensionally reduced on a circle.

The dimensional reduction of a d -dimensional CFT is generically a gapped theory in $d-1$ dimensions. Fortunately for our purposes, the exponential decay of correlations in a gapped theory makes it very *flexible*: we can place it on many different geometries, and in this way extract myriad predictions for the d -dimensional CFT.

A gapped theory can be described by a local action for background fields, obtained by integrating out the gapped degrees of freedom. In the context of a dimensionally-reduced CFT (with thermal boundary conditions), we call this local action the "thermal effective action." It describes hydrodynamic observables of the CFT in equilibrium. The derivative expansion of the thermal effective action is an expansion in the inverse temperature $\beta = 1/T$. This construction was explained in [14, 127], and has been explored extensively in the hydrodynamics literature; see e.g. [26, 71, 123, 124, 126]. We review it in Section 3.2, along the way discussing some subtleties related to the Weyl anomaly.

Placing the thermal effective theory on $S^1 \times S^{d-1}$ leads to simple universal predictions for the density of CFT operators at large Δ . For example, in 3D CFTs, one obtains

$$\log \rho^{d=3}(\Delta, J) = 3\pi^{1/3} f^{1/3} (\Delta^2 - J^2)^{1/3} - \frac{2}{3} \log(\Delta^2 - J^2) + \mathcal{O}(\Delta^0). \quad (3.5)$$

Here, f is a theory-dependent positive real number, equal to minus the free energy density of the CFT, as we review in Section 3.2. The leading term in the high temperature partition function for the canonical ensemble of a CFT was first written down using hydrodynamic techniques in [27]. It was subsequently transformed to the microcanonical ensemble in [188].¹ The thermal effective theory approach in this work allows us to reproduce those results and systematically explore subleading corrections.

The quantity f controls the leading density of states in both 2D (where $f = \pi c/6$) and higher dimensions. However, unlike in 2D, where the Cardy formula is valid up to nonperturbative corrections in Δ , the entropy in higher dimensional CFTs receives perturbative corrections in $1/\Delta$, coming from higher-derivative terms in the thermal effective action. The derivation of (3.5) using the thermal effective action is given in Section 3.3. There, we also describe the leading higher-derivative corrections. (Furthermore in Section 3.3, we clarify some subtleties related to the Casimir energy on S^{d-1} in higher-dimensional CFTs.) We also briefly discuss nonperturbative corrections to the density of states in Section 3.3. Then, in Section 3.4, we compare these general formulas to free theories and holographic theories, determining Wilson coefficients in those cases by matching their partition functions to the effective theory.

In addition to the density of states, we will also find universal formulas for OPE coefficients of three heavy operators in higher- d CFTs.² Our strategy will be to put the theory on a higher-dimensional version of a genus-2 Riemann surface, obtained by gluing a pair of three-punctured S^d 's with three cylinders $S^{d-1} \times I$ (where I is an interval). We describe this "genus-2" geometry in detail in Section 3.5.³

A glaring problem is that the "genus-2" geometry is *not* a circle fibration, so it is not immediately obvious how to apply the thermal effective action. However, in a "high temperature" limit where the cylinders get short, the geometry contains shrinking circles. We claim that these shrinking circles can be treated like thermal circles in local regions that we call "hot spots"; see Figure 3.1. We furthermore conjecture that the effective action of the hot spots gives the singular part of the partition function

¹The density of states was also studied [147, 199].

²Formulas for heavy OPE coefficients weighted by light OPE coefficients, e.g. $C_{\text{HHH}} C_{\text{HLL}}^3$, were derived in [9] using crossing symmetry of six-point functions of local operators. By contrast, our focus will be on *un-weighted* heavy OPE coefficients C_{HHH} , which are controlled by different physics. For example, the leading behavior of C_{HHH} is determined by the free energy density f , which does not (to our knowledge) appear in a simple way in a six-point function of light local operators.

³A special case of this geometry with no angular fugacities was studied recently in [20].

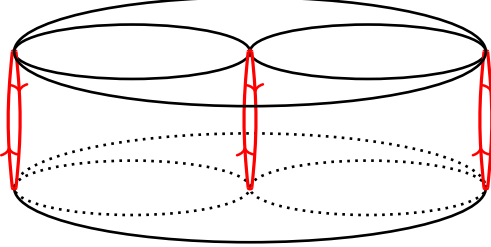


Figure 3.1: The "genus-2" geometry and its "hot spots." The top is a ball B^d with two balls removed. It is topologically equivalent to a three-punctured S^d . The bottom is the same. The top and bottom are glued together with three cylinders. In the limit that the cylinders get short, there are shrinking circles indicated in red that run down one cylinder and up another. The neighborhoods of each of these circles are "hot spots," where the thermal effective action receives a large contribution.

on our "genus-2" geometry. (The remaining parts of the geometry are not described by thermal EFT, but contribute non-singular corrections to the partition function at high temperature.) With the "hot spot" conjecture, we can determine the partition function in the regime where it is dominated by heavy CFT data.

To extract heavy-heavy-heavy OPE coefficients, we must furthermore understand the decomposition of the partition function into a higher-dimensional version of genus-2 (global) conformal blocks. These are interesting special functions that to our knowledge have not previously appeared in the CFT literature. We explore them in Section 3.6, determining their behavior at large Δ using the shadow formalism and saddle-point analysis. We then decompose the partition function into "genus-2" blocks using an appropriate inverse Laplace transform on the moduli space of "genus-2" conformal structures in higher dimensions. In the end, we obtain a universal formula for average squared heavy-heavy-heavy OPE coefficients in a d -dimensional CFT. For example, for three scalar operators with similar dimensions Δ in $d = 3$, we find

$$\rho^{d=3}(\Delta, 0)^3 (C_{\text{HHH}}^{d=3})^2 \sim \left(\frac{3}{2}\right)^{6\Delta} e^{3\sqrt{2\pi f\Delta}} \times \dots \quad (3.6)$$

where "... " are subleading corrections in Δ . We give a formula for OPE coefficients of three operators with arbitrary Lorentz representations (with spin held constant as $\Delta \rightarrow \infty$) in arbitrary d below in (3.242).

In Section 3.8, we apply similar (but simpler) methods to compute asymptotic thermal 1-point functions of heavy operators. This can be viewed as a particularly simple limit of heavy-heavy-heavy OPE coefficients.

In Section 3.9, we discuss (3.6), its generalizations, and some implications and future directions. In holographic theories, we speculate that (3.6) describes a three-point function of three black holes surrounded by highly entangled matter. Three point functions of three "pure" black holes are likely atypical from the point of view of (3.6), but perhaps could be determined from an appropriate holographic calculation. In Appendix A, we discuss a simple warmup example of the thermal effective action for a two-point function of momentum generators. In Appendix C, we discuss some aspects of free theories, including novel formulas for nonperturbative corrections to density of states. Other appendices contain detailed calculations to supplement the main text.

3.2 The thermal effective action

Consider a d -dimensional CFT at finite temperature T . Generically, thermal fluctuations cause equilibrium correlators to decay exponentially with distance:

$$\langle \mathcal{O}(\vec{x}_1) \mathcal{O}(\vec{x}_2) \rangle_\beta \sim e^{-|\vec{x}_1 - \vec{x}_2|/\xi}. \quad (3.7)$$

By dimensional analysis, the correlation length ξ must be inversely proportional to the temperature, $\xi \propto 1/T$. Exponentially-decaying correlators can be expanded in a series in δ -functions and their derivatives. (Equivalently, in momentum space, they can be expanded in a power series in momenta.) This expansion is summarized by a local effective action for background fields that we call the *thermal effective action*.

It is useful to adopt the geometric perspective on the thermal effective action explained in [14]. Equilibrium thermal correlators are computed by compactifying the Euclidean theory on a thermal circle of length $\beta = 1/T$. Generically, when a d -dimensional CFT is compactified on a circle, the result is a *gapped* theory in $(d-1)$ dimensions. A rough argument is that compactification of a CFT does not involve tuning any parameters, since all β are equivalent by d -dimensional scale invariance. Thus, it would be non-generic for the resulting $(d-1)$ -dimensional theory to be at a critical point. Instead, it will typically have a nonzero mass gap $m_{\text{gap}} \propto T$, and a finite correlation length $\xi = 1/m_{\text{gap}}$.⁴ We can think of this gapped theory as the modular transform of the d -dimensional CFT.

This argument fails when a symmetry protects gapless modes in the compactified theory, such as in free theories or supersymmetric compactifications (where we twist

⁴By contrast, when a theory with an intrinsic scale is compactified, one generally obtains different dynamics at different compactification radii. By tuning β it may be possible to reach a critical point. An example is 4D SU(2) pure Yang-Mills theory, which is expected to possess a critical point in the Ising universality class at a particular temperature, see e.g. [93] for a review.

by $(-1)^F$ around the circle). It could also fail in theories that spontaneously break a continuous symmetry at finite temperature, such as those recently constructed (in fractional spacetime dimensions) in [55]. It is currently unknown whether such theories exist in integer spacetime dimensions. See [55, 100] and references therein for more discussion. In this work, we will focus on theories that are gapped at finite temperature.

An efficient way to capture correlators of the CFT is to couple to classical background fields. For example, stress tensor correlators are captured by coupling to a d -dimensional background metric $G_{\mu\nu}$. If the metric possesses a circle isometry, then by a suitable choice of coordinates, we can put it in Kaluza-Klein form

$$G_{\mu\nu}dx^\mu dx^\nu = g_{ij}(\vec{x})dx^i dx^j + e^{2\phi(\vec{x})}(d\tau + A_i(\vec{x}))^2, \quad \tau \in [0, 1), \quad (3.8)$$

where the periodic direction is $x^0 = \tau$. The $(d-1)$ -dimensional fields are a metric g_{ij} , a gauge field A_i , and a dilaton ϕ . We choose conventions so that τ has periodicity 1. Thus, for the thermal compactification $S^1_\beta \times \mathbb{R}^{d-1}$ with the flat metric, we have $e^\phi = \beta$. However, it will be interesting in what follows to allow the $(d-1)$ -dimensional fields g_{ij}, A_i, ϕ to be spatially varying.

By our assumption above, the partition function of the d -dimensional CFT on the Kaluza-Klein geometry (3.8) becomes the partition function of a gapped $(d-1)$ -dimensional theory coupled to $(d-1)$ -dimensional background fields:

$$Z_{\text{CFT}}[G] = Z_{\text{gapped}}[g, A, \phi]. \quad (3.9)$$

The partition function of a trivially gapped QFT at long distances can be expanded in a sum of local counterterms in the background fields. In this case, we have⁵

$$Z_{\text{CFT}}[G] = Z_{\text{gapped}}[g, A, \phi] \sim e^{-S_{\text{th}}[g, A, \phi]}. \quad (3.10)$$

The thermal effective action S_{th} is a sum of local terms in g_{ij}, A_i, ϕ that captures Euclidean correlators at length scales that are large compared to the correlation length $\xi = 1/m_{\text{gap}}$ (equivalently, at momenta small compared to m_{gap}).⁶ In (3.10),

⁵A theory that spontaneously breaks a discrete symmetry at finite temperature can display mild violations of (3.10); see [55]. In general, if the finite temperature theory is nontrivially gapped, then the thermal effective action must include a nontrivial TQFT. We focus on the trivially gapped case in this work, though most of our results are simple to adapt to a more general thermal TQFT.

⁶Note that the thermal effective action *does not* in general capture long-distance real time observables, even at small nonzero frequencies $0 < \omega \ll m_{\text{gap}}$, where dissipation is an important effect.

" \sim " means agreement up to exponential corrections of the form $e^{-L/\xi}$, where L is a characteristic length scale.

In QFT, we usually have the freedom to add arbitrary local counterterms in background fields. This is called a change of "scheme." In the thermal effective action (3.10), it is important that we are only allowed to add local d -dimensional counterterms to the CFT (which enter S_{th} via dimensional reduction). We are *not* allowed to add arbitrary local $d-1$ -dimensional counterterms. Thus, S_{th} can contain physical, scheme-independent information.

The thermal effective action is highly constrained by symmetries. Firstly, coordinate-invariance in d -dimensions implies that S_{th} is invariant under $(d-1)$ -dimensional coordinate transformations, as well as gauge transformations of the KK gauge field A_i . For simplicity, in this work we focus on CFT_d 's with vanishing gravitational anomaly. When the gravitational anomaly is non-vanishing (for example in a 2D CFT with $c_L \neq c_R$), the anomaly must be matched by gravitational Chern-Simons terms in the thermal effective action; see [59, 75, 98, 125, 126] for more details. Such terms could be easily incorporated into the analysis that follows.⁷

Secondly, S_{th} is constrained by Weyl invariance of the d -dimensional theory. Under a Weyl transformation, the CFT partition function changes by

$$Z_{\text{CFT}}[e^{2\sigma} G] = Z_{\text{CFT}}[G] e^{-S_{\text{anom}}[G, \sigma]}, \quad (3.11)$$

where $S_{\text{anom}}[G, \sigma]$ is the contribution from the Weyl anomaly. Because ϕ transforms with a shift $\phi \rightarrow \phi + \sigma$ under τ -independent Weyl transformations, we can use (3.11) to completely determine the ϕ -dependence of $Z_{\text{CFT}}[G]$ [85]. Note that

$$Z_{\text{CFT}}[G] = Z_{\text{CFT}}[\widehat{G}] e^{-S_{\text{anom}}[\widehat{G}, \phi]}, \quad (3.12)$$

where $\widehat{G} \equiv e^{-2\phi} G$. Plugging in (3.10), this implies

$$\begin{aligned} S_{\text{th}}[g, A, \phi] &= S_{\text{th}}[\widehat{g}, A, 0] + S_{\text{anom}}[\widehat{G}, \phi] \\ &\equiv S[\widehat{g}, A] + S_{\text{anom}}[\widehat{G}, \phi]. \end{aligned} \quad (3.13)$$

In equation (3.13), $S_{\text{anom}}[\widehat{G}, \phi]$ plays the role of matching the Weyl anomaly in the thermal effective action. We discuss this contribution later in Section 3.2. The remaining term $S[\widehat{g}, A]$ is invariant under τ -independent Weyl transformations. It depends only on A_i , and the Weyl-invariant "effective metric"

$$\widehat{g}_{ij} \equiv e^{-2\phi} g_{ij}. \quad (3.14)$$

⁷We thank Yifan Wang for discussion on these points.

Note that \widehat{g} transforms as a metric under coordinate-transformations. Thus, $S[\widehat{g}, A]$ can be organized in a derivative expansion in coordinate invariants built out of \widehat{g} and A . Classifying the terms in $S[\widehat{g}, A]$ is similar to classifying local interactions in Einstein-Maxwell theory (without the freedom to perform field redefinitions). The first few terms are

$$S[\widehat{g}, A] = \int d^{d-1}x \sqrt{\widehat{g}} \left(-f + c_1 \widehat{R} + c_2 F^2 + \dots \right). \quad (3.15)$$

Here, \widehat{R} is the Riemann curvature built from the metric \widehat{g} , and $F_{ij} = \partial_i A_j - \partial_j A_i$ is the field strength of the KK gauge boson. Indices are everywhere contracted using \widehat{g} , for example

$$F^2 = \widehat{g}^{ik} \widehat{g}^{jl} F_{ij} F_{kl}. \quad (3.16)$$

This ensures that the derivative expansion for S_{th} becomes an expansion in \vec{p}/T , since \widehat{g}^{ij} contains a factor of $e^{2\phi}$, where $e^{-\phi}$ is a local temperature. Again, in (3.15), we have assumed gravitational anomalies are absent.

The construction of the thermal effective action (3.15) closely mimics the construction of the dilaton effective action in theories where scale invariance is spontaneously broken to d -dimensional Poincare invariance [137]. The key difference is that here we have an effective action in $(d-1)$ -dimensions instead of d dimensions.

The cosmological constant term

The leading term in the thermal effective action is a cosmological constant $-\int d^d x \sqrt{\widehat{g}} f$ for the effective metric \widehat{g} . The coefficient f has at least three important interpretations.

1. $-f$ is (the scheme-independent part of) the free energy density of the CFT at finite temperature in flat space.⁸ To see why, we place the theory on $\mathbb{R}^{d-1} \times S_\beta^1$, where the thermal circle has length β . In this geometry, the effective metric is $\widehat{g}_{ij} = \beta^{-2} \delta_{ij}$. Only the cosmological constant term in S_{th} is nonzero, and it contributes

$$F/T = -\log Z_{\text{CFT}}[\mathbb{R}^{d-1} \times S_\beta^1] = S_{\text{th}} = - \int d^d x f \beta^{-(d-1)} = -f T^{d-1} \text{vol } \mathbb{R}^{d-1}. \quad (3.17)$$

$$F/T = -\log Z_{\text{CFT}}[\mathbb{R}^{d-1} \times S_\beta^1] = S_{\text{th}} = - \int d^d x f \beta^{-(d-1)} = -f T^{d-1} \text{vol } \mathbb{R}^{d-1}.$$

⁸Our convention for f is opposite to the one in [119], $f_{\text{here}} = -f_{\text{there}}$.

Thus, the free energy density is $-fT^d$.

2. f is proportional to the thermal one-point function of the stress tensor in flat space \mathbb{R}^{d-1} . Lorentz and scale invariance dictate that

$$\langle T^{\mu\nu}(t, \vec{x}) \rangle_\beta = b_T T^d \left(\delta_0^\mu \delta_0^\nu - \frac{1}{d} \delta^{\mu\nu} \right), \quad (3.18)$$

for some dimensionless coefficient b_T . Meanwhile, the energy density can be computed from the derivative of the partition function⁹

$$-\langle T^{00}(0, \vec{x}) \rangle_\beta = -\frac{1}{\text{vol } \mathbb{R}^{d-1}} \frac{\partial}{\partial \beta} \log Z_{\text{CFT}}[\mathbb{R}^{d-1} \times S_\beta^1] = (d-1)fT^d. \quad (3.19)$$

Equating (3.18) and (3.19), we find $b_T = -df$. In particular, positivity and extensivity of the energy density on \mathbb{R}^{d-1} implies that f is positive:

$$f > 0. \quad (3.20)$$

3. $-f$ is the Casimir energy density of the CFT compactified on a circle. To see why, we choose x^1 as a time direction. The Hamiltonian density for the compactified theory is then

$$\frac{E_{\text{cas}}}{\text{vol}(S_\beta^1 \times \mathbb{R}^{d-2})} = -\langle T^{11} \rangle_\beta = -fT^d. \quad (3.21)$$

In particular, (3.20) gives a simple proof that the Casimir energy of a CFT compactified on a circle is always negative. Ultimately, this is a consequence of tracelessness of the stress tensor. The components T^{00} compute the energy in the thermal ensemble (which is positive), while the components T^{11} compute the energy in the compactified theory. The two have opposite signs by tracelessness of $T^{\mu\nu}$. This proof applies, for example, to electromagnetism.

Thus, the coefficient f is a simple and important observable of the CFT. We will see that it controls a huge amount of the physics at finite temperature. As a simple warmup example, in Appendix A, we show how f determines a (regularized) two-point function of momentum operators at finite temperature. This result can be understood both from "bootstrap" arguments using properties of stress tensor correlators, and from the thermal effective action.

⁹Note that we are using the conventions of Euclidean field theory, where the generator of time translations includes a minus sign $H = -\int d\vec{x} T^{00}$. The minus sign can be understood via Wick rotation from Lorentzian signature $T_E^{00} = (i)^2 T_L^{00}$.

Weyl anomaly terms

The Weyl anomaly terms $S_{\text{anom}}[\widehat{G}, \phi]$ in the thermal effective action were given in [85]. Let us write them down in detail. Such terms are of course absent when d is odd, so we focus on even d in this subsection.

As a review, the infinitesimal form of the Weyl anomaly in d dimensions is

$$\delta_\sigma(-\log Z_{\text{CFT}}[G]) = \int d^d x \sqrt{G} \sigma \mathcal{A}[G], \quad (3.22)$$

where δ_σ is defined by rescaling the metric $G \rightarrow (1 + 2\sigma)G$ with σ infinitesimal. Here, $\mathcal{A}[G]$ is a local functional of G such that (3.22) solves the Wess-Zumino consistency condition $[\delta_{\sigma_1}, \delta_{\sigma_2}] \log Z = 0$. The infinitesimal Weyl anomaly can be integrated by considering a family of metrics $e^{2t\sigma}G$ where $t \in [0, 1]$, using (3.22) to write a differential equation in t , and solving the differential equation. The result is the finite Weyl transformation rule (3.11), where S_{anom} is given by [187]

$$S_{\text{anom}}[G, \sigma] = \int_0^1 dt \int d^d x \sqrt{\det(e^{2t\sigma}G)} \sigma \mathcal{A}[e^{2t\sigma}G]. \quad (3.23)$$

The general solution of the Wess-Zumino consistency condition in d -dimensions is [33, 34]:

$$\int d^d x \sqrt{G} \sigma \mathcal{A}[G] = \frac{1}{(4\pi)^{d/2}} \int d^d x \sqrt{G} \sigma \left((-1)^{d/2} a_d E_d - \sum_k c_{dk} I_k^{(d)} \right) + \delta_\sigma S_{\text{ct}}. \quad (3.24)$$

Here, E_d is the Euler density,¹⁰ and $\sqrt{G} I_k^{(d)}$ are local Weyl-invariants of G . For example, in 4D there is one such Weyl-invariant, given by the square of the Weyl tensor:

$$I_1^{(4)} = C^2 = C_{\mu\nu\rho\sigma} C^{\mu\nu\rho\sigma} \quad (d = 4). \quad (3.25)$$

In 6D there are three such Weyl invariants $I_{k=1,2,3}^{(6)}$, and in general the number grows with d . The factor $1/(4\pi)^{d/2}$ in (3.24) is a convention.

The remaining terms $\delta_\sigma S_{\text{ct}}$ in (3.24) are Weyl variations of local counterterms. For instance, in 4D we can have

$$S_{\text{ct}} = -\frac{b}{12(4\pi)^2} \int d^d x \sqrt{G} R^2 \quad (d = 4), \quad (3.26)$$

¹⁰In 2D, we have $a_2 = c/6$, and in 4D we write $a_4 = a$.

which leads to a contribution $\delta_\sigma R^2 \sim b \square R$ in the Weyl anomaly. We sometimes refer to $\delta_\sigma S_{\text{ct}}$ as "b-type" terms. Such terms trivially obey the Wess-Zumino consistency condition. They are scheme-dependent because they can be shifted by adding local counterterms to the action of the CFT. We comment more on this below in Section 3.3.

Plugging these results into (3.23), we find S_{anom} for example in $d = 2$ and $d = 4$:

$$\begin{aligned} S_{\text{anom}}^{\text{2D}}[G, \sigma] &= -\frac{c}{24\pi} \int d^2x \sqrt{G} (\sigma R + (\partial\sigma)^2) \\ S_{\text{anom}}^{\text{4D}}[G, \sigma] &= \frac{a}{(4\pi)^2} \int d^4x \sqrt{G} \left(\sigma E_4 - 4\partial_\mu\sigma\partial_\nu\sigma(R^{\mu\nu} - \frac{1}{2}G^{\mu\nu}R) - 4(\partial\sigma)^2 \square\sigma - 2(\partial\sigma)^4 \right) \\ &\quad - \frac{c}{(4\pi)^2} \int d^4x \sqrt{G} \sigma C^2 + S_{\text{ct}}[e^{2\sigma}G] - S_{\text{ct}}[G]. \end{aligned} \quad (3.27)$$

Note that the scheme-dependent part of the Weyl anomaly $\delta_\sigma S_{\text{ct}}$ integrates trivially to give $S_{\text{ct}}[e^{2\sigma}G] - S_{\text{ct}}[G]$. The Weyl-invariant terms are also simple to integrate because the integrand (3.23) is t -independent for those terms.

Putting everything together, the Weyl-anomaly contribution to the thermal effective action is

$$\begin{aligned} S_{\text{anom}}[\widehat{G}, \phi] &= S_{\text{Euler}} \\ &\quad - \frac{1}{(4\pi)^{d/2}} \sum_k c_{dk} \int d^{d-1}x \sqrt{\widehat{g}} \phi \text{DR}[I_k^{(d)}[\widehat{G}]] + \text{DR}[S_{\text{ct}}[G]] - \text{DR}[S_{\text{ct}}[\widehat{G}]], \end{aligned} \quad (3.28)$$

(3.29)

where

$$S_{\text{Euler}} = \frac{(-1)^{d/2} a_d}{(4\pi)^{d/2}} \int_0^1 dt \int d^{d-1}x e^{dt\phi} \sqrt{\widehat{g}} \phi \text{DR}[E_d[e^{2t\phi}\widehat{G}]]. \quad (3.30)$$

Here, the dimensional reduction operation $\text{DR}[\dots]$ means evaluating in the KK metric (3.8) and integrating over τ .

Note that the $I_k^{(d)}$ terms in (3.28) are linear in ϕ , and thus can lead to temperature dependence of the form $\log(\beta/\beta_0)$ in certain geometries. Here, we note that the coefficient of $\log\beta$ is a genuine prediction of S_{th} , but the scale β_0 is scheme-dependent. The reason is that β_0 can be shifted by adding local Weyl-invariant counterterms to the action of the CFT:

$$S_{\text{CFT}} \rightarrow S_{\text{CFT}} + \frac{1}{(4\pi)^{d/2}} \int d^d x \sqrt{G} \sum_k r_k I_k^{(d)}. \quad (3.31)$$

This ambiguity shifts the coefficients of $\text{DR}[I_k^{(d)}]$ in the thermal effective action:

$$-c_{dk}\phi \rightarrow r_k - c_{dk}\phi, \quad (3.32)$$

and consequently shifts β_0 . This ambiguity will not play a further role in this work, since we will always consider CFTs in conformally-flat¹¹ geometries where $I_k^{(d)}$ vanishes.

Two dimensions

In two dimensions, a very nice thing happens. The cosmological constant term is the *only* local gauge-invariant combination of \widehat{g} and A_i that we can write down. Furthermore, there are no nontrivial local Weyl invariants. Thus, the Weyl-invariant part of the thermal effective action truncates to a single term!

$$S[\widehat{g}, A] = - \int d^1x \sqrt{\widehat{g}} f \quad (d = 2). \quad (3.33)$$

The action (3.33) describes equilibrium thermal physics in 2D to all perturbative orders in $1/T$. Using the connection between f and the Casimir energy (3.21), we find

$$f = \frac{2\pi c}{12}, \quad (3.34)$$

where c is the central charge.

This result is not a surprise. A 2D CFT at high temperature can be described by performing a modular transformation, reinterpreting the thermal circle as a spatial circle. The states propagating in the modular-transformed theory have energies $E_i = \frac{2\pi}{\beta}(\Delta_i - \frac{c}{12})$, where Δ_i are scaling dimensions in the CFT. The effective action (3.33) simply captures the contribution of the ground state in the modular transformed theory, with energy $E_0 = -\frac{2\pi}{\beta}\frac{c}{12}$. The energy gap to the next state is the "mass gap" of the thermal theory

$$m_{\text{gap}} = E_1 - E_0 = \frac{2\pi}{\beta}\Delta_1 \quad (d = 2). \quad (3.35)$$

States with energies at or above the mass gap $E_i - E_0 \geq m_{\text{gap}}$ contribute nonperturbative corrections in β of the form $e^{-2\pi\Delta_i/\beta}$, which are not captured by S_{th} .

3.3 The density of high-dimension states

The spectrum of a d -dimensional CFT is captured by the partition function on $S_\beta^1 \times S^{d-1}$. In this section, we compute this partition function using the thermal

¹¹We call a manifold "conformally-flat" if in a neighborhood of each point, the metric is Weyl-equivalent to a flat metric. This is sometimes called "locally conformally-flat." A 3-manifold is conformally-flat if and only if the Cotton tensor vanishes, and a d -manifold with $d \geq 4$ is conformally-flat if and only if the Weyl tensor vanishes.

effective action, and decompose the result into conformal characters to extract the density of high dimension states. We will recover the leading-order formulas from [27, 188], and also discuss subleading corrections. The precise expression for the partition function involves the Casimir energy of the CFT on S^{d-1} . To start, we review the Casimir energy and discuss some details of its relation to the thermal effective action.

The Casimir energy on S^{d-1}

The partition function on $S_\beta^1 \times S^{d-1}$ is a sum over states on S^{d-1} weighted by Boltzmann factors $e^{-\beta E_i}$. By the state-operator correspondence, states on S^{d-1} are in one-to-one correspondence with local CFT operators O_i . In even dimensions the energy E_i of the state $|O_i\rangle$ is equal to the dimension Δ_i plus a contribution from the Casimir energy on the sphere:

$$E_i = \Delta_i + E_0, \quad (3.36)$$

where Δ_i is the scaling dimension of O_i . For example, in 2D, the Casimir energy is $E_0 = -\frac{c}{12}$ (in units where the S^{d-1} has radius 1). The Casimir energy E_0 will play an important role in higher dimensions as well, so let us recall how to derive it.

We follow the discussion of [13]. Let $W[G] \equiv -\log Z_{\text{CFT}}[G]$, so that the Weyl anomaly is $W[e^{2\sigma}G] - W[G] = S_{\text{anom}}[G, \sigma]$. To compute the stress tensor on the cylinder $\mathbb{R} \times S^{d-1}$, we consider the Weyl rescaling from the plane to the cylinder

$$dr^2 + r^2 d\Omega_{d-1}^2 \rightarrow \frac{dr^2}{r^2} + d\Omega_{d-1}^2 = e^{-2\log r} \delta_{\mu\nu} dx^\mu dx^\nu, \quad (3.37)$$

which corresponds to $\sigma = -\log r$. Plugging this into $S_{\text{anom}}[G, \sigma]$, we obtain the partition function on the cylinder as a function of the partition function on the plane. Taking a derivative with respect to $G_{\mu\nu}$ and using that the one-point function $\langle T^{\mu\nu} \rangle$ on the plane vanishes, we obtain $\langle T^{\mu\nu} \rangle$ on the cylinder, from which we can read off the Casimir energy.

There is a small shortcut that will be useful in what follows. We can simply compute $W[G]$ on the infinite cylinder $\mathbb{R} \times S^{d-1}$ using the Weyl anomaly. This has an infinite part of the form $E_0 \text{vol } \mathbb{R}$, from which we can read off the Casimir energy E_0 . As an example, in 2D, we have

$$W[e^{-2\log r} \delta] - W[\delta] = -\frac{c}{24\pi} \int r dr d\theta \frac{1}{r^2} = -\frac{c}{12} \int d\tau \quad (d=2), \quad (3.38)$$

where we defined $\tau = \log r$. This gives the expected result $E_0 = -\frac{c}{12}$. In 4D, we find

$$\begin{aligned} W[e^{-2\log r}\delta] - W[\delta] &= \frac{a \text{vol } S^3}{(4\pi)^2} \int r^3 dr \left(\frac{6}{r^4} \right) + S_{\text{ct}}[e^{2\sigma}\delta] \\ &= \left(\frac{3a}{4} - \frac{3b}{8} \right) \int d\tau, \end{aligned} \quad (3.39)$$

where we used the form of S_{ct} in (3.26), together with the fact that the curvature of S^3 is $R = 6$. Thus, the Casimir energy in 4D is

$$E_0 = \frac{3a}{4} - \frac{3b}{8} \quad (d = 4). \quad (3.40)$$

- Choice of scheme

As noted in [13], the 4D Casimir energy (3.40) is scheme-dependent — it can be shifted by redefining the local counterterm coefficient b . Similar statements hold in any even $d \geq 4$. However, CFT data is scheme-independent. To study it, we are free to choose whatever scheme is most convenient.

In what follows, we will choose a scheme where $S_{\text{ct}} = 0$, so that b -type terms are absent from both the Casimir energy and the Weyl anomaly. To define such a scheme in practice, one must choose a regulator, compute the Weyl anomaly with that regulator, and then add appropriate local counterterms to cancel the b -type terms.¹²

In this $S_{\text{ct}} = 0$ scheme, the b -type terms $\text{DR}[S_{\text{ct}}]$ are not present in the thermal effective action, and the partition function on $S_\beta^1 \times S^{d-1}$ is given by

$$\text{Tr} [e^{-\beta(D+\varepsilon_0)}] \sim e^{-S_{\text{th}}} = e^{-S[\hat{g}, A] - S_{\text{Euler}}}, \quad (3.41)$$

where ε_0 is the a_d -type contribution to the Casimir energy alone. Here, " \sim " means equality up to exponentially suppressed corrections in $1/\beta$. S_{Euler} is given in (3.30). We have used that $S_\beta^1 \times S^{d-1}$ is conformally-flat to drop the Weyl-invariants $I_k^{(d)}$. In Appendix B, we describe how (3.41) comes about in a general scheme.

¹²This requires a sufficiently "flexible" regulator that we can compute the Weyl anomaly. For example it is not obvious how to do this with a lattice regulator. Furthermore, such a scheme choice might clash with other symmetries, e.g. SUSY [13]. We thank Zohar Komargodski for discussion on these points

The value of ε_0 was computed in general d in [113]:

$$\begin{aligned} \varepsilon_0 &\equiv a_d\text{-type contribution to Casimir energy on } S^{d-1} \\ &= \frac{\sqrt{\pi}}{\Gamma(\frac{1-d}{2})} a_d = \begin{cases} \frac{(d-1)!!}{(-2)^{d/2}} a_d, & d \text{ even,} \\ 0 & d \text{ odd,} \end{cases} \end{aligned} \quad (3.42)$$

where $(d-1)!! = (d-1) \cdots 3 \cdot 1$ for even d . Note that in 2D, we have $a_2 = c/6$.

The partition function from the thermal effective action

Let us now study the density of CFT operators with various dimensions and spins. We can obtain this from the partition function of the CFT on $S_\beta^1 \times S^{d-1}$ with a spin fugacity:

$$Z(\beta, \vec{\Omega}) = \text{Tr} \left[e^{-\beta(D+\varepsilon_0) + i\beta\vec{\Omega} \cdot \vec{M}} \right] \sim e^{-S[\hat{g}, A] - S_{\text{Euler}}}. \quad (3.43)$$

Here, D is the dilatation operator, \vec{M} are the $n := \lfloor \frac{d}{2} \rfloor$ generators of the Cartan subalgebra of the rotation group $\text{SO}(d)$, and $\vec{\Omega}$ are spin fugacities.

Geometrically, (3.43) is computed by a path integral on $S_\beta^1 \times S^{d-1}$, with a twist by $\beta\vec{\Omega}$ as we move around the thermal circle. The metric is

$$ds_{\text{cylinder}}^2 = \beta^2 d\tau^2 + ds_{\text{sphere}}^2, \quad (3.44)$$

where $\tau \in [0, 1]$ is a coordinate on S^1 and ds_{sphere}^2 is the metric on S^{d-1} .

To write down the metric on the sphere, let us choose coordinates that make Cartan rotations manifest. The Cartan generators are rotations in n orthogonal 2-planes. We use radius-angle coordinates $\{r_a, \theta_a\}$ for each plane ($a = 1, \dots, n$), so the Cartan generators are simply $i\partial_{\theta_a}$. If d is odd, we have an extra axis and we use the coordinate r_{n+1} for it. The radii satisfy the constraint $\sum_{a=1}^{n+\epsilon} r_a^2 = 1$, where $\epsilon = 0$ for even d and $\epsilon = 1$ for odd d . In these coordinates, the metric of the sphere is

$$ds_{\text{sphere}}^2 = \sum_{a=1}^{n+\epsilon} dr_a^2 + \sum_{a=1}^n r_a^2 d\theta_a^2, \quad (3.45)$$

where we have the constraint $\sum_{a=1}^{n+\epsilon} r_a dr_a = 0$.

In the twisted geometry that computes $Z(\beta, \vec{\Omega})$, we identify the points

$$(\tau, \theta_a) \sim (\tau + 1, \theta_a - \beta\Omega_a). \quad (3.46)$$

Because of this identification, shifts in τ with fixed θ_a are not periodic isometries, and thus the metric (3.45) is not in Kaluza-Klein (KK) form. To place it in KK

form, we redefine $\theta_a \rightarrow \theta_a + \beta\Omega_a\tau$, which removes the twist (3.46), and produces the new metric

$$\begin{aligned} ds^2 &= \beta^2 d\tau^2 + \sum_{a=1}^{n+\epsilon} dr_a^2 + \sum_{a=1}^n r_a^2 (d\theta_a + \beta\Omega_a d\tau)^2 \\ &= \beta^2 \left(1 + \sum_{a=1}^n r_a^2 \Omega_a^2 \right) \left(d\tau + \frac{1}{\beta} \sum_{a=1}^n \frac{r_a^2 \Omega_a}{1 + \sum_{b=1}^n r_b^2 \Omega_b^2} d\theta_a \right)^2 \\ &\quad + \sum_{a=1}^{n+\epsilon} dr_a^2 + \sum_{a,b=1}^n \left(r_a r_b \delta_{ab} - \frac{r_a^2 r_b^2 \Omega_a \Omega_b}{1 + \sum_{c=1}^n r_c^2 \Omega_c^2} \right) d\theta_a d\theta_b. \end{aligned} \quad (3.47)$$

Comparing (3.47) with (3.8), we identify a metric g_{ij} , a KK gauge field A_i , and a dilaton ϕ given by

$$\begin{aligned} e^{2\phi} &= \beta^2 \left(1 + \sum_{a=1}^n r_a^2 \Omega_a^2 \right), \\ A &= \frac{1}{\beta} \sum_{a=1}^n \frac{r_a^2 \Omega_a}{1 + \sum_{b=1}^n r_b^2 \Omega_b^2} d\theta_a, \\ g &= \sum_{a=1}^{n+\epsilon} dr_a^2 + \sum_{a,b=1}^n \left(r_a r_b \delta_{ab} - \frac{r_a^2 r_b^2 \Omega_a \Omega_b}{1 + \sum_{c=1}^n r_c^2 \Omega_c^2} \right) d\theta_a d\theta_b. \end{aligned} \quad (3.48)$$

The effective metric $\widehat{g} = e^{-2\phi} g$, together with A , then appears in the thermal effective action $S[\widehat{g}, A]$.

Explicitly, the cosmological constant term in the effective Lagrangian is

$$\sqrt{\widehat{g}} = T^{d-1} \left(1 + \sum_{i=1}^n r_i^2 \Omega_i^2 \right)^{-\frac{d}{2}} \prod_{i=1}^n r_i, \quad (3.49)$$

while the Maxwell and Einstein densities are

$$\begin{aligned} F^2 &= 8T^{-2} \left(\sum_{i=1}^n \Omega_i^2 - \frac{\sum_{i=1}^n r_i^2 \Omega_i^2 (1 + \Omega_i^2)}{1 + \sum_{i=1}^n r_i^2 \Omega_i^2} \right), \\ \widehat{R} &= T^{-2} \left(d(d+1) \frac{1 - \sum_{i=1}^n r_i^2 \Omega_i^4}{1 + \sum_{i=1}^n r_i^2 \Omega_i^2} - 2(2d-1) \left(1 - \sum_{i=1}^n \Omega_i^2 \right) \right). \end{aligned} \quad (3.50)$$

As expected, at high temperature, the cosmological constant term gives the leading contribution, while the Einstein and Maxwell terms are subleading by $1/T^2$, since they are two-derivative terms. Finally, the thermal effective action on our geometry

is given by integrating over S^{d-1} :

$$\begin{aligned} S[\widehat{g}, A] &= \int_{S^{d-1}} \sqrt{\widehat{g}} \left(-f + c_1 \widehat{R} + c_2 F^2 + \dots \right) \\ &= \frac{\text{vol } S^{d-1}}{\prod_{i=1}^n (1 + \Omega_i^2)} \left[-f T^{d-1} + (d-2) \left((d-1)c_1 + (2c_1 + \frac{8}{d}c_2) \sum_{i=1}^n \Omega_i^2 \right) T^{d-3} + \dots \right], \end{aligned} \quad (3.51)$$

where $\text{vol } S^{d-1} = \frac{2\pi^{d/2}}{\Gamma(d/2)}$ is the volume of the $d-1$ -sphere.¹³

Note that the cosmological constant predicts the entire leading term in (3.51) as a detailed function of the spin fugacities Ω_i . This leading term was first written down in [27].¹⁴ Using the thermal effective action, it is straightforward to incorporate more terms in S_{th} and characterize the form of subleading corrections. Overall, we obtain a formula for the thermal partition function of a CFT with a spin fugacity in a systematic expansion in $1/T$.

The leading term in (3.51) has poles at $\Omega_i = \pm i$. These poles are related to the unitarity bound because states close to the unitarity bound are not penalized by Boltzmann factors $e^{-\beta(\Delta-i\Omega J)}$ in this regime of angular fugacities. In our calculation, the poles come from locations on the sphere where $r_i = 1$ (and the remaining r_j vanish). Despite additional poles in the expressions (3.50), the higher-order corrections \widehat{R} and F^2 do *not* lead to further enhanced poles in the partition function. The reason is that \widehat{R} and F^2 are actually finite at $r_i = 1$ when $\Omega_i = \pm i$. We expect that this remains true for all higher-order corrections in the thermal effective action, so that the pole structure of (3.51) holds to arbitrary (perturbative) order in $1/T$.

¹³To evaluate (3.51), we use the following explicit coordinates on S^{d-1} . For even $d = 2n$, the integral is

$$\int_0^1 dr_1 \dots \int_0^1 dr_n \int_0^{2\pi} d\theta_1 \dots \int_0^{2\pi} d\theta_n \delta \left(\sqrt{r_1^2 + \dots + r_n^2} - 1 \right) \sqrt{\widehat{g}} \left(-f + c_1 \widehat{R} + c_2 F^2 + \dots \right),$$

and for odd $d = 2n + 1$, the integral is

$$\int_0^1 dr_1 \dots \int_0^1 dr_n \int_{-1}^1 dr_{n+1} \int_0^{2\pi} d\theta_1 \dots \int_0^{2\pi} d\theta_n \delta \left(\sqrt{r_1^2 + \dots + r_{n+1}^2} - 1 \right) \sqrt{\widehat{g}} \left(-f + c_1 \widehat{R} + c_2 F^2 + \dots \right).$$

To compute either case, we used the Feynman parametrization identity:

$$\frac{1}{A_1^{\alpha_1} \dots A_k^{\alpha_k}} = \frac{\Gamma(\alpha_1 + \dots + \alpha_k)}{\Gamma(\alpha_1) \dots \Gamma(\alpha_k)} \int_0^1 du_1 \dots \int_0^1 du_k \frac{\delta(u_1 + \dots + u_k - 1) u_1^{\alpha_1-1} \dots u_k^{\alpha_k-1}}{(u_1 A_1 + \dots + u_k A_k)^{\alpha_1+\dots+\alpha_k}}. \quad (3.52)$$

In order for (3.51) to be valid, we require that the convex hull of $1 + \Omega_i^2$ not contain 0. Otherwise, the integral diverges (as expected from the unitarity bound of the CFT).

¹⁴Our $\vec{\Omega}$ is related to the one in [27] by $i\vec{\Omega}_{\text{here}} = \vec{\Omega}_{\text{there}}$.

Specifically, we expect that the coefficient of T^{d-2k-1} is a degree- $2k$ polynomial in the Ω_i , times an overall factor $1/\prod_{i=1}^n (1 + \Omega_i^2)$.

Finally, let us compute S_{Euler} by plugging (3.48) into (3.30). In $d = 2, 4, 6$, we find

$$\begin{aligned} S_{\text{Euler}}^{d=2} &= 0, \\ S_{\text{Euler}}^{d=4} &= -\frac{a_4\beta}{12} \frac{(\Omega_1^2 - \Omega_2^2)^2}{(1 + \Omega_1^2)(1 + \Omega_2^2)}, \\ S_{\text{Euler}}^{d=6} &= -\frac{3a_6\beta}{80} \frac{1}{(1 + \Omega_1^2)(1 + \Omega_2^2)(1 + \Omega_3^2)} \\ &\quad \times \left[\Omega_1^6 + \Omega_2^6 + \Omega_3^6 - 4(\Omega_1^4(\Omega_2^2 + \Omega_3^2) + \Omega_2^4(\Omega_3^2 + \Omega_1^2) + \Omega_3^4(\Omega_1^2 + \Omega_2^2)) \right. \\ &\quad \left. + 21\Omega_2^2\Omega_3^2\Omega_1^2 + 5(\Omega_1^2\Omega_2^2 + \Omega_2^2\Omega_3^2 + \Omega_3^2\Omega_1^2) - 5(\Omega_1^4 + \Omega_2^4 + \Omega_3^4) \right]. \end{aligned} \quad (3.53)$$

In all these cases, S_{Euler} has the same functional form as expected from the $O(T^{-1})$ terms in the Weyl-invariant part of the thermal effective action $S[\hat{g}, A]$ — namely a polynomial of degree d in the Ω_i 's times $\beta/\prod_{i=1}^n (1 + \Omega_i^2)$. Thus, the effects of S_{Euler} cannot be distinguished from $S[\hat{g}, A]$ in the CFT partition function on $S^1 \times S^{d-1}$. It would be interesting to try to distinguish these terms in some example theories, perhaps by studying stress-tensor correlators in thermal flat space.

Leading asymptotic formula

From (3.51) we can extract the high energy density of states for any CFT¹⁵. Let us first consider the leading term of the high-temperature partition function:

$$\log Z(T, \Omega_i) = \frac{\text{vol } S^{d-1} f T^{d-1}}{\prod_{i=1}^n (1 + \Omega_i^2)} + O(T^{d-3}), \quad (3.54)$$

where $n = \lfloor d/2 \rfloor$. To extract the density of states, we perform an inverse Laplace transform on the partition function, which can be done by saddle point approximation. Before we do the general d case however, let us first do $d = 2$ and $d = 3$ explicitly.

We pause to note that we can compute either the asymptotic density of all operators of the CFT, including both primary and descendent operators, or the asymptotic density of only the conformal primary operators. We compute the latter by decomposing the partition function into the conformal characters. In d dimensions the characters

¹⁵A previous version of this paper had minor typos in the density of states that we have corrected. We thank Sasha Diatlyk and Yifan Wang for pointing them out to us.

are given by¹⁶

$$\chi_{\Delta, J_i}(\beta, \Omega_i) = \begin{cases} \frac{e^{-\beta\Delta} \chi_{J_i}(\beta\Omega_i)}{\prod_{i=1}^n (1 - e^{-\beta(1+i\Omega_i)})(1 - e^{-\beta(1-i\Omega_i)})}, & d \text{ even,} \\ \frac{e^{-\beta\Delta} \chi_{J_i}(\beta\Omega_i)}{(1 - e^{-\beta}) \prod_{i=1}^n (1 - e^{-\beta(1+i\Omega_i)})(1 - e^{-\beta(1-i\Omega_i)})}, & d \text{ odd,} \end{cases} \quad (3.55)$$

where $\chi_{J_i}(\theta_i)$ is the character of the $\text{SO}(d)$ representation $\lambda = (J_1, \dots, J_n)$. The partition function is a sum over characters, with an additional inclusion of the Casimir energy ε_0 defined in (3.42):

$$Z(T, \Omega_i) = e^{-\beta\varepsilon_0} \sum_{\Delta_i, J_i} \chi_{\Delta_i, J_i}(\beta, \Omega_i). \quad (3.56)$$

- $d = 2$

From (3.54), our high-temperature expression for the partition function in $d = 2$ is

$$\begin{aligned} Z(T, \Omega)_{d=2} &\approx \exp\left(\frac{2\pi fT}{1 + \Omega^2}\right) \\ &= \exp\left(\frac{4\pi^2 cT}{12(1 + \Omega^2)}\right), \end{aligned} \quad (3.57)$$

where we used the relation between f and c for 2D CFTs (3.34). We would like to take the inverse Laplace transform to extract the high-energy density of states. This calculation is precisely Cardy's calculation for the high-energy density of states [46], but we include it for completeness. It is convenient to first change variables:

$$\beta_L := \frac{1}{T} + \frac{i\Omega}{T}, \quad \beta_R := \frac{1}{T} - \frac{i\Omega}{T}, \quad (3.58)$$

which gives

$$Z(\beta_L, \beta_R)_{d=2} := \text{Tr}\left(e^{-\beta_L(\frac{\Delta-J}{2} - \frac{c}{24})} e^{-\beta_R(\frac{\Delta+J}{2} - \frac{c}{24})}\right) \approx e^{\frac{2\pi^2 c}{12} \left(\frac{1}{\beta_L} + \frac{1}{\beta_R}\right)}, \quad (3.59)$$

where we include the Casimir shift described in Sec 3.3. Taking the inverse Laplace transform then gives the following integral:

$$\rho_{d=2}^{\text{states}}(\Delta, J) \sim \frac{1}{2} \left[\frac{1}{2\pi i} \int_{\gamma-i\infty}^{\gamma+i\infty} d\beta_L e^{\frac{2\pi^2 c}{12\beta_L} + \beta_L(\frac{\Delta-J}{2} - \frac{c}{24})} \right] \left[\frac{1}{2\pi i} \int_{\gamma-i\infty}^{\gamma+i\infty} d\beta_R e^{\frac{2\pi^2 c}{12\beta_R} + \beta_R(\frac{\Delta+J}{2} - \frac{c}{24})} \right]. \quad (3.60)$$

¹⁶The characters (3.55) are for long representations of the conformal group. For special values of Δ, J_i (e.g. states at the unitarity bound), the representation may be shortened and the expression for the character will be modified. However, since we are interested in reading off the density of primary operators at large dimension, short representations will not play a role.

Although we can do this integral by saddle, it actually can be done exactly. The tree level piece is

$$\rho_{d=2}^{\text{states}}(\Delta, J) \sim \exp \left[\sqrt{\frac{2c}{3}} \pi \left(\sqrt{\frac{\Delta+J}{2}} - \frac{c}{24} + \sqrt{\frac{\Delta-J}{2}} - \frac{c}{24} \right) \right]. \quad (3.61)$$

We see this is none other than the Cardy formula [46]. If we do the integrals in (3.60) exactly¹⁷, we get

$$\begin{aligned} \rho_{d=2}^{\text{states}}(\Delta, J) &\sim \frac{\pi^2 c}{6\sqrt{(\Delta+J-\frac{c}{12})(\Delta-J-\frac{c}{12})}} I_1 \left(\sqrt{\frac{2c}{3}} \pi \sqrt{\frac{\Delta+J}{2}} - \frac{c}{24} \right) I_1 \left(\sqrt{\frac{2c}{3}} \pi \sqrt{\frac{\Delta-J}{2}} - \frac{c}{24} \right) \\ &= \frac{\sqrt{c}}{\sqrt{48}(\Delta+J-\frac{c}{12})^{3/4}(\Delta-J-\frac{c}{12})^{3/4}} \exp \left[\sqrt{\frac{2c}{3}} \pi \left(\sqrt{\frac{\Delta+J}{2}} - \frac{c}{24} + \sqrt{\frac{\Delta-J}{2}} - \frac{c}{24} \right) \right] \\ &\quad \times \left(1 + O(\Delta^{-1/2}) \right), \end{aligned} \quad (3.63)$$

where I_1 is a modified Bessel function of the first kind. The expression (3.63) indeed gives the known logarithmic corrections to Cardy's formula [47].

So far, (3.63) is counting the density of all states rather than the density of global or Virasoro primaries. A more natural object from the CFT perspective may be to count the density of primary operators. In order to generalize more easily to higher dimensions, we will now compute the asymptotic density of global (not Virasoro) primary operators. The calculation is almost identical, except now instead of taking the inverse Laplace transform of (3.59), we include the characters (3.55):

$$\int d\Delta dJ \rho_{d=2}^{\text{primaries}}(\Delta, J) e^{-\beta_L(\frac{\Delta-J}{2}-\frac{c}{24})} e^{-\beta_R(\frac{\Delta+J}{2}-\frac{c}{24})} \approx e^{\frac{2\pi^2 c}{12} \left(\frac{1}{\beta_L} + \frac{1}{\beta_R} \right)} (1-e^{-\beta_L})(1-e^{-\beta_R}). \quad (3.64)$$

¹⁷Strictly speaking the integral in (3.60) diverges. The precise statement is

$$\frac{1}{2\pi i} \int_{\gamma-i\infty}^{\gamma+i\infty} d\beta e^{\beta\Delta} \left(e^{\frac{\pi f}{\beta}} - 1 \right) = \sqrt{\frac{\pi f}{\Delta}} I_1 \left(\sqrt{4\pi f \Delta} \right). \quad (3.62)$$

This leads to an additional factor of $\delta(\Delta)$ in the inverse Laplace transform. However, since we are using this method to read off the large energy density of states, it does not affect our final expression (3.63).

Taking the inverse Laplace transform we then get

$$\begin{aligned} \rho_{d=2}^{\text{primaries}}(\Delta, J) &= \frac{c^{3/2}\pi^2}{\sqrt{432}(\Delta + J - \frac{c}{12})^{5/4}(\Delta - J - \frac{c}{12})^{5/4}} \\ &\times \exp\left[\sqrt{\frac{2c}{3}}\pi\left(\sqrt{\frac{\Delta+J}{2}} - \frac{c}{24} + \sqrt{\frac{\Delta-J}{2}} - \frac{c}{24}\right)\right] \\ &\times \left(1 + O(\Delta^{-1/2})\right). \end{aligned} \quad (3.65)$$

- $d = 3$

Now let us redo this analysis for $d = 3$. The logic is the same except now the form of the partition function is different:

$$Z(T, \Omega)_{d=3} \approx \exp\left(\frac{4\pi f T^2}{1 + \Omega^2}\right). \quad (3.66)$$

Using the same change variables (3.58) we get

$$Z(\beta_L, \beta_R)_{d=3} := \text{Tr}\left(e^{-\beta_L(\frac{\Delta-J}{2})} e^{-\beta_R(\frac{\Delta+J}{2})}\right) \approx \exp\left(\frac{4\pi f}{\beta_L \beta_R}\right). \quad (3.67)$$

To extract the density of states we again use an inverse Laplace transform:

$$\rho_{d=3}^{\text{states}}(\Delta, J) \approx \frac{1}{2} \left(\frac{1}{2\pi i}\right)^2 \int_{\gamma-i\infty}^{\gamma+i\infty} d\beta_L d\beta_R \exp\left(\frac{4\pi f}{\beta_L \beta_R} + \beta_L \left(\frac{\Delta-J}{2}\right) + \beta_R \left(\frac{\Delta+J}{2}\right)\right). \quad (3.68)$$

The integral in (3.68) is more complicated so now we do it via saddle point analysis.

The saddles in β_L, β_R are located at

$$\beta_L^* = \left(\frac{8\pi f(\Delta+J)}{(\Delta-J)^2}\right)^{1/3}, \quad \beta_R^* = \left(\frac{8\pi f(\Delta-J)}{(\Delta+J)^2}\right)^{1/3}. \quad (3.69)$$

This gives a remarkably simple expression for the tree-level density of states:

$$\rho_{d=3}^{\text{states}}(\Delta, J) \sim \exp\left[3\pi^{1/3} f^{1/3} (\Delta+J)^{1/3} (\Delta-J)^{1/3}\right]. \quad (3.70)$$

Keeping the one-loop terms we get

$$\rho_{d=3}^{\text{states}}(\Delta, J) \sim \frac{f^{1/3}}{\sqrt{3}\pi^{2/3}(\Delta+J)^{2/3}(\Delta-J)^{2/3}} \exp\left[3\pi^{1/3} f^{1/3} (\Delta+J)^{1/3} (\Delta-J)^{1/3}\right]. \quad (3.71)$$

The expression (3.71) again is counting the asymptotic density of states rather than conformal primaries. We can read off the density of primaries from the character

formula (3.55). We get

$$\rho_{d=3}^{\text{primaries}}(\Delta, J) \sim \frac{8\pi^{2/3} f^{5/3} (2J+1)\Delta}{\sqrt{3}(\Delta+J+\frac{1}{2})^{7/3}(\Delta-J-\frac{1}{2})^{7/3}} \exp \left[3\pi^{1/3} f^{1/3} \left(\Delta+J+\frac{1}{2} \right)^{1/3} \left(\Delta-J-\frac{1}{2} \right)^{1/3} \right]. \quad (3.72)$$

Note that in (3.72), $2J+1$ is the dimension of the spin J representation of $SO(3)$. This is reminiscent of the formulas found in [102, 128], where the density of a global symmetry representation ρ is proportional to its dimension $\dim \rho$. This comes about because the high temperature partition function can be approximated by a delta-function on a group (the rotation group in this case) centered at the identity, whose harmonic transform is the Plancherel measure $\dim \rho / \text{vol } G$.

- General d

For general $d > 3$, there are several chemical potentials to turn on, so the final leading formula for the density of states is a little more cumbersome. For simplicity, we will simply compute the tree-level asymptotic density of states (i.e. the value at the saddle-point, not including the Gaussian determinant). Note that because in this section we are computing the tree-level contribution, the formula is identical for states and for primaries.

First, let us consider the case where we only turn on information about one spin, for simplicity. The saddles in temperature and chemical potential are located at

$$T_* = \left(\frac{(\Delta + \varepsilon_0 - iJ\Omega_*)(1 + \Omega_*^2)}{(d-1)f \text{vol } S^{d-1}} \right)^{1/d},$$

$$\Omega_* = -i \frac{\sqrt{(\Delta + \varepsilon_0)^2 + (d-3)(d-1)J^2} - (\Delta + \varepsilon_0)}{J(d-3)}, \quad (3.73)$$

which lead to a high energy density of states of

$$\log \rho_d(\Delta, J) \sim \frac{d}{d-1} (\Delta + \varepsilon_0)^{\frac{d-1}{d}} \left(\frac{\text{vol } S^{d-1} f(d-1)}{2} \left(1 + \sqrt{1 + \frac{(d-3)(d-1)J^2}{(\Delta + \varepsilon_0)^2}} \right) \right)^{\frac{1}{d}}$$

$$\times \left(\frac{d-2}{d-3} - \frac{1}{d-3} \sqrt{1 + \frac{(d-3)(d-1)J^2}{(\Delta + \varepsilon_0)^2}} \right)^{1-\frac{2}{d}}. \quad (3.74)$$

This leading order formula matches the result in Equation (49) of [188].

The expression (3.74) reproduces (3.61) and (3.70) for $d = 2$ and $d = 3$ respectively. Note that to reproduce (3.70) we set the Casimir energy $\varepsilon_0 = 0$ and use the fact that

$$\lim_{d \rightarrow 3} \frac{(d-2)\Delta - \sqrt{\Delta^2 + (d-3)(d-1)J^2}}{d-3} = \frac{\Delta^2 - J^2}{\Delta}. \quad (3.75)$$

Now let us consider all the chemical potentials Ω_i turned on. The leading term for the partition function is given in (3.54), which means

$$\rho_d(\Delta, J_i) \sim \int dT d\Omega_i \exp \left(\frac{\Delta + \varepsilon_0}{T} + \frac{\text{vol } S^{d-1} f T^{d-1}}{\prod_{i=1}^n (1 + \Omega_i^2)} - \sum_{i=1}^n \frac{i \Omega_i J_i}{T} \right), \quad (3.76)$$

where for even dimensions, ε_0 is the Casimir energy as defined in (3.42). The saddle for the T integral is easy to compute, and is located at

$$T_* = \left(\frac{(\Delta + \varepsilon_0 - i \sum_i J_i \Omega_i) \prod_i (1 + \Omega_i^2)}{\text{vol } S^{d-1} f (d-1)} \right)^{1/d}. \quad (3.77)$$

Plugging this back into (3.76), we get

$$\begin{aligned} \rho_d(\Delta, J_i) &\sim \int d\Omega_i \exp \left[d(d-1)^{-\frac{d-1}{d}} (\text{vol } S^{d-1} f)^{\frac{1}{d}} \left(\Delta + \varepsilon_0 - i \sum_i J_i \Omega_i \right)^{\frac{d-1}{d}} \prod_i \left(1 + \Omega_i^2 \right)^{-\frac{1}{d}} \right]. \end{aligned} \quad (3.78)$$

We now want to find the saddles in the chemical potentials. Taking a derivative with respect to each Ω_j gives us the following equations to solve for the saddle $\Omega_{*,j}$:

$$-\frac{i(d-1)J_j}{2} = (\Delta + \varepsilon_0 - i \sum_i J_i \Omega_{*,i}) \frac{\Omega_{*,j}}{1 + \Omega_{*,j}^2}. \quad (3.79)$$

If we solve (3.79) for $\Omega_{*,j}$ for $j = 1, 2, \dots, \lfloor \frac{d}{2} \rfloor$, and plug into (3.78), we get the tree-level density of states (or primaries) in d dimensions. To describe the solution for (3.79), it is useful to define the quantity a as the following:

$$a := \frac{(\Delta + \varepsilon_0) - i \sum_i J_i \Omega_{*,i}}{d-1}. \quad (3.80)$$

a is a function of $\Delta + \varepsilon_0$ and the spins J_i , and it is a symmetric function of J_i . Each saddle point of Ω satisfies the following equations:

$$J_j = \frac{2ia\Omega_{*,j}^2}{1 + \Omega_{*,j}^2}, \quad \Omega_{*,j} = -i \frac{-a + \sqrt{a^2 + J_j^2}}{J_j}. \quad (3.81)$$

When we substitute this relation into (3.79), we get the density of states at leading order to be

$$\log \rho_d(\Delta, J_1, \dots, J_n) \sim d(\text{vol } S^{d-1} f)^{\frac{1}{d}} a^{\frac{d-1}{d}} \prod_{i=1}^n \left(\frac{1 + \sqrt{1 + \frac{J_i^2}{a^2}}}{2} \right)^{\frac{1}{d}}, \quad (3.82)$$

where a is the positive real solution of

$$\Delta + \varepsilon_0 = \lfloor \frac{d-1}{2} \rfloor a + \sum_i \sqrt{a^2 + J_i^2}. \quad (3.83)$$

Because the right-hand side of (3.83) is a monotonically increasing function of a , there is only one positive real a satisfying (3.83) for a given energy $\Delta + \varepsilon_0$ and spins J_i .

- Perturbative corrections to the density of states

Besides corrections coming from higher-loop terms in the saddle point analysis, the first nontrivial correction for $d > 2$ comes from higher derivative terms in the effective action of S_{th} in 3.51. Note that in $d = 2$ these corrections are absent (see 3.33). This is another way of understanding that the corrections to the first line of 3.63 are non-perturbatively suppressed in Δ (and come from the modular S transformation of the lightest non-vacuum operator).

For $d > 2$, the first correction comes from the Maxwell and Einstein terms in the effective action. This will turn out to induce a correction to the entropy of the form $\Delta^{\frac{d-3}{d}}$. To see this, let us look at our expression for the thermal effective action (3.51).

In $d = 3$ we have

$$\log Z_{d=3}(T, \Omega) = \frac{4\pi}{1 + \Omega^2} \left(fT^2 - \left(2c_1 + \left(2c_1 + \frac{8}{3}c_2 \right) \Omega^2 \right) + O(T^{-2}) \right). \quad (3.84)$$

From this we can extract a correction to the density of states from our saddle (3.69). We get

$$\begin{aligned} \log \rho_{d=3}^{\text{states}}(\Delta, J) &= 3\pi^{1/3} f^{1/3} (\Delta + J)^{1/3} (\Delta - J)^{1/3} - \frac{2}{3} \log(\Delta^2 - J^2) + \frac{1}{3} \log \left(\frac{f}{3\sqrt{3}\pi^2} \right) \\ &\quad - 8\pi c_1 + \frac{32c_2 J^2 \pi}{3(\Delta^2 - J^2)} + O(\Delta^{-1/3}), \\ \log \rho_{d=3}^{\text{primaries}}(\Delta, J) &= 3\pi^{1/3} f^{1/3} \left(\Delta + J + \frac{1}{2} \right)^{1/3} \left(\Delta - J - \frac{1}{2} \right)^{1/3} + \log \left(\frac{\Delta(2J+1)}{(\Delta^2 - (J + \frac{1}{2})^2)^{7/3}} \right) \\ &\quad + \log \left(\frac{8\pi^{2/3} f^{5/3}}{\sqrt{3}} \right) - 8\pi c_1 + \frac{32c_2 (J + \frac{1}{2})^2 \pi}{3(\Delta^2 - (J + \frac{1}{2})^2)} + O(\Delta^{-1/3}). \end{aligned} \quad (3.85)$$

Note that the size of the Maxwell term (c_2) compared to higher-derivative terms depends on the order of limits in Δ, J . If we take $\Delta \gg J \gg 1$, then the Maxwell term scales as Δ^{-2} (instead of Δ^0), can be neglected at this order in the derivative expansion. However, if we instead take a limit where Δ/J is fixed and then take Δ to infinity, then it is important.

For $d > 3$, we have the following correction to the density of states:

$$\begin{aligned} \log \rho_d(\Delta, J_1, \dots, J_n) &\sim d(\text{vol } S^{d-1} f)^{\frac{1}{d}} a^{\frac{d-1}{d}} \prod_{i=1}^n \left(\frac{1 + \sqrt{1 + \frac{J_i^2}{a^2}}}{2} \right)^{\frac{1}{d}} \\ &\quad - \frac{d-2}{f} (\text{vol } S^{d-1} f)^{\frac{3}{d}} a^{\frac{d-3}{d}} \left((d-1)c_1 - \left(2c_1 + \frac{8}{d}c_2 \right) \sum_i \frac{\sqrt{1 + J_i^2/a^2} - 1}{\sqrt{1 + J_i^2/a^2} + 1} \right) \prod_{i=1}^n \left(\frac{1 + \sqrt{1 + \frac{J_i^2}{a^2}}}{2} \right)^{\frac{3}{d}} \\ &\quad + O\left(a^{\frac{d-5}{d}}\right), \end{aligned} \quad (3.86)$$

where a is defined in (3.83). In order to trust the high-temperature expansion, we demand that the temperature at the saddle point be large. The saddle temperature (3.77) is proportional to $a^{\frac{1}{d}}$, with the remaining factors being $O(1)$. Therefore, we can expand our formula in a . We will discuss the regime of validity of our formulas in more detail in Sec 3.3.

If we keep the information from only one spin J , then we get a correction of the form

$$\begin{aligned} \log \rho_d(\Delta, J) &\sim \frac{d}{d-1} (\Delta + \varepsilon_0 - \alpha J)^{\frac{d-1}{d}} \left((d-1) \text{vol } S^{d-1} f \right)^{\frac{1}{d}} \left(1 + \frac{(d-3)\alpha J}{\Delta + \varepsilon_0} \right)^{\frac{1}{d}} \left(1 - \frac{\alpha J}{\Delta + \varepsilon_0} \right)^{1-\frac{2}{d}} \\ &\quad - \frac{(d-2)(\text{vol } S^{d-1} f)^{3/d}}{(d-1)^{\frac{d-3}{d}} f} (\Delta + \varepsilon_0 - \alpha J)^{\frac{d-3}{d}} (1 - \alpha^2)^{-3/d} \left((d-1)c_1 - \frac{8c_2 + 2c_1 d}{d} \alpha^2 \right) \\ &\quad + O\left((\Delta + \varepsilon_0)^{\frac{d-5}{d}}\right), \end{aligned} \quad (3.87)$$

where $\alpha := \frac{J}{\Delta + \varepsilon_0} \frac{d-1}{1 + \sqrt{1 + (d-1)(d-3)J^2/(\Delta + \varepsilon_0)^2}}$. Because $\Delta + \varepsilon_0$ is larger than J , $|\alpha|$ is always in between 0 and 1. The corrections from the Maxwell and Einstein terms are in fact more important than the Gaussian fluctuations about the saddle point.

Again, if $\Delta + \varepsilon_0 \gg |J|$, then $|\alpha| \ll 1$, so the Einstein (c_1) term dominates in 3.87 and the Maxwell (c_2) term is subleading. However, if $(\Delta + \varepsilon_0)/J$ is fixed as $\Delta \rightarrow \infty$, then $\alpha \sim O(1)$, and the two terms are comparable.

- Regime of validity

Because we are doing a high-temperature expansion, in order for our formulas to be valid, we need the saddle-point value of temperature, T_* , to be large. From (3.77), we see that we need to take $\Delta \gg f$. However, large Δ is not a sufficient condition — it is possible that the saddles in Ω are sufficiently close to i to make the saddle in T no longer large. This puts a condition on the twist $\Delta - \sum_i |J_i|$ of the operators. In particular, if m of the $\lfloor \frac{d}{2} \rfloor$ spins are large, meaning $|J_1|, \dots, |J_m| \gg \Delta - \sum_i |J_i|$, then

our universal entropy formula is only valid when

$$\Delta - \sum_i |J_i| \gg \left(f \prod_{i=1}^m |J_i| \right)^{\frac{1}{m+1}}. \quad (3.88)$$

For example, in CFT_3 , this is equivalent to the entropy formula only being valid in the regime

$$\Delta - |J| \gg \sqrt{f\Delta}. \quad (3.89)$$

(This can be seen easily by demanding the saddles in (3.69) are very small.) Operators outside of this window (for example operators along a Regge trajectory with Δ large but $\Delta - |J|$ growing slower than \sqrt{J}) will not obey our universal entropy formula.

In $d = 2$, the regime of validity is larger. In order to trust the saddle point analysis, it is only necessary to take $\Delta \rightarrow \infty$ with

$$\Delta - |J| \gg c \quad (3.90)$$

(or equivalently take $h, \bar{h} \gg c$).

- Non-perturbative corrections to the density of states

So far, we have discussed an infinite set of perturbative corrections in $1/T$ to $\log Z(T, \Omega_i)$, parametrized by an infinite set of terms in the thermal effective action. In this section we briefly consider nonperturbative corrections to $\log Z(T, \Omega_i)$, namely corrections that scale as $e^{-\#T}$.

In general we expect the first nonperturbative correction to be proportional to

$$e^{-2\pi m}, \quad (3.91)$$

where m is the mass of the lightest massive state in the dimensionally reduced theory. By dimensional analysis, $m \propto T$, so (3.91) is indeed a nonperturbative correction. The reason for (3.91) is the following. Consider the CFT on $S_\beta^1 \times S^{d-1}$ as a gapped theory on S^{d-1} . Corrections of the form (3.91) will be generated by world-line instantons associated with a massive particle moving along a great circle of S^{d-1} of length 2π . Similar world line instantons were studied in [39, 79, 99, 109, 110] in the context of the large-charge expansion.¹⁸

¹⁸We thank Yifan Wang for pointing out this interpretation and associated references.

We can also understand (3.91) from a Hamiltonian perspective. We can compute the partition function of the gapped theory on S^{d-1} by slicing the path integral on S^{d-2} spatial slices at various polar angles $\theta \in [0, \pi]$. These slices have varying radius $\sin \theta$, and therefore varying Hamiltonian $H(\theta)$. Overall, we time-evolve by Euclidean time π as we move from the south pole to the north pole of the S^{d-1} . This gives an expression for the partition function of the form

$$Z = \langle \psi_0 | \mathcal{T} \exp \left(- \int_0^\pi d\theta H(\theta) \right) | \psi_0 \rangle, \quad (3.92)$$

where $|\psi_0\rangle$ is the state in the S^{d-2} Hilbert space created by the path integral near the south pole, and \mathcal{T} denotes Euclidean time ordering. In general, the spectrum of $H(\tau)$ could be quite complicated. However, when β is small, most spatial slices are large compared to the mass gap, and we expect the low-lying spectrum of $H(\tau)$ to be close to the gapped spectrum in flat space \mathbb{R}^{d-2} . In particular, there is a contribution from a particle-antiparticle pair nucleated at the south pole, which propagate for Euclidean time π before annihilating at the north pole. This leads to 3.91.

In general, we expect similar corrections of the form $e^{-2\pi m_i}$ for each massive state in the gapped theory on \mathbb{R}^{d-2} . There will also be Lüscher corrections [159] that it would be interesting to study in more detail.

We can check the prediction (3.91) explicitly in free theories. In Appendix C, we write down the high-temperature expansions of the partition function for a d -dimensional free boson and free Dirac fermion respectively. In even dimensions, we write down the exact expression, including all non-perturbative corrections; in odd dimensions, the perturbative expansion is asymptotic rather than convergent, but we are still able to write down the first non-perturbative correction. In all cases, we show that the first non-perturbative correction at high temperature to the partition function take the form as predicted by (3.91).

3.4 Density of states: examples

In this section, we study partition functions of various CFTs to illustrate the general results of the previous sections. The examples we consider are the free scalar, the free scalar with a \mathbb{Z}_2 twist, the free fermion, and holographic CFTs where the entropy is well-approximated by that of a Kerr-AdS black hole. In these examples, we check the partition function against our general formula (3.51) and determine the unknown coefficients f , c_1 , and c_2 when the thermal effective action applies. Furthermore, in Appendix 3.9, we compare the predictions of the thermal effective

action to numerical bootstrap data for the 3D Ising model, obtaining an estimate for f .

Free scalar

Our first example is the free scalar in d dimensions. When compactified, this theory contains a gapless sector corresponding to a free scalar in one lower dimension. Therefore, it violates the central assumption of the thermal effective action, and the predictions of the thermal EFT should be violated in some way.

The partition function of this theory can be computed exactly. For a review, see Appendix C. Expanding the result at high temperature, we find for example

$$\log Z(T, \Omega_i) = \frac{1}{\prod_{i=1}^{\lfloor \frac{d}{2} \rfloor} (1 + \Omega_i^2)} \left(2\zeta(d)T^{d-1} - \frac{d-4-2\sum_{i=1}^{\lfloor \frac{d}{2} \rfloor} \Omega_i^2}{12} \zeta(d-2)T^{d-3} + O(T^{d-5}) \right). \quad (3.93)$$

Importantly, in even d , we find that the high temperature expansion contains a term proportional to T^0 , while in odd dimensions there is a term proportional to $\log T$. (When $d = 3$, the logarithm is visible in (3.93) via the pole in the ζ -function at 1.) Such terms are inconsistent with the derivative expansion of the thermal effective action (which contains powers of the form T^{d-2k-1} for integer k). They represent contributions from the gapless sector. We discuss these terms more explicitly in Appendix C.

Free scalar with a \mathbb{Z}_2 twist

To remove the gapless sector in the compactified free scalar, we can insert a \mathbb{Z}_2 twist on the S^1 , where we identify $\phi(\tau = 1) = -\phi(\tau = 0)$ as we go around the thermal circle. Computing the partition function with this twist inserted (this can be treated using methods in e.g. [80]), we find

$$\begin{aligned} \log Z(T, \Omega_i) = & \frac{1}{\prod_{i=1}^{\lfloor \frac{d}{2} \rfloor} (1 + \Omega_i^2)} \times \\ & \left(-2 \left(1 - \frac{1}{2^{d-1}} \right) \zeta(d)T^{d-1} + \left(1 - \frac{1}{2^{d-3}} \right) \frac{(d-4)-2\sum_{i=1}^{\lfloor \frac{d}{2} \rfloor} \Omega_i^2}{12} \zeta(d-2)T^{d-3} + O(T^{d-5}) \right). \end{aligned} \quad (3.94)$$

This result is now consistent with the thermal effective action (even though the compactification is no longer "thermal"). For example, when $d = 3$, the extra factor $(1 - 1/2^{d-3})$ cancels the pole in $\zeta(d-2)$, so there is no $\log T$ term. Matching with

(3.51), we get

$$\begin{aligned} f &= -\frac{2\zeta(d)}{\text{vol } S^{d-1}} \left(1 - \frac{1}{2^{d-1}}\right), \\ c_1 &= -\frac{(d-4)\zeta(d-2)}{12(d-1)(d-2)\text{vol } S^{d-1}} \left(1 - \frac{1}{2^{d-3}}\right), \\ c_2 &= \frac{d(2d-5)\zeta(d-2)}{48(d-1)(d-2)\text{vol } S^{d-1}} \left(1 - \frac{1}{2^{d-3}}\right), \end{aligned} \quad (3.95)$$

for a free scalar with a \mathbb{Z}_2 twist.

Note that $f < 0$ in (3.95). This is not a contradiction because the partition function computed in (3.94) is not a positive-definite sum of states (due to the insertion of the \mathbb{Z}_2 twist). In fact $f < 0$ implies a strong cancellation between \mathbb{Z}_2 -even and odd operators in the theory.

Free fermion

Next, let us consider a free Dirac fermion in d dimensions. We compactify the theory with thermal boundary conditions, where we do not insert $(-1)^F$. This leads to a massive $(d-1)$ -dimensional theory. (With the $(-1)^F$ operator inserted, there would be a gapless sector.)

We compute the partition function explicitly in Appendix C. The leading two terms in the free energy are given by

$$\begin{aligned} \log Z(T, \Omega_i) &= \frac{2^{\lfloor \frac{d}{2} \rfloor + 1}}{\prod_{i=1}^{\lfloor \frac{d}{2} \rfloor} (1 + \Omega_i^2)} \times \\ &\left[\left(1 - \frac{1}{2^{d-1}}\right) \zeta(d) T^{d-1} - \left(1 - \frac{1}{2^{d-3}}\right) \frac{(d-1) + \sum_{i=1}^{\lfloor \frac{d}{2} \rfloor} \Omega_i^2}{24} \zeta(d-2) T^{d-3} + O(T^{d-5}) \right]. \end{aligned} \quad (3.96)$$

Unlike in the free scalar case, the expression (3.96) has no $\log T$ terms or T^0 terms in even d , consistent with the thermal compactification being gapped. Matching with (3.51), we find

$$\begin{aligned} f &= \frac{2^{\lfloor \frac{d}{2} \rfloor + 1} \left(1 - \frac{1}{2^{d-1}}\right) \zeta(d)}{\text{vol } S^{d-1}}, \\ c_1 &= \frac{2^{\lfloor \frac{d}{2} \rfloor + 1} \left(1 - \frac{1}{2^{d-3}}\right) \zeta(d-2)}{24(d-2)\text{vol } S^{d-1}}, \\ c_2 &= -\frac{2^{\lfloor \frac{d}{2} \rfloor + 1} \left(1 - \frac{1}{2^{d-3}}\right) \zeta(d-2)}{96(d-2)\text{vol } S^{d-1}}, \end{aligned} \quad (3.97)$$

for the free fermion.

Holographic theories

Finally, let us consider CFTs dual to semiclassical Einstein gravity via AdS/CFT. We can estimate the partition functions of such theories by studying the thermodynamics of Kerr-AdS black holes (see e.g. [95]). By the holographic principle, a holographic CFT has the same partition function as its dual in AdS space. We get the following high-temperature partition function for a holographic CFT_d, $d \geq 3$:

$$\log Z = \frac{\text{vol } S^{d-1} (4\pi)^{d-1}}{4d^d G_N} \frac{\ell_{\text{AdS}}^{d-1} T^{d-1}}{\prod_{i=1}^{\lfloor d/2 \rfloor} (1 + \Omega_i^2)} \left(1 - \frac{d^2 \left((d-1) + \sum_{i=1}^{\lfloor d/2 \rfloor} \Omega_i^2 \right)}{16\pi^2 T^2} + \mathcal{O}\left(\frac{1}{T^4}\right) \right), \quad (3.98)$$

where ℓ_{AdS} is the characteristic length of the dual asymptotic AdS_{d+1} spacetime and G_N is the $d+1$ -dimensional Newton constant.

This is indeed consistent with the result (3.51) from the thermal effective action. Matching coefficients, we find¹⁹

$$\begin{aligned} f &= \frac{(4\pi)^{d-1} \ell_{\text{AdS}}^{d-1}}{4d^d G_N}, \\ c_1 &= \frac{(4\pi)^{d-3} \ell_{\text{AdS}}^{d-1}}{4(d-2)d^{d-2} G_N}, \\ c_2 &= -\frac{(4\pi)^{d-3} \ell_{\text{AdS}}^{d-1}}{32(d-2)d^{d-3} G_N}, \end{aligned} \quad (3.99)$$

for the thermal Wilson coefficients of a holographic CFT.

- Extended regime of validity for holographic theories

For holographic theories, the entropy of local operators with certain dimensions and spins can be approximated by the entropy of a black hole with the same quantum numbers, as long as the black hole is stable and has large area (in Planck units). In this section we examine where the entropy of Kerr black holes is trustworthy, and compare it to the range of validity of the EFT expansion in Section 3.3. We will find that for holographic theories, the universal formula for entropy has an extended regime of validity, compared to general CFTs. This is reminiscent of what happens

¹⁹The coefficients in (3.99) were also independently computed by Edgar Shaghoulian. We thank him for discussions related to these coefficients.

in two-dimensional CFTs, where the Cardy formula has an extended regime of validity for holographic theories [104].

When Kerr black holes in AdS spin too quickly, they suffer from a phenomenon called superradiant instability [43]. In the case of the Kerr-AdS black hole, it has an instability when any of the angular velocities Ω_i become larger than ℓ_{AdS}^{-1} . In particular, a stable Kerr-AdS black hole has a bound on quantity $E - \sum_i |J_i| \ell_{\text{AdS}}^{-1}$. For instance, in AdS_4 , the condition for stability is (see e.g. [133])

$$E - |J| \ell_{\text{AdS}}^{-1} > \sqrt{\frac{E \ell_{\text{AdS}}}{2G_N}}, \quad (3.100)$$

when the black hole has large mass and spin.²⁰ Translated to CFT data, the entropy for holographic theories is trustworthy when the twist obeys

$$\Delta - |J| \gtrsim \sqrt{f\Delta}, \quad (3.101)$$

where by \gtrsim we allow for an $O(1)$ constant on the RHS that we do not compute.²¹ A similar calculation shows that, for a holographic theory where m of the spins are taken to be large compared to the twist (i.e. $\Delta, |J_1|, \dots, |J_m| \gg \Delta - \sum_{i=1}^{\lfloor \frac{d}{2} \rfloor} |J_i|$), then the entropy is trustworthy when the twist obeys

$$\Delta - \sum_i |J_i| \gtrsim \left(f \prod_{i=1}^m |J_i| \right)^{\frac{1}{m+1}}. \quad (3.102)$$

We see that the functional form of the stability bound for Kerr-AdS black holes is very similar to the regime of validity (3.89) and (3.88) for the general entropy formula.

This is reminiscent of the extended regime of the Cardy formula for the case of CFT_2 : for theories holographically dual to large-radius gravity in AdS_3 , it was shown that there is a further extension of the validity of the Cardy formula in [104]. For holographic CFTs, the Cardy formula matches the Bekenstein-Hawking entropy of BTZ black holes, which only requires

$$\Delta - |J| \gtrsim c, \quad (3.103)$$

²⁰Meaning $EG_N \ell_{\text{AdS}}^{-1}, |J|G_N \ell_{\text{AdS}}^{-2} \gg 1$.

²¹The reason we allow this freedom is the possibility of the black holes being stable, but not yet dominating the canonical ensemble. This can occur for sufficiently light black holes, sometimes called "enigmatic black holes" [32, 104].

with $c \rightarrow \infty$ (rather than the usual $\Delta - |J| \gg c$ condition). In particular, it was shown that theories with a sufficiently sparse light spectrum (which is a necessary, but not sufficient condition for the theory to have a semiclassical Einstein gravity dual) have an extended Cardy regime of entropy. It would be interesting if one could prove a similar statement for higher dimensional CFTs.²²

3.5 A "genus-2" partition function

While the density of states of a CFT is encoded in the partition function on $S_\beta^1 \times S^{d-1}$, OPE coefficients are encoded in partition functions on other manifolds. In this work, we will be interested in "heavy-heavy-heavy" OPE coefficients c_{ijk} between operators with parametrically large scaling dimension. To study them, we can consider the partition function of the CFT on a manifold constructed by gluing a pair of three-punctured spheres along their punctures. In two dimensions, this produces a genus-2 Riemann surface. However, a similar construction works in higher dimensions. We will continue to refer to such a manifold as "genus-2" in higher dimensions, by analogy with the 2D case.

We pause to note that our final expression for "heavy-heavy-heavy" OPE coefficients is given at the end of Sec. 3.7, in Eqn (3.242). Readers only interested in the final result can skip to this part.

Conformal structures of a genus-2 manifold

In higher dimensions we can build a genus-2 manifold M_2 by taking two copies of the plane \mathbb{R}^d (more precisely its conformal compactification S^d), removing three balls from each plane, and gluing the boundaries of the balls with cylinders. In this construction, we can choose the positions and radii of the balls, as well as the lengths of the cylinders. We can additionally add angular twists by elements of $\text{SO}(d)$ as we move along each cylinder. This is a large number of parameters, but many of them are related by conformal symmetry.

In addition, if the CFT has a global symmetry Γ , we can introduce topological defects on M_2 , or equivalently a flat Γ -bundle over M_2 . Such flat bundles are parametrized by homomorphisms of the fundamental group of M_2 to Γ . For $d > 2$, \mathbb{R}^d with balls removed is simply connected, and the only homotopically non-trivial cycles on M_2 are those going through the cylinders between the two copies of \mathbb{R}^d . Therefore, the

²²Some works studying sparseness in higher- d CFT include [21, 116, 164]. In particular it would be interesting if the precise sparseness conditions in [164] implied the extended entropy formulas described in this section.

fundamental group is a free group with two generators, and flat Γ -bundles can be parametrized by decorating the cylinders by inserting topological defects transverse to these cycles. The situation is different for $d = 2$ since \mathbb{R}^2 with balls removed is already not simply connected, and there are additional generators of the fundamental group which go around the boundaries of the balls. Inserting topological defects transverse to these additional cycles on M_2 is equivalent to considering twisted sectors along the cylinders.

To understand the implications of conformal symmetry, it is helpful to ignore the Weyl anomaly and focus on the conformal structure of the manifold M_2 — i.e. properties of M_2 that are independent of the Weyl class of the metric. First, we can associate an (orientation-reversing) conformal group element to each cylinder as follows. Let x, x' be flat coordinates on the two copies of \mathbb{R}^d . A cylinder C that connects the two planes is Weyl-equivalent to an annulus in each plane. Using this Weyl-equivalence, each coordinate x and x' can be extended to cover C . Inside C , the coordinates x and x' are identified by an orientation-reversing conformal group element:

$$x = gx', \quad g \in G^- \quad (\text{inside } C). \quad (3.104)$$

Here, we denote the conformal group as $G = \text{SO}(d + 1, 1)$, and we write the orientation-reversing component of $O(d + 1, 1)$ as G^- . For example, if a cylinder of length β connects the unit spheres in each copy of the plane, then we have

$$g = e^{-\beta D} I, \quad (3.105)$$

where $I(x) = \frac{x}{x^2}$ is an inversion. More generally, suppose the cylinder is centered at $x = a$, has radius r and length βr , and includes an angular twist by $h \in \text{SO}(d)$. Then²³

$$g = e^{a \cdot P} e^{-(\beta - 2 \log r) D} h I e^{-a \cdot P}. \quad (3.106)$$

In the case of interest, we have three cylinders connecting two copies of the plane. This gives three group elements $(g_1, g_2, g_3) \in (G^-)^3$. However, the conformal structure of the resulting manifold is unchanged if we perform a conformal transformation $x \mapsto gx$ on the first plane or $x' \mapsto g'x'$ on the second. These conformal

²³The appearance of the quantity $\beta - 2 \log r$ reflects the fact that two planes glued by a cylinder with radius r and length βr is Weyl-equivalent to two planes glued by a cylinder with radius 1 and length $\beta - 2 \log r$. The Weyl transformation breaks the cylinder into three pieces of lengths $r \log r, r(\beta - 2 \log r), r \log r$, and flattens out the first and third piece into annuli.

transformations become gauge redundancies acting on the g_i :

$$(g_1, g_2, g_3) \sim (gg_1g'^{-1}, gg_2g'^{-1}, gg_3g'^{-1}). \quad (3.107)$$

Modding out by this gauge-redundancy, we obtain the moduli space of conformal structures as a double-quotient

$$\mathcal{M} = G \backslash (G^-)^3 / G, \quad (3.108)$$

where the left and right factors of G 's act on $(G^-)^3$ via (3.107). The action of the $G \times G$ gauge redundancies on $(G^-)^3$ is almost free, so the dimension of \mathcal{M} is

$$\dim \mathcal{M} = 3 \dim G^- - 2 \dim G = \dim G = \frac{(d+1)(d+2)}{2}. \quad (3.109)$$

For orientation, in 2D the parametrization of a genus-2 Riemann surface in terms of (g_1, g_2, g_3) is called a Whittaker parametrization. (The closely-related Schottky parametrization can be obtained by forming the combinations $\gamma_{ij} = g_i g_j^{-1}$, which satisfy $\gamma_{12}\gamma_{23}\gamma_{31} = 1$.) In 2D, the true moduli space of genus-2 surfaces is a quotient of \mathcal{M} by the mapping class group. The action of the mapping class group is unfortunately somewhat complicated in the Whittaker/Schottky parameterizations.

In higher dimensions, \mathcal{M} is again a covering space of the moduli space of conformal structures on M_2 . Topologically, M_2 is equivalent to a connected sum of two copies of $S^1 \times S^{d-1}$.²⁴

$$M_2 \cong (S^1 \times S^{d-1}) \# (S^1 \times S^{d-1}). \quad (3.110)$$

This can be seen by decomposing M_2 in the "dumbbell" channel where we slice Figure 3.3 down the middle into a left half and a right half. Each half is topologically a copy of $S^1 \times S^{d-1}$ with a ball removed, and the two halves are glued along an S^{d-1} . The mapping class group of this space was computed for $d = 3$ in [37]. This mapping class group will not play a further role in the present work. It will be interesting to explore its implications and other global aspects of higher-dimensional "higher-genus" surfaces in future work.

An important set of functions on \mathcal{M} are eigenvalues of the group elements $g_i^{-1}g_j \in \text{SO}(d+1, 1)$:

$$\text{eigenvalues}_{(d+2) \times (d+2)}(g_i^{-1}g_j) = \begin{cases} (e^{\pm\beta_{ij}}, e^{\pm i\vec{\theta}_{ij}}) & (\text{even } d), \\ (e^{\pm\beta_{ij}}, e^{\pm i\vec{\theta}_{ij}}, 1) & (\text{odd } d). \end{cases} \quad (3.111)$$

²⁴We thank Yifan Wang for pointing this out and directing us to reference [37].

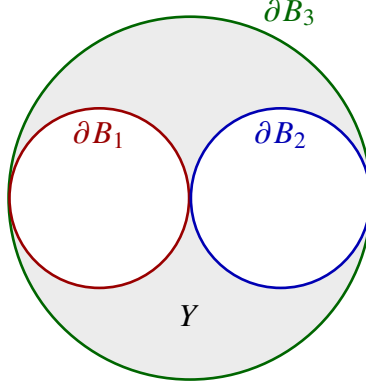


Figure 3.2: The space $Y = B_3 \setminus (B_1 \cup B_2)$. The boundary of Y has three S^{d-1} components given by $\partial B_1, \partial B_2, \partial B_3$ with radii 1, 1, 2, respectively. Note that in $d \geq 3$, Y has an $\text{SO}(d-1)$ rotational symmetry around the horizontal axis, and here we are depicting only a 2-dimensional slice.

These are indeed invariant under gauge-redundancies (3.107). We refer to the β_{ij} and $\vec{\theta}_{ij}$ as "relative" inverse temperatures and angles, for reasons that will become clear shortly. Note that there are $3 \lfloor \frac{d+2}{2} \rfloor$ relative temperatures/angles, which is not enough to parametrize the full moduli space when $d \geq 3$.

Choice of geometry

The partition function of a CFT on M_2 factors into a theory-independent part that depends on the precise metric and is determined by the Weyl anomaly, times a theory-dependent part that depends only on the conformal structure of M_2 . To get nontrivial information about the theory, it suffices to study only a single representative geometry for each conformal structure.

We will choose our geometry as follows. Let B_1 be the unit ball centered at $(-1, 0, \dots, 0)$, let B_2 be the unit ball centered at $(1, 0, \dots, 0)$, and let B_3 be the ball of radius 2 centered at the origin. All three balls are mutually tangent. From B_3 , we remove B_1 and B_2 . The resulting space $Y = B_3 \setminus (B_1 \cup B_2)$ has three S^{d-1} boundaries given by $\partial B_1, \partial B_2, \partial B_3$, see Figure 3.2. We now take a second copy of Y , which we call Y' , containing boundaries $\partial B'_1, \partial B'_2, \partial B'_3$. Finally, we glue each ∂B_i to $\partial B'_i$ with cylinders C_i whose ratios of length/radius are β_i , and we include angular twists $h_i \in \text{SO}(d)$ along each cylinder. See Figure 3.3 for an illustration.

This construction gives a particular choice of metric that is flat on Y, Y' and is the usual cylinder metric on the C_i . Note that the metric has curvature localized at the junctions between Y, Y' and the cylinders. However, it is everywhere conformally-flat because the plane, the cylinder, and a plane-cylinder junction are all conformally-

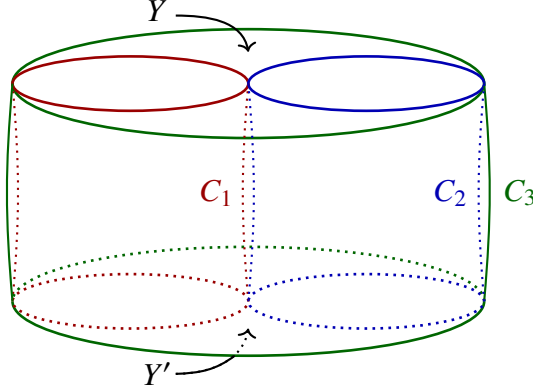


Figure 3.3: The manifold M_2 is obtained by taking two copies of Y and gluing corresponding boundary components with cylinders C_1, C_2, C_3 of inverse temperatures $\beta_1, \beta_2, \beta_3$ and angular twists h_1, h_2, h_3 , colored red, blue, and green, respectively. In the figure, we slightly bent the edges of the cylinders to help visualize them, but in the actual geometry the cylinders have constant radii. The figure also naively suggests that the lengths of the cylinders must be equal, but in reality they need not be related to each other.

flat. In terms of conformal structures, our geometry corresponds to

$$\begin{aligned} g_1 &= e^{-P^1} e^{-\beta_1 D} h_1 I e^{P^1}, \\ g_2 &= e^{P^1} e^{-\beta_2 D} h_2 I e^{-P^1}, \\ g_3 &= e^{D(2 \log 2 + \beta_3)} h_3 I, \end{aligned} \quad (3.112)$$

which gives a point in \mathcal{M} , parametrized by $\beta_1, \beta_2, \beta_3, h_1, h_2, h_3$.

A slight disadvantage of the parametrization (3.112) is that it is not permutation-symmetric among the three cylinders — C_3 is treated differently. However, an advantage is that it makes manifest an important $\text{SO}(d-1)$ symmetry that rotates all three balls around the x^1 axis, preserving their points of tangency.²⁵ We can act with an $\text{SO}(d-1)$ rotation on either Y or Y' , which means that the angular twists (h_1, h_2, h_3) are subject to a residual gauge redundancy

$$(h_1, h_2, h_3) \sim (k h_1 k'^{-1}, k h_2 k'^{-1}, k h_3 k'^{-1}), \quad k, k' \in \text{SO}(d-1). \quad (3.113)$$

Thus, overall, we can think of the parametrization (3.112) as a map

$$\text{SO}(d-1) \backslash (\text{SO}(1, 1) \times \text{SO}(d))^3 / \text{SO}(d-1) \rightarrow \mathcal{M}, \quad (3.114)$$

²⁵By contrast, we could restore manifest permutation symmetry by taking the balls to all have the same radius and be mutually tangent, but then the $\text{SO}(d-1)$ would act via a nontrivial conformal transformation.

where β_i parametrize the $\text{SO}(1, 1)$'s, the h_i parametrize the $\text{SO}(d)$'s, and the $\text{SO}(d-1)$'s act on the $\text{SO}(d)$'s via (3.113).

We claim that (3.112) is injective and covers an open subset of \mathcal{M} — in particular an open subset that contains the physical loci that will be important in what follows. These loci include the low temperature regime of large β_i , and a high temperature limit that will control the asymptotics of OPE coefficients. A first important check is that the two spaces in (3.114) have the same dimension. Indeed, they do, since

$$\begin{aligned} 3(1 + \dim \text{SO}(d)) - 2 \dim \text{SO}(d-1) &= 3 \left(1 + \frac{d(d-1)}{2}\right) - 2 \frac{(d-1)(d-2)}{2} \\ &= \frac{(d+1)(d+2)}{2}. \end{aligned} \tag{3.115}$$

In Section 3.7, we will show that the natural measure on \mathcal{M} is nonzero in the coordinates (3.112) at both low and high temperatures. This establishes that $\beta_1, \beta_2, \beta_3, h_1, h_2, h_3$ (modulo the gauge redundancy (3.113)) furnish good coordinates on \mathcal{M} for our purposes.

Consequently, it suffices to consider geometries of the form described above. These geometries contain all possible theory-dependent information about OPE coefficients of the CFT. In Appendix G, we show that there is a matching between quantum numbers specifying OPE coefficients and the dimension of the genus-2 moduli space $\dim \mathcal{M}$.

The partition function as a sum over states

The partition function on the above geometry is a weighted sum of squares of OPE coefficients. In this section, we derive this fact in detail, taking care with some of the subtleties of cutting and gluing in higher-dimensional CFTs.

Consider first the space $Y = B_3 \setminus (B_1 \cup B_2)$. This space has boundaries given by $\partial Y = \partial B_3 \sqcup -\partial B_1 \sqcup -\partial B_2$. Thus, the partition function $Z(Y)$ is an element of $\mathcal{H}_2 \otimes \mathcal{H}_1^* \otimes \mathcal{H}_1^*$, or equivalently a map $\mathcal{H}_1 \otimes \mathcal{H}_1 \rightarrow \mathcal{H}_2$, where \mathcal{H}_r is the Hilbert space on a sphere of radius r . A basis of states $|\mathcal{O}(x)\rangle_r$ in \mathcal{H}_r is given by the insertion of an operator $\mathcal{O}(x)$ inside a ball of radius r . The defining property of $Z(Y)$ is that its pairing with three basis elements is a conformal three-point function.

Let us state this more precisely. The Hermitian conjugate state to $|\mathcal{O}(x)\rangle_r \in \mathcal{H}_r$ can be obtained by inserting the following conjugate operator in a flat geometry outside

the ball of radius r :

$$[O^a(x)]^{\dagger_r} \equiv r^D [r^{-D} O^a(x)]^\dagger = \left(\frac{r}{|x|} \right)^{2\Delta} I^{-1}(\hat{x})_a{}^{\bar{a}} O_{\bar{a}}^\dagger \left(\frac{r^2 x}{x^2} \right). \quad (3.116)$$

Note that $[\dots]^\dagger = [\dots]^{\dagger_1}$ is the usual BPZ conjugation. The inversion tensor $I_{\bar{a}}{}^a$ is the solution to the conformal Ward identities for a two-point function of O^a and $O_{\bar{a}}^\dagger$:

$$\langle O_{\bar{a}}^\dagger(x) O^a(0) \rangle = \frac{I_{\bar{a}}{}^a(\hat{x})}{x^{2\Delta}}, \quad (3.117)$$

normalized so that $II^\dagger = 1$. With this notation, a projector onto the conformal multiplet of O inside \mathcal{H}_r can be written

$$|O|_r = |O^a(0)\rangle_r \langle O^a(0)[O^{a'}(0)]^{\dagger_r}\rangle^{-1} {}_r\langle O^{a'}(0)| + \text{descendants}, \quad (3.118)$$

where the inverse two-point function $\langle O^a(0)[O^{a'}(0)]^{\dagger_r}\rangle^{-1}$ should be understood as a matrix with indices a, a' . The indices a, a' are implicitly summed over in (3.118). The form of the sum over descendants is determined by the conformal algebra. A resolution of the identity on \mathcal{H}_r is given by summing over projectors $1 = \sum_O |O|_r$.

By composing $Z(Y)$ with resolutions of the identity on each of its three boundaries, we find an expression in terms of three-point functions:

$$\begin{aligned} Z(Y) &= \sum_{O_1, O_2, O_3} |O_3^\dagger|_2 Z(Y) (|O_1|_1 \otimes |O_2|_1) \\ &= \sum_{O_1, O_2, O_3} \langle O_1(-e) O_2(e) O_3(\infty e) \rangle \langle O_1(0)[O_1(0)]^\dagger \rangle^{-1} \langle O_2(0)[O_2(0)]^\dagger \rangle^{-1} \\ &\quad \times \langle O_3(\infty)[O_3(\infty)]^{\dagger_2} \rangle^{-1} |[O_3(\infty)]^{\dagger_2}\rangle_2 {}_1\langle O_1(0) | \otimes {}_1\langle O_2(0) |. \end{aligned} \quad (3.119)$$

For simplicity, we have omitted spin indices. This is a sum over states with coefficients given by a three-point function, where $e = (1, 0, \dots, 0)$ is a unit vector along the x^1 direction. Note that we define a primary operator at infinity *without* an inversion tensor:

$$O_3^c(\infty e) \equiv \lim_{L \rightarrow \infty} L^{2\Delta_3} O_3^c(L e). \quad (3.120)$$

To help restore symmetry among the three operators, we have chosen to insert the projector $|O_3^\dagger|$, as opposed to $|O_3|$ — this ensures that the three-point function contains $O_3(\infty)$ and not $O_3^\dagger(\infty)$.

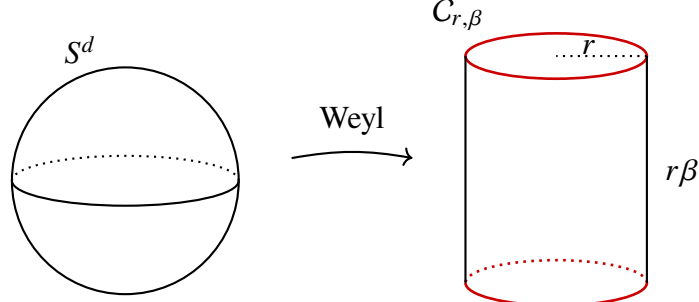


Figure 3.4: The sphere S^d is Weyl-equivalent to a "capped cylinder" $C_{r,\beta}$ with radius r and length $r\beta$. Each end cap is a ball (the interior of an S^{d-1}) of radius r . The "closed junctions" where the cylinder meets the end caps are highlighted in red.

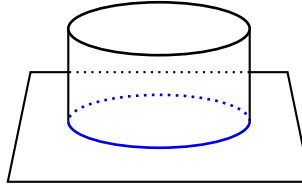


Figure 3.5: An "open junction," where a cylinder meets the complement of a ball in a flat plane. The junction is highlighted in blue.

The partition function of each cylinder C_i is simply $e^{-\beta_i(D+\varepsilon_0)} h_i$, where ε_0 is the Casimir energy (3.42), and $h_i \in \text{SO}(d)$ is the angular twist along the cylinder. One subtle ingredient is that we must also associate nontrivial "gluing" factors to junctions between cylinders and flat planes. To derive these gluing factors, let us start with the partition function on S^d (with unit radius). This is Weyl-equivalent to a cylinder of radius r and length $r\beta$, capped off by flat balls; see Figure 3.4. Let the capped cylinder be $C_{r,\beta}$, and denote the Weyl factor going from S^d to $C_{r,\beta}$ by $e^{2\omega_{r,\beta}}$. The Weyl anomaly implies

$$Z(C_{r,\beta}) = e^{-S_{\text{anom}}[g, \omega_{r,\beta}]} Z(S^d). \quad (3.121)$$

At the same time, $Z(C_{r,\beta})$ can be computed by cutting and gluing. The end caps are simply identity operators in radial quantization, $|1\rangle_r$. The cylinder contributes $e^{-\varepsilon_0\beta}$, where ε_0 is the Casimir energy on S^{d-1} . Let us define $Z_{\text{glue}}(r)$ as the factor associated to a junction between a cylinder and a flat end-cap, which we call a "closed junction". We find

$$Z(C_{r,\beta}) = |Z_{\text{glue}}(r)|^2 e^{-\varepsilon_0\beta} \implies |Z_{\text{glue}}(r)| = e^{\frac{1}{2}\varepsilon_0\beta} e^{-\frac{1}{2}S_{\text{anom}}[g, \omega_{r,\beta}]} Z(S^d)^{\frac{1}{2}}. \quad (3.122)$$

We calculate these gluing factors in various dimensions in Appendix F. For example, we find²⁶

$$|Z_{\text{glue}}(r)| = Z(S^d)^{\frac{1}{2}} \times \begin{cases} 1 & d \text{ odd}, \\ e^{c/12}(r/2)^{c/6} & d = 2, \\ e^{-7a/6}(r/2)^{-2a} & d = 4, \\ e^{37a_6/10}(r/2)^{6a_6} & d = 6. \end{cases} \quad (3.123)$$

Our geometry also contains four "open junctions" with the opposite curvature, where a cylinder joins a flat region that locally looks like the complement of a ball; see Figure 3.5. The gluing factor associated to an open junction is the inverse $Z_{\text{glue}}(r)^{-1}$ of the one associated to a closed junction. The reason is that we can perform an infinitesimal Weyl transformation on a plane to create a closed junction infinitesimally-close to an open junction. The Weyl anomaly is infinitesimal, so the gluing factors must multiply to 1.

Putting everything together, the partition function on our genus-2 manifold is

$$Z(M_2) = \frac{|Z_{\text{glue}}(2)|^2}{|Z_{\text{glue}}(1)|^4} \text{Tr}(Z(Y)^\dagger e^{-\beta_3(D+\varepsilon_0)} h_3^{-1} Z(Y) (e^{-\beta_1(D+\varepsilon_0)} h_1 \otimes e^{-\beta_2(D+\varepsilon_0)} h_2)). \quad (3.124)$$

Each group element $e^{-\beta_i D} h_i$ acts on the Hilbert space corresponding to the boundary component ∂B_i . Inserting our expression (3.119) for $Z(Y)$, we obtain the partition function as a sum over a triplet of primary operators

$$\begin{aligned} Z(M_2) &= \frac{|Z_{\text{glue}}(2)|^2}{|Z_{\text{glue}}(1)|^4} e^{-\varepsilon_0(\beta_1+\beta_2+\beta_3)} \\ &\times \sum_{O_1, O_2, O_3} \left(e^{-\beta_1\Delta_1 - \beta_2\Delta_2 - \beta_3\Delta_3} \right. \\ &\quad \langle O_1^{a'}(-e) O_2^{b'}(e) O_3^{c'}(\infty e) \rangle^* \langle h_1 \cdot O_1^a(-e) h_2 \cdot O_2^b(e) h_3 \cdot O_3^c(\infty e) \rangle \\ &\quad \times \langle O_1^a(0) [O_1^{a'}(0)]^\dagger \rangle^{-1} \langle O_2^b(0) [O_2^{b'}(0)]^\dagger \rangle^{-1} \langle O_3^c(\infty) [O_3^{c'}(\infty)]^\dagger \rangle^{-1} \\ &\quad \left. + \text{descendants} \right). \end{aligned} \quad (3.125)$$

Here, $h \cdot O$ denotes the action of a rotation $h \in \text{SO}(d)$ on a local operator:

$$h \cdot O^a = h O^a h^{-1} = \lambda(h^{-1})^a{}_b O^b, \quad (3.126)$$

where λ is the $\text{SO}(d)$ representation of O .

²⁶In $d = 4$, we write a_4 as a .

Let us choose the O_i to be an orthonormal basis of primaries with respect to the BPZ inner product. Using (3.116) and (3.120), we find

$$\langle O_3^c(\infty) [O_3^{c'}(\infty)]^{\dagger_2} \rangle = 2^{2\Delta_3} \delta_{c'}^c, \quad (3.127)$$

while the other two-point functions in (3.125), which involve standard BPZ conjugates $[\dots]^{\dagger}$, are identity matrices.

Let us furthermore expand the three-point functions in a basis of conformally-invariant three-point structures:

$$\begin{aligned} \langle O_1^a(-e) O_2^b(e) O_3^c(\infty e) \rangle &= \frac{1}{2^{\Delta_1+\Delta_2-\Delta_3}} \langle O_1^a(0) O_2^b(e) O_3^c(\infty e) \rangle \\ &= \frac{1}{2^{\Delta_1+\Delta_2-\Delta_3}} c_{123}^s V^{s;abc}(0, e, \infty). \end{aligned} \quad (3.128)$$

Here, s is a structure label, which runs over a finite-dimensional space of solutions V^s to the 3-point conformal Ward identities. Meanwhile, a, b, c are spin indices in the $SO(d)$ representations associated to the three operators. Each three-point structure comes with an associated OPE coefficient c_{123}^s , and a sum over s is implicit. We will discuss the space of three-point structures in more detail in Section 3.6.

Plugging everything in, we find an expression for the "genus-2" partition function as a sum over conformal blocks

$$Z(M_2) = \frac{|Z_{\text{glue}}(2)|^2}{|Z_{\text{glue}}(1)|^4} e^{-\varepsilon_0(\beta_1+\beta_2+\beta_3)} \sum_{O_1 O_2 O_3} (c_{123}^{s'})^* c_{123}^s B_{123}^{s's}, \quad (3.129)$$

where we have introduced the "genus-2" block $B_{123}^{s's}$

$$\begin{aligned} B_{123}^{s's}(\beta_i, h_i) &= 2^{-2\Delta_1-2\Delta_2} e^{-\beta_1\Delta_1-\beta_2\Delta_2-\beta_3\Delta_3} (V^{s';abc}(0, e, \infty))^* (h_1 h_2 h_3 \cdot V^s)^{abc}(0, e, \infty) \\ &+ \text{descendants.} \end{aligned} \quad (3.130)$$

The first term in (3.130) comes from primary states, and dominates in the "low temperature" limit $\beta_1, \beta_2, \beta_3 \gg 1$. The descendent terms involve three-point functions of descendant operators, contracted using the inverse of the Gram matrix. Such terms are determined by the conformal algebra.

The block $B_{123}^{s's}$ is naturally a function on the moduli space \mathcal{M} of conformal structures, and doesn't depend on the Weyl class of the metric. This fact is already hinted at in (3.130). Note that the factor $2^{-2\Delta_1-2\Delta_2}$ seems to violate permutation symmetry among the three operators. However, this is an artifact of our asymmetric conformal frame. We can restore manifest permutation symmetry by rewriting the block in

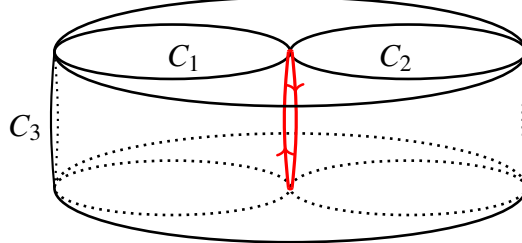


Figure 3.6: The thermal circle near the hot spot at the origin, highlighted in red. Starting from the top, we move along cylinder C_2 to the top, and then back along cylinder C_1 to the top.

terms of the "relative" temperatures β_{ij} , defined in (3.111), which are permutation-symmetric functions on \mathcal{M} . At low temperatures, we find

$$2^{-2\Delta_1-2\Delta_2} e^{-\beta_1\Delta_1-\beta_2\Delta_2-\beta_3\Delta_3} = e^{-\frac{\beta_{12}+\beta_{31}-\beta_{23}}{2}\Delta_1-\frac{\beta_{12}+\beta_{23}-\beta_{31}}{2}\Delta_2-\frac{\beta_{31}+\beta_{23}-\beta_{12}}{2}\Delta_3} + \dots, \quad (3.131)$$

which is manifestly symmetric under permuting 1, 2, 3. This is a nontrivial check on 3.130.

In Appendix G, we point out that the number of unbounded quantum numbers needed to specify the block $B_{123}^{s's}$ matches the dimension of the moduli space \mathcal{M} . This is analogous to the fact that the number of unbounded quantum numbers needed to specify a four-point conformal block (two: Δ and J) matches the number of cross-ratios for a four-point function (two: z and \bar{z}).

Hot spots and the thermodynamic limit

Because the geometry described in Section 3.5 is not a circle fibration, it is not immediately obvious how to compute the partition function using the thermal effective action. To make progress, we adopt the following assumption

Assumption. *The thermal effective action describes the contribution to the partition function from any region where the geometry locally looks like a circle fibration with a large local temperature.*

We call such a region a "hot spot."

For example, consider the origin in one of the copies of \mathbb{R}^d , where the balls B_1 and B_2 are tangent. Starting at the origin, there is a circular path of length $\beta_1 + \beta_2$ that runs along one cylinder C_2 , and then back along the other C_1 ; see Figure 3.6. In the limit where β_1, β_2 are both small, this circular path shrinks and we have a hot spot.

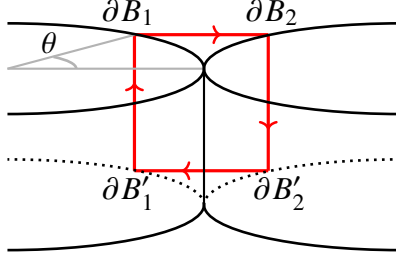


Figure 3.7: An approximation to the thermal circle, at an angle θ away from the origin. Starting at the top left, we move horizontally from ∂B_1 to ∂B_2 . Then we move down along C_2 to $\partial B'_2$. Then horizontally to the left to $\partial B'_1$, then up along C_1 to the starting point. The path has approximate length $\beta_1 + \beta_2 + 2\theta^2$.

To build some intuition, let us compute the leading contribution to the thermal effective action near this hot spot. The local temperature is highest at the origin, and decays away from it. To determine the local temperature precisely, we should find a (locally defined) conformal Killing vector field that moves around the hot spot's thermal circle. At leading order near the origin, we can guess what it looks like without too much calculation. Consider a path that starts at the point $(-1 + \cos \theta, \sin \theta, 0, \dots)$ on ∂B_1 . Move horizontally to the point $(1 - \cos \theta, \sin \theta, 0, \dots, 0)$ on ∂B_2 , through cylinder 2 to $\partial B'_2$, horizontally from $\partial B'_2$ to $\partial B'_1$, and back through cylinder 1 to the initial point on ∂B_1 , see Figure 3.7. This path has length

$$\beta_1 + \beta_2 + 4(1 - \cos \theta) \approx \beta_1 + \beta_2 + 2\theta^2 \quad (\theta \ll 1). \quad (3.132)$$

When θ is small, we expect this path to be close to the orbit of a local conformal Killing vector. Thus, the local temperature is approximately

$$\beta(\theta) \approx \beta_1 + \beta_2 + 2\theta^2. \quad (3.133)$$

The leading contribution to the thermal effective action near this hot spot is thus

$$-S_{\text{hot}}(\beta_1, \beta_2) \sim f \text{vol } S^{d-2} \int d\theta \frac{\sin^{d-2} \theta}{(\beta_1 + \beta_2 + 2\theta^2)^{d-1}}. \quad (3.134)$$

Here, $\text{vol } S^{d-2} \sin^{d-2} \theta$ comes from an integral over azimuthal angles. When $\beta_1 + \beta_2$ is small, the integral will be dominated by small $\theta \sim \sqrt{\beta_1 + \beta_2}$. To compute it, we can approximate $\sin^{d-2} \theta \approx \theta^{d-2}$ and extend the θ -integral from 0 to ∞ :

$$-S_{\text{hot}}(\beta_1, \beta_2) \sim f \text{vol } S^{d-2} \int_0^\infty \frac{d\theta \theta^{d-2}}{(\beta_1 + \beta_2 + 2\theta^2)^{d-1}} = \frac{f \text{vol } S^{d-1}}{(8(\beta_1 + \beta_2))^{\frac{d-1}{2}}}. \quad (3.135)$$

Note that the integral is dominated near the hot spot, i.e. in the neighborhood $\theta \sim \sqrt{\beta_1 + \beta_2}$. This justifies our use of the thermal effective action everywhere inside the integrand. Furthermore, when $\beta_1 + \beta_2$ is small, we find a large negative action from the hot spot, which translates into a large multiplicative contribution to the partition function $Z \sim e^{-S}$.

A more precise formula for the action of a hot spot

The fact that the integral (3.135) is dominated near the hot spot suggests a more precise and illuminating way to derive it. Let us assume that the action of a hot spot doesn't depend on the geometry far outside the neighborhood $\theta \sim \sqrt{\beta_1 + \beta_2}$. Thus, to compute it, it suffices to consider a "genus-1" version of the geometry discussed in Section 3.5, where we have only two balls B_1 and B_2 .

We claim that this "genus-1" geometry is Weyl equivalent to $S^1_{\beta_{12}} \times S^{d-1}$ with a special inverse temperature β_{12} that depends on β_1 and β_2 . The Weyl transformation that implements this equivalence essentially spreads out the hot-spot over the entire S^{d-1} , resulting in a uniform inverse temperature β_{12} . The result is

$$-S_{\text{hot}}(\beta_1, \beta_2) \sim \log Z_{S^1 \times S^{d-1}}(\beta_{12}) + \text{Weyl terms}, \quad (3.136)$$

where "Weyl terms" are possible contributions from the Weyl anomaly, and " \sim " indicates that both sides have the same singular parts as $\beta_1, \beta_2 \rightarrow 0$.

Now, β_{12} is determined by the conformal structure of our "genus-1" manifold, so we can read it off from the gluing group elements g_1 and g_2 associated to the two cylinders, given in (3.112). Gluing two copies of the plane with g_1 and g_2 is equivalent to gluing a single copy of the plane to itself with $g_1^{-1}g_2$. To read off β_{12} , we must simply diagonalize $g_1^{-1}g_2$:

$$g_1^{-1}g_2 = U e^{-\beta_{12}D + i\vec{\theta}_{12} \cdot \vec{M}} U^{-1}, \quad U \in \text{SO}(d+1, 1). \quad (3.137)$$

In other words, β_{12} is precisely the "relative" inverse temperature defined in (3.111).

There is a particularly nice expression for β_{12} when the angular fugacities are turned off. In this case, the group elements g_1, g_2 are built from conformal generators P^1, D, K^1 , that generate a $\text{PSL}(2, \mathbb{R})$ subgroup of the conformal group. Thus, we can obtain β_{12} by computing $g_1^{-1}g_2$ inside $\text{SL}(2, \mathbb{R})$ and comparing the trace of both sides of (3.137) as 2×2 matrices. We should compare them up to a sign, since the

1d conformal group $\text{PSL}(2, \mathbb{R})$ is a quotient of $\text{SL}(2, \mathbb{R})$ modulo ± 1 . This gives

$$\pm \text{Tr} \begin{pmatrix} e^{-\beta_{12}/2} & 0 \\ 0 & e^{\beta_{12}/2} \end{pmatrix} = \text{Tr} \begin{pmatrix} e^{\frac{\beta_1-\beta_2}{2}} (1 - 2e^{\beta_2}) & e^{\frac{\beta_1-\beta_2}{2}} + e^{\frac{\beta_2-\beta_1}{2}} - 2e^{\frac{\beta_1+\beta_2}{2}} \\ -2e^{\frac{\beta_1+\beta_2}{2}} & e^{\frac{\beta_2-\beta_1}{2}} (1 - 2e^{\beta_1}) \end{pmatrix}. \quad (3.138)$$

To find a solution, we must choose the $-$ sign, which gives

$$\beta_{12} = 2 \cosh^{-1} \left(2e^{\frac{\beta_1+\beta_2}{2}} - \cosh \left(\frac{\beta_1 - \beta_2}{2} \right) \right). \quad (3.139)$$

This is the inverse temperature at which we should evaluate (3.136).

In the limit where β_1, β_2 become small, the relative inverse temperature β_{12} has the expansion

$$\beta_{12} \sim \sqrt{8(\beta_1 + \beta_2)} - \frac{\beta_1^2 - 10\beta_1\beta_2 + \beta_2^2}{12\sqrt{2}\sqrt{\beta_1 + \beta_2}} + O(\beta_i^{5/2}) \quad (\beta_1, \beta_2 \ll 1). \quad (3.140)$$

Consequently, the leading contribution to the thermal effective action (3.54) is

$$-\log Z_{S^1 \times S^{d-1}}(\beta_{12}) \sim \frac{f \text{vol } S^{d-1}}{(8(\beta_1 + \beta_2))^{\frac{d-1}{2}}} + O(\beta_i^{-\frac{d-3}{2}}), \quad (\beta_1, \beta_2 \ll 1), \quad (3.141)$$

in perfect agreement with (3.135)! We have recovered our earlier result for the leading action of a hot spot. However, an advantage of this more abstract derivation is that we expect (3.136) and (3.139) to encompass all singular terms in the small β_1, β_2 limit.

This derivation is also straightforward to generalize to the case with angular fugacities. Let us think of the $S^1 \times S^{d-1}$ partition function as a class function $Z_{S^1 \times S^{d-1}}(g)$ of a conformal group element g . The old notation $Z_{S^1 \times S^{d-1}}(\beta, \vec{\theta})$ is obtained by setting $g = e^{-\beta D + \vec{\theta} \cdot \vec{M}}$. Then the above argument implies that the singular part of the action of a hot spot associated to two group elements g_1, g_2 is

$$-S_{\text{hot},12} \sim \log Z_{S^1 \times S^{d-1}}(g_1^{-1}g_2) + \text{Weyl terms}. \quad (3.142)$$

Let us comment on the Weyl anomaly terms in (3.142). In the genus-1 case, one can check that contributions from the Weyl anomaly to (3.142) vanish in the limit $\beta_1, \beta_2 \rightarrow 0$. In particular, they do not contribute to the singular part of the partition function in the high temperature limit. In what follows, we will assume that the same is true at higher genus, so that analogous Weyl terms can be ignored for our purposes. It would be nice to make these contributions more precise in an example theory.

The hot spot action for the genus-2 case

Let us finally apply this result to our "genus-2" partition function. We conjecture that the singular part of the log of the partition function as $\beta_1, \beta_2, \beta_3 \rightarrow 0$ is given by a sum of hot spot actions for each pair of tangent balls. Combined with (3.142), this implies

$$\begin{aligned} \log Z(M_2) &\sim -S_{\text{hot},12} - S_{\text{hot},23} - S_{\text{hot},31} \\ &\sim \log Z_{S^1 \times S^{d-1}}(g_1^{-1}g_2) + \log Z_{S^1 \times S^{d-1}}(g_2^{-1}g_3) + \log Z_{S^1 \times S^{d-1}}(g_3^{-1}g_1). \end{aligned} \quad (3.143)$$

Another way to state the conjecture is as follows. Consider the ratio

$$R(\beta_i) = \frac{Z(M_2)}{Z_{S^1 \times S^{d-1}}(g_1^{-1}g_2)Z_{S^1 \times S^{d-1}}(g_2^{-1}g_3)Z_{S^1 \times S^{d-1}}(g_3^{-1}g_1)}. \quad (3.144)$$

We conjecture that $R(\beta_i)$ has a finite limit as $\beta_i \rightarrow 0$:

$$R = \lim_{\beta_i \rightarrow 0} R(\beta_i) < \infty. \quad (3.145)$$

Intuitively, we imagine that dividing by the hot-spot partition function $Z_{S^1 \times S^{d-1}}(g_i^{-1}g_j)$ allows us to define a kind of renormalized "hot-spot operator" in the limit $\beta_i \rightarrow 0$ — a CFT operator that lives at a location where a circle shrinks to zero size. The quantity R is then a correlator of three such hot-spot operators. It would be very interesting to make this statement more precise and compute R in some example theories.

In this work, we will mostly be concerned with the leading singularity of the partition function that follows from (3.143). Using (3.54), this is

$$Z(M_2) \sim \exp \left(\frac{f \text{vol } S^{d-1}}{\beta_{12}^{d-1} \prod_a (1 + \Omega_{12,a}^2)} + \frac{f \text{vol } S^{d-1}}{\beta_{23}^{d-1} \prod_a (1 + \Omega_{23,a}^2)} + \frac{f \text{vol } S^{d-1}}{\beta_{31}^{d-1} \prod_a (1 + \Omega_{31,a}^2)} \right), \quad (3.146)$$

where the relative angular velocities are given by $\Omega_{ij,a} = \beta_{ij} \theta_{ij,a}$. We define the "high temperature" regime of the genus-2 partition function as $\beta_{ij} \rightarrow 0$, with $\vec{\Omega}_{ij}$ held fixed. This is the physical regime where the thermal effective action can be applied to each hot spot. Here, " \sim " means that the logs of both sides agree, up to subleading terms as $\beta_{ij} \rightarrow 0$.

If the CFT has a global symmetry Γ , we can decorate each cylinder by a topological defect associated to a group element γ_i ($i = 1, 2, 3$). If we do so, the coefficient

f in (3.146) for the (i, j) hot spot becomes a function of the conjugacy class of $\gamma_i \gamma_j^{-1} \in \Gamma$. Thus, in general, we can have a different f for each hot spot.

Note that the angular parameters $\vec{\theta}_{ij}$ scale to zero at high temperature. In this work, we will be particularly interested in a limit of low spin, where the $\vec{\Omega}_{ij}$ will scale to zero as well at an appropriate saddle point (so that the $\vec{\theta}_{ij}$ are parametrically smaller than the β_{ij}). Let us further expand the partition function in this regime. It will be convenient to parametrize the rotations h_i as a product of a rotation away from the x^1 axis, times an $\text{SO}(d-1)$ rotation:

$$h_i = \exp\left(\sum_{b=2}^d i\alpha_{i,b} M_{1b}\right) \exp\left(\sum_{2 \leq a < b \leq d} i\Phi_{i,ab} M_{ab}\right), \quad (3.147)$$

Here, $\vec{\alpha}_i = (\alpha_{i,2}, \dots, \alpha_{i,d})$ transforms like a vector under $\text{SO}(d-1)$, while the $\text{SO}(d-1)$ parameters $\vec{\Phi}_i = (\Phi_{i,23}, \dots, \Phi_{i,d-1,d})$ transform like an adjoint under $\text{SO}(d-1)$.

Recall that the h_i are subject to the gauge-redundancy (3.113). The right action of $\text{SO}(d-1)$ simultaneously shifts the $\vec{\Phi}_i$ (to leading order). Thus, the partition function must be translation-invariant in the $\vec{\Phi}_i$. Under the left action by $\text{SO}(d-1)$, the $\vec{\alpha}_i$ and $\vec{\Phi}_i$ transform linearly as $\text{SO}(d-1)$ vectors and adjoints, respectively. So the partition function must also be invariant under $\text{SO}(d-1)$ rotations of these variables.

Indeed, expanding (3.146) in small angles, we find

$$\begin{aligned} \frac{1}{\beta_{12}^{d-1} \prod_{a=1}^n (1 + \Omega_{12,a}^2)} &= \frac{1}{\beta_{12,0}^{d-1}} \left(1 - \frac{(\vec{\Phi}_1 - \vec{\Phi}_2)^2}{\beta_{12,0}^2} - 8(d+1) \frac{(\vec{\alpha}_1 + \vec{\alpha}_2)^2}{\beta_{12,0}^4} + \dots \right), \\ \frac{1}{\beta_{23}^{d-1} \prod_{a=1}^n (1 + \Omega_{23,a}^2)} &= \frac{1}{\beta_{23,0}^{d-1}} \left(1 - \frac{(\vec{\Phi}_2 - \vec{\Phi}_3)^2}{\beta_{23,0}^2} - 8(d+1) \frac{(\frac{1}{4}\vec{\alpha}_2 - \frac{1}{2}\vec{\alpha}_3)^2}{\beta_{23,0}^4} + \dots \right), \\ \frac{1}{\beta_{31}^{d-1} \prod_{a=1}^n (1 + \Omega_{31,a}^2)} &= \frac{1}{\beta_{31,0}^{d-1}} \left(1 - \frac{(\vec{\Phi}_3 - \vec{\Phi}_1)^2}{\beta_{31,0}^2} - 8(d+1) \frac{(\frac{1}{4}\vec{\alpha}_1 - \frac{1}{2}\vec{\alpha}_3)^2}{\beta_{31,0}^4} + \dots \right). \end{aligned} \quad (3.148)$$

This formula is valid when $\vec{\alpha}/\beta \ll 1$, and $\vec{\Phi}/\beta^{1/2} \ll 1$, and $\beta \ll 1$. Here, $\beta_{ij,0}$ denote the relative temperatures *when the angles are set to zero*. They are given by

$$\begin{aligned} \beta_{12,0} &= \sqrt{8(\beta_1 + \beta_2)} + \dots, \\ \beta_{23,0} &= \sqrt{8(\frac{1}{4}\beta_2 + \frac{1}{2}\beta_3)} + \dots, \\ \beta_{31,0} &= \sqrt{8(\frac{1}{4}\beta_1 + \frac{1}{2}\beta_3)} + \dots. \end{aligned} \quad (3.149)$$

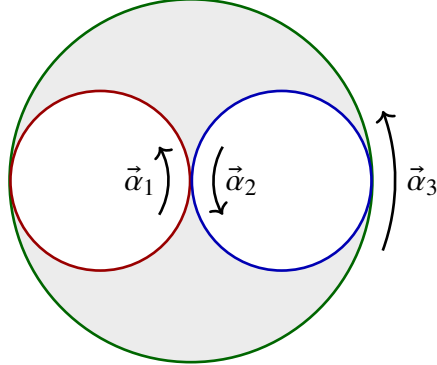


Figure 3.8: The partition function (3.148) penalizes rotations $\vec{\alpha}_i$ in such a way that the spheres behave like three interlocked gears. No matter what signs we choose for the $\vec{\alpha}_i$, there is no way to rotate the gears, since two of them will always be counter-rotating at their points of contact.

Let us understand some physical implications of (3.148). Terms like $(\vec{\alpha}_1 + \vec{\alpha}_2)^2$ come from rotating the spheres so that they rub against each other (Figure 3.8). The thermal effective action penalizes such rotations — the spheres behave like gears that are interlocked. It follows that there is no zero mode associated with moving the $\vec{\alpha}_i$'s: three mutually interlocked circular gears cannot be rotated. Meanwhile, terms like $(\vec{\Phi}_i - \vec{\Phi}_j)^2$ represent the effect of twisting the spheres by different amounts around their point of tangency. Such twists are also penalized by the effective action, but by a smaller power of $\beta_{ij,0}^2$. To summarize, the only zero mode in the angular parameters is associated to the gauge symmetry of right multiplication by $\text{SO}(d-1)$.

3.6 Genus-2 global conformal blocks

To determine the asymptotics of CFT OPE coefficients, we must invert the conformal block expansion (3.129) of the genus-2 partition function $Z(M_2)$. In particular, we will need the large- Δ limit of the genus-2 conformal blocks $B_{123}^{s's}$ in the high-temperature regime discussed in Section 3.5.

Our strategy will be to write an integral representation for the block using the "shadow formalism." In the large- Δ regime, the integral can be evaluated by saddle point, yielding simple closed-form expressions in the regimes of interest.

Review: shadow integrals for four-point blocks

Let us first review this strategy in the more familiar case of conformal blocks for four-point functions of local operators on \mathbb{R}^d [78, 89, 130, 193]. We will follow the notation and conventions of [130].

The central objects in the shadow formalism are principal series representations and their matrix elements. Let $\pi = (\Delta, \lambda)$ denote a conformal representation, where λ is a representation of $\text{SO}(d)$. The principal series corresponds to (unphysical) complex dimensions of the form $\Delta = \frac{d}{2} + is$, where $s \in \mathbb{R}$. States in a principal series representation are given by functions $f^a(x)$ that transform like conformal primaries with dimension Δ and rotation representation λ . Here, a is an index for λ . Such states admit a Hermitian inner product

$$(g|f) \equiv \int d^d x (g^a(x))^* f^a(x), \quad (3.150)$$

where the index a is summed over. Note that $(g^a(x))^*$ has scaling dimension $\frac{d}{2} - is = d - \left(\frac{d}{2} + is\right)$, so the integrand (including the measure $d^d x$) has scaling dimension 0. Furthermore, it transforms in the dual rotation representation λ^* , so the integrand is rotation-invariant. It follows that the pairing $(g|f)$ is conformally-invariant.

The principal series representation $\pi = (\frac{d}{2} + is, \lambda)$ is isomorphic to the "shadow" representation $\tilde{\pi} = (\frac{d}{2} - is, \lambda^R)$, where λ^R denotes the reflection of λ . This isomorphism is implemented by the shadow transform:

$$\mathbf{S}[f](x) = \int d^d y \langle \tilde{O}(x) \tilde{O}^\dagger(y) \rangle f(y), \quad (3.151)$$

where $\langle \tilde{O}(x) \tilde{O}^\dagger(y) \rangle$ denotes the unique (up to scale) conformal two-point structure between operators in the representations $\tilde{\pi}$ and $\tilde{\pi}^\dagger \equiv (\frac{d}{2} - is, \lambda^*)$.

Conformal three-point functions can be thought of as Clebsch-Gordon coefficients for a tensor product of principal series representations. Such three-point functions carry a structure label s that corresponds to different solutions of the conformal Ward identities:

$$V^{s;abc}(x_1, x_2, x_3) = \langle O_1^a(x_1) O_2^b(x_2) O_3^c(x_3) \rangle^{(s)}. \quad (3.152)$$

Here, $\langle \dots \rangle^{(s)}$ denotes a solution to the conformal Ward identities — not a physical three-point function. (In particular, it does not include an OPE coefficient.) The space of three-point structures is given by $(\lambda_1 \otimes \lambda_2 \otimes \lambda_3)^{\text{SO}(d-1)}$, where $\text{SO}(d-1)$ indicates the $\text{SO}(d-1)$ -invariant subspace [142]. We sometimes write V^s for a three-point structure, and we sometimes use the notation on the right-hand side of 3.152.

With these ingredients, we are ready to build conformal blocks. Four-point blocks are eigenfunctions of the conformal Casimir acting simultaneously on points 1 and

2, obeying certain boundary conditions. Using the inner product on principal series representations, we can instead easily build an eigenfunction called a "conformal partial wave" from two three-point structures:

$$\Psi_{\pi}^{s's}(x_1, \dots, x_4) = \int d^d x \langle O_3(x_3) O_4(x_4) \tilde{O}^\dagger(x) \rangle^{(s')} \langle O_1(x_1) O_2(x_2) O(x) \rangle^{(s)}. \quad (3.153)$$

Here, \tilde{O}^\dagger has representation $\tilde{\pi}^\dagger = (\frac{d}{2} - is, \lambda^*)$, so that it can be paired with $O(x)$ inside the integral. We omit spin indices for brevity.

The partial wave $\Psi_{\pi}^{s's}$ satisfies the same Casimir differential equations as a conformal block, but obeys different boundary conditions. However, it gets us "most of the way" to a block, and the block can be extracted from it with a small amount of extra work. The key point is that the space of solutions of the Casimir equations is two-dimensional. It is spanned by the conformal block, and a so-called "shadow" block for the representation $\tilde{\pi}$. It follows that the partial wave can be written as a linear combination of the block and its shadow:

$$\Psi_{\pi}^{s's} = S(\pi_3 \pi_4 [\tilde{\pi}^\dagger])^{s'} {}_t G_{\pi}^{t's} + S(\pi_1 \pi_2 [\pi])^s {}_t G_{\tilde{\pi}}^{s't}. \quad (3.154)$$

Here, the "shadow" coefficients $S(\pi_1 \pi_2 [\pi])^s {}_t$ are obtained by applying shadow transformations to a three-point structure. For example,

$$\mathbf{S}_3 V^s(x_1, x_2, x_3) = S(\pi_1 \pi_2 [\pi])^s {}_t V^t(x_1, x_2, x_3), \quad (3.155)$$

where \mathbf{S}_3 denotes the shadow transform (3.151) acting at x_3 . The reason these coefficients appear in (3.154) is explained in [130]. Starting from (3.154), we can isolate the block $G_{\pi}^{s's}$ using a "monodromy projection" [193], as we explain in more detail later.

To summarize, the shadow formalism gives a convenient integral representation of a partial wave, satisfying the same differential equations as a conformal block, and from which the block can be extracted. This approach will work for the genus-2 blocks $B_{123}^{s's}$ as well. Integral representations are particularly useful for studying large quantum number asymptotics, since we can use saddle point methods.

There exist alternative constructions of four-point conformal blocks via shadow-like integrals in Lorentzian signature [179]. These have the advantage of giving the block "on the nose," eschewing the need for a monodromy projection. Finding a similar Lorentzian shadow representation for the genus-2 block is an interesting problem for the future.

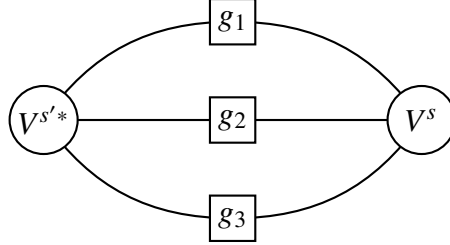


Figure 3.9: A "tensor diagram" for the genus-2 partial wave (3.158). The three-point structures V^s and $V^{s'*}$ are invariant tensors for a tensor product of three principal series representations, so they are represented as trivalent nodes. Each group element acts as a linear operator on a representation, so is a bivalent node. Lines connect together using the inner product (3.150). We act on each of the legs of V^s with group elements g_1, g_2, g_3 before contracting with $V^{s'*}$.

A genus-2 partial wave

The genus-2 conformal block $B_{123}^{s's}$ is a simultaneous eigenfunction of the conformal Casimir operators acting on each of the group elements g_1, g_2, g_3 . In more detail, let L^A ($A = 1, \dots, \dim G$) be the generators of the Lie algebra of G , realized as left-invariant vector fields on G . Then $\mathcal{D} = L^A L_A$ is a differential operator on G such that for any irrep π , we have

$$\mathcal{D}\pi(g) = \pi(g)C_2(\pi), \quad (3.156)$$

where $C_2(\pi)$ is the Casimir eigenvalue for π . Any matrix element of g in the representation π is thus an eigenfunction of \mathcal{D} . Viewing the conformal block as a matrix element of three group elements g_1, g_2, g_3 in the representations π_i , it follows that it must be a simultaneous eigenfunction of \mathcal{D} , acting on each of the g_i :

$$\mathcal{D}_i B_{123}^{s's} = C_2(\pi_i) B_{123}^{s's} \quad i = 1, 2, 3, \quad (3.157)$$

where \mathcal{D}_i indicates the action of \mathcal{D} on g_i . The block also diagonalizes the higher Casimirs of the conformal group, acting on each g_i .

By analogy with the four-point case, we can define a genus-2 partial wave as a principal series matrix element of g_i 's between a pair of three-point structures:

$$\begin{aligned} \Psi_{123}^{s's} &\equiv (V^{s'}|g_1 \otimes g_2 \otimes g_3|V^s) \\ &= \int d^d x_1 d^d x_2 d^d x_3 V^{s'*}(x_1, x_2, x_3) g_1 g_2 g_3 \cdot V^s(x_1, x_2, x_3). \end{aligned} \quad (3.158)$$

This is illustrated diagrammatically in Figure 3.9. The action of a conformal group element on an operator is

$$g \cdot O^a(x) = \Omega(x')^\Delta \lambda^a{}_b(R^{-1}(x')) O^b(x'). \quad (3.159)$$

The notation $g_1 g_2 g_3 \cdot V^s(x_1, x_2, x_3)$ indicates the simultaneous actions of g_1, g_2, g_3 on the three-point structure V^s , using the formula (3.159) at each point. The spin indices of the operators are implicitly contracted in (3.158). By construction, the partial wave also solves the Casimir equations (3.157).

Though we have not proven it, we expect that the space of solutions of the Casimir equations (3.157) is eight-dimensional, and is spanned by the block $B_{123}^{s's}$ and seven "shadow" blocks obtained by replacing $\pi_i \rightarrow \tilde{\pi}_i$ in various combinations:

$$\{B_{123}^{s's}, B_{\tilde{1}\tilde{2}\tilde{3}}^{s's}, \dots, B_{\tilde{1}\tilde{2}\tilde{3}}^{s's}\}.$$

The genus-2 partial wave is a linear combination of these 8 solutions. Applying similar logic to the derivation of (3.154), we expect it to have the form

$$\Psi_{123}^{s's} = (I^{-3} S_{\tilde{1}\tilde{2}\tilde{3}}^3)^{s'}_{\ t} B_{123}^{t's} + (\text{7 shadow blocks}). \quad (3.160)$$

Here $(S_{\tilde{1}\tilde{2}\tilde{3}}^3)^{s'}_t$ denotes the product of three shadow coefficients coming from performing the shadow transform of $\tilde{V}^{\dagger s'}$ on each of its external legs:

$$\begin{aligned} \mathbf{S}_1 \mathbf{S}_2 \mathbf{S}_3 \tilde{V}^{\dagger s'} &= (S_{\tilde{1}\tilde{2}\tilde{3}}^3)^{s'}_{\ v'} V^{v'} \\ &= S([\tilde{\pi}_1]^\dagger \tilde{\pi}_2^\dagger \tilde{\pi}_3^\dagger)^{s'}_{\ t'} S(\pi_1^\dagger [\tilde{\pi}_2^\dagger] \tilde{\pi}_3^\dagger)^{t'}_{\ u'} S(\pi_1^\dagger \pi_2^\dagger [\tilde{\pi}_3^\dagger])^{u'}_{\ v'} V^{v'}. \end{aligned} \quad (3.161)$$

(other expressions are possible, coming from doing the shadow transforms in other orders). Meanwhile, I^{-3} indicates the action of inverse inversion tensors $(I(e)^{-1})_a^{\bar{a}}$ on each operator. These are needed in order for the resulting three-point structure to transform in the dual representations $\lambda_1^*, \lambda_2^*, \lambda_3^*$, so that it can be paired with V^s . The seven shadow blocks in (3.160) will have similar coefficients, though we have not written them explicitly for brevity. We have not attempted to give a rigorous proof of (3.160), but instead have motivated it by analogy with the four-point case. We will verify (3.160) explicitly in the large- Δ limit where it is needed in Section 3.6.

Symmetries of the saddle point equations

We will be interested in the blocks and partial waves in the large- Δ limit. In this limit, the shadow integral (3.158) for the genus-2 partial wave can be evaluated by saddle point. The structure of the saddle point equations is complicated, and we will not attempt to solve them exactly for arbitrary g_i . However, there are some simple operations that permute the saddle points that will be helpful in exploring their structure. We derive them in this section.

Let us begin with the integral for a partial wave. For simplicity, we will work in $d = 1$; the results of this section will generalize straightforwardly to any d . The integral takes the form

$$\Psi_{\Delta_1, \Delta_2, \Delta_3} = \int dz_1 dz_2 dz_3 V_{\tilde{\Delta}_1, \tilde{\Delta}_2, \tilde{\Delta}_3}(z_1, z_2, z_3) g_1 g_2 g_3 \cdot V_{\Delta_1, \Delta_2, \Delta_3}(z_1, z_2, z_3), \quad (3.162)$$

where

$$V_{\Delta_1, \Delta_2, \Delta_3}(z_1, z_2, z_3) = \frac{1}{|z_{12}|^{\Delta_1 + \Delta_2 - \Delta_3} |z_{23}|^{\Delta_2 + \Delta_3 - \Delta_1} |z_{31}|^{\Delta_3 + \Delta_1 - \Delta_2}} \quad (3.163)$$

is a three-point structure for primaries with dimensions $\Delta_1, \Delta_2, \Delta_3$ in $1d$. Thinking of each g_i as an $SL(2, \mathbb{R})$ element, the action of g_i on each operator is given by

$$g_i \cdot \mathcal{O}(z_i) = (c_i z_i + d_i)^{-2\Delta_i} \mathcal{O} \left(\frac{a_i z_i + b_i}{c_i z_i + d_i} \right). \quad (3.164)$$

In the limit of large Δ_i , the integral is dominated by saddle points. Let us split the integrand into a rapidly-varying part that depends exponentially on Δ_i , and a part that is slowly-varying at large Δ_i . We define the saddle point equations as stationarity equations for the rapidly-varying part of the integrand. Concretely they are

$$\partial_{z_i} \log [V_{-\Delta_1, -\Delta_2, -\Delta_3}(z_1, z_2, z_3) g_1 g_2 g_3 \cdot V_{\Delta_1, \Delta_2, \Delta_3}(z_1, z_2, z_3)] = 0 \quad (i = 1, 2, 3). \quad (3.165)$$

This is a system of three coupled polynomial equations in the z_i , with coefficients that depend on the g_i . Note that the saddle-point equations are homogeneous in the Δ_i in our conventions. We denote the coordinates of the three points collectively as $\vec{p} = (z_1, z_2, z_3)$.

Suppose that we can find a saddle point $\vec{p}_* = (z_{1*}, z_{2*}, z_{3*})$, i.e. a solution of (3.165), as a function of the Δ_i . A simple operation that relates different saddle points is

$$\tau \vec{p}_* \equiv (g_1^{-1} z_1, g_2^{-1} z_2, g_3^{-1} z_3) \Big|_{\Delta_i \rightarrow \tilde{\Delta}_i}, \quad (3.166)$$

where we can approximate $\tilde{\Delta}_i \approx -\Delta_i$ at large Δ_i . The fact that $\tau \vec{p}_*$ is a saddle point of (3.162) follows from symmetry of the integrand under the change of variables $z_i \rightarrow g_i^{-1} z_i$ and $\Delta_i \rightarrow \tilde{\Delta}_i$.

However there is another less-obvious operation that relates saddle points to each other, coming from the \mathbb{Z}_2^3 shadow symmetry of the partial wave. We start by

rewriting (3.162) by introducing a shadow transformation on z_1 :

$$\begin{aligned}
& \Psi_{\Delta_1, \Delta_2, \Delta_3} \\
&= \frac{1}{S([\Delta_1] \tilde{\Delta}_2 \tilde{\Delta}_3)} \int dz_1 dz'_1 dz_2 dz_3 \frac{1}{z_{11'}^{2\Delta_1}} V_{\Delta_1, \tilde{\Delta}_2, \tilde{\Delta}_3}(z'_1, z_2, z_3) g_1 g_2 g_3 \cdot V_{\Delta_1, \Delta_2, \Delta_3}(z_1, z_2, z_3) \\
&= \frac{S([\Delta_1] \Delta_2 \Delta_3)}{S([\Delta_1] \tilde{\Delta}_2 \tilde{\Delta}_3)} \int dz'_1 dz_2 dz_3 V_{\Delta_1, \tilde{\Delta}_2, \tilde{\Delta}_3}(z'_1, z_2, z_3) g_1 g_2 g_3 \cdot V_{\tilde{\Delta}_1, \Delta_2, \Delta_3}(z'_1, z_2, z_3).
\end{aligned} \tag{3.167}$$

In the second line, we performed the integral over z_1 and used that the two-point function $z_{11'}^{-2\Delta_1}$ is G -invariant.

The resulting integral (3.167) has the same form as (3.162), except that Δ_1 and $\tilde{\Delta}_1$ have been swapped, and z_1 has been swapped with z'_1 . Thus, a saddle point of (3.167) is given by

$$(z'_1, z_2, z_3) = \vec{p}_*|_{\Delta_1 \rightarrow \tilde{\Delta}_1}. \tag{3.168}$$

So far, we have managed to find a saddle point for a different integral — not the original integral we started with.

However, in the large Δ_i limit, z'_1 can be related to z_1 using the integral on the first line of (3.167). The integral over z_1 takes the form of a shadow transform, and the shadow transform is dominated by its own saddle point at large Δ_i , as we explain in Appendix 3.9. Let us denote the saddle point obtained by shadow-transforming $V_{\Delta_1, \Delta_2, \Delta_3}(z_1, z_2, z_3)$ at site z_1 by

$$s_{[\Delta_1] \Delta_2 \Delta_3}(\vec{p}) \equiv -\frac{2\Delta_1 z_2 z_3 - (\Delta_1 + \Delta_2 - \Delta_3) z_1 z_3 - (\Delta_1 - \Delta_2 + \Delta_3) z_1 z_2}{2\Delta_1 z_1 - (\Delta_1 + \Delta_2 - \Delta_3) z_2 - (\Delta_1 - \Delta_2 + \Delta_3) z_3} \quad (\Delta_i \gg 1). \tag{3.169}$$

Note that $s_{[\Delta_1] \Delta_2 \Delta_3}$ satisfies the identity

$$z_1 = s_{[\tilde{\Delta}_1] \Delta_2 \Delta_3}(s_{[\Delta_1] \Delta_2 \Delta_3}(z_1, z_2, z_3), z_2, z_3), \tag{3.170}$$

which is related to the fact that the square of the shadow transform is proportional to the identity.

In our case, we have

$$z'_1 = s_{[\Delta_1] \tilde{\Delta}_2 \tilde{\Delta}_3}(z_1, z_2, z_3). \tag{3.171}$$

Using (3.170), we can solve this as

$$z_1 = s_{[\tilde{\Delta}_1] \tilde{\Delta}_2 \tilde{\Delta}_3}(z'_1, z_2, z_3). \tag{3.172}$$

Putting everything together, we find a saddle point of the original integrand (3.162)

$$\begin{aligned}\sigma_1 \vec{p}_* &\equiv (s_{[\tilde{\Delta}_1]\tilde{\Delta}_2\tilde{\Delta}_3}(\vec{p}_*|_{\Delta_1 \rightarrow \tilde{\Delta}_1}), z_{2*}|_{\Delta_1 \rightarrow \tilde{\Delta}_1}, z_{3*}|_{\Delta_1 \rightarrow \tilde{\Delta}_1}) \\ &= (s_{[\Delta_1]\tilde{\Delta}_2\tilde{\Delta}_3}(\vec{p}_*), z_{2*}, z_{3*})|_{\Delta_1 \rightarrow \tilde{\Delta}_1}.\end{aligned}\quad (3.173)$$

Note that $\sigma_1 \vec{p}_*$ may or may not coincide with \vec{p}_* . We can similarly define operations σ_2 and σ_3 by cyclic permutations of (3.173). Note that $\sigma_i^2 = 1$ and the σ_i are mutually commuting. One can also show that $\tau = \sigma_1 \sigma_2 \sigma_3$.

The σ_i operations give a homomorphism from \mathbb{Z}_2^3 into the group of permutations of the saddle solutions. The behavior of this homomorphism can jump when any of the Δ_i crosses 0, since the saddle point analysis of the shadow integral for z_1, z'_1 becomes invalid if Δ_1 's is small. Indeed, we will see that such jumps happen in practice.

Low temperature saddles

We are now ready to explore the saddle points of the partial wave integral in different regimes. Let us begin by exploring low temperature $\beta_i \rightarrow \infty$, where it will be easy to distinguish the block from shadow blocks. We study high-temperature saddles (which will be our main interest) in the next section.

As a reminder, we will use the parametrization \mathcal{M} given in (3.112). For simplicity, let us first turn off the angular fugacities by setting $h_i = 1$. The shadow integral (3.158) then has an $\text{SO}(d-1)$ symmetry, so we can locate its saddle points by specializing the points to the x^1 axis: $x_i = (z_i, 0, \dots, 0)$.

The $\text{SO}(d-1)$ -symmetry also means that the local rotations $R_\mu{}^\nu(x')$ associated to each group element g_i are trivial, since the centralizer of $\text{SO}(d-1) \subset \text{SO}(d)$ is trivial. Thus, each group element acts in a simple way on the x -axis:

$$g_i \cdot O^a(x) = \Omega_i(x')^\Delta O^a(g_i x). \quad (3.174)$$

The tensor structures in the numerators of the three-point structures are identical to what they would be in a standard configuration $(x_1, x_2, x_3) = (0, e, \infty)$. The remaining factors are the same as in the $\text{SL}(2, \mathbb{R})$ transformation of conformal three-point structures in 1D. Thus, the integrand restricted to the x^1 -axis becomes

$$\begin{aligned}I(x_i) &= V^{s'*}(x_1, x_2, x_3) g_1 g_2 g_3 \cdot V^s(x_1, x_2, x_3) \\ &= V^{s'*}(0, e, \infty) V^s(0, e, \infty) V_{\tilde{\Delta}_1, \tilde{\Delta}_2, \tilde{\Delta}_3}(z_1, z_2, z_3) g_1 g_2 g_3 \cdot V_{\Delta_1, \Delta_2, \Delta_3}(z_1, z_2, z_3),\end{aligned}\quad (3.175)$$

where $V_{\Delta_1, \Delta_2, \Delta_3}(z_1, z_2, z_3)$ are 1d conformal three-point functions, and the g_i act via (3.164).

In the small temperature limit $\beta_i \rightarrow \infty$, it is straightforward to find at least one solution to the saddle point equations (3.165). We naively expand the equations in the $\beta_i \rightarrow \infty$ limit to obtain

$$\begin{aligned} 0 &= \frac{(\Delta_1 - \Delta_2 + \Delta_3)z_2 + (\Delta_1 + \Delta_2 - \Delta_3)z_3 - 2\Delta_1 z_1}{z_{12}z_{31}} - \frac{2\Delta_1}{z_1 + 1} + O(e^{-\beta_i}), \\ 0 &= \frac{(\Delta_2 + \Delta_3 - \Delta_1)z_1 + (\Delta_1 + \Delta_2 - \Delta_3)z_3 - 2\Delta_2 z_2}{z_{12}z_{23}} - \frac{2\Delta_2}{z_2 - 1} + O(e^{-\beta_i}), \\ 0 &= \frac{(\Delta_2 + \Delta_3 - \Delta_1)z_1 + (\Delta_1 + \Delta_3 - \Delta_2)z_2 - 2\Delta_3 z_3}{z_{31}z_{23}} + O(e^{-\beta_i}). \end{aligned} \quad (3.176)$$

These have the solution

$$\vec{p}_{0,0,0} \equiv \left(\frac{3\Delta_1 - \Delta_2 + \Delta_3}{\Delta_1 + \Delta_2 - \Delta_3}, \frac{\Delta_1 - 3\Delta_2 - \Delta_3}{\Delta_1 + \Delta_2 - \Delta_3}, \frac{\Delta_2 - \Delta_1}{\Delta_3} \right) + O(e^{-\beta_i}). \quad (3.177)$$

Then, using the operations defined in Section 3.6, we can generate seven additional saddles:

$$\begin{aligned} \vec{p}_{1,0,0} &\equiv \sigma_1 \vec{p}_{0,0,0}, \\ \vec{p}_{0,1,0} &\equiv \sigma_2 \vec{p}_{0,0,0}, \\ \vec{p}_{0,0,1} &\equiv \sigma_3 \vec{p}_{0,0,0}, \\ \vec{p}_{1,1,0} &\equiv \sigma_1 \sigma_2 \vec{p}_{0,0,0} = \tau \vec{p}_{0,0,1}, \\ \vec{p}_{1,0,1} &\equiv \sigma_1 \sigma_3 \vec{p}_{0,0,0} = \tau \vec{p}_{0,1,0}, \\ \vec{p}_{0,1,1} &\equiv \sigma_1 \sigma_3 \vec{p}_{0,0,0} = \tau \vec{p}_{1,0,0}, \\ \vec{p}_{1,1,1} &\equiv \sigma_1 \sigma_2 \sigma_3 \vec{p}_{0,0,0} = \tau \vec{p}_{0,0,0}. \end{aligned} \quad (3.178)$$

As an aside, these additional saddles are more subtle to see directly from the saddle point equations because they involve points scaling towards singularities. For example, in the solution

$$\vec{p}_{1,0,0} = \left(-1 + \frac{\Delta_1 - \Delta_2 + \Delta_3}{4\Delta_1} e^{-\beta_1} + \dots, \frac{\Delta_1 + 3\Delta_2 + \Delta_3}{\Delta_1 - \Delta_2 + \Delta_3} + \dots, \frac{\Delta_1 + \Delta_2}{\Delta_3} + \dots \right), \quad (3.179)$$

the point z_1 approaches the center of the ball B_1 at $z_1 = -1$, which is a singularity of the saddle point equations at low temperatures. To find the solution $\vec{p}_{1,0,0}$ directly, we cannot use (3.176). Instead, we must re-expand the equations near the singularity and re-solve them in a small-temperature expansion, resulting in (3.179).

Let us denote the saddle point integral along a steepest descent contour through $\vec{p}_{a,b,c}$ by $I_{a,b,c}$. Plugging in the different solutions, we find that the $I_{a,b,c}$ have the following behavior in the small temperature regime (as a function of the β_i):

$$\begin{aligned} I_{0,0,0} &\sim e^{-\beta_1\Delta_1-\beta_2\Delta_2-\beta_3\Delta_3}, \\ I_{1,0,0} &\sim e^{-\beta_1\tilde{\Delta}_1-\beta_2\Delta_2-\beta_3\Delta_3}, \\ I_{0,1,0} &\sim e^{-\beta_1\Delta_1-\beta_2\tilde{\Delta}_2-\beta_3\Delta_3}, \\ &\dots \\ I_{1,1,1} &\sim e^{-\beta_1\tilde{\Delta}_1-\beta_2\tilde{\Delta}_2-\beta_3\tilde{\Delta}_3}. \end{aligned} \tag{3.180}$$

More formally, if we consider monodromies $M_i : \beta_i \rightarrow \beta_i + 2\pi i$, then each saddle point integral is an eigenfunction of the monodromies $M_{1,2,3}$ with different eigenvalues. The block is the solution to the Casimir equations with monodromies $M_i B_{123}^{s's} = e^{-2\pi i \Delta_i} B_{123}^{s's}$. It follows that $I_{0,0,0}$ is the block at low temperatures, while the other saddle point contours give shadow blocks.

Let us finally turn back on the angular fugacities h_1, h_2, h_3 . In the low-temperature limit, they do not move the saddle point $\vec{p}_{0,0,0}$. Performing the gaussian integral around $\vec{p}_{0,0,0}$, and multiplying by the inverse of the triple shadow coefficient computed in (3.346), we find a nontrivial cancellation of Δ -dependent factors, resulting in

$$\begin{aligned} ((I^{-3} S_{\tilde{1}^\dagger \tilde{2}^\dagger \tilde{3}^\dagger}^3)^{-1})^{s' t'} \Psi_{123}^{t' s} \Big|_{\vec{p}_{0,0,0}} &= 2^{-2\Delta_1-2\Delta_2} e^{-\Delta_1\beta_1-\Delta_2\beta_2-\Delta_3\beta_3} \\ &\times V^{s'*}(0, e, \infty) (h_1 h_2 h_3 \cdot V^s)(0, e, \infty) \\ &\times (1 + O(\Delta_i^{-1}, e^{-\beta_i})), \end{aligned} \tag{3.181}$$

where the $\vec{p}_{0,0,0}$ subscript means we evaluate the saddle point integral around $\vec{p}_{0,0,0}$. This result agrees precisely with the formula for the block from summing over states (3.130). This is a check on our assertion that $I_{0,0,0}$ computes the block, and also on our ansatz (3.160) for the partial wave as a sum of blocks.

High temperature saddles

We define the high temperature regime as $\beta_{ij} \rightarrow 0$ with $\vec{\Omega}_{ij} = \beta_{ij}^{-1} \vec{\theta}_{ij}$ fixed. In terms of the coordinates β_i, h_i , this means that $h_i \rightarrow 1$ at high temperatures. Our strategy will be to start with the infinite temperature case $\beta_i = 0$ and $h_i = 1$, and then work in perturbation theory at small β_i . At infinite temperature, we restore $\text{SO}(d-1)$ symmetry, so we can again look for solutions along the x^1 axis.

It is not obvious a-priori that perturbation theory around infinite temperature makes sense — what if the block had a singularity at infinite temperature? However, we find in practice that the block is nonsingular at infinite temperature, and this strategy works. Relatedly, we do not find any evidence of a nontrivial difference in the order of limits $\beta_i \rightarrow 0$ and $\Delta_i \rightarrow \infty$. This situation is somewhat different from the “*t*-channel” $z, \bar{z} \rightarrow 1$ limit of four-point conformal blocks, where the blocks have nontrivial log or power-law singularities, and one must be careful about orders of limits [176, 185]. It would be nice to understand these differences in more detail.

In the infinite temperature limit $\beta_i = 0$, one saddle point is relatively easy to find. We naively expand the saddle point equations and solve them to give

$$\vec{q}_0 \equiv \left(\frac{2\Delta_3}{2\Delta_2 - \Delta_3}, -\frac{2\Delta_3}{2\Delta_1 - \Delta_3}, \frac{2(\Delta_2 - \Delta_1)}{\Delta_1 + \Delta_2} \right) + O(\beta_i). \quad (3.182)$$

Interestingly, it turns out that $\sigma_1 \vec{q}_0 = \sigma_2 \vec{q}_0 = \sigma_3 \vec{q}_0 = \tau \vec{q}_0$, so the operations defined in Section 3.6 generate only one additional high temperature saddle, namely $\tau \vec{q}_0$.

However, it turns out that there are three additional high temperature saddles where the points x_1, x_2, x_3 scale towards each other in the high temperature limit. For example, we find a solution \vec{q}_{12} given by

$$\vec{q}_{12} \equiv \left(-\frac{\beta_2 \Delta_1 + \beta_1 (\Delta_1 + \Delta_3)}{2\Delta_3}, \frac{\beta_1 \Delta_2 + \beta_2 (\Delta_2 + \Delta_3)}{2\Delta_3}, \frac{\beta_1 (\Delta_1^2 - \Delta_2^2 - \Delta_3^2) + \beta_2 (\Delta_1^2 - \Delta_2^2 + \Delta_3^2)}{4\Delta_3^2} \right) + O(\beta_i^2). \quad (3.183)$$

Here, all three points scale toward $x = 0$ (the point where balls B_1 and B_2 are tangent) as $\beta_i \rightarrow 0$. Similarly, we find a solution \vec{q}_{23} where the x_i scale toward the point where balls B_2 and B_3 are tangent, and a solution \vec{q}_{31} where the x_i scale toward the point where balls B_3 and B_1 are tangent. The action of σ_i and τ on these solutions is given by

$$\sigma_2 \vec{q}_{12} = \sigma_1 \vec{q}_{12} = \vec{q}_{12}, \quad \sigma_3 \vec{q}_{12} = \tau \vec{q}_{12}, \quad (3.184)$$

and cyclic permutations of these relations. The saddle points $\tau \vec{q}_{ij}$ are new — they involve two points scaling towards a singularity, while one remains at a finite position. Thus, overall, we have eight high-temperature saddles given by $\vec{q}_0, \vec{q}_{12}, \vec{q}_{23}, \vec{q}_{31}$, and their images under τ .

These saddle points yield eight solutions of the conformal Casimir equations in the high temperature regime. But which one(s) corresponds to the block? To answer this, let us start at low temperature, where we know that the block corresponds to

$\vec{p}_{0,0,0}$. As we dial from low to high temperature, we find that each low temperature saddle point transitions smoothly to a high temperature saddle. Although we have not proved analytically which saddle becomes which, we can track them numerically; see for example Figure 3.10.

Interestingly, the matching between low- and high-temperature saddles depends on the signs of the Δ_i . The saddle point equations depend projectively on the Δ_i , so more precisely only the signs of their ratios matter. We will be most interested in the case where all Δ_i/Δ_j are positive, where we find

$$\begin{array}{ccc}
 \text{low temperature} & \longrightarrow & \text{high temperature} \\
 \hline
 \vec{p}_{0,0,0} & \longrightarrow & \vec{q}_0 \\
 \vec{p}_{1,1,0} & \longrightarrow & \vec{q}_{12} \\
 \vec{p}_{0,1,1} & \longrightarrow & \vec{q}_{23} \\
 \vec{p}_{1,0,1} & \longrightarrow & \vec{q}_{31}
 \end{array} \quad (\Delta_i/\Delta_j > 0). \quad (3.185)$$

The remaining mappings from low to high temperature are obtained by acting with τ , for example $\tau\vec{p}_{0,0,0} \rightarrow \tau\vec{q}_0$.

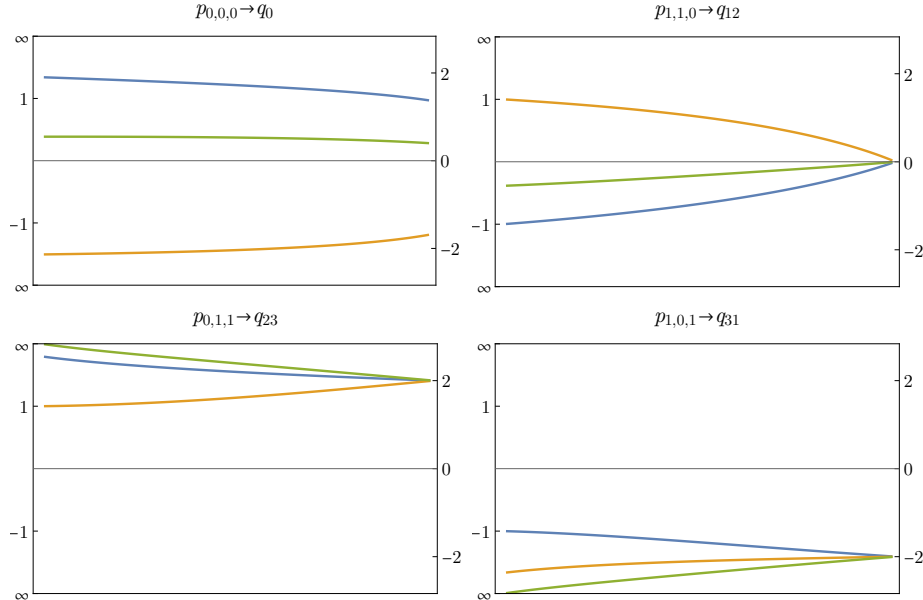


Figure 3.10: Evolution of saddle points from low to high temperature when $\Delta_i/\Delta_j > 0$ for some representative values of Δ_i . The blue curve is x_1 , the orange curve is x_2 , and the green curve is x_3 . Here, we set all three temperatures equal $\beta_i = \beta$. The horizontal axis is $t = e^{-\beta}$, with low temperatures near $t = 0$ and high temperatures near $t = 1$.

How is this compatible with the fact that the σ_i operations act differently on the high temperature and low temperature saddle points? The key is that the map from

low to high temperature depends on the signs of the Δ_i 's, and the σ_i operations can flip these signs. We can capture these rules as follows. Let us define maps $H_{\pm,\pm,\pm}$ that take low temperature saddle points to high temperature saddle points by continuation in β_i , with the signs of $(\Delta_1, \Delta_2, \Delta_3)$ corresponding to the signs in the subscript of $H_{\pm,\pm,\pm}$. For example, when all of the Δ_i are positive, the map H_{+++} is given by 3.185. We claim that the σ_i interchange the maps $H_{\pm\pm\pm}$ in the following way:

$$\begin{aligned} H_{s_1s_2s_3}(\vec{p}) &= \sigma_1 H_{(-s_1)s_2s_3}(\sigma_1 \vec{p}), \\ H_{s_1s_2s_3}(\vec{p}) &= \sigma_2 H_{s_1(-s_2)s_3}(\sigma_2 \vec{p}), \\ H_{s_1s_2s_3}(\vec{p}) &= \sigma_3 H_{s_1s_2(-s_3)}(\sigma_3 \vec{p}). \end{aligned} \quad (3.186)$$

In other words, conjugating by σ_i flips the sign of the i -th subscript in $H_{\pm\pm\pm}$. Intuitively, this is because σ_i flips the sign of Δ_i in 3.173.

With the rules (3.185) defining H_{+++} , the relations (3.186), and the action of σ_i, τ on the low and high temperature saddles, we can predict how any low temperature saddle continues to a high temperature saddle, for various signs of the Δ_i . We have verified these predictions numerically in examples. It would be nice to prove them analytically.

To summarize, as we continue from low to high temperature, with $\Delta_i/\Delta_j > 0$, the saddle point $\vec{p}_{0,0,0}$ continues to \vec{q}_0 . We will assume that no Stokes phenomena occur during this continuation, so that the saddle point integral through $\vec{p}_{0,0,0}$ continues to the saddle point integral through \vec{q}_0 . Another way to think about this is that the saddle point integral automatically solves the conformal Casimir equation, in perturbation theory in $1/\Delta$. The assumption of no Stokes phenomena is the same as the assumption that perturbation theory in $1/\Delta$ can be used to solve the Casimir equations at large Δ for all temperatures.

Thus, let us focus on the saddle point \vec{q}_0 . Away from infinite temperature, the positions of the points in the \vec{q}_0 saddle get corrected, and we can compute these corrections in a systematic expansion in β_i and the angles $\vec{\alpha}_i$ and $\vec{\Phi}_i$ defined in

(3.147) (still in the large- Δ limit). For example, x_1 shifts by

$$\begin{aligned}\delta x_1^1 &= \frac{(\Delta_1^2 + (\Delta_2 - \Delta_3)^2)(2\Delta_2 + \Delta_3)}{4\Delta_2(2\Delta_2 - \Delta_3)\Delta_3}\beta_1 + \frac{\Delta_2(4\Delta_1^2 - \Delta_3^2)(\Delta_1^2 + \Delta_2^2 - \Delta_3^2)}{4\Delta_1^2\Delta_3(2\Delta_2 - \Delta_3)^2}\beta_2 \\ &\quad - \frac{(\Delta_1^2 - \Delta_2^2)\Delta_3(\Delta_1^2 - \Delta_2^2 + \Delta_3^2)}{2\Delta_1^2\Delta_2(2\Delta_2 - \Delta_3)^2}\beta_3 + O(\beta^2, \vec{\alpha}^2), \\ \delta \vec{x}_1 &= \frac{(\Delta_1^2 + (\Delta_2 - \Delta_3)^2)(2\Delta_2 + \Delta_3)}{4\Delta_2\Delta_3(2\Delta_2 - \Delta_3)}\vec{\alpha}_1 + \frac{\Delta_2(4\Delta_1^2 - \Delta_3^2)(\Delta_1^2 + \Delta_2^2 - \Delta_3^2)}{4\Delta_1^2\Delta_3(2\Delta_2 - \Delta_3)^2}\vec{\alpha}_2 \\ &\quad + \frac{(\Delta_1^2 - \Delta_2^2)\Delta_3(\Delta_1^2 - \Delta_2^2 + \Delta_3^2)}{2\Delta_1^2\Delta_2(2\Delta_2 - \Delta_3)^2}\vec{\alpha}_3 + O(\beta\vec{\alpha}, \vec{\Phi}\vec{\alpha}).\end{aligned}\tag{3.187}$$

Here, $\delta \vec{x}_1$ indicates the components of x_1 perpendicular to the x_1^1 axis, and $O(\beta^2, \vec{\alpha}^2)$ and $O(\beta\vec{\alpha}, \vec{\Phi}\vec{\alpha})$ stand for quadratic corrections in the $\beta_i, \vec{\alpha}_i, \vec{\Phi}_i$ of the indicated form. The $\vec{\alpha}_i$ appear at second order in δx_1^1 , as required by $SO(d-1)$ invariance.

Plugging this corrected \vec{q}_0 into the saddle point integral, and taking into account the 1-loop determinant, we finally find the high temperature behavior of the block at large Δ :

$$\begin{aligned}B_{123}^{s',s} &= \frac{(2\Delta_1)^{2\Delta_1-d}(2\Delta_2)^{2\Delta_2-d}(2\Delta_3)^{2\Delta_3-d}}{2^{3d/2}(\Delta_1 + \Delta_2 + \Delta_3)^{2\Delta_1+2\Delta_2+2\Delta_3-3d}} V^{s'*}(0, e, \infty) h_1 h_2 h_3 V^s(0, e, \infty) \\ &\quad \times \exp\left(-\frac{\Delta_1\Delta_2}{\Delta_3}(\beta_1 + \beta_2) - \frac{\Delta_2\Delta_3}{\Delta_1}\left(\frac{\beta_2}{4} + \frac{\beta_3}{2}\right) - \frac{\Delta_1\Delta_3}{\Delta_2}\left(\frac{\beta_1}{4} + \frac{\beta_3}{2}\right) + O(\Delta\beta^2, \Delta\vec{\alpha}^2)\right) \\ &\quad (\beta_i, |\vec{\alpha}_i|, |\vec{\Phi}_i| \ll 1, \Delta_i \gg 1).\end{aligned}\tag{3.188}$$

Recall that this formula only holds in the chamber $\Delta_i/\Delta_j > 0$. When the signs of ratios Δ_i/Δ_j are different, the high temperature behavior of the block is in general controlled by a different saddle. Our derivation so far has been for principal series representations $\Delta_i \in \frac{d}{2} + i\mathbb{R}_{\geq 0}$. However, we can now analytically continue the result to real Δ_i by simultaneously rotating the Δ_i clockwise in the complex plane.

In (3.188), we only kept linear order terms in β_i in the exponent. Later, we will argue that the higher order terms in $\beta, \vec{\alpha}, \vec{\Phi}$ do not contribute to the leading asymptotics of OPE coefficients, at large Δ and finite J . Such terms can potentially become important at large- J , but we leave the analysis of this case to future work. Note also that in (3.188), we have $h_i = 1 + O(\alpha_i, \Phi_i)$. We study one consequence of the Φ_i^2 terms in h_i later in Section 3.7.

As was the case at low temperatures, the apparent breaking of 1-2-3 permutation symmetry in (3.188) is due to using non-permutation symmetric coordinates on the

moduli space \mathcal{M} . Switching to the relative temperatures β_{ij} , the exponent in 3.188 becomes the beautifully permutation-symmetric

$$\exp\left(-\frac{\Delta_1\Delta_2}{8\Delta_3}\beta_{12}^2 - \frac{\Delta_2\Delta_3}{8\Delta_1}\beta_{23}^2 - \frac{\Delta_3\Delta_1}{8\Delta_2}\beta_{31}^2 + O(\Delta\beta^2, \Delta\vec{\alpha}^2)\right). \quad (3.189)$$

Let us make a few additional observations about the result (3.188). We define a "scaling block" as the primary term in 3.130. Because the full block is a sum of scaling blocks with nonnegative coefficients, we should have the inequality

$$B_{123} \geq 2^{-2\Delta_1-2\Delta_2} e^{-\beta_1\Delta_1-\beta_2\Delta_2-\beta_3\Delta_3} \quad (h_i = 1). \quad (3.190)$$

Let us check this at high temperatures. Our calculation of the block is valid in the regime $\Delta \gg 1$ and $\beta \ll 1$. Thus, we can ignore $\beta\Delta$ compared to Δ and just compare the Δ -dependent terms out front:

$$\frac{(2\Delta_1)^{2\Delta_1-d}(2\Delta_2)^{2\Delta_2-d}(2\Delta_3)^{2\Delta_3-d}}{2^{3d/2}(\Delta_1 + \Delta_2 + \Delta_3)^{2\Delta_1+2\Delta_2+2\Delta_3-3d}} \geq 2^{-2\Delta_1-2\Delta_2}. \quad (3.191)$$

Indeed, we find that numerically, the above inequality holds when $\Delta_i > 0$. It is saturated when $\Delta_1 = \Delta_2 = \Delta_3/2$, and in this case the high temperature block and the scaling block are exactly the same (up to the order we've computed them)! One speculative interpretation is that the full genus-2 block at large Δ may be a scaling block in an appropriate Weyl frame that depends on the Δ_i . Our choice of Weyl frame in Section 3.5 happens to be the appropriate frame for $\Delta_1 = \Delta_2 = \Delta_3/2$. Other Weyl frames would be best suited to other Δ_i . The large- Δ limit of Virasoro blocks also simplifies in an appropriate Weyl frame [161, 206].

3.7 OPE coefficients of heavy operators

"Heavy-heavy-heavy" OPE coefficients are encoded in the partition function of the CFT on the genus-2 manifold M_2 via (3.129). In Section 3.5, using the thermal effective action and the "hot spot" hypothesis, we calculated the leading expression (3.146) for the partition function in the high-temperature regime discussed in Section 3.5. In Section 3.6, we obtained an expression (3.188) for a conformal block in the same regime. Finally, in this section, we will combine these ingredients to obtain an asymptotic formula for "heavy-heavy-heavy" OPE coefficients by inverting the conformal block decomposition of the partition function.

Review: inverting a genus-1 partition function

Before discussing how to invert a genus-2 partition function, let us revisit the genus-1 case, phrasing it in language that will generalize to genus-2. Conformal blocks for

the genus-1 partition function on $S^1 \times S^{d-1}$ are just conformal characters $\chi_{\Delta,J}(\beta, \Omega_i)$. For simplicity, let us work in $d = 1$, where the characters have the simple form

$$\chi_{\Delta}(\beta) = \frac{e^{-\Delta\beta}}{1 - e^{-\beta}} \quad (d = 1), \quad (3.192)$$

and the partition function has the decomposition

$$Z(\beta) = \int d\Delta p(\Delta) \chi_{\Delta}(\beta), \quad (3.193)$$

which is essentially a Laplace transform of the density of states $p(\Delta)$. It is straightforward to decompose $Z(\beta)$ into characters via an inverse Laplace transform, as we did in Section 3.3. However, let us pause to understand this transform in group-theoretic language.

The conformal characters can be viewed as functions on the group $\mathrm{SL}(2, \mathbb{R})$ that are invariant under conjugation, i.e. class functions. They are naturally eigenfunctions of the Casimir differential operator \mathcal{D} defined in Section 3.6. In terms of β , this leads to the eigenvalue equation

$$\mathcal{D}\chi_{\Delta}(\beta) = \frac{1 + e^{-\beta}}{1 - e^{-\beta}} \chi'_{\Delta}(\beta) + \chi''_{\Delta}(\beta) = \Delta(\Delta - 1)\chi_{\Delta}(\beta). \quad (3.194)$$

(Here, we abuse notation and write \mathcal{D} both for the differential operator $L^A L_A$ on the group $\mathrm{SL}(2, \mathbb{R})$, and for the differential operator (3.194) acting on β .) Because the Casimir eigenvalue $\Delta(\Delta - 1)$ is the same for Δ and $\tilde{\Delta} = 1 - \Delta$, the shadow character $\chi_{\tilde{\Delta}}(\beta)$ satisfies the same differential equation as $\chi_{\Delta}(\beta)$.

Because of its group-theoretic origin, \mathcal{D} is naturally self-adjoint in the Haar measure on $\mathrm{SL}(2, \mathbb{R})$. When acting on class functions, this implies that \mathcal{D} defined in (3.194) is self-adjoint with respect to the quotient measure on the space of conjugacy classes of $\mathrm{SL}(2, \mathbb{R})$. The quotient measure is given by the famous Weyl integration formula (and can be computed using the Faddeev-Popov procedure):

$$d\mu = d\beta (e^{\beta/2} - e^{-\beta/2})^2. \quad (3.195)$$

Self-adjointness of \mathcal{D} immediately implies an orthogonality relation

$$\int d\mu \chi_{\Delta}(\beta) \chi_{\tilde{\Delta}'}(\beta) = 0 \quad \text{unless } \Delta = \Delta' \text{ or } \Delta = \tilde{\Delta}', \quad (3.196)$$

where the integral can follow any contour such that the boundary terms from integrating \mathcal{D} by parts vanish. For our applications, we can integrate over an infinite

contour parallel to the imaginary axis $\beta = \beta_0 + it$, which gives

$$\oint d\mu \chi_\Delta(\beta) \chi_{\Delta'}(\beta) = \oint d\beta e^{(\Delta' - \Delta)\beta} = 2\pi i \delta(\Delta - \Delta'). \quad (3.197)$$

This allows us to invert the partition function by integrating against a shadow block:

$$p(\Delta) = \frac{1}{2\pi i} \oint d\mu \chi_{\Delta}(\beta) Z(\beta) = \frac{1}{2\pi i} \oint d\beta e^{\Delta\beta} (1 - e^{-\beta}) Z(\beta), \quad (3.198)$$

which is the usual inverse Laplace transform.

Before proceeding, let us make a comment about the choice of contour. By analogy with Euclidean inversion formulae for local correlation functions, we could have instead tried to decompose $Z(\beta)$ in characters for principal series representations, which take the form

$$\chi'_s(\beta) = \chi_{\frac{1}{2}+is}(\beta) + \chi_{\frac{1}{2}-is}(\beta) = \frac{e^{is\beta} + e^{-is\beta}}{e^{\beta/2} - e^{-\beta/2}}. \quad (3.199)$$

Principal series characters are naturally orthonormal with respect to $d\mu$, when integrated along a *real* contour $\beta \in \mathbb{R}$. However, this kind of orthogonality is unsuitable for decomposing a physical partition function. The reason is that $Z(\beta)$ typically possesses a high-temperature singularity on the real axis of the form $Z(\beta) \sim e^{1/\beta^a}$ for some positive power a . This high-temperature singularity cannot be integrated against $\chi'_s(\beta)$ along a real contour in a simple way.²⁷ Using a complex contour as in 3.198 bypasses this issue by avoiding the singularity.

An inverse Laplace transform for genus-2 blocks

Let us now assemble analogous ingredients in the genus-2 case. Let $d\mu$ be the natural quotient measure on the moduli space $\mathcal{M} = G \backslash (G^-)^3 / G$, descending from the product of Haar measures on $(G^-)^3$. Consider a contour integral of a block against a shadow block

$$\oint d\mu B_{123}^{s's} B_{\tilde{1}'\tilde{2}'\tilde{3}'}^{t't}. \quad (3.200)$$

(We do not specify the precise contour for now.) The block and shadow block are both simultaneous eigenfunction of the Casimir operators \mathcal{D}_i acting on each group element g_i . Because of their group-theoretic origin, these operators are naturally

²⁷Interestingly, there is usually no problem with decomposing correlators of local operators in principal series representations. Doing so leads to Euclidean inversion formulas, which typically involve integrable power-like singularities. It would be nice to better understand the distinction between these cases.

self-adjoint in the measure $d\mu$. If the contour is such that there are no boundary terms from integrating the \mathcal{D}_i by parts, then the above integral must be proportional to δ -functions restricting π_i and π'_i to be the same

$$\oint d\mu B_{123}^{s's} B_{\bar{1}'\bar{2}'\bar{3}'\dagger}^{t't} \propto \delta_{\pi_1\pi'_1} \delta_{\pi_2\pi'_2} \delta_{\pi_3\pi'_3}, \quad (3.201)$$

where

$$\delta_{\pi\pi'} = \delta(\Delta - \Delta') \delta_{\lambda\lambda'}. \quad (3.202)$$

To find the constant of proportionality in (3.201), we will assume that the contour is a complex contour in β_i that can be deformed to low temperature and evaluated in that regime. This is analogous to the inverse Laplace transform (3.198), where we can choose any contour of the form $\beta = \beta_0 + it$. Moving the contour to low temperatures, we can evaluate the orthogonality relation (3.201) using the low-temperature expansion of the blocks (3.130). When inverting a partition function, we can instead deform the contour into the high temperature regime and look for a saddle point.

Computing the measure

The first step is to compute the quotient measure $d\mu$ via the Faddeev-Popov procedure. There are a few wrinkles in doing so, so let us work through the computation in full. Recall that the quotient space \mathcal{M} can be redundantly parametrized by $(g_1, g_2, g_3) \in G^- \times G^- \times G^-$. We would like to fix a gauge by writing g_i in terms of β_i, h_i as in (3.112). For the moment, let us also imagine that we have chosen a non-redundant parametrization of the h_i in terms of angles, so that overall the g_i are specified in terms of $n = \dim G$ parameters which we call y . Our gauge-fixing condition is $g_i = \bar{g}_i(y)$. An appropriate gauge-fixing function is

$$Q(g_1, g_2, g_3) = \int dy \delta(g_1, \bar{g}_1) \delta(g_2, \bar{g}_2) \delta(g_3, \bar{g}_3), \quad (3.203)$$

where dy is any measure on the coordinates y , and $\delta(g, g')$ is a unit-normalized δ -function (in the Haar measure) on the group supported at $g = g'$.

Consider now a gauge-invariant function $f(g_1, g_2, g_3)$. We formally define its integral over the moduli space as

$$\int_{\mathcal{M}} d\mu f = \int \frac{dg_1 dg_2 dg_3}{(\text{vol}G)^2} f(g_1, g_2, g_3), \quad (3.204)$$

where dg_i are Haar measures. Following the usual FP procedure, we insert 1 in the form of an integral over gauge orbits of Q , divided by its average over gauge orbits

$$\int_{\mathcal{M}} d\mu f = \int \frac{dg_1 dg_2 dg_3}{(\text{vol}G)^2} dg dg' \frac{Q(gg_1g'^{-1}, gg_2g'^{-1}, gg_3g'^{-1})}{\widehat{Q}(g_1, g_2, g_3)} f(g_1, g_2, g_3), \quad (3.205)$$

where

$$\widehat{Q}(g_1, g_2, g_3) \equiv \int dg dg' Q(gg_1g'^{-1}, gg_2g'^{-1}, gg_3g'^{-1}). \quad (3.206)$$

Now we change variables $g_i \rightarrow g^{-1}g_i g'$ and use gauge-invariance of f and \widehat{Q} to obtain

$$\int_{\mathcal{M}} d\mu f = \int dg_1 dg_2 dg_3 \frac{f(g_1, g_2, g_3)}{\widehat{Q}(g_1, g_2, g_3)} Q(g_1, g_2, g_3) = \int dy \frac{f(\bar{g}_1, \bar{g}_2, \bar{g}_3)}{\widehat{Q}(\bar{g}_1, \bar{g}_2, \bar{g}_3)}. \quad (3.207)$$

This is our gauge-fixed integral and $1/\widehat{Q}$ is the FP determinant, which we now compute.

We have

$$\widehat{Q}(\bar{g}_1, \bar{g}_2, \bar{g}_3) = \int dg dg' dy' \prod_{i=1}^3 \delta(g\bar{g}_i(y)g'^{-1}, \bar{g}_i(y')). \quad (3.208)$$

The δ -functions are supported for g, g' near the identity and y' near y . Thus, we can write

$$g = 1 + \xi, \quad g' = 1 + \xi', \quad (3.209)$$

where ξ, ξ' are elements of the Lie algebra of G , and we can furthermore Taylor expand the \bar{g}_i in $y' = y + dy$. We have

$$\begin{aligned} \delta(g\bar{g}_i(y)g'^{-1}, \bar{g}_i(y')) &= \delta(\bar{g}_i(y)^{-1}g\bar{g}_i(y)g'^{-1}, \bar{g}_i(y)^{-1}\bar{g}_i(y')) \\ &= \delta(1 + \bar{g}_i(y)^{-1}\xi\bar{g}_i(y) - \xi', 1 + dy \cdot \bar{g}_i(y)^{-1}\partial_y\bar{g}_i(y)) \\ &= \delta(\text{Ad}_{\bar{g}_i^{-1}}\xi - \xi' - dy \cdot \bar{g}_i^{-1}\partial_y\bar{g}_i), \end{aligned} \quad (3.210)$$

where in the last line, we have a δ function on the Lie algebra \mathfrak{g} , and Ad_g denotes the adjoint action of g . The gauge-fixed measure is thus

$$d\mu = \frac{dy}{\widehat{Q}} = \det \begin{pmatrix} \text{Ad}_{\bar{g}_1^{-1}} & -\mathbf{1} & -\bar{g}_1^{-1}\partial_{y^1}\bar{g}_1 & \cdots & -\bar{g}_1^{-1}\partial_{y^n}\bar{g}_1 \\ \text{Ad}_{\bar{g}_2^{-1}} & -\mathbf{1} & -\bar{g}_2^{-1}\partial_{y^1}\bar{g}_2 & \cdots & -\bar{g}_2^{-1}\partial_{y^n}\bar{g}_2 \\ \text{Ad}_{\bar{g}_3^{-1}} & -\mathbf{1} & -\bar{g}_3^{-1}\partial_{y^1}\bar{g}_3 & \cdots & -\bar{g}_3^{-1}\partial_{y^n}\bar{g}_3 \end{pmatrix} dy^1 \cdots dy^n \quad (3.211)$$

The object inside the determinant is a $3n \times 3n$ matrix. Choosing an orthonormal basis of \mathfrak{g} , $\text{Ad}_{\bar{g}_i^{-1}}$ becomes an $n \times n$ block, and each $\mathbf{1}$ becomes an $n \times n$ identity matrix. Finally, $-\bar{g}_i^{-1} \partial_{y^j} \bar{g}_i$ is an element of \mathfrak{g} , which we can think of as a column vector of height n .

- Partial gauge fixing

In our parametrization of \mathcal{M} in terms of temperatures $\beta_1, \beta_2, \beta_3$ and rotations $h_1, h_2, h_3 \in \text{SO}(d)$, we write the moduli space as

$$\mathcal{M} = G \backslash (G^-)^3 / G \cong \text{SO}(d-1) \backslash (\text{SO}(1,1) \times \text{SO}(d))^3 / \text{SO}(d-1), \quad (3.212)$$

where the two copies of $\text{SO}(d-1)$ act by left and right multiplication on the h_i . Above, we obtained the measure from fully gauge-fixing both the left and right action of G . However, it will be more convenient to only partially fix the gauge, leaving the $\text{SO}(d-1) \times \text{SO}(d-1)$ gauge redundancy un-fixed. Let us determine how the above computation should be modified in this case.

Let $y = (\beta_1, \beta_2, \beta_3, h_1, h_2, h_3)$ now be coordinates on $(\text{SO}(1,1) \times \text{SO}(d))^3$, and let us write $K = \text{SO}(d-1)$, with Lie algebra \mathfrak{k} . The y have an action of $K \times K$ given by $y \mapsto kyk'^{-1}$ and an invariant measure dy . Once again, we should consider the average over gauge orbits of the gauge-fixing function

$$\widehat{\mathcal{Q}}(g_1, g_2, g_3) \equiv \int dg dg' dy \prod_i \delta(gg_1g'^{-1}, \bar{g}_i(y)). \quad (3.213)$$

We can factorize g into

$$g = k \gamma, \quad (3.214)$$

where $k \in K$, and γ is a representative of the quotient $K \backslash G$. The measure on G similarly splits as

$$dg = dk d\gamma, \quad (3.215)$$

where dk is the measure on K , and $d\gamma$ is a right- G -invariant measure on $K \backslash G$. To be more precise, let T^a be an orthonormal basis of generators of \mathfrak{g} , and let the generators of $\mathfrak{k} \subset \mathfrak{g}$ be the T^a with $a = 1, \dots, \dim K$. Then we can take the γ to be the image under the exponential map of the remaining generators T^a with $a = \dim K + 1, \dots, \dim G$.

Inserting this decomposition into (3.213), we find

$$\begin{aligned}
\widehat{\mathcal{Q}}(g_1, g_2, g_3) &\equiv \int dk d\gamma dk' d\gamma' dy \prod_i \delta(k\gamma g_1 \gamma'^{-1} k'^{-1}, \bar{g}_i(y)) \\
&= \int dk d\gamma dk' d\gamma' dy \prod_i \delta(\gamma g_1 \gamma'^{-1}, \bar{g}_i(k^{-1} y k')) \\
&= (\text{vol}K)^2 \int d\gamma d\gamma' dy \prod_i \delta(\gamma g_1 \gamma'^{-1}, \bar{g}_i(y)) \\
&= (\text{vol}K)^2 \int d\xi d\xi' dy \prod_i \delta(\text{Ad}_{g_i^{-1}} \xi - \xi' - dy \cdot \bar{g}_i^{-1} \partial_y \bar{g}), \quad (3.216)
\end{aligned}$$

where we have written

$$\gamma = \exp(\xi), \quad \gamma' = \exp(\xi'). \quad (3.217)$$

The only differences from before are that now ξ and ξ' are restricted to generators of γ — i.e. T^a with $a = \dim K + 1, \dots, \dim G$, and furthermore we must divide by $(\text{vol}K)^2$. The partially gauge-fixed measure is thus

$$d\mu = \frac{1}{(\text{vol}K)^2} \det \begin{pmatrix} \text{Ad}_{\bar{g}_1^{-1}} \Pi_\gamma^\dagger & -\Pi_\gamma^\dagger & -\bar{g}_1^{-1} \partial_{y^1} \bar{g}_1 & \cdots & -\bar{g}_1^{-1} \partial_{y^m} \bar{g}_1 \\ \text{Ad}_{\bar{g}_2^{-1}} \Pi_\gamma^\dagger & -\Pi_\gamma^\dagger & -\bar{g}_2^{-1} \partial_{y^1} \bar{g}_2 & \cdots & -\bar{g}_2^{-1} \partial_{y^m} \bar{g}_2 \\ \text{Ad}_{\bar{g}_3^{-1}} \Pi_\gamma^\dagger & -\Pi_\gamma^\dagger & -\bar{g}_3^{-1} \partial_{y^1} \bar{g}_3 & \cdots & -\bar{g}_3^{-1} \partial_{y^m} \bar{g}_3 \end{pmatrix} dy^1 \cdots dy^m, \quad (3.218)$$

where Π_γ is an $(n - \dim K) \times n$ matrix implementing the orthogonal projection onto the generators of γ , and Π_γ^\dagger is its adjoint. Finally, $m = n + 2 \dim K$. Overall, this again gives a $3n \times 3n$ matrix.

Let us finally plug in (3.112) to write the measure (3.218) in terms of the parameters β_i, h_i . We found it difficult to compute the measure exactly for generic parameters.²⁸ However, we can compute it in various limits. At low temperatures, we find

$$d\mu = \frac{2^{5d}}{(\text{vol SO}(d-1))^2} \prod_{i=1}^3 e^{d\beta_i} d\beta_i dh_i, \quad (\text{low temperature}), \quad (3.219)$$

where dh_i denotes Haar measures on $\text{SO}(d)$. At high temperature, we find

$$d\mu = \frac{2^{4d}}{(\text{vol SO}(d-1))^2} \prod_{i=1}^3 d\beta_i d\vec{\alpha}_i d\vec{\Phi}_i, \quad (\text{high temperature}), \quad (3.220)$$

²⁸The reason is that (3.218) is the determinant of a large symbolic matrix, which is extremely difficult for *Mathematica* to handle.

where $\vec{\alpha}_i$ and $\vec{\Phi}_i$ are the angles defined in (3.147).²⁹

- Orthogonality relation for genus-2 blocks

With the measure in hand, let us determine the correct orthogonality relation for genus-2 blocks. We will take the contour to be a real contour for the group elements $h_i \in \mathrm{SO}(d)$, and a complex contour running parallel to the imaginary axis for the β_i . The key idea will be to deform the β_i contour into the low-temperature region, where the blocks are given by the simple formula

$$B_{123}^{s's} = 2^{-2\Delta_1-2\Delta_2} e^{-\Delta_1\beta_1-\Delta_2\beta_2-\Delta_3\beta_3} V^{s'}(0, e, \infty)^* h_1 h_2 h_3 V^s(0, e, \infty) \times (1 + O(e^{-\beta_i})). \quad (3.222)$$

Consider a shadow block with complex-conjugated three-point structures

$$B_{\tilde{1}'^\dagger \tilde{2}'^\dagger \tilde{3}'^\dagger}^{t'^* t^*} = 2^{-2(d-\Delta'_1)-2(d-\Delta'_2)} e^{-(d-\Delta'_1)\beta_1-(d-\Delta'_2)\beta_2-(d-\Delta'_3)\beta_3} \times V^{t'}(0, e, \infty) h_1 h_2 h_3 V^t(0, e, \infty)^* (1 + O(e^{-\beta_i})). \quad (3.223)$$

Integrating the block and the shadow block against each other using the low-temperature measure (3.219), we find

$$\begin{aligned} & \oint d\mu B_{123}^{s's} B_{\tilde{1}'^\dagger \tilde{2}'^\dagger \tilde{3}'^\dagger}^{t'^* t^*} \\ &= \frac{2^{5d}}{(\mathrm{vol} \mathrm{SO}(d-1))^2} \int \left(\prod_i d\beta_i dh_i \right) 2^{-4d} e^{-\beta_1(\Delta_1-\Delta'_1)-\beta_2(\Delta_2-\Delta'_2)-\beta_3(\Delta_3-\Delta'_3)} \\ & \quad \times V^{s'}(0, e, \infty)^* h_1 h_2 h_3 V^s(0, e, \infty) \times V^{t'}(0, e, \infty) h_1 h_2 h_3 V^t(0, e, \infty)^*. \end{aligned} \quad (3.224)$$

To perform the integral over the h_i , we can use the Schur orthogonality formula, which states that for any compact group G with unitary representations λ, λ'

$$\int dg \langle a|\lambda(g)|b\rangle \langle c|\lambda'(g^{-1})|d\rangle = \langle a|d\rangle \langle c|b\rangle \frac{\mathrm{vol} G}{\dim \lambda} \delta_{\lambda\lambda'}. \quad (3.225)$$

²⁹We can find an interpolating result between high and low temperatures by setting the angles to zero, $\vec{\alpha}_i = 0, \vec{\Phi}_i = 0$. In this case, *Mathematica* is able to compute the determinant for general β_i , giving

$$\begin{aligned} d\mu = & \left(-8e^{\beta_1} - 8e^{\beta_2} + \frac{1}{2}e^{\beta_1-\beta_2-\beta_3} + \frac{1}{2}e^{-\beta_1+\beta_2-\beta_3} - 2e^{\beta_1+\beta_2-\beta_3} + e^{-\beta_3} + 32e^{\beta_1+\beta_2+\beta_3} \right)^d \\ & \times \frac{1}{(\mathrm{vol} \mathrm{SO}(d-1))^2} \prod_{i=1}^3 d\beta_i d\vec{\alpha}_i d\vec{\Phi}_i \quad (\vec{\alpha}_i = 0, \vec{\Phi}_i = 0). \end{aligned} \quad (3.221)$$

This indeed agrees with both 3.219 and 3.220 in the appropriate limits.

The integral over β_i gives δ -functions of the form $\delta(\Delta_i - \Delta'_i)$, as in the inverse Laplace transform (3.198). Overall, we find the orthogonality relation

$$\begin{aligned} &= \frac{V^t(0, e, \infty)^* V^s(0, e, \infty)}{2^d \text{vol SO}(d-1)} \frac{V^{s'}(0, e, \infty)^* V^{t'}(0, e, \infty)}{2^d \text{vol SO}(d-1)} \prod_{i=1}^3 2\pi \delta(\Delta_i - \Delta'_i) \frac{2^d \text{vol SO}(d)}{\dim \lambda_i} \delta_{\lambda_i, \lambda'_i} \\ &= T^{ts} T^{s't'} \prod_{i=1}^3 2\pi \delta(\Delta_i - \Delta'_i) \frac{2^d \text{vol SO}(d)}{\dim \lambda_i} \delta_{\lambda_i, \lambda'_i}, \end{aligned} \quad (3.226)$$

where we have introduced the three-point pairing matrix

$$T^{ts} = \frac{V^t(0, e, \infty)^* V^s(0, e, \infty)}{2^d \text{vol SO}(d-1)}. \quad (3.227)$$

Recall that the structure V^s is a tensor with an index for each of the representations $\lambda_1, \lambda_2, \lambda_3$, and V^{t*} carries indices for the dual representations $\lambda_1^*, \lambda_2^*, \lambda_3^*$. The indices of V^s and V^{t*} are implicitly contracted in the three point pairing (3.227). The pairing matrix T^{ts} shows up in other contexts related to harmonic analysis on the conformal group, and is discussed more extensively in [130, 151].

To summarize, if the partition function has an expansion in conformal blocks

$$Z = \sum_{\lambda_1, \lambda_2, \lambda_3} \int d\Delta_1 d\Delta_2 d\Delta_3 P_{123}^{ss'} B_{123}^{s's}, \quad (3.228)$$

then the conformal block coefficients $P_{123}^{ss'}$ are given by the inversion formula

$$P_{123}^{ss'} = (T^{-1})^{st} (T^{-1})^{t's'} \frac{1}{(2\pi)^3} \prod_{i=1}^3 \left(\frac{\dim \lambda_i}{2^d \text{vol SO}(d)} \right) \oint d\mu Z B_{\tilde{1}^* \tilde{2}^* \tilde{3}^*}^{t'^* t^*}. \quad (3.229)$$

In both (3.228) and (3.229), a sum over repeated three point structure indices s, t, s', t' is implicit.

Putting everything together

We are finally ready to put everything together and perform the genus-2 Laplace transform at high temperature. Let us recall the important formulas. The shadow block at high temperature is given by

$$\begin{aligned} B_{\tilde{\pi}_1 \tilde{\pi}_2 \tilde{\pi}_3}^{t'^* t^*} &= \frac{1}{2^{3d/2}} \left(\prod_{i=1}^3 \left(\frac{2\Delta_i}{\Delta_1 + \Delta_2 + \Delta_3} \right)^{d-2\Delta_i} \right) e^{\frac{\Delta_1 \Delta_2}{8\Delta_3} \beta_{12,0}^2 + \frac{\Delta_2 \Delta_3}{8\Delta_1} \beta_{23,0}^2 + \frac{\Delta_1 \Delta_3}{8\Delta_2} \beta_{31,0}^2 + O(\Delta \beta_i^2, \Delta \vec{\alpha}^2)} \\ &\times V^{t'}(0, e, \infty) \prod_{i=1}^3 e^{i\alpha_i \cdot M_{i,\alpha}} e^{i\Phi_i \cdot M_{i,\Phi}} V^t(0, e, \infty)^*, \end{aligned} \quad (3.230)$$

where we use the shorthand notation

$$\begin{aligned}\alpha_i \cdot M_{i,\alpha} &= \sum_{b=2}^d \alpha_{i,b} M_{i,1b}, \\ \Phi_i \cdot M_{i,\Phi} &= \sum_{2 \leq a < b \leq d} \Phi_{i,ab} M_{i,ab},\end{aligned}\tag{3.231}$$

where $M_{i,ab}$ denotes a rotation generator with indices ab acting on the i -th point in the representation λ_i . The partition function at high temperature is given by

$$\begin{aligned}Z = \exp \left(\frac{f_{12} \text{vol } S^{d-1}}{\beta_{12,0}^{d-1}} \left(1 - \frac{(\vec{\Phi}_1 - \vec{\Phi}_2)^2}{\beta_{12,0}^2} - 8(d+1) \frac{(\vec{\alpha}_1 + \vec{\alpha}_2)^2}{\beta_{12,0}^4} + \dots \right) \right. \\ \left. + \frac{f_{23} \text{vol } S^{d-1}}{\beta_{23,0}^{d-1}} \left(1 - \frac{(\vec{\Phi}_2 - \vec{\Phi}_3)^2}{\beta_{23,0}^2} - 8(d+1) \frac{(\frac{1}{4}\vec{\alpha}_2 - \frac{1}{2}\vec{\alpha}_3)^2}{\beta_{23,0}^4} + \dots \right) \right. \\ \left. + \frac{f_{31} \text{vol } S^{d-1}}{\beta_{31,0}^{d-1}} \left(1 - \frac{(\vec{\Phi}_3 - \vec{\Phi}_1)^2}{\beta_{31,0}^2} - 8(d+1) \frac{(\frac{1}{4}\vec{\alpha}_1 - \frac{1}{2}\vec{\alpha}_3)^2}{\beta_{31,0}^4} + \dots \right) \right).\end{aligned}\tag{3.232}$$

Here, we have allowed for different free energy densities f_{ij} at each hot spot. This would arise if we inserted topological defects into the partition function, for example symmetry operators, as discussed in Section 3.5. Our main case of interest is where $f_{ij} = f$ (the thermal free energy density), but it is just as straightforward to do the computation for general f_{ij} . Finally, the measure at high temperature is

$$d\mu = \frac{2^{4d}}{(\text{vol SO}(d-1))^2} \prod_{i=1}^3 d\beta_i d^{d-1} \vec{\alpha}_i d^{\frac{(d-1)(d-2)}{2}} \vec{\Phi}_i.\tag{3.233}$$

We would now like to integrate (3.229) to extract the density of OPE coefficients. We deform the contour so that it passes through the regime of high temperature. We will organize the calculation as follows. We split the integrand into the form

$$(\text{quickly varying}) \times (\text{slowly varying}).\tag{3.234}$$

Here "quickly varying" includes terms that are exponential in large parameters like Δ or $1/\beta^\#$, while "slowly varying" includes everything else. We look for a saddle point of the "quickly varying" terms, writing them as a gaussian centered at this saddle point, times perturbative corrections. Meanwhile, we expand the (slowly varying) part perturbatively around the saddle point.

One simplification of this way of organizing the calculation is that, because we are working in the regime $J \ll \Delta$, terms in the conformal block of the form $V^* h_1 h_2 h_3 V$

will be included among the slowly-varying terms, and will not affect the location of the saddle point. By symmetry, the saddle point will be located at $\vec{\alpha}_i = \vec{\Phi}_i = 0$.

Let us analyze the size of fluctuations around the saddle point. In particular, we would like to determine which terms must be kept in our approximation to the conformal block and the partition function. The quickly-varying (i.e. exponential in Δ) part of the block has the schematic form

$$B \sim e^{-\Delta\beta - \Delta\beta^2 - \Delta\vec{\alpha}^2 + \dots}, \quad (3.235)$$

where "... " are higher-order corrections in β, α, Φ . Meanwhile, the quickly-varying part of the partition function has the form

$$Z \sim \exp\left(\frac{1}{\beta^{\frac{d-1}{2}}} \left(1 - \frac{\vec{\Phi}^2}{\beta} - \frac{\vec{\alpha}^2}{\beta^2}\right)\right). \quad (3.236)$$

Here, β schematically denotes the individual β_i , not the relative $\beta_{ij,0}$.

The saddle point equation for β will set $\Delta \sim \beta^{-(d+1)/2}$. Plugging this in, we find

$$ZB \sim \exp\left(\frac{1}{\beta^{\frac{d-1}{2}}} - \frac{\vec{\Phi}^2}{\beta^{\frac{d+1}{2}}} - \frac{\vec{\alpha}^2}{\beta^{\frac{d+3}{2}}} - \frac{\vec{\alpha}^2}{\beta^{\frac{d+1}{2}}}\right). \quad (3.237)$$

There are two $\vec{\alpha}^2$ terms: one coming from the block (3.235) and one coming from the partition function (3.236). We see that the $\vec{\alpha}^2$ term coming from the partition function is more important — it is enhanced by an additional power of $1/\beta$. Thus, we can ignore the quadratic $\vec{\alpha}$ -dependence of the conformal block. In other words, the terms written explicitly in (3.230) are sufficient for our purposes. Overall, the characteristic size of fluctuations in the angular variables coming from (3.148) is

$$\vec{\alpha} \sim \beta^{\frac{d+3}{4}} \sim \Delta^{-\frac{1}{2} - \frac{1}{d+1}}, \quad \vec{\Phi} \sim \beta^{\frac{d+1}{4}} \sim \Delta^{-\frac{1}{2}}. \quad (3.238)$$

The saddle point for the quickly-varying terms is located at $\vec{\alpha}_i = 0, \vec{\Phi}_i = 0$, and

$$\beta_{12,0} = \left(\frac{4(d-1)f_{12}\text{vol } S^{d-1}\Delta_3}{\Delta_1\Delta_2}\right)^{\frac{1}{d+1}}, \quad (3.239)$$

together with cyclic permutations of (3.239). The Hessian matrix at the saddle point splits into three separate blocks: a block for the β_i , a block for the $\vec{\alpha}_i$, and a block for the $\vec{\Phi}_i$. Thus, we can calculate the 1-loop determinant separately in each of these

sets of variables. The determinant for the β_i and $\vec{\alpha}_i$ variables is straightforward:

$$\begin{aligned} \text{1-loop } \beta_i \text{ factor} &= \left(\frac{(\beta_{12,0}\beta_{23,0}\beta_{31,0})^{d+3}}{4f_{12}f_{23}f_{31}} \left(\frac{\pi}{2(d^2-1)\text{vol } S^{d-1}} \right)^3 \right)^{\frac{1}{2}}, \\ \text{1-loop } \vec{\alpha}_i \text{ factor} &= \left(\frac{(\beta_{12,0}\beta_{23,0}\beta_{31,0})^{d+3}}{4f_{12}f_{23}f_{31}} \left(\frac{\pi}{2(d+1)\text{vol } S^{d-1}} \right)^3 \right)^{\frac{d-1}{2}}. \end{aligned} \quad (3.240)$$

To compute the $\vec{\Phi}_i$ determinant, we must fix the $\text{SO}(d-1)$ gauge redundancy that simultaneously shifts the $\vec{\Phi}_i$. For example, we can set $\vec{\Phi}_3 = 0$ and compute the 1-loop determinant in $\vec{\Phi}_1, \vec{\Phi}_2$, multiplying the result by $\text{vol } \text{SO}(d-1)$ to account for the volume of the $\text{SO}(d-1)$ orbit. This gives

$$\begin{aligned} \text{1-loop } \vec{\Phi}_i \text{ factor} \\ = \text{vol } \text{SO}(d-1) \left(\left(\frac{\text{vol } S^{d-1}}{\pi} \right)^2 \left(\frac{f_{12}f_{23}}{(\beta_{12,0}\beta_{23,0})^{d+1}} + \frac{f_{12}f_{31}}{(\beta_{12,0}\beta_{31,0})^{d+1}} + \frac{f_{23}f_{31}}{(\beta_{23,0}\beta_{31,0})^{d+1}} \right) \right)^{-\frac{(d-2)(d-1)}{4}}. \end{aligned} \quad (3.241)$$

Putting everything together, plugging in the saddle point values (3.239), we find the asymptotic conformal block coefficients

$$\begin{aligned} P_{123}^{ss'} \sim (T^{-1})^{ss'} \left(\prod_{i=1}^3 \frac{\dim \lambda_i}{\text{vol } \text{SO}(d)} \right) \frac{\pi^{\frac{(d+2)(d-2)}{2}} (4(d-1))^{\frac{d^2}{2} - \frac{3}{d+1} + \frac{5}{2}}}{2^{\frac{d}{2}} (d+1)^{\frac{3d}{2}}} \left(8f_{12}f_{23}f_{31}(\text{vol } S^{d-1})^3 \right)^{\frac{d}{d+1}} \\ \times \frac{(\Delta_1 + \Delta_2 + \Delta_3)^{2(\Delta_1 + \Delta_2 + \Delta_3) - 3d}}{(\Delta_1^2 + \Delta_2^2 + \Delta_3^2)^{\frac{(d-2)(d-1)}{4}} \prod_{i=1}^3 (2\Delta_i)^{2\Delta_i - \frac{d(d-1)}{2(d+1)}}} \\ \times \exp \left[(d+1) \left(\frac{\text{vol } S^{d-1}}{2} \right)^{\frac{2}{d+1}} \left(f_{12}^{\frac{2}{d+1}} \left(\frac{\Delta_1\Delta_2}{8(d-1)\Delta_3} \right)^{\frac{d-1}{d+1}} + \text{cycl.} \right) \right], \end{aligned} \quad (3.242)$$

where "+cycl." denotes a sum over cyclic permutations of 123. This result is valid for large Δ_i with the spin-representations λ_i fixed, up to subleading corrections at large Δ_i . Our approximation for the asymptotic squared OPE coefficients is then

$$(c_{123}^{s'})^* c_{123}^s \sim \frac{P_{123}^{ss'}}{\rho_1 \rho_2 \rho_3}, \quad (3.243)$$

where ρ_i are the densities of states of the CFT computed in Section 3.3 for the representations $\pi_i = (\Delta_i, \lambda_i)$. (In the case, where we refine the partition function with topological defects, the density ρ_i should be the appropriate density of states with that defect inserted.)

As an example, let us study $P_{123}^{ss'}$ for identical-dimension scalars in various dimensions. In 2D, the rotation representations are one dimensional, there is a unique conformal three-point structure, and the corresponding T matrix is simply $T = 1/2$. Plugging this in, we find the high energy density of (global primary) OPE coefficients in 2D:

$$2D : P_{\Delta\Delta\Delta} \sim \left(\frac{3}{2}\right)^{6\Delta-9} \frac{f^2 e^{\frac{9}{2}(\pi^2 f^2 \Delta)^{1/3}}}{\pi \Delta^5}. \quad (3.244)$$

In 3D, the T matrix is diagonalized in the q -basis of [142]. Specifically, it is given by [130]

$$T^{[q_1 q_2 q_3], [q'_1 q'_2 q'_3]} = \frac{1}{2^3 2\pi} \prod_{i=1}^3 \binom{2J_i}{J_i + q_i}^{-1} \delta_{q_i q'_i}. \quad (3.245)$$

Plugging this into (3.242), we find the high energy density of OPE coefficients in 3D:

$$3D : P_{(\Delta, J_1)(\Delta, J_2)(\Delta, J_3)}^{[q_1 q_2 q_3], [q'_1 q'_2 q'_3]} \sim \left(\frac{3}{2}\right)^{6\Delta} \frac{2^{\frac{49}{4}} f^{\frac{9}{4}} e^{3\sqrt{2\pi f \Delta}}}{3^{\frac{19}{2}} \pi^{\frac{1}{4}} \Delta^{\frac{31}{4}}} \prod_{i=1}^3 (2J_i + 1) \binom{2J_i}{J_i + q_i} \delta_{q_i q'_i}. \quad (3.246)$$

- A subleading correction

It is straightforward to take into account perturbative corrections around the saddle point. For example, let us highlight the leading correction that is not proportional to the $T^{ss'}$ three-point structure matrix. It comes from the Φ^2 term in the expansion of

$$V^{t'}(0, e, \infty) \prod_i e^{i\Phi_i \cdot M_i \cdot \Phi} V^t(0, e, \infty)^* \quad (3.247)$$

in the genus-2 block. Performing the Gaussian integral and using the fact that $M_{1,\Phi} + M_{2,\Phi} + M_{3,\Phi} = 0$ (because the three-point structures are $\text{SO}(d-1)$ -invariant), we find a multiplicative correction of the form

$$\vec{\Phi}_i^2\text{-correction} = \left(1 - (d-1) \frac{\Delta_1^2 \Delta_2^2 M_{3,\Phi}^2 + \Delta_2^2 \Delta_3^2 M_{1,\Phi}^2 + \Delta_3^2 \Delta_1^2 M_{2,\Phi}^2}{\Delta_1 \Delta_2 \Delta_3 (\Delta_1^2 + \Delta_2^2 + \Delta_3^2)}\right). \quad (3.248)$$

Here, $M_{i,\Phi}^2$ are the Casimirs of the $\text{SO}(d-1)$ subgroup of $\text{SO}(d)$. As discussed in [130], the three-point pairing matrix $T^{s's}$ can be simultaneously diagonalized together with the $M_{i,\Phi}^2$. For example, in three dimensions, we have $M_{i,\Phi}^2 = q_i^2$ in the q -basis. It will be interesting in the future to compute the full spin-dependence of the asymptotic OPE coefficients by computing the genus-2 blocks in the regime of finite J/Δ .

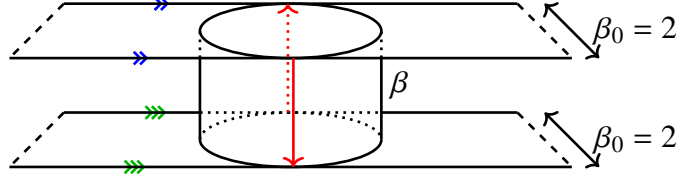


Figure 3.11: A geometry that encodes a sum of squares of thermal one-point functions. The top surface is a copy of thermal flat space $S^1_{\beta_0=2} \times \mathbb{R}^{d-1}$, with a unit ball removed. The ball is tangent to itself because it wraps completely around the thermal circle of length $\beta_0 = 2$. The bottom is the same as the top. The top and bottom are connected by a cylinder of length β and angular twist $h \in \text{SO}(d)$. The periodicity of each copy of thermal flat space is illustrated via arrow marks, indicating loci that should be identified. The hot spot thermal circle (red) runs down the cylinder in the front of the figure, and back up the cylinder in the back of the figure.

3.8 Asymptotics of thermal 1-point functions

We can also use the techniques developed in this work to determine asymptotics of thermal 1-point functions. (In fact, one can think of high-energy thermal 1-point functions as a particular limit of heavy-heavy-heavy OPE coefficients.) One nice thing about this exercise is that, because the blocks are so simple, we can easily invert the partition function for arbitrary J/Δ . For brevity, we will only determine the leading exponential form of the thermal 1-point coefficients, leaving 1-loop determinants and subleading corrections for later work.

Recall that the 1-point function of a primary operator \mathcal{O} at inverse temperature β_0 is fixed by symmetries to be [119]

$$\langle \mathcal{O}^{\mu_1 \dots \mu_J} \rangle_{\beta_0} = \frac{b_{\mathcal{O}}}{\beta_0^\Delta} (e^{\mu_1} \dots e^{\mu_J} - \text{traces}), \quad (3.249)$$

where $e = (1, 0, \dots, 0)$ is a unit vector in the Euclidean time direction, and $b_{\mathcal{O}}$ is an operator-dependent thermal 1-point coefficient. Only even-spin traceless symmetric tensors have nonvanishing thermal 1-point functions.

We can build a geometry that measures squares of the 1-point coefficients $b_{\mathcal{O}}$ as follows. We start with two copies of thermal flat space $S^1_{\beta_0=2} \times \mathbb{R}^{d-1}$ at inverse temperature $\beta_0 = 2$. From each copy, we drill out unit balls, so that the balls wrap around the thermal circle and are self-tangent. We then glue the boundaries of the two balls together with a cylinder of length β (not equal to β_0 !) and angular twist $h \in \text{SO}(d)$; see Figure 3.11. By the cutting and gluing arguments of Section 3.5,

this geometry computes

$$\begin{aligned} Z &= \frac{1}{|Z_{\text{glue}}(1)|^2} \sum_O \langle O \rangle_{\beta_0=2} \langle h \cdot O \rangle_{\beta_0=2} e^{-\beta(\Delta+\varepsilon_0)} \\ &= \frac{1}{|Z_{\text{glue}}(1)|^2} \sum_O \frac{b_O^2}{2^{2\Delta}} q_J \mathcal{P}_J(\cos \theta) e^{-\beta(\Delta+\varepsilon_0)}. \end{aligned} \quad (3.250)$$

Here, we used the fact that thermal 1-point functions are $\text{SO}(d-1)$ -invariant to write h as a rotation away from the e -axis by an angle θ . The function $\mathcal{P}_J(\cos \theta)$ is a Gegenbauer polynomial, given by

$$\mathcal{P}_J(x) = {}_2F_1(-J, J+d-2, \frac{d-1}{2}, \frac{1-x}{2}), \quad (3.251)$$

and q_J is given by

$$q_J = \frac{\Gamma(\frac{d-2}{2})\Gamma(J+d-2)}{2^J \Gamma(d-2)\Gamma(J+\frac{d-2}{2})}. \quad (3.252)$$

In the limit $\beta \rightarrow 0$, this geometry develops a hot spot. The emergent thermal circle goes down the cylinder starting at a point of tangency, and then back up the diametrically opposite side of the cylinder to the starting point. To determine the hot-spot partition function, we should find the conformal group element that glues the plane to itself near this hot spot. On the each copy of the plane, we have a thermal periodicity

$$x \sim e^{2P^1} x, \quad x' \sim e^{2P^1} x', \quad (3.253)$$

where P^1 generates translations in the Euclidean time direction. Meanwhile, the cylinder induces an identification between the two coordinates

$$x = e^{-\beta D} h I x'. \quad (3.254)$$

The hot-spot thermal circle thus corresponds to the group element

$$g_{\text{hot}} = e^{-2P^1} (e^{-\beta D} h I)^{-1} e^{2P^1} (e^{-\beta D} h I). \quad (3.255)$$

We can define a relative temperature and angle from the eigenvalues of g_{hot} :

$$(e^{\pm\beta_{\text{rel}}}, e^{\pm i\theta_{\text{rel}}}, 1, \dots, 1) = \text{eigenvalues}(g_{\text{hot}}). \quad (3.256)$$

Note that h can be brought to the form of a rotation between the 1 and 2 axes. Then $\text{SO}(d-2)$ symmetry guarantees that the eigenvalues of g_{hot} take the above form. The leading contribution to the partition function from the hot spot is

$$Z \sim \exp \left(\frac{f \text{vol} S^{d-1}}{\beta_{\text{rel}}^{d-1} (1 + \Omega_{\text{rel}}^2)} \right) = \exp \left(\frac{f \text{vol} S^{d-1}}{\beta_{\text{rel},0}^{d-1}} \left(1 - 32(d+1) \frac{\theta^2}{\beta_{\text{rel},0}^4} + \dots \right) \right), \quad (3.257)$$

where

$$\beta_{\text{rel},0} = \cosh^{-1} \left(1 - 8e^\beta + 8e^{2\beta} \right) = 4\sqrt{\beta} + \dots \quad (3.258)$$

is the relative inverse temperature when $\theta = 0$, and this formula is valid for $\theta^2/\beta^2 \ll 1$ and $\beta \ll 1$. Formula (3.257) is the analog of (3.148) from the genus-2 calculation.

All that remains is to invert (3.257) to determine the asymptotics of the coefficients b_O . In doing so, we can use the orthogonality relation for Gegenbauer polynomials

$$\int_0^\pi d\theta \sin^{d-2} \theta \mathcal{P}_J(\cos \theta) \mathcal{P}_{J'}(\cos \theta) = n_J \delta_{JJ'}, \quad (3.259)$$

where

$$n_J = \frac{\pi \Gamma(J+1)}{\Gamma(\frac{d-2}{2})^2 (J + \frac{d-2}{2}) \Gamma(J+d-2)}. \quad (3.260)$$

When we integrate $\mathcal{P}_J(\cos \theta)$ in θ against the Gaussian in (3.257), the integral will be dominated by small θ with fixed θJ . In this regime, we can use an approximation for the Gegenbauer function in terms of a Bessel function (which plays an important role in dispersive bounds on scattering amplitudes [52]):

$$\lim_{J \rightarrow \infty, \theta J \text{ fixed}} \mathcal{P}_J(\cos \theta) = \frac{\Gamma(\frac{d-1}{2})}{(\theta J/2)^{\frac{d-3}{2}}} J_{\frac{d-3}{2}}(\theta J) = \int \frac{d\vec{n}}{\text{vol } S^{d-2}} e^{i J \vec{n} \cdot \vec{\theta}}. \quad (3.261)$$

Here, $J_\alpha(x)$ is a Bessel function. In the right-hand formula, \vec{n} is a point on the unit S^{d-2} , and we think of $\vec{\theta}$ as a vector in \mathbb{R}^{d-1} with norm $|\vec{\theta}| = \theta$. The idea is that $\mathcal{P}_J(\cos \theta)$ satisfies a wave equation on S^{d-1} . In the limit of large J with small θ , we can zoom in near the locus $\theta = 0$, where the S^{d-1} becomes flat space \mathbb{R}^{d-1} . We are left with a linear combination of solutions to the wave equation in flat space, i.e. plane waves. In this limit, the measure $d\theta \sin^{d-2} \theta$ becomes equivalent to the usual measure $d^{d-1} \vec{\theta}$ on \mathbb{R}^{d-1} .

Thus, overall, the angular integral from inverting the partition function takes the form

$$\begin{aligned} & \int \frac{d\vec{n}}{\text{vol } S^{d-2}} \int d^{d-1}\vec{\theta} e^{iJ\vec{n}\cdot\vec{\theta}} \exp\left(-\frac{32(d+1)f\text{vol } S^{d-1}}{\beta_{\text{rel},0}^{d+3}}\vec{\theta}^2\right) \\ &= \exp\left(-\frac{\beta_{\text{rel},0}^{d+3}}{128(d+1)f\text{vol } S^{d-1}}J^2\right) \times \text{1-loop determinant.} \end{aligned} \quad (3.262)$$

At the same time, we must perform an inverse Laplace transform in β . This integral can be done by saddle point, with the overall result

$$\frac{b_O^2 \rho(\Delta, J)}{2^\Delta} q_J n_J \sim \exp\left(\frac{1}{\Delta} \left(\frac{d+1}{d-1}\Delta^2 - \frac{d-1}{d+1}J^2\right) \left(\frac{(d-1)f\text{vol } S^{d-1}}{2^{2d-1}\Delta}\right)^{\frac{2}{d+1}}\right), \quad (3.263)$$

where $\rho(\Delta, J)$ is the density of states for traceless symmetric tensors.

3.9 Discussion

In this paper, we studied the asymptotic behavior of CFT data at large energy. Using the thermal effective action, we looked at both the density of states and the three-point-functions of heavy operators as a function of Δ, J . There are a number of interesting future directions to study.

Density of states

The formula (3.74) for the density of states is valid in a specific region of Δ, J . For example, in CFT_3 , it is valid when

$$\Delta - |J| \gg \sqrt{f\Delta}. \quad (3.264)$$

This notably has no overlap with the regime of large spin with fixed twist described by the lightcone bootstrap [92, 138]. Naively, the lightcone bootstrap suggests that the spectrum of interacting CFT should look like Mean Field Theory in this regime [6, 91, 195]. It would be interesting if one could prove this statement using some kind of effective action, perhaps by compactifying the CFT on a null circle. It would be also interesting to study how the spectrum of operators can behave *between* these regions. For instance, for interacting 3D CFTs, is the density of states at large spin with twist obeying

$$\Delta^0 \ll \Delta - |J| \ll \sqrt{f\Delta} \quad (3.265)$$

universal or theory-dependent?

One could also ask to further refine our general entropy formulas. In [128], a universal formula for CFT_d with global symmetry was found. It would be nice to combine them and obtain universal formulas as a function of energy, spin, and global charges.

In Section 3.4, we compared the predictions of the thermal effective action to exact results in free theories and Einstein gravity, finding excellent agreement. In Appendix 3.9, we give a preliminary comparison between the thermal effective action for the $S^1 \times S^2$ partition function and numerical bootstrap data for the 3D Ising CFT. One could also consider other theories where a large number of operators are known from numerics, e.g. the $O(2)$ model [63, 152]. Obtaining accurate information about large-twist operators is a challenge for the numerical bootstrap, which seems to be most sensitive to the lowest-twist Regge trajectories [195]. (Computing a large number of heavy-heavy-heavy OPE coefficients with the numerical bootstrap is likely even more challenging.)

In 2D CFTs, it is possible to make very precise statements about the spectrum of high energy states using more sophisticated tools than Laplace transforms and saddle point approximations; see e.g. [24, 73, 94, 168, 170, 174, 175]. Such techniques typically rely on nonperturbative input coming from modular invariance. Is it possible to derive similarly precise statements in higher dimensions? What additional information about the partition function is needed?

Effective actions

We parametrized our ignorance of the $d-1$ -dimensional gapped theory upon compactifying on a thermal circle via an effective action, with an infinite set of Wilson coefficients. Can we place bounds on these Wilson coefficients? For instance, as discussed in Section 3.2, we know that $f > 0$. Are there similar bounds (in either direction) on c_1 , c_2 , or other higher-derivative Wilson coefficients? One possible approach is to consider Weinberg-like sum rules relating two-point functions in the IR (described by the thermal effective action) and the UV (described by the CFT), as was recently done in [70]. Another approach is to consider the compactified theory in $(d-2, 1)$ (Lorentzian) signature and study dispersive bounds on scattering, following e.g. [2, 50, 137].

It may also be interesting to study perturbative examples. For example, the value of f in the 3D $O(N)$ models at large N was computed long ago by Sachdev [186]. To our knowledge, higher Wilson coefficients in the thermal effective action, like the

coefficients of F^2 and \widehat{R} , have not yet been computed for the $O(N)$ models.

In this work, we obtained all of our results purely using equilibrium hydrodynamical information. Recently, there has been a surge of progress in non-equilibrium hydrodynamics for CFTs; see [35, 150] for reviews. What additional CFT data can be predicted using this more sophisticated machinery? See [74, 131] for recent work in this direction. Can one study non-equilibrium dynamics at higher genus?

There has also been tremendous recent progress applying other effective actions to characterize asymptotic CFT data, for example the effective theory of large charge [111, 121, 167]. One way of summarizing our "hot spot" analysis of the genus-2 partition function is the idea of using an EFT in the part of a geometry where it is valid (the hot spots), and factoring out the part where the EFT is not valid (the region away from the hot spots). Can this "hot spot" idea be useful in other contexts like large charge?

Three-point functions and genus-2 blocks

So far, we calculated asymptotic OPE coefficients to leading order at large Δ , with fixed spin. It would be interesting to allow the spin to grow large with Δ , as we did for the density of states. In particular, this would require a more general expression for the genus-2 conformal block at large quantum numbers.

Genus-2 blocks are interesting objects in their own right, and it would be interesting to study their properties more systematically, both at large and non-large quantum numbers. For example, can we find recursion relations for genus-2 blocks similar to those in [86, 139, 140, 177, 206]? Can we explore genus-2 blocks from the perspective of integrability [120]? Is there a clearer understanding of the interesting saddle-point dynamics uncovered in Section 3.6? Do there exist Lorentzian shadow representations [179] or holographic representations [114] for higher-genus blocks, and do they admit any interesting kinematic limits? The literature on global conformal blocks for correlation functions of local operators is vast, but global genus-2 blocks are essentially unexplored.

We would also like to understand how to systematically improve our three-point function result. For the density of states, we understand how to systematically improve the result by keeping further terms in the thermal effective action. However, for the three-point function, corrections come in two types: higher derivative terms in the effective action (which are easy to include), and corrections to the hot spot assumption, as discussed in Sec. 3.5. In order to understand how to systematically

improve the estimate for the HHH three-point functions, we need to understand contributions to the partition function outside of the hot spot regions, namely understanding the quantity R defined in (3.145). Explicitly computing examples of "genus-two" partition functions, either for free or holographic theories, could be instructive.

It is also worthwhile to compare our result to known results CFT₂. In [67], it was shown that HHH, HHL, and HLL asymptotic density of states for Virasoro primary operators are all related to analytic continuations of the DOZZ formula — the structure constants of Liouville theory. In higher dimensions, asymptotic formulas for HLL OPE coefficients have been studied using Tauberian techniques and inversion formulae [169, 176, 185]. Furthermore, it is well-known that HHL OPE coefficients are related to thermal one-point functions. These computations, together with our genus-2 computation seem to involve different physics. It would be extremely interesting if there were a unifying perspective or formula similarly to 2D.

Bootstrap axioms and crossing equations

To what extent are our results for the density of states and OPE coefficients encoded in the usual bootstrap conditions — namely unitarity and crossing symmetry of local correlation functions? In 2D, modular invariance is known to be independent from crossing symmetry of local correlators. By analogy, this suggests that perhaps the formulas we derived from the thermal effective action are *independent* from the usual bootstrap axioms.³⁰ If so, should we enlarge the axioms to include them? What is the minimal set of extra axioms that we need? In 2D, modular invariance can be interpreted as crossing symmetry of twist operators. Can our results in higher dimensions be interpreted in terms of traditional bootstrap axioms applied to appropriate twist operators?

As we mentioned briefly in Section 3.5, there exists another decomposition of the genus-2 partition function $Z(M_2)$ into a sum over states: the "dumbbell" channel, which expresses $Z(M_2)$ as a sum of squares of 1-point functions on $S^1 \times S^{d-1}$. The dumbbell channel has its own conformal blocks, which as far as we know have not been studied in detail. (The blocks discussed in Section 3.8 can be thought of as a limiting case of these dumbbell blocks.) Furthermore, one can formulate a crossing equation relating the dumbbell channel to the channel considered in this work. As

³⁰We thank Dalimil Mazáč for pointing this out.

pointed out in [64] for $d = 2$, this crossing equation enjoys manifest positivity properties needed for numerical bootstrap applications. It would be very interesting to explore it in both two-dimensional and higher-dimensional theories.

Ensembles and holographic theories

There is an important difference between our higher-dimensional result for asymptotic OPE coefficients and the 2D results of [44, 67]. The results of [44, 67] were for OPE coefficients of *Virasoro* primaries, while our results are for OPE coefficients of *global* primaries. In the case of the density of states, there isn't a huge difference between Virasoro and global primaries. But the story is different for OPE coefficients, where descendant states play an important role. We can see this by comparing the leading exponential behavior of Virasoro and global OPE coefficients in 2D:

$$P_{\Delta\Delta\Delta}^{\text{global}} \sim \left(\frac{3}{2}\right)^{6\Delta} \quad \gg \quad P_{\Delta\Delta\Delta}^{\text{Virasoro}} \sim \left(\frac{27}{16}\right)^{3\Delta}. \quad (3.266)$$

We see that typical global primaries have much larger OPE coefficients than typical Virasoro primaries.³¹ In other words, the statistics of CFT data in a theory with Virasoro symmetry has more structure than is captured by $P_{\Delta\Delta\Delta}^{\text{global}}$.

These statements are interesting to consider in a holographic CFT. In a holographic 2D CFT, a high energy Virasoro primary is interpreted as a black hole microstate, while a Virasoro descendant is a black hole orbited by boundary gravitons. We have found that states with boundary gravitons typically have much larger OPE coefficients than pure black hole microstates. While we don't have an analog of Virasoro symmetry in higher dimensions, we can conjecture an analogous statement for higher-dimensional CFTs: we expect that typical states of black holes with orbiting matter have much larger OPE coefficients than pure black hole microstates. It would be very interesting to make this more precise, for example by performing a holographic computation of OPE coefficients of pure black hole microstates via an appropriate wormhole geometry.

The authors of [58] used $P_{\Delta\Delta\Delta}^{\text{Virasoro}}$ to define an interesting "ensemble" of CFT data. In their ensemble, OPE coefficients are (almost) gaussian random variables whose variance is set by $P_{\Delta\Delta\Delta}^{\text{Virasoro}}/\rho(\Delta)$ ³. Remarkably, the predictions of this ensemble turn out to agree with bulk 3D gravity. The result (3.266) indicates that an analogous ensemble based on $P_{\Delta\Delta\Delta}^{\text{global}}$ would not have refined-enough information to recover

³¹Similarly, by comparing scaling blocks and full genus-2 blocks in the high temperature regime, we conclude that typical states have much larger OPE coefficients than typical global primaries.

bulk gravity in 2D (presumably also in higher d). However, it is interesting to ask whether any interesting physics *would* be captured by an ensemble built from $P_{\Delta\Delta\Delta}^{\text{global}}$. In the spirit of [17, 20, 58, 122], we can imagine starting with a completely general ensemble of CFT data. We can refine this ensemble with knowledge of the partition functions on $S_\beta^1 \times S^{d-1}$ and the "genus-2" geometry M_2 . We could additionally refine the ensemble with other information like local correlation functions and thermal one-point functions. At what point does the refined ensemble begin to make nontrivial predictions that can be tested in additional observables, and what are those predictions?

Bulk locality for thermal observables

HPPS famously conjectured that any unitary CFT with large c_T and a large gap Δ_{gap} in the spectrum of higher-spin single-trace operators should agree with a local gravitational EFT in AdS [107]. Recently, there has been significant progress proving this statement for correlators of local operators in the CFT vacuum [3, 19, 51, 103, 135]. However, holography implies analogous statements in nontrivial backgrounds as well — in particular a thermal background. For example, the Wilson coefficients f, c_1, c_2 , etc. in the thermal effective action of a theory satisfying HPPS conditions should agree with those of Einstein gravity, up to small corrections suppressed by $1/\Delta_{\text{gap}}$. How can we prove the emergence of black hole physics using field-theoretic methods? Can we formulate dispersion relations in a black hole background? For recent work in these direction, see [49].

Completing the square in the thermal bootstrap

An interesting feature of our formulas (3.250) and (3.257) is that they provide a kind of sum rule for squares of thermal 1-point coefficients b_O^2 . Such a sum rule could in principle be used to "complete the square" in the bootstrap equations studied in [118, 119].

The works [118, 119] studied crossing symmetry of thermal two-point functions, which have an expansion in products $c_{\phi\phi O} b_O$, where $c_{\phi\phi O}$ are bulk OPE coefficients. Unfortunately, we do not know the sign of $c_{\phi\phi O} b_O$, and this prevents one from applying traditional numerical bootstrap techniques [181]. (The same issue appears in the study of boundary and defect two-point functions [148].) Ideally, one would like to complete the square by finding other crossing equations in which $c_{\phi\phi O}$ and b_O appear quadratically. Then, one can treat $c_{\phi\phi O} b_O$ as an off-diagonal element in a positive-definite 2×2 matrix and apply numerical bootstrap techniques for mixed

correlators [139].

A crossing equation where $c_{\phi\phi O}$ appears quadratically is easy to find: it is just the usual crossing equation for vacuum four-point functions! Tantalizingly, the formulas (3.250) and (3.257) have b_O appearing quadratically, but unfortunately they are not as precise as the usual four-point crossing equation, due to our use of the hot-spot ansatz. It would be interesting to go beyond the hot-spot ansatz and find a sum rule precise enough to be used in the numerical bootstrap.

"Sphere packing" and other hot-spot geometries

In addition to the "genus-2" manifold M_2 studied in this work, there are many additional geometries that encode statistics of CFT data and can be studied using the hot-spot idea. Partition functions on these geometries are examples of "generalized spectral form factors" [20].

As a simple example, consider a higher-genus generalization of M_2 , where we take two copies of \mathbb{R}^d , drill out $n > 3$ balls from each copy, and connect the boundaries of the balls with cylinders. The partition function on this geometry encodes a sum of squared n -point correlation functions of the CFT, schematically

$$\sum_{O_1, \dots, O_n} |\langle O_1 \cdots O_n \rangle|^2 e^{-\sum_i \beta_i \Delta_i}. \quad (3.267)$$

If two balls are tangent in (both copies of) \mathbb{R}^d , we obtain a hot spot when the corresponding cylinders shrink to zero length.

The hot spot ansatz is most useful when there are a maximal number of hot spots, and all other moduli of the geometry are frozen. Thus, we should consider configurations where most of the balls are mutually tangent — i.e. sphere packings!³² For example, the packing shown in Figure 3.12 encodes interesting asymptotics of CFT four-point functions.

We can construct an even more general "higher genus" manifold as follows. We take m copies of \mathbb{R}^d and drill out various numbers of balls from each copy, such that there are an even number of balls in total. We then connect pairs of balls with cylinders. This computes a sum of products of m correlation functions

$$\sum_{O_1, \dots, O_n} \underbrace{\langle \cdots \rangle \cdots \langle \cdots \rangle}_m e^{-\sum_i \beta_i \Delta_i}. \quad (3.268)$$

³²See [76, 105] for other connections between sphere packing and conformal field theory.

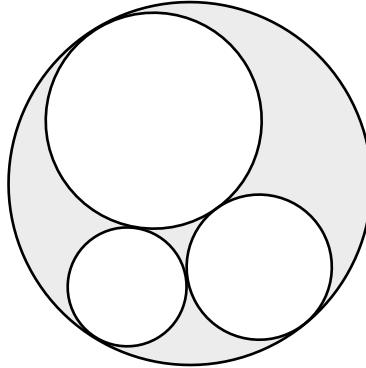


Figure 3.12: A ball with three mutually-tangent balls removed. If we take two copies of this space and glue the boundaries of the balls together with cylinders, analogously to Figure 3.3, we obtain a geometry that computes a sum of squares of CFT four-point functions. When the cylinders shrink, this "sphere packing" geometry contains hot spots at each of the six points of tangency.

Again, hot spots can emerge when cylinders shrink to zero.

Of course, CFT n -point functions for $n > 3$ are determined in terms of 2- and 3-point functions. In this work we have determined asymptotics of 2- and 3-point functions, and it is interesting to ask whether our results can be used to predict partition functions on higher genus geometries, and whether the results agree with the hot-spot ansatz at higher genus. In two dimensions, it is known that crossing symmetry of local four-point functions and torus one-point functions implies crossing symmetry on arbitrary Riemann surfaces. However, we expect that in higher dimensions, hot spot results for higher genus manifolds provide a nontrivial refinement of the statistics computed in this work.

Appendix A Thermal two-point function of momentum generators

In Section 3.3, we study the response of a CFT on $S^1_\beta \times S^{d-1}$ when we twist by a rotation of S^{d-1} . In this appendix, as a warmup, we study the leading term in the twisting parameter in the high temperature limit. This computation reduces to a two-point function of momenta in thermal flat space. We determine this two-point function directly from Ward identities, and then show how the same result can be understood using the thermal effective action.

At high temperature, the radius of curvature of the sphere becomes unimportant, and we can approximate $S^1_\beta \times S^{d-1}$ as thermal flat space $S^1_\beta \times \mathbb{R}^{d-1}$. A rotation generator on the sphere locally looks like a translation on \mathbb{R}^{d-1} . Thus, it suffices to study the

thermal expectation value of a translation group element

$$\langle e^{\vec{a} \cdot \vec{P}} \rangle_\beta = \langle 1 \rangle_\beta + \frac{1}{2} a_i a_j \langle P^i P^j \rangle_\beta + \dots \quad (3.269)$$

The momentum P^i is the integral of T^{0i} on a spatial slice at fixed Euclidean time τ (which can take any value, by conservation):

$$P^i = - \int d\vec{x} T^{0i}(\tau, \vec{x}). \quad (3.270)$$

The $O(a)$ term in (3.269) vanishes by rotation-invariance. For simplicity, in this section we set $\beta = 1$, restoring it when needed by dimensional analysis.

Using Ward identities

Let us focus on the quadratic term in (3.269), given by an integrated two-point function of stress tensors:

$$\frac{1}{\text{vol } \mathbb{R}^{d-1}} \frac{1}{2} a_i a_j \langle P^i P^j \rangle_\beta = \frac{1}{2} a_i a_j \int d\vec{x}_1 \langle T^{0i}(0, \vec{x}_1) T^{0j}(x_2) \rangle_\beta. \quad (3.271)$$

Here, we separated the momentum generators in Euclidean time, placing the first at time $\tau_1 = 0$ and the second at time τ_2 . We furthermore divided by $\text{vol } \mathbb{R}^{d-1}$ to obtain a finite result, and used translation-invariance in \mathbb{R}^{d-1} to fix the second stress tensor at $x_2 = (\tau_2, \vec{x}_2)$.

We claim that the integrated two-point correlator (3.271) is determined by the *one-point* function of the stress tensor at finite temperature. To understand why, we must express it in terms of operators in the dimensionally-reduced $d-1$ -dimensional theory. The first step is to average over Euclidean times τ_1 and τ_2 . However, this averaging is subtle because $T^{0i}(x_1)$ and $T^{0j}(x_2)$ become coincident, and contact terms can contribute. Such contact terms are actually crucial to the calculation, so let us take a moment to define them carefully.

We define (un-normalized) one- and two-point functions of the stress tensor by

$$\sqrt{G(x)} \langle T^{\mu\nu}(x) \rangle = 2 \frac{\delta Z}{\delta G_{\mu\nu}(x)}, \quad (3.272)$$

$$\sqrt{G(x)} \sqrt{G(y)} \langle T^{\mu\nu}(x) T^{\rho\sigma}(y) \rangle = 4 \frac{\delta^2 Z}{\delta G_{\mu\nu}(x) \delta G_{\rho\sigma}(y)}, \quad (3.273)$$

where $Z[G]$ is the partition function. Our definition of the two-point function (3.273) applies at both coincident and non-coincident points, and thus suffices to specify all contact terms. Diffeomorphism invariance of $Z[G]$ implies that

$$0 = \int d^d x \mathcal{L}_\xi G_{\mu\nu} \frac{\delta Z}{\delta G_{\mu\nu}}, \quad (3.274)$$

where \mathcal{L}_ξ denotes the Lie derivative with respect to a vector field ξ^μ . Taking an additional derivative with respect to $G_{\rho\sigma}(y)$, and evaluating in a locally flat metric $G_{\mu\nu} = \delta_{\mu\nu}$, we obtain the following Ward identity for conservation of the stress tensor inside a two-point correlator

$$\begin{aligned} & \int d^d x (\partial_\mu \xi_\nu(x)) \langle T^{\mu\nu}(x) T^{\rho\sigma}(y) \rangle \\ &= (\xi \cdot \partial) \langle T^{\rho\sigma}(y) \rangle + (\partial \cdot \xi) \langle T^{\rho\sigma}(y) \rangle - \partial_\mu \xi^\rho \langle T^{\mu\sigma}(y) \rangle - \partial_\mu \xi^\sigma \langle T^{\mu\rho}(y) \rangle. \end{aligned} \quad (3.275)$$

We can use this identity to average the correlator (3.271) over Euclidean time. Consider the vector field

$$\xi^i(\tau, \vec{x}) = -a^i \tau, \quad \xi^0(\tau, \vec{x}) = 0, \quad (3.276)$$

where $\tau \in [0, 1]$. Since τ is periodic, ξ^i has the shape of a "sawtooth" function, with a discontinuity at $\tau = 0$. In particular, we have

$$\partial_\tau \xi^i = a^i (\delta(\tau) - 1). \quad (3.277)$$

Applying (3.275), we find

$$\int d\vec{x}_1 a_i a_j \langle T^{0i}(0, \vec{x}_1) T^{0j}(y) \rangle_\beta = \int d\tau_1 d\vec{x}_1 a_i a_j \langle T^{0i}(\tau_1, \vec{x}_1) T^{0j}(y) \rangle_\beta + a^2 \langle T^{00}(y) \rangle_\beta, \quad (3.278)$$

where we used $\partial \cdot \xi = 0$ and translation invariance $\xi \cdot \partial \langle T^{\rho\sigma} \rangle_\beta = 0$. The right-hand side of (3.278) is the two-point correlator averaged over Euclidean time, plus a nontrivial contact term $a^2 \langle T^{00}(y) \rangle$ that is a consequence of diffeomorphism invariance.

It is natural to define the $d-1$ dimensional stress tensor $t^{ij}(\vec{x})$ and KK current $j^i(\vec{x})$ via derivatives with respect to g_{ij} and A_i in the Kaluza-Klein parametrization (3.8). For example, we have

$$\begin{aligned} \sqrt{g(\vec{x})} \langle t^{ij}(\vec{x}) \rangle &\equiv \frac{\delta Z}{\delta g_{ij}(\vec{x})}, \\ \langle j^i(\vec{x}) j^j(\vec{y}) \rangle &\equiv \frac{\delta^2 Z}{\delta A_i(\vec{x}) \delta A_j(\vec{y})}. \end{aligned} \quad (3.279)$$

A key property of the KK parametrization (3.8) is that gauge transformations $A_i(\vec{x}) \rightarrow A_i(\vec{x}) + \partial_i \lambda(\vec{x})$ are diffeomorphisms of the d -dimensional metric. Consequently, diff-invariance implies that $\langle j^i(\vec{x}) j^j(\vec{y}) \rangle$ is exactly conserved, *even at coincident points*. This will be important in a moment.

At separated points $t^{ij}(\vec{x})$ and $j^i(\vec{x})$ are equivalent to Euclidean time averages of $T^{ij}(\tau, \vec{x})$ and $T^{0i}(\vec{x})$, respectively. However, at coincident points, they differ from naïve averages by contact terms. In particular, the definitions (3.279) and (3.273) imply (on a flat geometry)

$$\langle j^i(\vec{x}_1) j^j(\vec{x}_2) \rangle = \int d\tau_1 d\tau_2 \langle T^{0i}(x_1) T^{0j}(x_2) \rangle + \delta(\vec{x}_1 - \vec{x}_2) \int d\tau_1 \langle T^{ij}(x_1) \rangle. \quad (3.280)$$

The contact term on the right-hand side arises from the quadratic term in A_i in the KK metric: $G_{ij} = g_{ij} + e^{2\phi} A_i A_j$.

Integrating (3.280) over \vec{x}_1 , and combining it with the average of (3.278) over τ_2 , we find

$$\int d\vec{x}_1 a_i a_j \langle T^{0i}(0, \vec{x}_1) T^{0j}(y) \rangle_\beta = a_i a_j \int d\vec{x}_1 \langle j^i(\vec{x}_1) j^j(\vec{x}_2) \rangle - a_i a_j \langle T^{ij} \rangle_\beta + \vec{a}^2 \langle T^{00} \rangle_\beta. \quad (3.281)$$

Finally, we will argue that the integrated correlator $\int d\vec{x}_1 \langle j^i(\vec{x}_1) j^j(\vec{x}_2) \rangle$ vanishes. We can think of it as the momentum-space two-point function $\langle j^i(\vec{p}) j^j(-\vec{p}) \rangle$, evaluated at zero momentum. Rotation-invariance and conservation imply that the momentum-space two-point function takes the form

$$\langle j^i(\vec{p}) j^j(-\vec{p}) \rangle = (\vec{p}^i \vec{p}^j - \delta^{ij} \vec{p}^2) G(|\vec{p}|). \quad (3.282)$$

If the finite-temperature theory has a nonzero mass gap, then $G(|\vec{p}|)$ must be regular near zero momentum (otherwise its Fourier transform would have support at long distances.) Thus, at low momenta, we have

$$\langle j^i(\vec{p}) j^j(-\vec{p}) \rangle = c(\vec{p}^i \vec{p}^j - \delta^{ij} \vec{p}^2) + O(\vec{p}^4). \quad (3.283)$$

In particular, $\langle j^i(\vec{p}) j^j(-\vec{p}) \rangle$ vanishes at $\vec{p} = 0$. Note that conservation of $j^i(\vec{x})$ at coincident points is crucial here. Without it, the momentum-space correlator could have an $O(\vec{p}^0)$ contact term of the form δ^{ij} .

It is instructive to understand this vanishing result in position space as well. In the position-space integral $\int d\vec{x}_1 a_i a_j \langle j^i(\vec{x}_1) j^j(\vec{x}_2) \rangle$, we can write $a_i = \partial_i(\vec{a} \cdot \vec{x}_1)$. Integrating by parts and using conservation, we obtain a boundary term at infinity:

$$a_i a_j \int d\vec{x}_1 \langle j^i(\vec{x}_1) j^j(\vec{x}_2) \rangle = \lim_{R \rightarrow \infty} a_j \int_{|\vec{x}|=R} dS_i(\vec{a} \cdot \vec{x}_1) \langle j^i(\vec{x}_1) j^j(\vec{x}_2) \rangle, \quad (3.284)$$

where dS_i is the surface normal for the sphere $|\vec{x}| = R$. This boundary term (3.284) vanishes provided the two-point function decays sufficiently quickly at large $|\vec{x}|$. In other words,

$$a_i a_j \int d\vec{x}_1 \langle j^i(\vec{x}_1) j^j(\vec{x}_2) \rangle = 0 \quad \text{if} \quad \lim_{|\vec{x}| \rightarrow \infty} |\vec{x}|^{d-1} \langle j^i(\vec{x}) j^j(0) \rangle = 0. \quad (3.285)$$

This condition certainly holds when the finite-temperature theory has a mass gap (since the correlator decays exponentially). However, it also holds more generally. For example, if the finite-temperature theory possesses a massless sector, we expect the current two-point function to decay no slower than a correlator of conserved currents in a $d-1$ dimensional CFT: $\langle j(\vec{x}) j(0) \rangle \sim |\vec{x}|^{-2(d-2)}$. In that case, (3.285) will be satisfied as long as $d > 3$.

Finally, using (3.285) in (3.281), we find

$$\int d\vec{x}_1 a_i a_j \langle T^{0i}(0, \vec{x}_1) T^{0j}(y) \rangle_\beta = -a_i a_j \langle T^{ij} \rangle_\beta + \vec{a}^2 \langle T^{00} \rangle_\beta = -(fd) \vec{a}^2, \quad (3.286)$$

where we used (3.18) for the one-point functions $\langle T^{\mu\nu} \rangle_\beta$. We conclude

$$\langle e^{\vec{a} \cdot \vec{P}} \rangle_\beta = 1 - \frac{fd}{2} T^{d+1} \vec{a}^2 \text{vol} \mathbb{R}^{d-1} + \dots, \quad (3.287)$$

where we have restored factors of T by dimensional analysis. To apply this result to $S_\beta^1 \times S^{d-1}$ with a twist by a rotation of S^{d-1} , we can make the replacement

$$\vec{a}^2 \text{vol} \mathbb{R}^{d-1} \rightarrow \int_{S^{d-1}} d\Omega_{d-1} |v|^2, \quad (3.288)$$

where v is the Killing vector on S^{d-1} implementing the rotation.

Using the thermal effective action

The thermal effective action gives an efficient way to package the Ward identity calculations above and extend them to arbitrary nonlinear order in \vec{a} . Let us see how it recovers the result (3.269). The correlator $\langle e^{\vec{a} \cdot \vec{P}} \rangle$ is captured by the geometry $S_\beta^1 \times \mathbb{R}^{d-1}$ with a twist of \vec{a} around the thermal circle, i.e. an identification

$$(\tau, \vec{x}) \sim (\tau + 1, \vec{x} - \vec{a}). \quad (3.289)$$

To use the thermal effective action, we must put the metric into Kaluza Klein form. We undo the twist with a coordinate transformation

$$\vec{x}' = \vec{x} - \tau \vec{a}. \quad (3.290)$$

This essentially implements averaging over Euclidean time (3.278) by spreading out the twist over the thermal circle. The metric changes to

$$\begin{aligned} d\vec{x}^2 + d\tau^2 &= (d\vec{x}' + \vec{a}d\tau)^2 + d\tau^2 \\ &= d\vec{x}'^2 - \frac{(\vec{a} \cdot d\vec{x}')^2}{1 + \vec{a}^2} + (1 + \vec{a}^2) \left(d\tau + \frac{\vec{a} \cdot d\vec{x}'}{1 + \vec{a}^2} \right)^2. \end{aligned} \quad (3.291)$$

The effective metric is thus

$$\widehat{g}_{ij} = \frac{1}{1 + \vec{a}^2} \left(\delta_{ij} - \frac{a_i a_j}{1 + \vec{a}^2} \right), \quad (3.292)$$

and the thermal effective action is

$$S[\widehat{g}, A] = -f \text{vol } \mathbb{R}^{d-1} \sqrt{\widehat{g}} = -f \text{vol } \mathbb{R}^{d-1} (1 + \vec{a}^2)^{-d/2}. \quad (3.293)$$

Finally, the partition function is

$$e^{-S[\widehat{g}, A]} = e^{f \text{vol } \mathbb{R}^{d-1} (1 + \vec{a}^2)^{-d/2}} = e^{f \text{vol } \mathbb{R}^{d-1}} \left(1 - \frac{fd}{2} \vec{a}^2 \text{vol } \mathbb{R}^{d-1} + \dots \right), \quad (3.294)$$

in agreement with (3.269).

These manipulations are clearly easier and more efficient than those in the previous section. However, detailed manipulations of correlators are instructive as well. For instance, they tell us that (3.269) holds even when the thermal theory is not gapped, as long as $d > 3$. It would be interesting to determine which other results from the thermal effective action continue to hold in non-gapped thermal theories. We leave this problem for future work.

Appendix B Scheme independence

In Section 3.3, we derived (3.41) by working in a scheme where b -type terms S_{ct} are absent from the Weyl anomaly. In this appendix, we describe how (3.41) comes about in a general scheme. The point is that the scheme dependence of the Casimir energy and the thermal effective action cancel each other. For concreteness, let us work in 4D. The partition function on $S_\beta^1 \times S^3$ is

$$\text{Tr} \left[e^{-\beta(D + \frac{3a}{4} - \frac{3b}{8})} \right] \sim e^{-S_{\text{th}}} = e^{-S[\widehat{g}, A] - S_{\text{Euler}} - \text{DR}[S_{\text{ct}}[G]] + \text{DR}[S_{\text{ct}}[\widehat{G}]]}, \quad (3.295)$$

where we have used that $S_\beta^1 \times S^{d-1}$ is conformally-flat to drop Weyl-invariants. Meanwhile, we have

$$\text{DR}[S_{\text{ct}}[G]] = \text{DR}[S_{\text{ct}}[\widehat{G}]] = \int_{S^3} d^3x \sqrt{g} \int_0^1 \beta d\tau \left(-\frac{b}{12(4\pi)^2} R^2 \right) = -\frac{3b}{8} \beta, \quad (3.296)$$

where we used that $R = 6$ on S^3 . Thus, we can cancel the b -dependence on the left-hand side with $\text{DR}[S_{\text{ct}}[G]]$ on the right-hand side, leaving

$$\text{Tr} \left[e^{-\beta(D+\frac{3a}{4})} \right] \sim e^{-S[\widehat{g}, A] + \text{DR}[S_{\text{ct}}[\widehat{G}]] - S_{\text{Euler}}}. \quad (3.297)$$

The combination $-S[\widehat{g}, A] + \text{DR}[S_{\text{ct}}[\widehat{G}]]$ is then scheme-independent, and equal to $S[\widehat{g}, A]$ in the scheme of Section 3.3.

Of course, this cancellation was not an accident. The b -term contribution to the Casimir energy is

$$E_0|_{b\text{-type}} = \frac{1}{\text{vol } \mathbb{R}} S_{\text{ct}}|_{\mathbb{R} \times S^{d-1}}. \quad (3.298)$$

Because S_{ct} is local, it follows that

$$\beta E_0|_{b\text{-type}} = \text{DR}[S_{\text{ct}}]|_{S_\beta^1 \times S^{d-1}}. \quad (3.299)$$

Said another way, the b -term in the Casimir energy is precisely what matches the b -term contribution to the Weyl anomaly on the cylinder. Since the b -term in the thermal effective action was determined by Weyl anomaly matching, it must cancel with the Casimir energy. This argument generalizes to arbitrary d .

Appendix C More on free theories

Partition function of free scalar theories

In this section we review the partition function of a free scalar theory on $\mathbb{R} \times S_R^{d-1}$. This space is conformally equivalent to the Euclidean space \mathbb{R}^d . The energy E of the state on $\mathbb{R} \times S_R^{d-1}$ is related to the scaling dimension Δ of the corresponding field on \mathbb{R}^d via:

$$E = \Delta/R. \quad (3.300)$$

The equation of motion of the free scalar field on $\mathbb{R} \times S_R^{d-1}$ is

$$\left[-\frac{\partial^2}{\partial t^2} + \nabla_{S_R^{d-1}}^2 - \xi \mathcal{R} \right] \phi = 0, \quad (3.301)$$

where ξ is the conformal coupling in d dimensions, $\xi = \frac{d-2}{4(d-1)}$, and \mathcal{R} is the Ricci scalar of S_R^{d-1} , $\mathcal{R} = \frac{(d-1)(d-2)}{R^2}$. The spherical harmonics in d dimension, $Y_l^{(d)}$, are eigenfunctions of $\nabla_{S_R^{d-1}}^2$, with eigenvalue $-l(l+d-2)$, where l is a non-negative integer. We can then construct an orthonormal set of solutions as

$$\phi_l \propto e^{-iEt} Y_l^{(d)}, \quad E = \frac{l + \frac{d-2}{2}}{R}, \quad (3.302)$$

whose elements become each mode after quantization. Note that $Y_l^{(d)}$ is the representation of $Spin(d)$ with the highest weight $(l, 0, \dots, 0)$ in the standard Cartan-Weyl labeling scheme.

We will write down the case of even dimension and odd dimension separately because the group structure of $SO(d)$ is slightly different in these two cases.

Even dimensions

The spherical harmonics $Y_l^{(d)}$ are also eigenfunctions of ∂_{θ_a} in the coordinate system (3.45). The eigenvalues m_a ($a = 1, \dots, n$) of ∂_{θ_a} are integers, and they obey the following relation:

$$l = 2m_0 + |m_1| + \dots + |m_n|, \quad (3.303)$$

where m_0 is a non-negative integer. The multiplicity of this specific eigenvalue is $\binom{n+m_0-2}{m_0}$. Therefore, in even d ($d > 2$), the partition function of a free scalar field is

$$Z(T, \Omega_i) = \prod_{m_0=0}^{\infty} \left(\prod_{m_1=-\infty}^{\infty} \dots \prod_{m_{d/2}=-\infty}^{\infty} \frac{1}{1 - e^{-\frac{1}{T}(2m_0 + \sum_i |m_i| + d/2 - 1 + i \sum_i m_i \Omega_i)}} \right)^{\binom{d/2+m_0-2}{m_0}}, \quad (3.304)$$

where the sums over i in (3.304) run from $i = 1, \dots, \frac{d}{2}$. From this we can read off $\log Z$. The first two terms in the high-temperature expansion are as in (3.93).

The higher order terms in $\log Z$ come with a factor proportional to $\sim \zeta(d - 2k)T^{d-2k-1}$ for integer k . Because the zeta function vanishes at negative even integers, this means the high-temperature perturbative expansion for $\log Z$ of a free scalar field in even dimensions truncates after the $O(1/T)$ term [147]. The further corrections after the perturbative expansion in $1/T$ are non-perturbatively suppressed in T . In fact, using techniques similar to [45], we can get an exact expression for $\log Z$ for free scalar field theories in even d . For completeness, we write these expressions in the following section.

Odd dimensions

In odd d , the relation between the eigenvalues l and m_a is

$$l = m'_0 + |m_1| + \dots + |m_{\frac{d-1}{2}}|, \quad (3.305)$$

where m'_0 is a non-negative integer. The multiplicity of this specific eigenvalue state is $\binom{\frac{d-1}{2}+m_0-1}{m_0}$, where $m_0 = \lfloor \frac{m'_0}{2} \rfloor$. Therefore, the partition function of a free scalar

field is

$$Z(T, \Omega_i) = \prod_{m_0=0}^{\infty} \left(\prod_{m_1=-\infty}^{\infty} \cdots \prod_{m_{\frac{d-1}{2}}=-\infty}^{\infty} \frac{1}{1 - e^{-\frac{1}{T}(2m_0 + \sum_i |m_i| + d/2 - 1 + i \sum_i m_i \Omega_i)}} \right)^{\left(\frac{d-3}{2} + m_0\right)} \\ \times \prod_{m_0=0}^{\infty} \left(\prod_{m_1=-\infty}^{\infty} \cdots \prod_{m_{\frac{d-1}{2}}=-\infty}^{\infty} \frac{1}{1 - e^{-\frac{1}{T}(2m_0 + \sum_i |m_i| + d/2 + i \sum_i m_i \Omega_i)}} \right)^{\left(\frac{d-3}{2} + m_0\right)}, \quad (3.306)$$

where the sums over i in (3.306) run from $i = 1, \dots, \frac{d-1}{2}$. When we take the log and expand at high temperature, we arrive at the same result as in (3.93).

In even d , the expansion in inverse powers of T truncates after the $O(T^{-1})$ term. In odd d , however, the expansion never truncates. This is because the higher order terms have a factor proportional to $\sim \zeta(d - 2k)T^{d-2k-1}$. For odd d , this never vanishes. Moreover, due to the factorial growth of the zeta function at large, negative, odd values of the argument, the expansion in inverse powers of T is in fact asymptotic rather than convergent. Finally (due to a pole of the zeta function at argument 1), there is a $\log T$ term in the high-temperature expansion as well (see (4.13) of [128] for this $\log T$ term in the case of $d = 3$.) We write an explicit expression for all perturbative terms in odd dimensions in the previous section.

Gapless sector in the free scalar

As noted in Sec 3.4, the free scalar in d dimensions is a somewhat pathological example for our purposes, due to the presence of a gapless sector upon compactification on S^1 , namely the $d-1$ -dimensional free scalar CFT. As a result, the partition function at high temperature contains terms proportional to $O(T^0)$ and $O(\log T)$ in even- d and odd- d respectively. These terms cannot be produced by the thermal effective action, and must come from the gapless sector. In this appendix we understand them explicitly (see also [61] for earlier discussion of such terms).

An important subtlety is that the $d-1$ dimensional gapless sector is *not* conformally coupled to curvature in $d-1$ dimensions. To see why, we start with a conformally-coupled scalar in d -dimensions. This contains a term in the Lagrangian $\frac{1}{2}\xi_d \mathcal{R}\phi^2$ with coefficient

$$\xi_d = \frac{d-2}{4(d-1)} \quad (\text{conformal coupling in } d\text{-dimensions}). \quad (3.307)$$

When we dimensionally reduce on S^1 , we do not obtain a conformally-coupled scalar in $d-1$ dimensions, because $\xi_d \neq \xi_{d-1}$. Instead, the $d-1$ -dimensional scalar has a particular mass deformation turned on. To be more precise, it satisfies the equation of motion

$$\mathcal{D}\phi = \left(-\nabla_{d-1}^2 + \xi_d \mathcal{R}\right) \phi = 0, \quad (3.308)$$

where ∇_{d-1}^2 is the $d-1$ dimensional Laplacian. By contrast, a conformally-coupled scalar would satisfy

$$\tilde{\mathcal{D}}\phi = \left(-\nabla_{d-1}^2 + \xi_{d-1} \mathcal{R}\right) \phi = 0 \quad (d-1\text{-dimensional conformal coupling}). \quad (3.309)$$

The partition function of the gapless sector in our case is $(\det \mathcal{D})^{-1/2}$. By contrast, reference [134] computed the sphere partition function of a conformally-coupled free scalar, i.e. $(\det \tilde{\mathcal{D}})^{-1/2}$. For our purposes, we can follow the methods of [134], but we will obtain different results because we have a different equation of motion (3.308).³³

Following [134], the contribution to $-\log Z_{S^1 \times S^{d-1}}$ from the gapless sector is

$$F = \sum_{n=0}^{\infty} m_n \left[-\log(\mu R) + \log \left(n + \frac{d-2}{2} \right) \right], \quad (3.310)$$

where

$$m_n := \frac{(2n+d-2)(n+d-3)!}{(d-2)!n!} \quad (3.311)$$

is the dimension of the n -th traceless symmetric tensor representation of $\text{SO}(d)$. Here, R is the radius of the S^{d-1} , and μ is a mass scale coming from the regulator. In our case, the temperature sets the regulator scale, so we have $\mu = T$.

The sum (3.310) diverges, but we can use ζ -function regularization to make it finite. In even d , the R -dependence of (3.310) formally drops out. However, in odd d it remains, giving a nontrivial $\log T$ term in $\log Z$. The ζ -function regulated sum is

$$F_s := \sum_{n=0}^{\infty} \frac{m_n}{\left(n + \frac{d-2}{2}\right)^s}. \quad (3.312)$$

The $\log T$ term is given by $F_{s=0}$ and the T^0 term is given by $\partial_s F_s|_{s=0}$. These values for the first few d are given in Table 3.1. They indeed agree with the corresponding terms in the high-temperature expansion of the partition function of the free scalar on $S^1 \times S^{d-1}$, as we explicitly write in Appendix C.

³³We are grateful to Yifan Wang for discussions related to this point.

d	$F_{s=0}$	$\partial_s F_s _{s=0}$
3	$\frac{1}{12}$	$-\frac{\log 2}{12} - \zeta'(-1)$
4	0	$-\frac{\zeta(3)}{4\pi^2}$
5	$-\frac{17}{2880}$	$\frac{11 \log 2}{2880} + \frac{\zeta'(-1)}{24} - \frac{7\zeta'(-3)}{24}$
6	0	$\frac{\pi^2 \zeta(3) + 3\zeta(5)}{48\pi^4}$
7	$\frac{367}{483840}$	$-\frac{211 \log 2}{483840} - \frac{3\zeta'(-1)}{640} + \frac{7\zeta'(-3)}{192} - \frac{31\zeta'(-5)}{1920}$
8	0	$-\frac{8\pi^4 \zeta(3) + 30\pi^2 \zeta(5) + 45\zeta(7)}{2880\pi^6}$

Table 3.1: Values for $F_{s=0}$ and $\partial_s F_s|_{s=0}$ for various dimensions, with F_s defined in (3.312). These provide the coefficients of the $O(\log T)$ and $O(T^0)$ terms respectively in the free energy of a free scalar field in d dimensions.

The a -anomaly of the free scalar

As an aside, we can use similar techniques to compute the a -anomaly of a free scalar theory in d dimensions. The value of the a anomaly is well-known in $d = 2, 4, 6$ [82]; see e.g. [15] for a calculation in 6D. In general d it was computed in [96, 97], which we review here.

Here we study the free scalar field in d dimensions conformally coupled to S^d , as was precisely done in [134]. As discussed in Appendix F, the a -anomaly is related to the sphere partition function by³⁴

$$\log Z(S_r^d) = -\frac{(-1)^{d/2} a_d d!}{(4\pi)^{d/2}} \text{vol } S^d \log(\mu r), \quad (3.313)$$

where μ is a regulator scale. Thus, we can read off a_d from the $\log r$ term in the sphere free energy. We find the general answer

$$a_d = \frac{(-1)^{\frac{d}{2}+1}}{2\Gamma(\frac{d+2}{2})\Gamma(d+2)} \int_0^1 dt (d+4t^2) \left(t - \frac{d}{2} + 1\right)_{d-1} \quad (d \text{ even, } d > 2), \quad (3.314)$$

where $(x)_n$ is the Pochhammer symbol $(x)_n \coloneqq \frac{\Gamma(x+n)}{\Gamma(x)}$. The integrand is of course a polynomial in t for positive integer d , so the integral is trivial in practice. This formula requires $d > 2$ because the sphere partition function of the (noncompact) free boson in $d = 2$ is ill-defined. The first few values of a_d are listed in Table 3.2.

³⁴References [96, 97] use a different convention for the a anomaly where $\frac{(-1)^{d/2} a_d^{\text{here}} d! \text{vol } S^d}{(4\pi)^{d/2}} = a_d^{\text{here}}$.

d	4	6	8	10	12
a_d	$\frac{1}{360}$	$\frac{1}{9072}$	$\frac{23}{5443200}$	$\frac{263}{1796256000}$	$\frac{133787}{29422673280000}$

Table 3.2: Values for the conformal a -anomaly of a free scalar field in d dimensions, with d even. For general d , see (3.314).

Non-perturbative corrections for free scalars

From the second section of this appendix, we have the perturbative corrections in $1/T$ for the free scalar field in d dimensions. For even d , they truncate after the $O(1/T)$ term (see e.g. [41, 81]). From the techniques in [45] we can in fact compute the exact high-temperature partition function. It is given by the following.

Define the auxiliary function for even d :

$$f(d, T) := \zeta(d) T^{d-1} - \frac{(-1)^{d/2}}{(2\pi)^{d-2}} \left[\frac{\zeta(d-1)}{2} - \frac{(d-1)\zeta(d)}{4\pi^2 T} + \sum_{n=1}^{\infty} \frac{e^{-4\pi^2 T n} \sigma_{d-1}(n)}{n^{d-1}} \sum_{i=0}^{d-2} \frac{(4\pi^2 T n)^i}{\Gamma(i+1)} \right], \quad (3.315)$$

where σ is the divisor sigma function: $\sigma_{d-1}(n) := \sum_{\ell|n} \ell^{d-1}$. Then the general even d free scalar is

$$\log Z_d(T) = \sum_{i=0}^{d/2-2} c_{2i-(d-1)}(d) f(d-2i, T), \quad (3.316)$$

where $c_{2i}(d)$ is the coefficient of the β^{2i} term in the expansion of $\frac{\sinh(\beta)}{2^{d-1} \sinh^d(\beta/2)}$ about $\beta = 0$.³⁵

For example at $d = 4$ and $d = 6$, (3.316) reduces to the following two equations³⁶:

$$\log Z_{d=4}(T) = \frac{\pi^4}{45} T^3 - \frac{\zeta(3)}{4\pi^2} + \frac{1}{240T} - \sum_{n=1}^{\infty} \frac{4\sigma_3(n) e^{-4\pi^2 T n}}{n} \left(\pi^2 T^2 + \frac{T}{2n} + \frac{1}{8\pi^2 n^2} \right), \quad (3.319)$$

³⁵This function comes about from writing the logarithm of the free boson partition function as

$$\log Z(T) = - \sum_{j=0}^{\infty} \frac{j+d/2-1}{d/2-1} \binom{j+d-3}{d-3} \log(1 - e^{-\frac{1}{T}(j+\frac{d-2}{2})}), \quad (3.317)$$

doing the Taylor expansion of the logarithm, and finally resumming over j , giving (see e.g. [61])

$$\log Z(T) = \sum_{n=1}^{\infty} \frac{\sinh(\frac{n}{T})}{n 2^{d-1} \sinh^d(\frac{n}{2T})}. \quad (3.318)$$

³⁶These perturbative terms here reproduce, e.g. [165].

$$\begin{aligned} \log Z_{d=6}(T) = & \frac{2\pi^6}{945}T^5 - \frac{\pi^4}{540}T^3 + \frac{\pi^2\zeta(3) + 3\zeta(5)}{48\pi^4} - \frac{31}{60480T} \\ & + \sum_{n=1}^{\infty} e^{-4\pi^2 n T} \left[\frac{4\sigma_5(n)}{3n} \left(\pi^4 T^4 + \frac{\pi^2 T^3}{n} + \frac{3T^2}{4n^2} + \frac{3T}{8n^3 \pi^2} + \frac{3}{32n^4 \pi^4} \right) \right. \\ & \left. + \frac{\sigma_3(n)}{3n} \left(\pi^2 T^2 + \frac{T}{2n} + \frac{1}{8n^2 \pi^2} \right) \right]. \end{aligned} \quad (3.320)$$

For a free scalar field in odd dimensions, the perturbative expansion in $1/T$ no longer truncates. The perturbative expansion is

$$\begin{aligned} \log Z_d(T) \sim & \sum_{n=1}^{\frac{d-1}{2}} c_{-2n}(d) \zeta(2n+1) T^{2n} \\ & + F_{s=0} \log T + \partial_s F_s|_{s=0} + \sum_{n=1}^{\infty} c_{2n}(d) \zeta(-2n+1) T^{-2n}, \end{aligned} \quad (3.321)$$

where in (3.321), $F_{s=0}$ and $\partial_s F_s|_{s=0}$ are defined in (3.312), and $c_{2i}(d)$ is defined again as the coefficient of the β^{2i} term in the expansion of $\frac{\sinh(\beta)}{2^{d-1} \sinh^d(\beta/2)}$ about $\beta = 0$.

At large n , $|c_{2n}(d)| \sim (2\pi)^{-2n}$. On the other hand, $|\zeta(-2n+1)| \sim \frac{(2n)!}{(2\pi)^{2n}}$. Thus the expression (3.321) is an asymptotic series with divergent piece growing like

$$\log Z_d(T) \sim \sum_n \frac{(2n)!}{(4\pi^2 T)^{2n}}. \quad (3.322)$$

From techniques in resurgence, this implies the first non-perturbative correction to (3.321) scales as $e^{-4\pi^2 T}$, just as in even dimensions.

These results are consistent with the worldline instanton corrections discussed in Section 3.3 (even though in this example there is also a gapless sector upon compactification). When the free boson is compactified on a circle with thermal boundary conditions, the mass of the lightest KK mode is $m_{KK} = 2\pi T$. Therefore, (3.91) predicts a correction to $\log Z$ of the form $e^{-4\pi^2 T}$, which is precisely consistent with what we found in both even and odd d .

We can also study the free scalar with a \mathbb{Z}_2 twist around the thermal circle. For example, in $d = 4$, we find

$$\log Z_{d=4}^{\mathbb{Z}_2\text{-twisted}}(T) = -\frac{7\pi^4}{360}T^3 + \frac{1}{240T} + O(e^{-2\pi^2 T}). \quad (3.323)$$

In this case, the lightest KK mode has mass $m_{KK} = \pi T$, and the nonperturbative corrections are indeed of the form $e^{-2\pi m_{KK}} = e^{-2\pi^2 T}$.

Partition function of free fermion theories

In this section, we review the partition function of a free massless Dirac fermion in d dimensions on $\mathbb{R} \times S_R^{d-1}$. We can construct the partition function from the solution of the Dirac equation:

$$\left(\Gamma^0 \frac{\partial}{\partial t} + \Gamma^i \nabla_i \right) \psi = 0, \quad (3.324)$$

where Γ^μ ($\mu = 0, 1, \dots, d-1$) are gamma matrices, and ∇_i ($i = 1, \dots, d-1$) is the covariant derivative on the sphere.

The spectrum of the Dirac operator on S^{d-1} has been considered in e.g. [40]. The Dirac operator on S^{d-1} , $\mathcal{X} \equiv \Gamma^i \nabla_i$, has the following eigenvalues:

$$\mathcal{X} \psi_{\pm\rho} = \pm i \left(\rho + \frac{d-1}{2} \right) \psi_{\pm\rho}, \quad \rho = 0, 1, 2, \dots \quad (3.325)$$

Because $\Gamma^0{}^2 = -\mathbf{1}$ and $\{\Gamma^0, \mathcal{X}\} = 0$, we find the solution of the Dirac equation as

$$\psi = e^{iEt} \left(\psi_{\pm\rho} \pm \Gamma^0 \psi_{\pm\rho} \right), \quad E = \rho + \frac{d-1}{2}. \quad (3.326)$$

From [40] we see the solutions are representations of $\text{Spin}(d)$ with highest weight $\left(\rho + \frac{1}{2}, \frac{1}{2}, \dots, \frac{1}{2} \right)$ for odd d and $\left(\rho + \frac{1}{2}, \frac{1}{2}, \dots, \frac{1}{2}, \pm \frac{1}{2} \right)$ for even d where ρ is the eigenvalue of the Dirac operator in (3.325).

In odd dimensions, we have a complete set of solution of the Dirac equation with eigenvalues as follows:

$$\begin{aligned} E &= \rho + \frac{d-1}{2}, \\ \rho &= m_0 + m'_1 + \dots + m'_{\frac{d-1}{2}}, \\ m_a &= \pm \left(m'_a + \frac{1}{2} \right), \quad \left(a = 1, \dots, \frac{d-1}{2} \right), \end{aligned} \quad (3.327)$$

where $m_0, m'_1, \dots, m'_{\frac{d-1}{2}}$ are non-negative integers. Here E is the energy of the state and m_a is the eigenvalue of the rotation generator ∂_{θ_a} . The multiplicity of states with eigenvalues $(E, m_1, \dots, m_{\frac{d-1}{2}})$ is $\binom{\frac{d-3}{2} + m_0}{m_0}$. Finally we get an additional tower of states from quantizing the field $\bar{\psi}$. Therefore, the partition function of a free fermion in odd dimensions is

$$Z(T, \Omega_i) = \prod_{m_0=0}^{\infty} \prod_{m_1 \in \mathbb{Z} + \frac{1}{2}} \dots \prod_{m_{\frac{d-1}{2}} \in \mathbb{Z} + \frac{1}{2}} \left(1 + e^{-\frac{1}{T}(m_0 + \sum_i |m_i| + \frac{d-1}{4} + i \sum_i m_i \Omega_i)} \right)^{2 \binom{\frac{d-3}{2} + m_0}{m_0}}, \quad (3.328)$$

where the sums over i run from $1, \dots, \frac{d-1}{2}$. Taking a log and expanding at high temperature recovers (3.96).

In even dimensions, we can do a very similar calculation. We have a complete set of solutions to the Dirac equation with eigenvalues as follows:

$$\begin{aligned} E &= \rho + \frac{d}{2}, \\ \rho &= m_0 + m'_1 + \dots + m'_{\frac{d}{2}}, \\ m_a &= \pm \left(m'_a + \frac{1}{2} \right), \quad \left(a = 1, \dots, \frac{d}{2} \right), \end{aligned} \quad (3.329)$$

where m_0, m'_1, \dots, m'_n are nonnegative integers. The multiplicity of the states with eigenvalues $(E, m_1, \dots, m_{\frac{d}{2}})$ is $\binom{\frac{d}{2} + m_0 - 2}{m_0}$. Therefore, the partition function of a free fermion in even dimensions is

$$Z(T, \vec{\Omega}) = \prod_{m_0=0}^{\infty} \prod_{m_1 \in \mathbb{Z} + \frac{1}{2}} \dots \prod_{m_{\frac{d}{2}} \in \mathbb{Z} + \frac{1}{2}} \left(1 + e^{-\frac{1}{T}(m_0 + \sum_i |m_i| + \frac{d-2}{4} + i \sum_i m_i \Omega_i)} \right)^{2 \binom{\frac{d}{2} + m_0 - 2}{m_0}}, \quad (3.330)$$

where the sums over i in (3.330) run from $1, \dots, \frac{d}{2}$. This gives the same answer as (3.96).

Non-perturbative corrections for free fermions

We can repeat the same analysis in previous section to find the non-perturbative corrections for the free energy of a free Dirac fermion in d dimensions. When we turn off the spin fugacities, we can rewrite (3.328), (3.330), as

$$\log Z_d^f(T) = \sum_{n=1}^{\infty} \frac{2^{\lfloor \frac{d}{2} \rfloor + 1} (-1)^{n+1} e^{-\frac{(d-1)n}{2T}}}{n(1 - e^{-\frac{n}{T}})^{d-1}}. \quad (3.331)$$

In even dimensions, this admits the following (exact) high-temperature expansion. First, we define the auxiliary function for even d as

$$\begin{aligned} g(d, T) &\coloneqq 2^{d/2} \left(1 - \frac{1}{2^{d-1}} \right) \zeta(d) T^{d-1} + \frac{(-1)^{d/2} (d-1)(2^d - 2) \zeta(d)}{\pi^d 2^{3d/2} T} \\ &+ \frac{(-1)^{d/2}}{2^{\frac{d}{2}-2} \pi^{d-2}} \sum_{n=1}^{\infty} \frac{e^{-2\pi^2 T n} (-1)^n \sigma_{d-1}^{\text{odd}}(n)}{n^{d-1}} \sum_{i=0}^{d-2} \frac{(2\pi^2 T n)^i}{\Gamma(i+1)}, \end{aligned} \quad (3.332)$$

where

$$\sigma_{d-1}^{\text{odd}}(n) \coloneqq \sum_{\substack{\ell|n, \\ \ell \text{ odd}}} \ell^{d-1}. \quad (3.333)$$

We also define the function $\tilde{c}_i(d)$ as the β^i term in the expansion of $\frac{\beta^d e^{-\frac{\beta(d-1)}{2}}}{(1-e^{-\beta})^{d-1}}$ about $\beta = 0$.³⁷ Then the partition function of a free Dirac fermion in even d dimensions at temperature T is

$$\log Z_d^f(T) = \sum_{i=1}^{d-1} 2^{\frac{i+1}{2}} \tilde{c}_i(d) g(d+1-i, T). \quad (3.334)$$

For instance, (3.334) for $d = 4, 6$ reduces to

$$\begin{aligned} \log Z_{d=4}^f(T) &= \frac{7\pi^4}{90} T^3 - \frac{\pi^2}{12} T + \frac{17}{480T} \\ &+ \sum_{n=1}^{\infty} (-1)^n e^{-2\pi^2 T n} \left(\frac{4\pi^2}{n} \sigma_3^{\text{odd}}(n) T^2 + \frac{4}{n^2} \sigma_3^{\text{odd}}(n) T + \frac{\sigma_1^{\text{odd}}(n)}{n} + \frac{2\sigma_3^{\text{odd}}(n)}{n^3 \pi^2} \right), \end{aligned} \quad (3.335)$$

and

$$\begin{aligned} \log Z_{d=6}^f(T) &= \frac{31\pi^6}{1890} T^5 - \frac{7\pi^4}{216} T^3 + \frac{\pi^2}{32} T - \frac{367}{24192T} \\ &+ \sum_{n=1}^{\infty} (-1)^{n+1} e^{-2\pi^2 T n} \left[\frac{2\pi^4}{3n} \sigma_5^{\text{odd}}(n) T^4 + \frac{4\pi^2}{3n^2} \sigma_5^{\text{odd}}(n) T^3 + \left(\frac{2\sigma_5^{\text{odd}}(n)}{n^3} + \frac{5\pi^2 \sigma_3^{\text{odd}}}{3n} \right) T^2 \right. \\ &\quad \left. + \left(\frac{2\sigma_5^{\text{odd}}(n)}{\pi^2 n^4} + \frac{5\sigma_3^{\text{odd}}(n)}{3n^2} \right) T + \left(\frac{\sigma_5^{\text{odd}}(n)}{\pi^4 n^5} + \frac{5\sigma_3^{\text{odd}}(n)}{6\pi^2 n^3} + \frac{3\sigma_1^{\text{odd}}(n)}{8n} \right) \right]. \end{aligned} \quad (3.336)$$

In odd dimensions, the perturbation theory in $1/T$ no longer truncates. Rather, it looks like

$$\log Z_d^f(T) \sim \sum_{n=1}^{\infty} 2^{\frac{d+1}{2}} \left(1 - 2^{n-d} \right) \zeta(d+1-n) \tilde{c}_n(d) T^{d-n}, \quad (3.337)$$

where the $n = d$ term in (3.337) is $\tilde{c}_d(d) 2^{\frac{d+1}{2}} \log 2$. The sum in (3.337) is an asymptotic expansion. At large odd n , $|\tilde{c}_n(d)| \sim (2\pi)^{-n}$ and $|\zeta(d+1-n)| \sim \frac{n!}{(2\pi)^n}$. The sum then diverges, growing as

$$\log Z_d^f(T) \sim \sum_n \frac{n!}{(2\pi^2 T)^n}. \quad (3.338)$$

From the techniques in resurgence, this implies the first non-perturbative correction of (3.337) scales as $e^{-2\pi^2 T}$, just as in even dimensions.

In a free fermion theory compactified on a circle with thermal boundary conditions, we have $m_{KK} = \pi T$, so that (3.91) predicts a non-perturbative correction of the form $e^{-2\pi^2 T}$, consistent with what we found in both even and odd dimensions.

³⁷Like in the free scalar case, up to an overall constant, this comes from (3.331) upon setting $n = 1$.

Appendix D Wilson coefficients for the 3D Ising model

In this appendix, we discuss estimates of the high-temperature partition function of the 3D Ising model. In Appendix A of [119], the coefficient f for the 3D Ising model was estimated by constructing the partition function with $\Omega = 0$ as a sum over the spectrum of known operators, which has numerically been computed up to about dimension 8 [195]. In this appendix, we perform a similar analysis, but including spin-dependence. Note that there is a balance in choosing the temperature — if the temperature is too low, then truncating the thermal effective action becomes a poor approximation; if the temperature is too high, then truncating the partition function to a finite sum of characters becomes inaccurate.³⁸

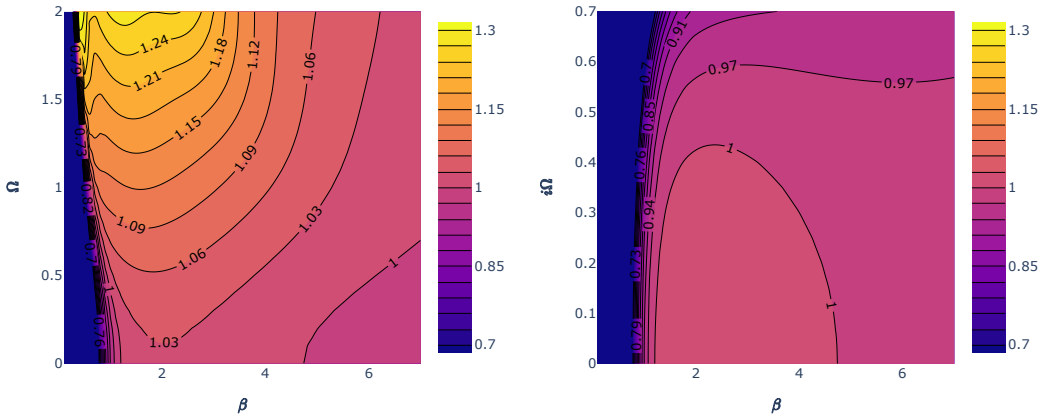


Figure 3.13: Contour plots of the ratio of the estimated partition function to the leading term in the thermal effective action with $f = 0.153$, i.e. $Z^{\text{3D Ising}}(\beta, \Omega)/\exp\left(4\pi\frac{0.153}{\beta^2(1+\Omega^2)}\right)$, as a function of β, Ω for real Ω (left) and imaginary Ω (right). The ratio is very close to 1 for intermediate temperatures $1 \lesssim \beta \lesssim 5$ and small angles $|\Omega| \lesssim 0.5$.

From Monte-Carlo techniques, it has been estimated that $f_{\text{3D Ising}} \sim 0.153$ [143, 145, 198]. In Figure 3.13, we plot the ratio of the computed partition function to the estimate from the first term in the thermal effective action (3.54) with $f = 0.153$. For the values of β and Ω shown in the figure, the ratio is quite close to 1. We can also independently fit f from the partition function. By studying temperatures with $1.5 < \beta < 3$ and chemical potentials $|\Omega| < 0.6$, we estimate that $f \sim 0.15$, consistent with [143, 145, 198].

³⁸Much like the porridge in *Goldilocks and the Three Bears* [196], it is important to pick a temperature that is just right.

We can also try to estimate higher-derivative Wilson coefficients in the effective action of the 3D Ising model, such as c_1, c_2 . Unfortunately, we do not have a clear enough picture of the high-dimension spectrum to estimate these coefficients with reliable precision. However, our best fits suggest that $c_2 < 0$ (we are not yet able to reliably estimate the sign of c_1).

In general, accessing large twist operators is challenging for the numerical bootstrap, which seems most sensitive to low-twist operators—particularly "double twist" operators [195]. Furthermore, the numerical bootstrap studies done so far are blind to certain parts of the operator spectrum of the 3D Ising model, such as odd-spin \mathbb{Z}_2 -even operators, or parity-odd operators.³⁹ Such sectors would need to be included to reliably compute the partition function at higher temperatures. See [117, 207] for recent work accessing these sectors with other methods.

Appendix E The shadow transform of a three-point function at large Δ

The formula for OPE coefficients depends on the triple shadow coefficient $S_{\tilde{1}\tilde{2}\tilde{3}}^3$ given in (3.161). In this appendix, we compute this coefficient at large Δ_i . First consider a single shadow transform applied to a three-point function with large Δ 's. The shadow transform is

$$\langle O_1^a(x_1) O_2^b(x_2) S[O_3] \bar{c}(x_3) \rangle^{(s)} \equiv \int d^d x_0 \langle \tilde{O}^{\bar{c}}(x_3) \tilde{O}_c^{\dagger}(x_0) \rangle \langle O_1^a(x_1) O_2^b(x_2) O_3^c(x_0) \rangle^{(s)}. \quad (3.339)$$

Here, a, b, c are spin indices for the representations $\lambda_1, \lambda_2, \lambda_3$. The operator \tilde{O}^{\dagger} has Lorentz representation λ_3^* , so we write its index as a lowered c index. The operator \tilde{O} has Lorentz representation λ_3^R (the reflected representation), and we indicate this with a barred index.

The three-point function is

$$\langle O_1^a(x_1) O_2^b(x_2) O_3^c(x_3) \rangle^{(s)} = V^{s;abc}(x_1, x_2, x_3). \quad (3.340)$$

We will be interested in restricting this three-point function to a single axis $x_i = z_i e$ with unit vector $e \in S^{d-1} \subset \mathbb{R}^d$. We get two different answers, depending on the cyclic ordering of the points

$$V^{s;abc}(z_1 e, z_2 e, z_3 e) = \begin{cases} \frac{V^{s;abc}(0, e, \infty)}{|z_{12}|^{\Delta_1 + \Delta_2 - \Delta_3} |z_{23}|^{\Delta_2 + \Delta_3 - \Delta_1} |z_{31}|^{\Delta_3 + \Delta_1 - \Delta_2}} & (z_1 < z_2 < z_3, \text{ or cycl.}), \\ \frac{V^{s;abc}(e, 0, \infty)}{|z_{12}|^{\Delta_1 + \Delta_2 - \Delta_3} |z_{23}|^{\Delta_2 + \Delta_3 - \Delta_1} |z_{31}|^{\Delta_3 + \Delta_1 - \Delta_2}} & (z_2 < z_1 < z_3, \text{ or cycl.}). \end{cases} \quad (3.341)$$

³⁹Though there are preliminary results for some of these sectors from the stress tensor bootstrap [84].

The tensors $V^{s;abc}(0, e, \infty)$ and $V^{s;abc}(e, 0, \infty)$ are related to each other by a rotation by π in the 1-2 direction applied simultaneously to all three indices. The operator at ∞ is defined by (3.120).

To compute the shadow transform, we can use conformal symmetry to choose a simple configuration of the points. We pick $(x_1, x_2, x_3) = (0, e, \infty)$, where e is a unit vector in the x^1 direction. The two-point function becomes a tensor depending on the unit vector e that maps $\lambda_3 \rightarrow \lambda_3^R$:

$$\langle \tilde{O}^{\bar{c}}(\infty e) \tilde{O}_c^\dagger(0) \rangle = I^{\bar{c}}_c(e). \quad (3.342)$$

For example, in the case of a spinor representation in 4D, we have $I^{\dot{\alpha}}_\alpha(e) \propto (e \cdot \bar{\sigma})^{\dot{\alpha}}_\alpha$.

The shadow transform will be dominated by a saddle point on the x^1 -axis, by $\text{SO}(d-1)$ invariance. Its location depends only on the z_0 -dependent factors in the three-point function

$$V^{s;abc}(0, e, z_0 e) \propto |z_0|^{\Delta_1 - \Delta_2 - \Delta_3} |1 - z_0|^{\Delta_2 - \Delta_1 - \Delta_3}. \quad (3.343)$$

This has the saddle solution

$$z_{0*} = \frac{\Delta_2 + \Delta_3 - \Delta_1}{2\Delta_3}. \quad (3.344)$$

The tensor structure that multiplies the answer depends on the location of the saddle. Taking into account the gaussian fluctuations around the saddle, we find

$$\begin{aligned} & \langle O_1^a(0) O_2^b(e) \mathbf{S}[O_3]^{\bar{c}}(\infty) \rangle^{(s)} \\ &= i \left(\frac{\pi}{\Delta_3} \right)^{d/2} \left(\left(\frac{\Delta_1 + \Delta_3 - \Delta_2}{2\Delta_3} \right)^2 \right)^{\frac{\Delta_2 - \Delta_1 - \Delta_3 + \frac{d}{2}}{2}} \left(\left(\frac{\Delta_2 + \Delta_3 - \Delta_1}{2\Delta_3} \right)^2 \right)^{\frac{\Delta_1 - \Delta_2 - \Delta_3 + \frac{d}{2}}{2}} \\ & \quad \times I^{\bar{c}}_c(e) \times \begin{cases} V^{s;abc}(0, e, \infty) & 0 < z_{0*} < 1, \\ V^{s;abc}(e, 0, \infty) & \text{otherwise.} \end{cases} \end{aligned} \quad (3.345)$$

If we perform the shadow transform three times, we find that $z_{0*} \in (0, 1)$ twice, and once it lies outside of this range. Thus, the cyclic ordering of the arguments to V^s get swapped twice, resulting in the same ordering after three transforms. The overall effect is to multiply by Δ -dependent factors and act on each index with $I^{\bar{c}}_c(e)$.

Overall, we find

$$\begin{aligned}
& (I(e)^{-1})_a^{\bar{a}} (I(e)^{-1})_b^{\bar{b}} (I(e)^{-1})_c^{\bar{c}} \langle \mathbf{S}[\tilde{O}_1^\dagger]_{\bar{a}}(0) \mathbf{S}[\tilde{O}_2^\dagger]_{\bar{b}}(e) \mathbf{S}[\tilde{O}_3^\dagger]_{\bar{c}}(\infty) \rangle^{(s'*)} \\
&= V_{abc}^{s'*}(0, e, \infty) \times e^{\frac{i\pi(d-2)}{4}} \left(\frac{\pi i}{\Delta_1} \right)^{d/2} \left(\frac{\pi i}{\Delta_2} \right)^{d/2} \left(\frac{\pi i}{\Delta_3} \right)^{d/2} \\
&\quad \times \left(\frac{(\Delta_1 + \Delta_2 - \Delta_3)(\Delta_1 + \Delta_2 + \Delta_3)}{4\Delta_1\Delta_2} \right)^{\Delta_1 + \Delta_2 - \Delta_3 - \frac{d}{2}} \left(\frac{(\Delta_3 + \Delta_1 - \Delta_2)(\Delta_1 + \Delta_2 + \Delta_3)}{4\Delta_3\Delta_1} \right)^{\Delta_3 + \Delta_1 - \Delta_2 - \frac{d}{2}} \\
&\quad \times \left(\frac{(\Delta_2 + \Delta_3 - \Delta_1)(\Delta_1 + \Delta_2 + \Delta_3)}{4\Delta_2\Delta_3} \right)^{\Delta_2 + \Delta_3 - \Delta_1 - \frac{d}{2}}. \tag{3.346}
\end{aligned}$$

Here, $V^{s'*}$ indicates the complex conjugate of the three-point structure $V^{s'}$. For the purposes of this calculation, we should think of it simply as a three-point structure for operators in the representations $\tilde{\pi}_i^\dagger$. We have written (3.346) so that its phase is manifest when Δ_i is on the principal series $\Delta_i \in \frac{d}{2} + i\mathbb{R}_{\geq 0}$ (with positive imaginary part). Finally, we included inverse two-point structures $I(e)^{-1}$, since they are needed in (3.181).

Appendix F Gluing factors

In this appendix, we determine the gluing factor $|Z_{\text{glue}}(r)|$ coming from a junction between a d -dimensional cylinder of radius r and a flat end-cap given by a d -dimensional ball. Our strategy is to start with the partition function on S^d (with radius 1) and perform a Weyl transformation to a cylinder $C_{r,\beta}$ of radius r and length βr with two flat end-caps. We will integrate the Weyl anomaly to compute S_{anom} and deduce $|Z_{\text{glue}}(r)|$ via (3.122).

Recall that on a conformally-flat geometry, with the scheme $S_{\text{ct}} = 0$ discussed in Section 3.3, the finite form of the Weyl anomaly is

$$\begin{aligned}
\log Z[e^{2\omega}g] - \log Z[g] &= -S_{\text{anom}}[g, \omega] \\
&= -\frac{(-1)^{d/2}a_d}{(4\pi)^{d/2}} \int_0^1 dt \int d^d x \omega \sqrt{g} e^{dt\omega} E_d[e^{2t\omega}g]. \tag{3.347}
\end{aligned}$$

To compute the Weyl anomaly between the sphere and the capped cylinder, we first need the Riemann tensor for a Weyl rescaling of S^d . Let us write the metric on S^d as

$$ds_{S^d}^2 = d\phi^2 + \sin^2 \phi ds_{S^{d-1}}^2. \tag{3.348}$$

We will be interested in Weyl rescalings $\tilde{g} = e^{2\omega} g_{S^d}$, where ω is a function of ϕ alone. In this case, the Riemann tensor simplifies:

$$\begin{aligned} \tilde{R}_{\mu\nu}^{\rho\sigma} &= e^{-2\omega} \left[(1 - 2\omega' \cot \phi - \omega'^2) (\delta_\mu^\rho \delta_\nu^\sigma - \delta_\mu^\sigma \delta_\nu^\rho) \right. \\ &\quad \left. + (\omega' \cot \phi + \omega'^2 - \omega'') (\delta_\mu^1 \delta_1^\rho \delta_\nu^\sigma - \delta_\nu^1 \delta_1^\rho \delta_\mu^\sigma - \delta_\mu^1 \delta_1^\sigma \delta_\nu^\rho + \delta_\nu^1 \delta_1^\sigma \delta_\mu^\rho) \right], \end{aligned} \quad (3.349)$$

where the index 1 represents the ϕ coordinate, and ω', ω'' denote derivatives of ω with respect to ϕ . The Euler density is

$$\begin{aligned} \tilde{E}_d &= \frac{1}{2^{d/2}} \epsilon^{\mu_1 \dots \mu_d} \epsilon_{\nu_1 \dots \nu_d} \tilde{R}_{\mu_1 \mu_2}^{\nu_1 \nu_2} \dots \tilde{R}_{\mu_{d-1} \mu_d}^{\nu_{d-1} \nu_d} \\ &= d! e^{-d\omega} (1 - 2\omega' \cot \phi - \omega'^2)^{\frac{d-2}{2}} (1 - \omega' \cot \phi - \omega''). \end{aligned} \quad (3.350)$$

Plugging this result into (3.347), we find

$$\begin{aligned} \log Z[e^{2\omega} g] - \log Z[g] &= -\frac{(-1)^{d/2} d! a_d}{2^{d-1} \Gamma(\frac{d}{2})} \int_0^1 dt \int_0^\pi d\phi \omega (\sin \phi)^{d-1} (1 - 2t\omega' \cot \phi - t^2 \omega'^2)^{\frac{d-2}{2}} (1 - t\omega' \cot \phi - t\omega''). \end{aligned} \quad (3.351)$$

Now let us examine the Weyl factor that relates the sphere to $C_{r,\beta}$. We will impose a symmetry under $\phi \rightarrow \pi - \phi$, so that it suffices to consider the range $0 \leq \phi \leq \frac{\pi}{2}$. The Weyl factor is

$$\omega(\phi) = \begin{cases} \log \frac{e^{\beta/2} r \tan(\phi/2)}{\sin \phi} & 0 \leq \phi \leq \phi_0 \\ \log \frac{r}{\sin \phi} & \phi_0 \leq \phi \leq \pi/2, \end{cases} \quad (3.352)$$

where $\phi_0 = 2 \tan^{-1}(e^{-\beta/2})$. As a check, consider first the range $0 \leq \phi < \phi_0$. There, we have

$$\begin{aligned} e^{2\omega} (d\phi^2 + \sin^2 \phi ds_{S^{d-1}}^2) &= e^\beta r^2 \left(\frac{\tan^2(\phi/2)}{\sin^2 \phi} d\phi^2 + \tan^2(\phi/2) ds_{S^{d-1}}^2 \right) \\ &= d\rho^2 + \rho^2 ds_{S^{d-1}}^2, \end{aligned} \quad (3.353)$$

where $\rho = e^{\beta/2} r \tan(\phi/2)$. This is the metric on the flat ball, i.e. the first end cap. Similarly, for $\phi_0 \leq \phi \leq \pi/2$, we have

$$e^{2\omega} (d\phi^2 + \sin^2 \phi ds_{S^{d-1}}^2) = \left(\frac{r d\phi}{\sin \phi} \right)^2 + r^2 ds_{S^{d-1}}^2 = d\tau^2 + r^2 ds_{S^{d-1}}^2, \quad (3.354)$$

where $\tau = r \log \tan(\phi/2)$, which is the metric on the cylinder. Thus, (3.352) describes how the first hemisphere $0 \leq \phi \leq \pi/2$ maps to half of the capped cylinder. The remaining hemisphere should be treated symmetrically under $\phi \rightarrow \pi - \phi$. In practice, this means integrating the anomaly over $\phi \in [0, \pi/2]$ and including a factor of 2.

Plugging the Weyl factor (3.352) into (3.351) is subtle because ω'' has a δ -function singularity at $\phi = \phi_0$. In (3.351), this δ -function gets multiplied by a function of ω' , which is discontinuous at the support of the δ -function! To get the correct result, we must regularize ω by smoothing out the discontinuities in its derivatives. For example, we can model ω' near ϕ_0 as

$$\omega'(\phi) = \frac{1}{2} \left(\omega'_+ + \omega'_- + (\omega'_+ - \omega'_-) \operatorname{erf}\left(\frac{\phi - \phi_0}{\epsilon}\right) \right), \quad (3.355)$$

where ϵ is a small regulator, and ω'_\pm are the values of ω' to the left and the right of the discontinuity. Plugging this into (3.351), expanding to leading order in ϵ , and writing $\phi = \phi_0 + \epsilon x$, we obtain integrals of the form

$$\int dx e^{-x^2} \operatorname{erf}(x)^n = \frac{1 + (-1)^n}{2} \frac{\sqrt{\pi}}{n+1}, \quad (3.356)$$

which give finite, calculable contributions. Applying this procedure, we can obtain the contribution to (3.351) from an infinitesimal neighborhood of ϕ_0 :

$$(\text{contribution near } \phi_0) = \begin{cases} \frac{a_2}{2} \log(r \cosh \frac{\beta}{2}) & d = 2, \\ \frac{a_4}{4} \log(r \cosh \frac{\beta}{2}) \frac{\sinh \beta - 4 \cosh \beta - 6}{4(\cosh \beta + 1)} & d = 4, \\ \dots & \end{cases} \quad (3.357)$$

The detailed expressions here will not matter for our purposes. The important observation is that the contributions (3.357) all vanish when $r = 1$ and $\beta = 0$. We will take advantage of this fact shortly.

Before computing the full result from plugging (3.352) into (3.351), let us use a shortcut to determine its r -dependence. From cutting and gluing, we expect the capped cylinder partition function to take the form

$$\log Z(C_{r,\beta}) = \log |Z_{\text{glue}}(r)|^2 - \varepsilon_0 \beta, \quad (3.358)$$

where ε_0 is the Casimir energy on a unit S^{d-1} , given in (3.42). We can determine the r -dependence of the right-hand side by starting with a cylinder $C_{1,\beta}$ of radius 1 and performing a Weyl rescaling $g \rightarrow r^2 g$ to get $C_{r,\beta}$. Because the integral of the

d	2	4	6	8	10	12	14
$f(d)$	1	$\frac{7}{3}$	$\frac{37}{5}$	$\frac{1066}{35}$	$\frac{3254}{21}$	$\frac{72428}{77}$	$\frac{949484}{143}$

Table 3.3: Values of $f(d)$ for the first few even d .

Euler density is topological, a constant Weyl rescaling gives the same anomaly on the capped cylinder as on the sphere. In other words, we have

$$\log Z(C_{r,\beta}) - \log Z(C_{1,\beta}) = \log Z(S_r^d) - \log Z(S^d), \quad (3.359)$$

where S_r^d is the sphere with radius r . On the sphere, we can easily integrate the Weyl anomaly using $E_d[g_{S^d}] = d!$ to give

$$\log Z(S_r^d) - \log Z(S^d) = -\frac{(-1)^{d/2} a_d d!}{(4\pi)^{d/2}} \text{vol } S^d \log r = -2(-1)^{d/2} \left(\frac{d}{2}\right)! a_d \log r. \quad (3.360)$$

Combining (3.358), (3.359), and (3.360), we conclude

$$\log |Z_{\text{glue}}(r)|^2 = \log |Z_{\text{glue}}(1)|^2 - 2(-1)^{d/2} \left(\frac{d}{2}\right)! a_d \log r. \quad (3.361)$$

Thus, we have completely fixed the β and r dependence of $\log Z(C_{r,\beta})$, and the only remaining unknown is $\log Z(C_{1,0}) = \log |Z_{\text{glue}}(1)|^2$. As noted above, when $r = 1$ and $\beta = 0$, the contribution to the Weyl anomaly near ϕ_0 vanishes. Furthermore, the contribution from the cylinder region vanishes as well since $\phi_0 = \frac{\pi}{2}$. We are left with an integral over the end cap $\phi \in [0, \pi/2]$ alone:

$$\begin{aligned} & \log |Z_{\text{glue}}(1)|^2 - \log Z(S^d) \\ &= \frac{(-1)^{d/2} a_d d!}{2^{d-2} \Gamma(d/2)} \int_0^1 dt \int_0^1 dx [(1-t)(1-x)(1+t+x-xt)]^{\frac{d-2}{2}} (1-t) \log(x+1), \end{aligned} \quad (3.362)$$

where we made the change of variables $x = \cos \phi$. We have not found a simple closed-form formula for $\log |Z_{\text{glue}}(1)|^2$ in general d . However, it is straightforward to plug different values of d into (3.362) and perform the resulting elementary integrals. We find that

$$\log |Z_{\text{glue}}(r)|^2 = \log Z(S_{r/2}^d) - (-1)^{d/2} f(d) a_d, \quad (3.363)$$

where $Z(S_{r/2}^d)$ is the partition function on a sphere of radius $r/2$ (determined by (3.360)), and $f(d)$ takes rational values for even d ; see table 3.3.

Appendix G Counting quantum numbers in the genus-2 block

A four point function of local operators depends on two independent cross ratios z and \bar{z} . These cross ratios are roughly conjugate to the quantum numbers Δ and J labeling the internal representation. By varying z, \bar{z} independently, we can extract information about Δ and J independently (for example, using Caron-Huot's Lorentzian inversion formula [48]).

Note that the internal operator in a four-point function may transform in a complicated $\text{SO}(d)$ representation whose Young diagram has multiple rows with lengths (m_1, m_2, \dots, m_n) , where $n = \lfloor \frac{d}{2} \rfloor$ and $m_1 = J$. However, in a fixed four-point function, only $m_1 = J$ is unbounded. The remaining m_i are bounded.

In this appendix, we point out a similar match between unbounded quantum numbers in the genus-2 block $B_{123}^{s's}$ and the dimension of the moduli space of genus-2 conformal structures $\dim \mathcal{M} = \dim \text{SO}(d+1, 1)$. Before explaining the general case, let us describe the matching in $d = 2$ and $d = 3$.

In $d = 2$, there is a unique three-point structure, so the labels s, s' take only one value. The only unbounded quantum numbers in the block are the dimensions and spins of the three exchanged operators. This gives six quantum numbers, which matches $\dim \mathcal{M} = 6$ in $d = 2$.

In $d = 3$, we again have six unbounded quantum numbers from the dimensions and spins of the exchanged operators. However, we must also take into account the 3-point structure labels s, s' . One way to count them is to work in the embedding space. (The counting is even easier in the q -basis, but our embedding-space discussion will be useful later.) In the embedding space formalism, a spin- J operator becomes a homogeneous function $\mathcal{O}(X, Z)$ of an embedding coordinate $X \in \mathbb{R}^{d+1, 1}$ and a polarization vector $Z \in \mathbb{C}^{d+1, 1}$, subject to orthogonality conditions $X^2 = Z^2 = X \cdot Z = 0$, and a gauge redundancy $Z \sim Z + \lambda X$. The operator $\mathcal{O}(X, Z)$ has homogeneity $-\Delta$ in X and J in Z . A general three-point structure for such operators is given by

$$\langle \mathcal{O}_1(X_1, Z_1) \mathcal{O}_2(X_2, Z_2) \mathcal{O}_3(X_3, Z_3) \rangle \ni \frac{V_1^{J_1-\ell_2-\ell_3} V_2^{J_2-\ell_3-\ell_1} V_3^{J_3-\ell_1-\ell_2} H_{23}^{\ell_1} H_{31}^{\ell_2} H_{12}^{\ell_3}}{X_{12}^{\Delta_1+\Delta_2-\Delta_3} X_{23}^{\Delta_2+\Delta_3-\Delta_2} X_{31}^{\Delta_3+\Delta_1-\Delta_2}} \\ (\ell_2 + \ell_3 \leq J_1, \ell_3 + \ell_1 \leq J_2, \ell_1 + \ell_2 \leq J_3), \quad (3.364)$$

where H_{ij} and V_i are standard polynomials in the polarization vectors [69]. The three point structure is labeled by integers ℓ_1, ℓ_2, ℓ_3 , which are constrained by the

requirement that the correlator should be a polynomial in the Z_i .

The ℓ_i are unbounded in the limit of large spin J_i . However, there is a relation between the H_{ij} and V_i :

$$(V_1 H_{23} + V_2 H_{13} + V_3 H_{12} + 2V_1 V_2 V_3)^2 = 2H_{12} H_{13} H_{23}. \quad (3.365)$$

Using this relation, we can always reduce one of the λ_i to zero, so the number of unbounded quantum numbers labeling the three-point structures in 3D is $3 - 1 = 2$. The conformal block is labeled by two three-point structures, so this gives $2 \times 2 = 4$ additional unbounded quantum numbers for the block. Overall, we have $6 + 4 = 10 = \dim \mathcal{M}$ in 3D.

We are now ready to tackle the d -dimensional case. In the d -dimensional embedding formalism, an operator \mathcal{O} becomes a homogeneous function of an embedding coordinate $X \in \mathbb{R}^{d+1,1}$ and polarization vectors $W_1, \dots, W_n \in \mathbb{C}^{d+1,1}$, where $n = \lfloor \frac{d}{2} \rfloor$. (We conventionally write $W_1 = Z$.) More formally, \mathcal{O} is a locally holomorphic section of a line bundle over the flag variety $\mathcal{V}_{d+1,1}$ of $\mathrm{SO}(d+1, 1)$, which has (X, W_1, \dots, W_n) as projective coordinates. The number of these coordinates, subject to orthogonality relations and modulo gauge redundancies, is the same as the complex dimension of the flag variety, which is

$$\dim_{\mathbb{C}} \mathcal{V}_{d+1,1} = \frac{1}{2} (\dim \mathrm{SO}(d+1, 1) - \dim T) = \frac{1}{2} \left(\frac{(d+1)(d+2)}{2} - \left\lfloor \frac{d+2}{2} \right\rfloor \right), \quad (3.366)$$

where T is the maximal torus of $\mathrm{SO}(d+1, 1)$. See [68, 136] for more discussion on the embedding formalism for general tensors.

For example, in $d = 3$, this gives $\dim_{\mathbb{C}} \mathcal{V}_{4,1} = 4$, which is the correct number of degrees of freedom in the vectors $X, Z \in \mathbb{R}^{4,1}$. We can see this explicitly by restricting to the Poincare section $X = (1, x^2, x)$ and $Z = (1, 2x \cdot z, z)$. Here $x \in \mathbb{R}^3$ is unconstrained, and z is a null vector in 3D, modulo rescaling, which corresponds to a single angle on the celestial circle.

A three-point function $\langle \mathcal{O}_1 \mathcal{O}_2 \mathcal{O}_3 \rangle$ is a section of a line bundle over three copies of $\mathcal{V}_{d+1,1}$, satisfying invariance under $\mathrm{SO}(d+1, 1)$. In the large quantum number limit, the number of quantum numbers labeling such sections is

$$\#(\mathbb{Z}\text{-valued 3-pt structure labels}) = 3 \dim_{\mathbb{C}} \mathcal{V}_{d+1,1} - \dim \mathrm{SO}(d+1, 1). \quad (3.367)$$

Finally, a genus-2 block has two three-point structure labels s, s' , together with $\dim T = \lfloor \frac{d+2}{2} \rfloor$ quantum numbers for each of the three internal operators. Overall, the number of unbounded quantum numbers is

$$2(3 \dim \mathcal{V}_{d+1,1} - \dim \mathrm{SO}(d+1, 1)) + 3 \dim T = \dim \mathrm{SO}(d+1, 1) = \dim \mathcal{M}. \quad (3.368)$$

Chapter 4

ANGULAR FRACTALS IN THERMAL QFT

4.1 Introduction

Many aspects of conformal field theories (CFTs) are universal at high energies. A famous example is Cardy's formula, which states that the entropy of local operators at sufficiently high energies takes a universal form in all unitary, compact 2D CFTs [46] (see [168, 170, 175] for a precise formulation). Equivalently, the partition function of a 2D CFT

$$\mathrm{Tr} [e^{-\beta H + i\theta J}] \quad (4.1)$$

is universal in the high temperature regime $\beta \rightarrow 0$ with $\theta \sim O(\beta)$.

The derivation of Cardy's formula uses invariance of the torus partition function under the modular transformation $S : \tau \mapsto -1/\tau$. By instead using the full modular group $\mathrm{PSL}(2, \mathbb{Z})$, one finds similar universal behavior as $\beta \rightarrow 0$, near *any rational angle* $\theta = \frac{2\pi p}{q}$, see e.g. [24]. This leads to universal "spin-refined" versions of the density of states. For example, in the case $\frac{p}{q} = \frac{1}{2}$, the modular transformation $\tau \mapsto \frac{-\tau}{2\tau-1}$ gives the universal behavior of

$$\mathrm{Tr} [e^{-\beta(H-i\Omega J)} (-1)^J] = \mathrm{Tr} [e^{-\beta H + i\theta J}]_{\theta=\pi+\beta\Omega}, \quad (4.2)$$

in the regime $\beta \rightarrow 0$ with $\Omega \sim O(1)$. For any given 2D CFT, the logarithm of (4.2) is 1/4 the logarithm of (4.1) at high temperature, leading to a universal result for the difference between densities of even- and odd-spin operators in 2D CFTs.¹

While modular invariance is not available on $S^{d-1} \times S^1$ in higher dimensions, higher dimensional CFTs still display forms of universality at high energies, both in their density of states [7, 25, 27, 147, 188, 189, 199], and OPE coefficients [25, 74]. A central insight from [14, 27, 127] is that the high temperature behavior of a CFT can be captured by a "thermal Effective Field Theory (EFT)" that efficiently encodes the constraints of conformal symmetry and locality. In [7, 25, 188, 189], thermal EFT plays the role of a surrogate for the modular S -transformation (as well as modular transformations on genus-2 surfaces).

¹Modular invariance on higher genus surfaces also leads to universal results for OPE coefficients in 2D CFTs, as derived in [36, 44, 72, 115, 141], and unified in [67].

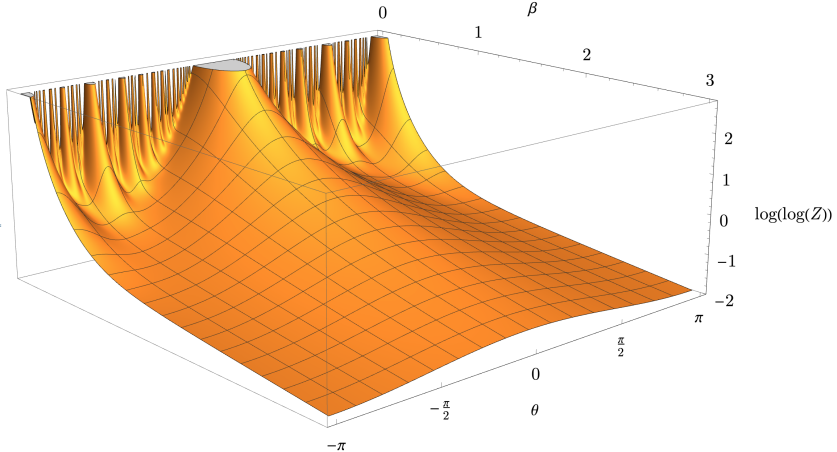


Figure 4.1: A qualitative picture of $\log(\log(Z))$ in the 3D Ising CFT, where $Z = \text{Tr}(e^{-\beta H + i\theta J})$ is the $S^2 \times S^1$ partition function. To construct this picture, we took the leading terms in the EFT description around each rational angle (up to denominator 15), and combined them with a root-mean-square. We give more detail in Appendix 4.10.

In this work, we will be interested in "spin-refined" information about the CFT density of states in general dimensions. In particular, we will study the partition function (4.1) with high temperature ($\beta \ll 1$) and finite angles $\vec{\theta}$. (In higher dimensions we promote $\vec{\theta}$ and \vec{J} to vectors with $\lfloor d/2 \rfloor$ components coming from the rank of $SO(d)$.) The regime $\vec{\theta} = \beta \vec{\Omega}$ with fixed $\vec{\Omega}$ is captured by thermal EFT as discussed in [14, 25, 27, 127, 188]. However, when $\vec{\theta}$ does not scale to zero as $\beta \rightarrow 0$, the naïve EFT description breaks down.

A simple example of a partition function with finite $\vec{\theta}$ is (4.2): the relative density of even-spin and odd-spin operators with respect to some particular Cartan generator J of the rotation group. This observable is naïvely outside the regime of validity of the thermal EFT, since θ remains finite as $\beta \rightarrow 0$.

More generally, we can consider a partition function that includes a rotation by finite rational angles in each of the Cartan directions:²

$$\text{Tr} \left[e^{-\beta(H - i\vec{\Omega} \cdot \vec{J})} R \right], \quad \text{where} \quad R = e^{2\pi i \left(\frac{p_1}{q_1} J_1 + \dots + \frac{p_n}{q_n} J_n \right)}. \quad (4.3)$$

Using a trick that was applied in [10] to study superconformal indices near roots of unity, we will find a *different* EFT description for this partition function, in terms of the thermal EFT on a background geometry with inverse temperature $q\beta$ and spatial manifold S^{d-1}/\mathbb{Z}_q , where $q = \text{lcm}(q_1, \dots, q_n)$. This determines the small- β

²In parity-invariant theories, we can also include reflections.

expansion of (4.3) in terms of the usual Wilson coefficients of thermal EFT, up to new subleading contributions from "Kaluza-Klein vortices" that we classify. For example, the effective free energy density of (4.3), coming from the leading term in the thermal effective action, is smaller than the usual free energy density by a factor of $1/q^d$. In particular, the effective free energy density of even-spin minus odd-spin operators described by (4.2) is smaller by $1/2^d$. (This generalizes the factor of $1/4$ in 2D.)³

The EFT descriptions around each rational angle patch together to create fractal-like behavior in the high-temperature partition function; see Figure 4.1 for an illustration in the 3D Ising CFT. It is remarkable that effective field theory constrains the asymptotics of the partition function in such an intricate way, even in higher dimensions.

Kaluza-Klein vortices appear whenever the rational rotation R does not act freely on the sphere S^{d-1} . Each vortex creates a defect in the thermal EFT, whose action can be written systematically in a derivative expansion in background fields. By contrast, when R generates a group that acts freely, no vortex defects are present, and the complete perturbative expansion of (4.3) in β is determined in terms of thermal EFT Wilson coefficients, with no new undetermined parameters.

While most of our discussion and examples are focused on CFTs, our formalism also applies to general QFTs. In particular, using thermal effective field theory, we derive a relation between the partition function at temperature T with a discrete isometry of order q inserted, to the partition function with no insertion at temperature T/q , in the thermodynamic limit.⁴ For example, we have

$$-\log \text{Tr}_{\mathcal{H}(\mathcal{M}_L)} [e^{-\beta H} R] \sim -\frac{1}{q} \log \text{Tr}_{\mathcal{H}(\mathcal{M}_L)} [e^{-q\beta H}] + \text{topological + KK defects} \quad (\text{as } L \rightarrow \infty). \quad (4.4)$$

Here, \mathcal{M}_L is a spatial manifold of characteristic size L , with associated Hilbert space $\mathcal{H}(\mathcal{M}_L)$, R is a discrete isometry of order q , and " \sim " denotes agreement to all perturbative orders in $1/L$. The relation (4.4) holds whenever the theory is gapped at inverse temperature $q\beta$. We write the most general relation in (4.32), which we check

³Note that simply taking the density of states computed in [25] and inserting the phase R into the trace will *not* give the correct answer to the partition function. For a demonstration of this in 2D, see Appendix B of [24].

⁴We are extremely grateful to Luca Delacretaz for emphasizing the general QFT case to us.

in both massive and massless examples. An interesting consequence of this simple formula is that twists by discrete isometries can be sensitive to lower-temperature phases of the theory. For example, the partition function of QCD at temperature $T > \Lambda_{\text{QCD}}$, twisted by a discrete isometry with order q , becomes sensitive to physics below the confinement scale when $T/q < \Lambda_{\text{QCD}}$.

This universality of partition functions with spacetime symmetry insertions is in contrast to the case for global symmetry insertions. The insertion of a global symmetry generator operator is equivalent to turning on a new background field in the thermal EFT. The dependence of the effective action on this background field introduces new Wilson coefficients that are not necessarily related in a simple way to the Wilson coefficients without the global symmetry background; see e.g. [102, 128, 174].

The paper is organized as follows. In Section 4.2, we present a derivation of our main result: a systematic study of the high temperature expansion of the partition function of any quantum field theory with the insertion of a discrete isometry. In Section 4.3, we look in more detail at the Kaluza-Klein vortices that appear on S^{d-1} when the discrete isometry (which is a rational rotation in this case) has fixed points. In Section 4.4, we discuss subtleties that appear for fermionic theories. In Section 4.5, we give several examples in free theories that illustrate our general results. In Section 4.6, we consider thermal effective actions with topological terms. In Section 4.7, we apply our results to holographic CFTs. In Section 4.8, we look at irrational θ . In Section 4.9, we discuss non-perturbative corrections in temperature. Finally in Section 4.10, we conclude and discuss future directions.

4.2 Folding and unfolding the partition function

Thermal effective action and finite velocities

Equilibrium correlators of generic interacting QFTs at finite temperature are expected to have a finite correlation length. Equivalently, the dimensional reduction of a generic interacting QFT on a Euclidean circle is expected to be gapped. When this is the case, long-distance finite-temperature observables of the QFT can be captured by a local "thermal effective action" of background fields [14, 27, 127]. For example, consider the partition function of a QFT_d on $\mathcal{M}_L \times S^1_\beta$, where the spatial

$d-1$ -manifold \mathcal{M}_L has size L . In the thermodynamic limit of large L , we have

$$\begin{aligned} \text{Tr}_{\mathcal{H}(\mathcal{M}_L)}[e^{-\beta H_L}] &= Z_{\text{QFT}}[\mathcal{M}_L \times S_\beta^1] \\ &= Z_{\text{gapped}}[\mathcal{M}_L] \\ &\sim e^{-S_{\text{th}}[g, A, \phi]} + \text{nonperturbative in } 1/L \quad (L \rightarrow \infty), \end{aligned} \quad (4.5)$$

where $\mathcal{H}(\mathcal{M}_L)$ is the Hilbert space of states on \mathcal{M}_L , and H_L is the Hamiltonian. Here, the thermal effective action S_{th} depends on a $d-1$ -dimensional metric g_{ij} , a Kaluza-Klein gauge field A_i , and a dilaton ϕ , which can be obtained by placing the d -dimensional metric in Kaluza-Klein (KK) form

$$G_{\mu\nu}dx^\mu dx^\nu = g_{ij}(\vec{x})dx^i dx^j + e^{2\phi(\vec{x})}(d\tau + A_i(\vec{x}))^2, \quad (4.6)$$

where $\tau \sim \tau + \beta$ is a periodic coordinate along the thermal circle. The derivative expansion for S_{th} becomes an expansion in inverse powers of the length L .

If the spatial manifold \mathcal{M}_L possesses a continuous isometry ξ , then we can additionally twist the partition function by the corresponding charge Q_ξ :

$$\text{Tr}_{\mathcal{H}(\mathcal{M}_L)}[e^{-\beta(H_L - i\alpha Q_\xi)}]. \quad (4.7)$$

Geometrically, this twist corresponds to a deformation of the background fields g, A, ϕ that depends on $\alpha\xi$. In the thermodynamic limit, we can describe (4.7) using the thermal effective action, provided that the background fields g, A, ϕ remain finite as $L \rightarrow \infty$. In particular, the combination $\alpha\xi$ must remain finite as $L \rightarrow \infty$. The physical reason is that $i\alpha$ represents the velocity of the system in the direction of ξ in the canonical ensemble. This velocity must remain finite in order to have a good thermodynamic limit.

By contrast, suppose that \mathcal{M}_L possesses a nontrivial discrete isometry R with finite order $R^q = 1$. If we twist the partition function by R ,

$$\text{Tr}_{\mathcal{H}(\mathcal{M}_L)}[e^{-\beta H}R], \quad (4.8)$$

then physically this corresponds to a system whose "velocity" is of order L . The background fields g, A, ϕ naively do not have a good thermodynamic limit, and we cannot apply the thermal effective action in an obvious way.

- Example: CFT partition function

An important example for us is the partition function of a CFT_d on $S^{d-1} \times S_\beta^1$. Conformal invariance dictates that

$$\text{Tr}\left[e^{-\beta(H - i\vec{\Omega} \cdot \vec{J})}\right] = \text{Tr}_{\mathcal{H}(S_L^{d-1})}\left[e^{-L\beta(H_L - i\vec{\Omega} \cdot \vec{J}_L)}\right]. \quad (4.9)$$

On the left-hand side, we have the usual partition function of the CFT on a sphere of radius 1. On the right-hand side, H_L denotes the Hamiltonian on a sphere S_L^{d-1} of radius L , and \vec{J}_L are generators of isometries of the sphere, normalized so that the corresponding Killing vectors are finite in the flat-space limit $L \rightarrow \infty$. (For example, for a rotation of the sphere by an angle ϕ , a Killing vector with a finite flat-space limit is $\frac{1}{L} \frac{\partial}{\partial \phi}$.)

When β is small, we can set $L = O(1/\beta)$ on the right-hand side and try to apply the thermal effective action (4.5). We find that in order to have a good thermodynamic limit as $\beta \rightarrow 0$, the angular potentials $\vec{\Omega}$ must remain finite. Phrased in terms of the rotation angle $\vec{\theta} = \beta \vec{\Omega}$, we find that $\vec{\theta}$ must scale to zero as $\beta \rightarrow 0$. Provided this is the case, the $1/L$ expansion of the thermal effective action gives an expansion in small β for the CFT partition function.

We can also understand condition $\vec{\theta} \rightarrow 0$ more explicitly from a direct computation using the thermal effective action. In a CFT, the thermal effective action is constrained by d -dimensional Weyl invariance. The most general coordinate- and Weyl-invariant action takes the form^{5,6}

$$S_{\text{th}} = \int \frac{d^{d-1} \vec{x}}{\beta^{d-1}} \sqrt{\hat{g}} \left(-f + c_1 \beta^2 \hat{R} + c_2 \beta^2 F^2 + \dots \right) + S_{\text{anom}}. \quad (4.10)$$

Here $\hat{g} = e^{-2\phi} g$, \hat{R} is the Ricci scalar built from \hat{g} , F^2 is a Maxwell term, etc. The term S_{anom} accounts for Weyl anomalies (which are not important for the present discussion).

On the geometry $S^{d-1} \times S^1_\beta$, we can easily determine g, A, ϕ and evaluate S_{th} [25]:

$$S_{\text{th}} = \frac{\text{vol } S^{d-1}}{\prod_{i=1}^n (1 + \Omega_i^2)} \left[-f T^{d-1} + (d-2) \left((d-1)c_1 + \left(2c_1 + \frac{8}{d} c_2 \right) \sum_{i=1}^n \Omega_i^2 \right) T^{d-3} + \dots \right]. \quad (4.11)$$

We see that terms of order $T^{d-1-k} = \beta^{k-d+1}$ in the high-temperature expansion of S_{th} are multiplied by a polynomial in the angular potentials Ω_i of degree k (see e.g. examples in [31]). Consequently, $\theta_i \rightarrow 0$ as $\beta \rightarrow 0$ is necessary for the high-temperature expansion to be well-behaved.

⁵For simplicity, here we assume that the theory is free of gravitational anomalies.

⁶Note that [25] worked in conventions where τ has periodicity 1, and β is absorbed into the field ϕ . In this paper, we instead use conventions where τ has dimensionful periodicity β (later we will also have other periodicities) so that explicit powers of β appear in the action (4.10), as required by dimensional analysis. To convert from the conventions of [25] to the conventions in this work, one shifts the dilaton by $\phi \rightarrow \phi + \log \beta$.

To summarize, the thermal effective action can describe "small" angles $\theta \sim \beta\Omega$, where the angular velocity remains finite in the thermodynamic limit. However, results from the thermal effective action like (4.11) break down outside this regime. How can we access more general angles?

Spin-refined partition functions: warm-up in 2D CFT

As a warm-up, in 2D CFT, we can compute partition functions at more general angles using modular invariance. Let us review how this works and derive some example results. For convenience, we write the partition function as

$$Z(\tau, \bar{\tau}) = \text{Tr} \left[e^{2\pi i \tau (L_0 - \frac{c}{24}) - 2\pi i \bar{\tau} (\bar{L}_0 - \frac{c}{24})} \right], \quad (4.12)$$

where $\tau = \frac{i\beta}{2\pi} + \frac{\theta}{2\pi}$ and $\bar{\tau} = \tau^*$.⁷ The high temperature behavior of $Z(\tau, \bar{\tau})$ at small angles can be obtained by performing the modular transformation $\tau \rightarrow -1/\tau$ (similarly for $\bar{\tau}$) and approximating by the contribution of the vacuum state. The result agrees with the thermal effective action:

$$\text{Tr} \left[e^{-\beta(H - i\Omega J)} \right] \sim e^{-S_{\text{th}}} = \exp \left[\frac{\text{vol } S^1}{(1 + \Omega^2)} \frac{f}{\beta} \right] = \exp \left[\frac{4\pi^2}{\beta(1 + \Omega^2)} \frac{c}{12} \right] \quad (\text{CFT}_2), \quad (4.13)$$

where $f = \frac{2\pi c}{12}$. Here, we assume $c_L = c_R$ for simplicity. In this case, only the cosmological constant term appears in the thermal effective action in 2D.

Now let us instead assume that $\frac{\theta}{2\pi}$ is close to a nonzero rational angle $\frac{p}{q}$, so that $\tau, \bar{\tau}$ are very close to $\frac{p}{q}$. Following [24], we can perform a different modular transformation to map $(\tau, \bar{\tau})$ close to $\pm i\infty$ and approximate the partition function by the vacuum state in the new channel. For example, let us study the partition function with an insertion of $(-1)^J$ given in (4.2). In this case, we have

$$\begin{aligned} \tau &= \frac{1}{2} + \frac{\beta\Omega}{2\pi} + \frac{i\beta}{2\pi} \\ \bar{\tau} &= \frac{1}{2} + \frac{\beta\Omega}{2\pi} - \frac{i\beta}{2\pi}, \quad \beta \ll 1, \quad \Omega \sim O(1). \end{aligned} \quad (4.14)$$

Modular invariance is the statement

$$Z(\gamma \circ \tau, \gamma \circ \bar{\tau}) = Z(\tau, \bar{\tau}), \quad \gamma \in \text{PSL}(2, \mathbb{Z}). \quad (4.15)$$

⁷Note that in this section, τ denotes the modular parameter of the torus, while in other sections τ denotes Euclidean time. We hope this will not cause confusion.

An appropriate transformation in this case is

$$\gamma = \pm \begin{pmatrix} -1 & 0 \\ 2 & -1 \end{pmatrix} \in \mathrm{PSL}(2, \mathbb{Z}), \quad (4.16)$$

which leads to

$$\mathrm{Tr} \left[e^{-\beta(H-i\Omega J)} (-1)^J \right] = \mathrm{Tr} \left[e^{2\pi i \tilde{\tau}(L_0 - \frac{c}{24}) - 2\pi i \tilde{\tau}^*(\bar{L}_0 - \frac{c}{24})} \right] \sim \exp \left[\frac{1}{4} \frac{4\pi^2}{\beta(1+\Omega^2)} \frac{c}{12} \right],$$

where $\tilde{\tau} = -\frac{1}{2} + \frac{\pi i}{2\beta(1-i\Omega)}$, $\tilde{\tau}^* = \tilde{\tau}^*$. (4.17)

On the right-hand side, we approximated the trace by the contribution of the vacuum state in the $\beta \rightarrow 0$ limit. We find that the partition function weighted by $(-1)^J$ grows exponentially in $1/\beta$, with an exponent that is $1/4$ of the un-weighted case (4.13).

For a general angle $\frac{\theta}{2\pi}$ close to $\frac{p}{q}$, we repeat the same logic above but with a more complicated modular transformation, namely

$$\gamma = \pm \begin{pmatrix} -(p^{-1})_q & b \\ q & -p \end{pmatrix} \in \mathrm{PSL}(2, \mathbb{Z}), \quad (4.18)$$

where $(p^{-1})_q$ is the inverse of p modulo q , and b is chosen so the matrix has determinant 1. We get

$$\mathrm{Tr} \left[e^{-\beta(H-i\Omega J)} e^{2\pi i \frac{p}{q} J} \right] \sim \exp \left[\frac{1}{q^2} \frac{4\pi^2}{\beta(1+\Omega^2)} \frac{c}{12} \right]. \quad (4.19)$$

In general, we find that the partition function of a 2D CFT weighted by $e^{2\pi i \frac{p}{q} J}$ grows exponentially in $1/\beta$, with an exponent that is $1/q^2$ of the un-weighted case (4.13).

Because modular invariance is not available in higher dimensions, it will be useful to rederive (4.19) in a different way. We now describe two (related) approaches that can generalize to higher dimensions.

Folding and unfolding

Thermal EFT naively breaks down in spin-refined partition functions like (4.2) because the large spacetime symmetry $(-1)^J$ moves us outside the thermodynamic limit. One way to recover an EFT description is to perform a change of coordinates that makes $(-1)^J$ look more like a global symmetry.

For example, consider a spin-refined partition function of a 2D QFT (not necessarily conformal) on $S_L^1 \times S_\beta^1$,

$$\mathrm{Tr} \left[e^{-\beta H} (-1)^J \right], \quad (4.20)$$

where $(-1)^J$ denotes a rotation of the spatial circle S_L^1 by π . We can reinterpret *one* copy of the QFT on $S_L^1 \times S_\beta^1$ as *two* copies of the QFT on $(S_L^1/\mathbb{Z}_2) \times S_\beta^1$, with topological defects that glue the two copies to each other, see the middle of Figure 4.2. In this picture, the operator $(-1)^J$ becomes a topological defect that simply permutes the two copies of the QFT as we move along the time direction. If we begin in one copy of the QFT and move by β in Euclidean time, we pass once through the $(-1)^J$ defect and go to the other copy. Moving by β again, we pass through the $(-1)^J$ defect again and end up in the first copy. Thus, inserting $(-1)^J$ into the partition function creates a new effective thermal circle of length 2β .

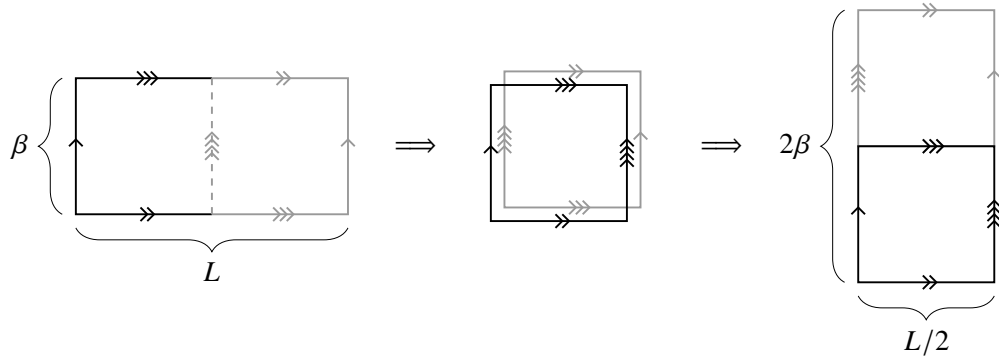


Figure 4.2: Left: The torus partition function with spatial cycle of length L , inverse temperature β , and an insertion of $(-1)^J$. The $(-1)^J$ insertion means we must glue the top and bottom of the figure with a half shift around the spatial circle. We split the figure into a left and right half using the trivial defect (vertical dashed line), and for convenience we color the right half grey. **Middle:** Placing the black and grey rectangles on top of each other, we can interpret this same observable as the partition function of two copies of the QFT (black and grey) on an $(L/2) \times \beta$ rectangle, with boundary conditions inherited from the left figure. **Right:** Finally, we can re-stack the two copies of the QFT, resulting in a single copy of the QFT with a new spatial circle of length $L/2$ and an effective thermal circle of length 2β . Note that the effective thermal circle is nontrivially fibered over the new spatial circle.

This reinterpretation of the path integral with a $(-1)^J$ insertion is illustrated in Figure 4.2. One wrinkle (that is clear in the figure) is that the effective thermal $S_{2\beta}^1$ is nontrivially fibered over the spatial circle S_L^1/\mathbb{Z}_2 : when we go once around the new spatial circle, the $S_{2\beta}^1$ shifts by β .

So far, we have considered a rotation angle of π . However, it is straightforward to study nearby rotation angles of the form $\theta = \pi + \beta\Omega$. On the left-hand side of Figure 4.2, we simply insert an additional topological operator along the spatial cycle that implements the small rotation $e^{i\beta\Omega J}$. Following the manipulations in the

figure, we end up with a product of two such operators on the new spatial cycle S_L^1/\mathbb{Z}_2 , which together implement a rotation of $2\beta\Omega$.

The advantage of this rewriting of the path integral is that we can now smoothly take the thermodynamic limit $L \rightarrow \infty$ and use the thermal effective action. The effective inverse temperature is 2β , the rotation angle is $2\beta\Omega$, and the effective spatial cycle is S_L^1/\mathbb{Z}_2 .

In fact, the above construction is straightforward to generalize to twists by any rational angle:

$$\text{Tr} \left[e^{-\beta(H-i\Omega J)+2\pi i \frac{p}{q} J} \right]. \quad (4.21)$$

We interpret (4.21) as the partition function of q copies of the QFT on the space S_L^1/\mathbb{Z}_q , with appropriate topological defects that glue the copies together. The operator $e^{2\pi i \frac{p}{q} J}$ becomes a topological defect that permutes the copies of the QFT as we move around the Euclidean time circle. This creates an effective thermal circle $S_{q\beta}^1$, which is fibered over S_L^1/\mathbb{Z}_q . We can now apply thermal EFT on S_L^1/\mathbb{Z}_q .

- Example: 2D CFT

As an example application, we can recover our previous answer for the spin-refined partition function of a 2D CFT. For a twist by $(-1)^J$, we find

$$\text{Tr} \left[e^{-\beta(H-i\Omega J)} (-1)^J \right] \sim e^{-S_{\text{th}}[S^1/\mathbb{Z}_2 \times S_{2\beta}^1]} = \exp \left[\frac{2\pi c}{12} \frac{\text{vol}(S^1/\mathbb{Z}_2)}{2\beta(1+\Omega^2)} \right] = \exp \left[\frac{1}{4} \frac{4\pi^2}{\beta(1+\Omega^2)} \frac{c}{12} \right]. \quad (4.22)$$

In the action, we obtain one factor of $\frac{1}{2}$ from the smaller spatial cycle S^1/\mathbb{Z}_2 , and another factor of $\frac{1}{2}$ from the larger thermal circle, resulting in an overall factor of $\frac{1}{4}$ that agrees with the result from modular invariance (4.17).⁸

More generally, for a twist by $\frac{2\pi p}{q}$, the thermal effective action gives

$$\text{Tr} \left[e^{-\beta(H-i\Omega J)} e^{\frac{2\pi i p}{q} J} \right] \sim e^{-S_{\text{th}}[S^1/\mathbb{Z}_q \times S_{q\beta}^1]} = \exp \left[\frac{2\pi c}{12} \frac{\text{vol}(S^1/\mathbb{Z}_q)}{q\beta(1+\Omega^2)} \right] = \exp \left[\frac{1}{q^2} \frac{4\pi^2}{\beta(1+\Omega^2)} \frac{c}{12} \right]. \quad (4.23)$$

⁸The fact that the thermal circle is nontrivially fibered plays no role here because the thermal effective action is the integral of a local coordinate-invariant quantity that does not detect global features of the bundle. In a theory with a gravitational anomaly, the thermal effective action would contain an additional 1-dimensional Chern-Simons for the Kaluza-Klein gauge field, which can detect the nontrivial topological structure of the thermal circle bundle; see Section 4.6. The nontrivial topology also enters into nonperturbative corrections; see Section 4.9.

We find that the effective free energy at high temperature for the spin-refined partition function (4.21) is down by a factor of q^2 , in agreement with (4.19). Note that the precise permutation of the copies of the CFT implemented by $e^{2\pi i \frac{p}{q} J}$ depends on p , but the length of the resulting thermal circle does not. Consequently the partition function is independent of p , up to nonperturbative corrections as $\beta \rightarrow 0$.⁹

- Higher dimensions

The above construction works for $d > 2$ as well, and on more general geometries. Consider a QFT_d on any $(d-1)$ -dimensional spatial manifold \mathcal{M}_L with a discrete isometry R of finite order $R^q = 1$. Again, we can reinterpret one copy of the QFT on $\mathcal{M}_L \times S_\beta^1$ as q copies of the QFT on $(\mathcal{M}_L / \mathbb{Z}_q) \times S_\beta^1$, with topological defects that glue the copies to each other. In this picture, R is represented as a topological defect that simply permutes the q copies of the QFT as we move along the time direction, creating an effective inverse temperature $q\beta$.

The EFT bundle

Before exploring further consequences of this idea, it will be helpful to adopt a more abstract, geometrical perspective on this construction. Consider again a d -dimensional QFT with spatial manifold \mathcal{M}_L . Given an isometry $U \in \text{Iso}(\mathcal{M}_L)$, the partition function twisted by U^{10}

$$\text{Tr}_{\mathcal{H}(\mathcal{M}_L)} [e^{-\beta H} U] \quad (4.24)$$

is computed by the path integral of the CFT on the mapping torus

$$M_{\beta, U} \equiv (\mathcal{M}_L \times \mathbb{R}) / \mathbb{Z}, \quad (4.25)$$

where $\mathbb{Z} = \langle h \rangle$ is generated by

$$\begin{aligned} h : \mathcal{M}_L \times \mathbb{R} &\rightarrow \mathcal{M}_L \times \mathbb{R}, \\ h : (\vec{x}, \tau) &\mapsto (U\vec{x}, \tau + \beta), \end{aligned} \quad (4.26)$$

where \vec{x} is a coordinate on \mathcal{M}_L .

Now let us specialize to $U = R$, where R has order q . In this case, the q -th power of h acts very simply: it leaves \mathcal{M}_L invariant, and shifts τ by $q\beta$:

$$h^q : (\vec{x}, \tau) \mapsto (\vec{x}, \tau + q\beta). \quad (4.27)$$

⁹There is p -dependence if the theory is fermionic (see Section 4.4) or has a gravitational anomaly (see Section 4.6).

¹⁰Here, we abuse notation and write U for both the isometry and the operator implementing its action on the Hilbert space $\mathcal{H}(\mathcal{M}_L)$.

Consequently, it is useful to decompose $\mathbb{Z} \cong q\mathbb{Z} \times \mathbb{Z}_q = \langle h^q \rangle \times (\langle h \rangle / \langle h^q \rangle)$, and obtain the mapping torus $M_{\beta,R}$ via two successive quotients. We first quotient by $q\mathbb{Z} \cong \langle h^q \rangle$ (which turns \mathbb{R} into $S^1_{q\beta}$), and then quotient by $\mathbb{Z}_q = \langle h \rangle / \langle h^q \rangle$:

$$M_{\beta,R} = ((\mathcal{M}_L \times \mathbb{R})/q\mathbb{Z})/\mathbb{Z}_q = (\mathcal{M}_L \times S^1_{q\beta})/\mathbb{Z}_q. \quad (4.28)$$

The quotient $(\mathcal{M}_L \times S^1_{q\beta})/\mathbb{Z}_q$ on the right-hand side of (4.28) can be viewed as a bundle in two different ways. Firstly, it is a \mathcal{M}_L -bundle over $S^1_{q\beta}/\mathbb{Z}_q \cong S^1_\beta$. This is the usual point of view of the trace as a spatial manifold evolving over Euclidean time β . However, we can alternatively view $(\mathcal{M}_L \times S^1_{q\beta})/\mathbb{Z}_q$ as an $S^1_{q\beta}$ bundle over $\mathcal{M}_L/\mathbb{Z}_q$. We call this latter description the "EFT bundle." In Section 4.2, the EFT bundle was a nontrivial $S^1_{q\beta}$ bundle over S^1_L/\mathbb{Z}_q . As we saw, the virtue of the EFT bundle is that the thermodynamic limit $L \rightarrow \infty$ is straightforward: we can dimensionally reduce along the effective thermal circle $S^1_{q\beta}$ without leaving the thermodynamic limit. The theory is then described by thermal EFT with effective inverse temperature $q\beta$ and spatial cycle $\mathcal{M}_L/\mathbb{Z}_q$.

Suppose for the moment that the action of R on \mathcal{M}_L is free, so that $\mathcal{M}_L/\mathbb{Z}_q$ is smooth. (This is the case, for example, for a rational rotation of the spatial circle in 2D.) For any term in the thermal effective action that is the integral of a local density, the effect of the quotient by \mathbb{Z}_q is simply to multiply its contribution by $1/q$. Thus, we conclude

$$-\log \text{Tr} [e^{-\beta H} R] \sim -\frac{1}{q} \log \text{Tr} [e^{-q\beta H}] + \text{topological} \quad (\text{if the } R \text{ action is free}). \quad (4.29)$$

Here, " \sim " denotes agreement to all perturbative orders in the $1/L$ expansion. The term "topological" indicates potential contributions from a finite number of terms capable of detecting the topology of the EFT bundle, which cannot be written as the integral of a local gauge/coordinate-invariant density. We discuss such terms in Section 4.6.

Let us pause to note that the result (4.29) really only requires that the theory be gapped at inverse temperature $q\beta$ (not necessarily at inverse temperature β), since we only use locality of the thermal effective action on the right-hand side.

- Adding "small" isometries

Just as before, we can also consider inserting into the trace an additional "small" isometry $U = e^{i\beta(\alpha Q_\xi)}$, where ξ is a Killing vector on \mathcal{M}_L , Q_ξ is its corresponding

charge, and α is the corresponding thermodynamic potential. We will be mainly interested in the case where U commutes with the discrete isometry R , so we assume this henceforth. The insertion of U can be thought of as a topological defect that wraps \mathcal{M}_L . Consequently, the defect wraps q times around the base of the EFT bundle $\mathcal{M}_L/\mathbb{Z}_q$, resulting in an effective rotation U^q . We conclude that

$$-\log \text{Tr} [gR] \sim -\frac{1}{q} \log \text{Tr} [g^q] + \text{topological} \quad (\text{if the } R \text{ action is free}), \quad (4.30)$$

where $g = e^{-\beta H}U$.

In fact, this argument applies to any global symmetry element V as well, so (4.30) holds when g is multiplied by a global symmetry group element: $g = e^{-\beta H}UV$. We can think of V as implementing a nontrivial flat connection for a background gauge field coupled to the global symmetry. In this case, the "topological" terms in (4.30) could include contributions from nontrivial topology of this connection.

We can also understand the insertion of "small" isometries geometrically. Again, the idea is to view the mapping torus $M_{\beta,UR}$ as the result of two successive quotients

$$M_{\beta,UR} = ((\mathcal{M}_L \times \mathbb{R})/\langle h^q \rangle)/\mathbb{Z}_q = M_{q\beta,U^q}/\mathbb{Z}_q, \\ \text{where } h : (\vec{x}, \tau) \mapsto (UR\vec{x}, \tau + \beta), \quad (4.31)$$

where $\mathbb{Z}_q = \langle h \rangle/\langle h^q \rangle$, and we have used $(UR)^q = U^q$. On the right-hand side, we have the mapping torus $M_{q\beta,U^q}$ which is described by the thermal effective action at inverse temperature $q\beta$, with small isometries U^q turned on. The effect of the \mathbb{Z}_q quotient is to multiply the contribution of any integral of a local density by $1/q$. This again leads to (4.30).¹¹

The work [10] uses similar ideas to characterize superconformal indices of 4D CFTs near roots of unity. Our novel contribution is to apply these ideas in not-necessarily-supersymmetric, not-necessarily-conformal theories, on general spatial geometries, and also to describe the effects of Kaluza-Klein vortices (see below), which do not appear in superconformal indices.

- Non-free actions and Kaluza-Klein vortex defects

What happens if the action of R is not free? For example, in a 3D QFT on $S^2 \times S^1_\beta$, the action of $(-1)^J$ (where J is the Cartan generator of the rotation group) has fixed

¹¹When U and R don't commute, the same logic works but we have $M_{q\beta,(UR)^q}/\mathbb{Z}_q$ on the right-hand side of (4.31). We can still use thermal EFT, since $(UR)^q$ is $O(\beta)$ close to the identity.

points at the north and south poles of S^2 . In this case, the EFT bundle degenerates at the fixed loci of nontrivial elements of \mathbb{Z}_q , namely $R, \dots, R^{q-1} \in \mathbb{Z}_q$. After dimensional reduction, these degeneration loci becomes defects \mathfrak{D}_i (with i labelling the set of defects) in the $d - 1$ dimensional thermal effective theory. We call them "Kaluza-Klein vortex defects" because the KK gauge field A has nontrivial holonomy around them, as we explain in Section 4.3.

Each defect \mathfrak{D}_i contributes to the partition function a coordinate-invariant effective action $S_{\mathfrak{D}_i}$ of the background fields g, A, ϕ *in the infinitesimal neighborhood of \mathfrak{D}_i* . We then have the more general result

$$-\log \text{Tr} [gR] \sim -\frac{1}{q} \log \text{Tr} [g^q] + \text{topological} + \sum_{\mathfrak{D}_i} S_{\mathfrak{D}_i}. \quad (4.32)$$

We conjecture that for generic interacting QFTs, the KK vortex defects will be gapped. (In fact, in this work, we will study several examples of free theories where the appropriate defects are still gapped.) In this case, each $S_{\mathfrak{D}_i}$ will be a local functional of g, A, ϕ .

In CFTs, the defect actions $S_{\mathfrak{D}_i}$ are additionally constrained by Weyl-invariance, just like the bulk terms in the thermal effective action. We will determine the explicit form of $S_{\mathfrak{D}} := \sum_{\mathfrak{D}_i} S_{\mathfrak{D}_i}$ in CFTs later in Section 4.3. For now, we simply note that the leading term in the derivative expansion of $S_{\mathfrak{D}_i}$ in a CFT is a cosmological constant localized on \mathfrak{D}_i :¹²

$$S_{\mathfrak{D}_i} = a_{\mathfrak{D}_i} \int_{\mathfrak{D}_i} \frac{d^{n_i} y}{(q\beta)^{n_i}} \sqrt{\hat{g}|_{\mathfrak{D}_i}} + \text{higher derivatives.} \quad (4.33)$$

Here, we assume that \mathfrak{D}_i is n_i -dimensional, y are coordinates on the defect, and $\hat{g}|_{\mathfrak{D}_i}$ denotes the pullback of $\hat{g} = e^{-2\phi} g$ to \mathfrak{D}_i . This term behaves like β^{-n_i} as $\beta \rightarrow 0$. In the case $n_i = 0$, i.e. when \mathfrak{D}_i is point-like (for example the north/south poles of S^2), the "cosmological constant" becomes simply a constant.

- Example: CFT in general d

As an example application, consider a d -dimensional CFT on $S^{d-1} \times S^1_\beta$. Although our discussion so far has been somewhat abstract, and we have used only basic geometry and principles of EFT, our conclusion (4.32) makes powerful predictions

¹² $S_{\mathfrak{D}_i}$ itself can also have topological terms; if the topological term has no derivatives (i.e. the Wilson line of the KK photon), it will contribute at the same order in β as the defect cosmological constant.

about CFT spectra. For example, to leading order as $\beta \rightarrow 0$, the defect term $S_{\mathfrak{D}}$ does not contribute, so very generally we obtain a higher dimensional generalization of (4.23),

$$\log \text{Tr}[e^{-\beta(H-i\vec{\Omega}\cdot\vec{J})} R] \sim \frac{1}{q^d} \frac{\text{vol}S^{d-1}}{\prod_{i=1}^n (1+\Omega_i^2)} \frac{f}{\beta^{d-1}} + \dots, \quad (4.34)$$

valid for any element R of the Cartan subgroup of $\text{SO}(d)$ with order q . For example, the relative density of even- and odd-spin operators (with respect to any Cartan generator) grows exponentially at a rate precisely $1/2^d$ times the rate for the un-weighted density of states.

Unlike in $d = 2$, the thermal effective action in $d > 2$ can have more than just a cosmological constant term. Consequently, the "..." in (4.34) includes higher-derivative corrections (in addition to possible vortex defect contributions). However, these higher-derivative corrections can be predicted in the same way: they differ from the un-spin-refined case by replacing $\beta \rightarrow q\beta$ and multiplying by $1/q$ to account for the smaller spatial manifold.

The results (4.34) and (4.32) display an important difference between partition functions weighted by spacetime symmetries and partition functions weighted by global symmetries. If we replace R with a global symmetry element, this corresponds to turning on new background gauge fields in the thermal effective action, whose contributions are captured by Wilson coefficients that are not active when the global symmetry generators are turned off. For example, the density of states weighted by a global symmetry generator U is controlled by a U -dependent free energy density f_U with no (obvious) relation to f when $U \neq 1$ (see e.g. [102, 128]). By contrast, the density of states weighted by different discrete *spacetime* symmetries are all controlled by the same f (and the same higher Wilson coefficients like c_1, c_2, \dots), in a predictable way.

Finally, let us describe the possible discrete rotations R for which (4.34) applies. Let us write $R = e^{i\vec{\theta}\cdot\vec{J}}$. In order for R to have finite order q , we must have $\vec{\theta} = 2\pi(\frac{p_1}{q_1}, \dots, \frac{p_n}{q_n})$, where the p_i/q_i are rational numbers (which we assume are in reduced form, so that p_i and q_i are relatively prime). The order of R is $q = \text{lcm}(q_1, \dots, q_n)$.

When d is even, the action of \mathbb{Z}_q is free if all $q_i = q$. In this case, the quotient S^{d-1}/\mathbb{Z}_q is a lens space $L(q; p_1, \dots, p_n)$, and there are no vortex defects \mathfrak{D} . If instead there exists at least one $q_i \neq q$, then the group element R^{q_i} will have a

fixed locus S^{2k-1} , where k is the number of q_j 's such that $q_j|q_i$, and there will be a corresponding defect \mathfrak{D} at this location (or rather its image after quotienting by \mathbb{Z}_q). Note that it is possible for fixed loci to intersect, creating higher codimension defects. For example, if $\vec{\theta} = 2\pi(1, \frac{1}{2}, \frac{1}{3})$, the element R^2 has a fixed S^3 , the element R^3 has its own fixed S^3 , and the two S^3 's intersect along an S^1 . Quotienting by \mathbb{Z}_6 , we obtain a defect localized on $S^3/\mathbb{Z}_3 \subset S^5/\mathbb{Z}_6$, a defect localized on $S^3/\mathbb{Z}_2 \subset S^5/\mathbb{Z}_6$, and they intersect along an $S^1 \in S^5/\mathbb{Z}_6$. In this case, the thermal effective action will include terms localized on the defects and their intersection. When d is odd, any element of $\text{SO}(d)$ necessarily has a nontrivial fixed locus, since there is a direction left invariant by the Cartan generators.

If the theory has a reflection symmetry, then we can more generally consider $R \in O(d)$. The above arguments continue to hold, essentially unmodified. When R includes a reflection, the base of the EFT bundle S^{d-1}/\mathbb{Z}_q can be non-orientable. For example, if we take R to be the parity operator $R : \vec{n} \rightarrow -\vec{n}$, then $S^{d-1}/\mathbb{Z}_2 = \mathbb{RP}^{d-1}$, which is non-orientable in odd d . Note that the parity operator acts freely, so in this case we can apply (4.30).

4.3 Kaluza-Klein vortex defects

In this section, we explore the form of the defect action $S_{\mathfrak{D}}$ that contributes whenever the group generated by the discrete rotation R does not act freely. For simplicity, we will restrict our attention to CFT's in d -dimensions on a spatial sphere S^{d-1} .

Background fields and EFT gauge

As before, we wish to compute the partition function of a CFT on the geometry $M_{q\beta,U^q}/\mathbb{Z}_q$, where the mapping torus in the numerator is $M_{q\beta,U^q} = (S^{d-1} \times \mathbb{R})/\langle h^q \rangle$, the group in the denominator is $\mathbb{Z}_q = \langle h \rangle/\langle h^q \rangle$, and the action of h is given by

$$h : (\vec{n}, \tau) \mapsto (UR\vec{n}, \tau + \beta) = (e^{i(\frac{2\pi p_a}{q_a} + \beta\Omega_a)J^a} \vec{n}, \tau + \beta). \quad (4.35)$$

First, let us be more precise about the form of the background fields in this geometry. Following [25], we use radius-angle coordinates on the sphere S^{d-1} . These are given by a pair of radius and angle $\{r_a, \theta_a\}$ for each orthogonal 2-plane ($a = 1, \dots, n = \lfloor \frac{d}{2} \rfloor$). If d is odd, we have an additional radial coordinate r_{n+1} . Together, the radii satisfy the constraint $\sum_{a=1}^{n+\epsilon} r_a^2 = 1$, where $\epsilon = 0$ in even d and $\epsilon = 1$ in odd d .

To write the metric on $M_{q\beta,U^q}$ in Kaluza-Klein form, we switch to co-rotating

coordinates

$$\varphi_a \equiv \theta_a - \Omega_a \tau, \quad (4.36)$$

where τ is the coordinate on \mathbb{R} . In co-rotating coordinates, the action of h simplifies to

$$h : (r_a, \varphi_a, \tau) \mapsto (r_a, \varphi_a + \frac{2\pi p_a}{q_a}, \tau + \beta). \quad (4.37)$$

In particular h^q , becomes simply a shift $h^q : \tau \mapsto \tau + q\beta$. Thus, quotienting by $\langle h^q \rangle$ to obtain $M_{q\beta, U^q}$ makes τ periodic with period $q\beta$.

The metric of $M_{q\beta, U^q}$ in co-rotating coordinates takes the Kaluza-Klein form

$$ds^2 = g + e^{2\phi} (d\tau + A)^2, \quad (4.38)$$

where the fields g, A, ϕ are given by [25]

$$e^{2\phi} = 1 + \sum_{a=1}^n r_a^2 \Omega_a^2, \quad (4.39)$$

$$A = \sum_{a=1}^n \frac{r_a^2 \Omega_a}{1 + \sum_b r_b^2 \Omega_b^2} d\varphi_a, \quad (4.40)$$

$$g = \sum_{a=1}^{n+\epsilon} dr_a^2 + \sum_{a,b=1}^n \left(r_a r_b \delta_{ab} - \frac{r_a^2 r_b^2 \Omega_a \Omega_b}{1 + \sum_{c=1}^n r_c^2 \Omega_c^2} \right) d\varphi_a d\varphi_b. \quad (4.41)$$

The metric of the EFT bundle $M_{q\beta, U^q} / \mathbb{Z}_q$ is locally the same as (4.38). Consequently, we can choose a local trivialization of the EFT bundle such that the fields g, A, ϕ are identical to (4.39) in each patch. However, such a local trivialization will have nontrivial transition functions between patches that contribute to holonomies of the Kaluza-Klein connection along various cycles (including around the defect locus).

If we like, we can perform a gauge transformation that makes the transition functions trivial, at the cost of introducing new contributions to A . We refer to such a gauge as "EFT gauge" because it will be convenient for discussing the EFT limit of the CFT on this geometry. In EFT gauge, the curvature $F = dA$ has δ -function type singularities at the fixed-loci of R whose coefficients reflect the topology of the EFT bundle.

- Example: 2D CFT

Let us illustrate these ideas with an example. Consider a 2D CFT, where the action of h is given by $h : (\varphi, \tau) \mapsto (\varphi + \frac{2\pi p}{q}, \tau + \beta)$. The metric on $M_{q\beta, U^q}$ is

$$\begin{aligned} ds^2 &= d\tau^2 + d\theta^2 = d\tau^2 + (d\varphi + \Omega d\tau)^2 \\ &= \underbrace{(1 - \frac{\Omega^2}{1+\Omega^2})d\varphi^2}_{g} + \underbrace{(1 + \Omega^2)(d\tau + \frac{\Omega}{1+\Omega^2}d\varphi)^2}_{e^{2\phi}} + \underbrace{\frac{\Omega}{1+\Omega^2}d\varphi^2}_{A}. \end{aligned} \quad (4.42)$$

To choose a local trivialization of the EFT bundle, we first specify two intervals in the φ coordinate:

$$I_1 = \{\varphi : 0 < \varphi < \frac{2\pi}{q}\}, \quad I_2 = \{\varphi : -\epsilon < \varphi < \epsilon\}, \quad (4.43)$$

with $0 < \epsilon < \frac{\pi}{q}$. We denote their images in S^1/\mathbb{Z}_q by U_1 and U_2 , respectively. Together U_1 and U_2 cover the quotient space S^1/\mathbb{Z}_q ; see Figure 4.3.

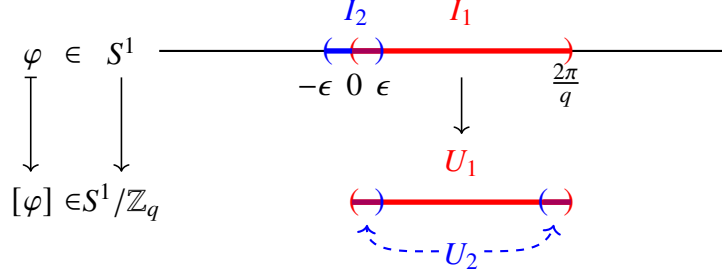


Figure 4.3: The open intervals I_1 and I_2 are subsets of S^1 . Their images under the quotient map $S^1 \rightarrow S^1/\mathbb{Z}_q$ are U_1 and U_2 , respectively, which together cover S^1/\mathbb{Z}_q . We can choose a gauge where the KK fields g, A, ϕ are given by (4.42) in each of U_1 and U_2 . However, in this gauge, there will be a nontrivial transition function between U_1 and U_2 .

The bundle projection $\pi : M_{q\beta, U^q}/\langle h \rangle \rightarrow S^1/\mathbb{Z}_q$ acts by $\pi : [(\varphi, \tau)] \mapsto [\varphi]$, where $[(\varphi, \tau)]$ denotes an equivalence class modulo the action of h , and $[\varphi]$ denotes an equivalence class modulo $\frac{2\pi p}{q}$. Over each open set U_1, U_2 , we must define trivialization maps

$$\phi_{U_i} : \pi^{-1}(U_i) \rightarrow U_i \times S^1_{q\beta}. \quad (4.44)$$

We choose them as follows. Given $p \in \pi^{-1}(U_i)$, thought of as an equivalence class modulo $\langle h \rangle$, let (φ, τ) be a representative of the equivalence class such that φ is contained in I_i . Then we define

$$\phi_{U_i}(p) = ([\varphi], \tau). \quad (4.45)$$

Note that τ is well-defined modulo $q\beta$ because the only elements of $\langle h \rangle$ that map the I_i to themselves are powers of h^q . With this local trivialization, the fields g, A, ϕ are given by (4.42) in each patch. In particular, we have $A = \frac{\Omega}{1+\Omega^2} d\varphi$ in both patches.

However, the data of the Kaluza-Klein connection includes both the value of A in each patch, as well as the transition functions between patches. We must also determine these transition functions.

There are two overlap regions to consider. The first is $(0, \epsilon)$. In this region, the transition function is trivial. The second overlap region is the image of $(-\epsilon, 0) \subset I_2$ in S^1/\mathbb{Z}_q , which coincides with the image of $(\frac{2\pi}{q} - \epsilon, \frac{2\pi}{q}) \subset I_1$ in S^1/\mathbb{Z}_q . Note that (φ, τ) for $\varphi \in (-\epsilon, 0)$ is equivalent modulo $\langle h \rangle$ to $(\varphi + \frac{2\pi}{q}, \tau + (p^{-1})_q \beta)$, where $\varphi + \frac{2\pi}{q} \in (\frac{2\pi}{q} - \epsilon, \frac{2\pi}{q})$. Here, $(p^{-1})_q$ denotes the inverse of $p \bmod q$, i.e. it satisfies $p(p^{-1})_q = qn + 1$ for some integer n . Thus, the transition function in this second overlap region is

$$\phi_{U_2} \circ \phi_{U_1}^{-1} : ([\varphi], \tau) \mapsto ([\varphi], \tau - (p^{-1})_q \beta). \quad (4.46)$$

The holonomy of the connection gets a nontrivial contribution from the transition functions.¹³

$$-\oint A = -\frac{2\pi}{q} \frac{\Omega}{1+\Omega^2} - (p^{-1})_q \beta. \quad (4.47)$$

(The holonomy is an example of the "topological" terms discussed in Section 4.6 which can contribute in the thermal effective action, but are not the integral of a local gauge/coordinate invariant density.)

To go to EFT gauge, we perform a gauge transformation (i.e. a φ -dependent redefinition of τ) that trivializes the transition functions. One possible choice is

$$\tau' = \tau - (p^{-1})_q \beta \left\lfloor \frac{\varphi}{2\pi/q} \right\rfloor. \quad (4.48)$$

Note that the function $\left\lfloor \frac{\varphi}{2\pi/q} \right\rfloor$ is multi-valued on the entire circle S^1 , but there is no problem defining it inside the intervals I_1, I_2 where we perform the gauge transformation. In terms of τ' , the transition functions are now trivial in both overlap regions. (A quick way to see why is to note that τ' is invariant under the h -action (4.37).) The gauge field becomes

$$A' = A + d\tau - d\tau' = \frac{\Omega}{1+\Omega^2} d\varphi + (p^{-1})_q \beta \delta(\varphi) d\varphi \quad (\text{EFT gauge}). \quad (4.49)$$

The holonomy $-\oint A'$ is still given by (4.47), but that is now manifest in the local expression for the gauge field (4.49).

¹³The parallel transport equation is $d\tau + A = 0$, so the holonomy of τ is computed by $-\oint A$.

- Example: 3D CFT

Now consider the same setup in a 3D CFT. The metric on S^2 is

$$ds_{S^2}^2 = dr_1^2 + dr_2^2 + r_1^2 d\varphi^2 \quad (r_1^2 + r_2^2 = 1). \quad (4.50)$$

Essentially all of the above discussion goes through un-modified, with the radii r_1, r_2 coming along for the ride. We can again go to EFT gauge, and the gauge field (4.49) now gets interpreted as a gauge field on S^2 . This time, A has δ -function-localized curvature at the north and south poles:

$$dA = \mp(p^{-1})_q \beta \delta(\vec{n}, \vec{n}_\pm) d^2\vec{n} + \text{nonsingular}, \quad (4.51)$$

where $\delta(\vec{n}, \vec{n}')$ represents a δ -function on S^2 , and \vec{n}_\pm are the north/south poles.

- EFT gauge in general

More generally, we go to EFT gauge as follows. First choose a fundamental domain F for the quotient map $S^{d-1} \rightarrow S^{d-1}/\mathbb{Z}_q$. Define an integer valued function $k(\vec{n})$ by

$$\begin{aligned} k(\vec{n}) &= 0 \text{ if } \vec{n} \in F, \\ k(R\vec{n}) &= 1 + k(\vec{n}). \end{aligned} \quad (4.52)$$

In words, $k(\vec{n})$ counts the power of R needed to move from somewhere in F to \vec{n} . Again, $k(\vec{n})$ is multi-valued if we try to define it on the entire sphere, but we only need to define it inside a collection of open sets that cover S^{d-1}/\mathbb{Z}_q . For example, in the 2D case considered above, we had $k(\varphi) = (p^{-1})_q \lfloor \frac{\varphi}{2\pi/q} \rfloor$.

Finally, we define

$$\tau' \equiv \tau - \beta k(\vec{n}(r_a, \varphi_a)). \quad (4.53)$$

In the coordinates (r_a, φ_a, τ') , h acts simply by shifting angles φ_a :

$$h : (r_a, \varphi_a, \tau') \mapsto (r_a, \varphi_a + \frac{2\pi p_a}{q_a}, \tau'). \quad (4.54)$$

Consequently, a local trivialization of the EFT bundle defined using the τ' coordinate has trivial transition functions. The gauge field is given by

$$A' = A + d\tau - d\tau' = \sum_{a=1}^n \frac{r_a^2 \Omega_a}{1 + \sum_b r_b^2 \Omega_b^2} d\varphi_a + \beta dk(\vec{n}(r_a, \varphi_a)). \quad (4.55)$$

The curvature dA' has δ -function contributions $\beta d^2 k(\vec{n})$ at the fixed loci of powers of R .

Effective action

Following the logic of the thermal effective action, let us now equip the EFT bundle with a more general metric G and try to write down a local action of G . We will demand that G satisfy the following conditions:

- It possesses a circle isometry, so that it can be written in Kaluza-Klein form (4.38).
- In EFT gauge, the curvature dA is a sum of δ -function singularities of the form $\beta d^2 k(\vec{n})$, plus something smooth on S^{d-1}/\mathbb{Z}_q . (This ensures that the Kaluza-Klein bundle has the same topology as $M_{q\beta,V^q}/\mathbb{Z}_q$.)
- g and $e^{2\phi}$ should be smooth on S^{d-1}/\mathbb{Z}_q .

Here, a field is "smooth on S^{d-1}/\mathbb{Z}_q " if it lifts to a smooth \mathbb{Z}_q -invariant field on S^{d-1} .

In the limit $\beta \rightarrow 0$, we can separate each of the background fields into a long-wavelength part, with wavelengths much longer than β , and a short-wavelength part, with wavelengths comparable to (or smaller than) β . The long-wavelength parts become background fields for the thermal EFT. Meanwhile, the short-wavelength parts become operator insertions in that EFT.

In our case, the δ -function curvature singularities $dA \sim \beta d^2 k(\vec{n})$ are short-wavelength. They determine the insertion of an operator in the thermal EFT, which is described by the defect action $S_{\mathcal{D}}$. This action is a functional of the long-wavelength parts of g, A, ϕ . As mentioned in Section 4.2, we will assume that the defect is gapped, so that the action functional is local and can be organized in a derivative expansion. To construct it, we should compute curvatures and other invariants of g, A, ϕ , and *throw away δ -function singularities*. Since g and ϕ are smooth, this effectively amounts to the replacement

$$dA \rightarrow d\tilde{A} \equiv dA - \beta d^2 k(\vec{n}). \quad (4.56)$$

Henceforth, we leave this replacement implicit. In other words, when we write dA in the defect action, we mean its long-wavelength part $d\tilde{A}$, with δ -functions thrown away.

The defects live at singularities in the quotient space S^{d-1}/\mathbb{Z}_q . How should we write an action for long wavelength fields near these singularities? Recall that the long-wavelength parts of g, A, ϕ lift to smooth \mathbb{Z}_q -invariant fields on S^{d-1} . We will

write $S_{\mathfrak{D}}$ as a functional of these \mathbb{Z}_q -invariant lifts, integrated over the preimage of the defect locus modulo \mathbb{Z}_q , which we denote by $\tilde{\mathfrak{D}}$. We also conventionally divide by q , which ensures that Wilson coefficients of defects living at singularities with the same local structure (but possibly different global structure) are the same.

The action should be invariant under gauge/coordinate transformations that preserve the defect locus. For now, we ignore the possibility of nontrivial Weyl anomalies on the defect \mathfrak{D} , and we impose that $S_{\mathfrak{D}}$ be Weyl-invariant as well. Consequently, it will be a functional of A and the Weyl-invariant combination $\hat{g} = e^{-2\phi} g$.

Consider an n -dimensional defect \mathfrak{D} whose preimage $\tilde{\mathfrak{D}}$ is the fixed locus of an element $R^l \in \langle R \rangle$ with order m . Given a point p on $\tilde{\mathfrak{D}}$, we can choose a vielbein \hat{e}_i^a at p satisfying $\delta_{ab} \hat{e}_i^a \hat{e}_j^b = \hat{g}_{ij}$, where a, b are indices for the local rotation group $\text{SO}(d-1)$. The group $\langle R^l \rangle \cong \mathbb{Z}_m$ acts as a subgroup of the local rotation group $\text{SO}(d-1)$, so the \hat{e}_i^a can be classified into representations of this \mathbb{Z}_m . Singlets under \mathbb{Z}_m represent directions parallel to the defect. They are acted upon by an $\text{SO}(n) \subset \text{SO}(d-1)$ that commutes with \mathbb{Z}_m . Hence, altogether the \hat{e}_i^a can be classified into representations of $\mathbb{Z}_m \times \text{SO}(n)$.

To build the defect action, we enumerate curvature tensors built from \hat{g} and A , in a derivative expansion, and contract them with \hat{e}_i^a to build $\mathbb{Z}_m \times \text{SO}(n)$ invariants I_i with d_i derivatives. The defect action is then

$$S_{\mathfrak{D}} = \frac{1}{q} \int_{\tilde{\mathfrak{D}}} d^n y \sqrt{\hat{g}|_{\tilde{\mathfrak{D}}}} \left(\sum_i a_i (q\beta)^{d_i - n} I_i \right), \quad (4.57)$$

where $\hat{g}|_{\tilde{\mathfrak{D}}}$ denotes the pullback of \hat{g} to $\tilde{\mathfrak{D}}$, and y are coordinates on the defect. The factors of $q\beta$ are supplied using dimensional analysis.

Finally, to evaluate the defect action on $M_{q\beta, V^q} / \mathbb{Z}_q$, we simply plug in the expressions (4.39), (4.40), (4.41), which are precisely the \mathbb{Z}_q -lifts to S^{d-1} of the long-wavelength parts of g, A, ϕ .

In what follows, we will sometimes use the notation \mathfrak{D} to refer to *both* a defect on S^{d-1} / \mathbb{Z}_q and the lift $\tilde{\mathfrak{D}}$ of the defect locus to S^{d-1} . We hope this will not cause confusion.

Example: point-like vortex defects in 3D CFTs

As an example, consider a 3D CFT, where R acts by the discrete rotation $\varphi \rightarrow \varphi + \frac{2\pi p}{q}$. The action of R fixes the north and south poles of S^2 . Consequently, there are two

point-like vortex defects: $\mathfrak{D}_{p/q}$ located at the north pole, and its orientation reversal $\mathfrak{D}_{-p/q}$ located at the south pole. Let us focus on $\mathfrak{D}_{p/q}$.

Classifying the vielbein at the north pole into representations of \mathbb{Z}_q , we have basis elements \hat{e}_+^i, \hat{e}_-^i with charges $+p$ and $-p$, respectively. We normalize them so that $\hat{e}_\pm \cdot (\hat{e}_\pm)^* = 1$. To build basic \mathbb{Z}_q -invariant curvatures, we begin with tensors $\hat{\nabla}_i \cdots \hat{\nabla}_j \hat{R}$ and $\hat{\nabla}_i \cdots \hat{\nabla}_j F_{kl}$, where $F = dA$, \hat{R} is the curvature scalar built from \hat{g} , and $\hat{\nabla}$ denotes a covariant derivative with respect to \hat{g} . We then contract their indices with \hat{e}_\pm^l in such a way that the total \mathbb{Z}_q charge vanishes. The action at each order in a derivative expansion is a polynomial in these basic \mathbb{Z}_q -invariants.

Note that we cannot build valid terms in the action by multiplying two \mathbb{Z}_q -charged objects to obtain a \mathbb{Z}_q -singlet. For example, $(\hat{e}_+^i \hat{\nabla}_i \hat{R})(\hat{e}_-^j \hat{\nabla}_j \hat{R})$ is not admissible. The reason is that $\hat{e}_+^i \hat{\nabla}_i \hat{R}$ individually vanishes, due to \mathbb{Z}_q -invariance.

Proceeding in this way, the leading invariants in a derivative expansion are

$$S_{\mathfrak{D}_{p/q}} \ni 1, \hat{\star}F, \hat{R}, (\hat{\star}F)^2, \dots, \quad (4.58)$$

where $\hat{\star}F = i\hat{e}_+^k \hat{e}_-^l F_{kl}$ is the Hodge star of F in the metric \hat{g} . Concretely, the action is

$$S_{\mathfrak{D}_{p/q}} = \frac{1}{q} \left(a_{0,p/q} + (q\beta)a_{1,p/q} \hat{\star}F + (q\beta)^2 \left(a_{2,p/q} \hat{R} + a_{3,p/q} (\hat{\star}F)^2 \right) + \dots \Big|_{\mathfrak{D}_{p/q}} \right), \quad (4.59)$$

where $(\dots)|_{\mathfrak{D}_{p/q}}$ denotes evaluation at the preimage of the defect on S^2 — in this case the north pole. We have written the Wilson coefficients as $a_{i,p/q}$ to emphasize that they depend on the rotation fraction p/q . In bosonic theories, the $a_{i,x}$ are periodic in x with period 1, while in fermionic theories, they are periodic in x with period 2.

At higher orders in derivatives, we can also include laplacians $\hat{\nabla}^2$, as well as q -th powers of charged derivatives $(\hat{e}_\pm \cdot \nabla)^q$. However, note that the background fields on $M_{q\beta,U^q}$ given in (4.39), (4.40), and (4.41) are invariant not only under \mathbb{Z}_q , but under the full maximal torus $\text{SO}(2)$. Consequently, terms involving charged derivatives $(\hat{e}_\pm \cdot \nabla)^q$ will actually vanish on $M_{q\beta,U^q}/\mathbb{Z}_q$, and in practice we only need to keep polynomials in $\hat{\nabla}^{2k} \hat{\star}F$ and $\hat{\nabla}^{2k} \hat{R}$.

Plugging in the fields on $M_{q\beta,U^q}$, we find

$$\begin{aligned} \hat{\star}F|_\pm &= \pm 2\Omega, \\ \hat{R}|_\pm &= 2 + 10\Omega^2, \end{aligned} \quad (4.60)$$

where $(\cdots)|_{\pm}$ denotes the north/south poles of S^2 . Thus, summing up the contributions from the north and south poles, the total defect contribution to $\text{Tr}[e^{-\beta H}UR]$ is

$$\begin{aligned} S_{\mathfrak{D}} = & \frac{a_{0,p/q} + a_{0,-p/q}}{q} + 2\beta\Omega(a_{1,p/q} - a_{1,-p/q}) \\ & + \frac{(q\beta)^2}{q}((2 + 10\Omega^2)(a_{2,p/q} + a_{2,-p/q}) + 4\Omega^2(a_{3,p/q} + a_{3,-p/q})) + \dots \end{aligned} \quad (4.61)$$

In general, the point-like defect action at each order β^k is a polynomial in Ω that is even if k is even and odd if k is odd. We will verify this structure in several examples below.

There is an important distinction between the terms (4.61) arising in the defect action $S_{\mathfrak{D}}$ and the "bulk" terms (4.11). Note that the bulk terms contain poles at $\Omega_a = \pm i$. Physically, such poles arise because a great circle $r_a = 1$ of the spinning S^{d-1} approaches the speed of light as $\Omega_a \rightarrow \pm i$. The measure $\sqrt{\hat{g}}$ becomes singular at the great circle, and the integral over r_a cannot be deformed away from the singularity because it is at an endpoint of the integration contour. By contrast, the defects $\mathfrak{D}_{\pm p/q}$ are located at the north and south poles of S^2 , where this phenomenon does not occur, and thus their contributions do not have poles at $\Omega = \pm i$. In general, the action of a defect \mathfrak{D} on $M_{q\beta,V^q}/\mathbb{Z}_q$ can have poles at $\Omega_a = \pm i$ if and only if the support of \mathfrak{D} intersects the great circle $r_a = 1$. We will see an example in the next subsection.

Example: vortex defects in 4D CFTs

Consider now a 4D CFT, where R acts by discrete rotations on each of the angles $\varphi_1 \rightarrow \varphi_1 + \frac{2\pi p_1}{q_1}$ and $\varphi_2 \rightarrow \varphi_2 + \frac{2\pi p_2}{q_2}$. If $q_1 \neq q_2$, we have two 1-dimensional vortex defects $\mathfrak{D}^{(1)}$ and $\mathfrak{D}^{(2)}$. The first defect $\mathfrak{D}^{(1)}$ is located at the fixed locus of R^{q_1} , which is given by $(r_1, r_2) = (1, 0)$ with $\varphi_1 \in [0, \frac{2\pi}{q}]$, where $q := \text{lcm}(q_1, q_2)$. The second defect $\mathfrak{D}^{(2)}$ is located at the fixed locus of R^{q_2} , which is given by $(r_1, r_2) = (0, 1)$ with $\varphi_2 \in [0, \frac{2\pi}{q}]$.

Let us focus on $\mathfrak{D}^{(1)}$ for now. On $\mathfrak{D}^{(1)}$, the leading term in the effective action is a cosmological constant $\int d\phi_1 \sqrt{\hat{g}|_{\mathfrak{D}^{(1)}}}$, as usual. At the first subleading order in a derivative expansion, we have the term $\int d\varphi_1 \sqrt{\hat{g}|_{\mathfrak{D}^{(1)}}} i \hat{e}_+^k \hat{e}_-^l F_{kl}$, which can be written more simply as $\int \hat{\star} F$.

The Wilson coefficients of a defect depend only on the geometry of the singularity

where the defect lives. To describe this geometry, it is helpful to introduce the co-prime integers

$$\begin{aligned} P_1 &:= \frac{p_1 q_2}{(q_1, q_2)}, & Q_1 &:= \frac{q_1}{(q_1, q_2)}, \\ P_2 &:= \frac{p_2 q_1}{(q_1, q_2)}, & Q_2 &:= \frac{q_2}{(q_1, q_2)}, \end{aligned} \quad (4.62)$$

where (q_1, q_2) is the greatest common divisor of q_1, q_2 . The structure of the singularity at $\mathfrak{D}^{(1)}$ is determined by the action of R^{q_1} , which is

$$R^{q_1} : \varphi_2 \mapsto \varphi_2 + \frac{2\pi P_2}{Q_2}. \quad (4.63)$$

Thus, the Wilson coefficients of $\mathfrak{D}^{(1)}$ should depend only on P_2/Q_2 . However, there is a subtlety in fermionic theories: Note that R^{q_1} implements a rotation by $2\pi p_1$, which is $(-1)^{p_1 F}$ in fermionic theories. Thus, the Wilson coefficients of $\mathfrak{D}^{(1)}$ can additionally depend on $(-1)^{p_1}$ in that case. Consequently, we will write the Wilson coefficients of $\mathfrak{D}^{(1)}$ as $a_{i, P_2/Q_2, (-1)^{p_1}}$ to emphasize the data they depend on. (We will see subtleties of a similar flavor in Section 4.4.)

Putting everything together, the action $S_{\mathfrak{D}^{(1)}}$ takes the form

$$\begin{aligned} S_{\mathfrak{D}^{(1)}} &= \frac{1}{q} \left(\frac{a_{0, P_2/Q_2, (-1)^{p_1}}}{q\beta} \int d\varphi_1 \sqrt{\hat{g}} |_{\mathfrak{D}} + a_{1, P_2/Q_2, (-1)^{p_1}} \int \hat{\star} F + \dots \right) \\ &= \frac{2\pi}{q(1 + \Omega_1^2)} \left(\frac{a_{0, P_2/Q_2, (-1)^{p_1}}}{q\beta} + 2a_{1, P_2/Q_2, (-1)^{p_1}} \Omega_2 + \dots \right), \end{aligned} \quad (4.64)$$

where in the second line, we evaluated the action in the background $M_{q\beta, U^q}/\mathbb{Z}_q$. Note that because $\mathfrak{D}^{(1)}$ lives on the great circle $r_1 = 1$, its action has poles at $\Omega_1 = \pm i$.

Adding similar terms for $\mathfrak{D}^{(2)}$, the total defect contribution to $\text{Tr}[e^{-\beta H} U R]$ is

$$\begin{aligned} S_{\mathfrak{D}} &= \frac{2\pi}{q^2 \beta} \left(\frac{a_{0, P_2/Q_2, (-1)^{p_1}}}{1 + \Omega_1^2} + \frac{a_{0, P_1/Q_1, (-1)^{p_2}}}{1 + \Omega_2^2} \right) \\ &\quad + \frac{4\pi}{q} \left(a_{1, P_2/Q_2, (-1)^{p_1}} \frac{\Omega_2}{1 + \Omega_1^2} + a_{1, P_1/Q_1, (-1)^{p_2}} \frac{\Omega_1}{1 + \Omega_2^2} \right) + \dots, \end{aligned} \quad (4.65)$$

where "..." represents higher-order terms in β coming from higher dimension operators in the defect action.

4.4 Fermionic theories

In this section, we describe some subtleties associated with partition functions of fermionic theories. Again, for simplicity we mostly restrict our discussion to CFT_d

on a spatial sphere S^{d-1} , though the final conclusion (4.84) holds in a general QFT. In short, the results (4.30) and (4.32) work in fermionic CFTs as well, but we must take care to keep track of the spin structure of the manifold (in particular whether we have periodic or antiperiodic boundary conditions for fermions around S_β^1 and $S_{q\beta}^1$), and we must consider the rotation R as an element of $\text{Spin}(d)$.

Review of 2D

Let us first review fermionic CFTs in 2D. In 2D, we need to specify the boundary conditions of the fermions around both the space and time circles. This defines four different fermion partition functions:

$$\begin{aligned} Z_{R,+}(\tau, \bar{\tau}) &:= \text{Tr}_R \left(e^{2\pi i \tau (L_0 - \frac{c}{24})} e^{-2\pi i \bar{\tau} (\bar{L}_0 - \frac{c}{24})} \right) \\ Z_{R,-}(\tau, \bar{\tau}) &:= \text{Tr}_R \left((-1)^F e^{2\pi i \tau (L_0 - \frac{c}{24})} e^{-2\pi i \bar{\tau} (\bar{L}_0 - \frac{c}{24})} \right) \\ Z_{NS,+}(\tau, \bar{\tau}) &:= \text{Tr}_{NS} \left(e^{2\pi i \tau (L_0 - \frac{c}{24})} e^{-2\pi i \bar{\tau} (\bar{L}_0 - \frac{c}{24})} \right) \\ Z_{NS,-}(\tau, \bar{\tau}) &:= \text{Tr}_{NS} \left((-1)^F e^{2\pi i \tau (L_0 - \frac{c}{24})} e^{-2\pi i \bar{\tau} (\bar{L}_0 - \frac{c}{24})} \right). \end{aligned} \quad (4.66)$$

The partition functions in (4.66) are not independent. The partition functions $Z_{R,+}$, $Z_{NS,+}$, and $Z_{NS,-}$ are invariant under different subgroups of $SL(2, \mathbb{Z})$ and can transform into each other. More precisely, $Z_{R,-}$ is invariant under all of $SL(2, \mathbb{Z})$; and $Z_{R,+}$, $Z_{NS,+}$, and $Z_{NS,-}$ are invariant under the congruence subgroups $\Gamma_0(2)$, Γ_θ , and $\Gamma^0(2)$ respectively, which are defined as

$$\begin{aligned} \Gamma_0(2) &= \left\{ \begin{pmatrix} a & b \\ c & d \end{pmatrix} \in SL(2, \mathbb{Z}), \quad c \text{ even} \right\} \\ \Gamma_\theta &= \left\{ \begin{pmatrix} a & b \\ c & d \end{pmatrix} \in SL(2, \mathbb{Z}), \quad a+b \text{ odd}, c+d \text{ odd} \right\} \\ \Gamma^0(2) &= \left\{ \begin{pmatrix} a & b \\ c & d \end{pmatrix} \in SL(2, \mathbb{Z}), \quad b \text{ even} \right\}. \end{aligned} \quad (4.67)$$

Finally they transformation into each other as

$$\begin{aligned} Z_{R,+}(-1/\tau, -1/\bar{\tau}) &= Z_{NS,-}(\tau, \bar{\tau}), \\ Z_{NS,+}(\tau + 1, \bar{\tau} + 1) &= Z_{NS,-}(\tau, \bar{\tau}). \end{aligned} \quad (4.68)$$

The NS sector partition function (with or without a $(-1)^F$ insertion) at low temperature is well-approximated by the vacuum state (which is a bosonic state), with Casimir energy $-\frac{c}{12}$:

$$\text{Tr}_{NS}(e^{-\beta(\Delta - \frac{c}{12})}) \sim e^{\frac{\beta c}{12}}, \quad \beta \gg 1. \quad (4.69)$$

The Ramond sector ground state, in contrast, has a Casimir energy of $E_{gs} - \frac{c}{12}$ where E_{gs} is the Ramond ground-state energy, a non-negative number that is theory-dependent.¹⁴ Finally, the Ramond ground-state may not necessarily be unique, so we call the degeneracy $N_{gs} \in \mathbb{N}$.

$$\text{Tr}_R(e^{-\beta(\Delta - \frac{c}{12})}) \sim N_{gs} e^{-\beta(E_{gs} - \frac{c}{12})}, \quad \beta \gg 1. \quad (4.70)$$

To study the high temperature behavior of the NS-sector partition function with an arbitrary phase $e^{2\pi i p/qJ}$ inserted (with $0 \leq p/q < 2$ and p, q coprime)

$$\text{Tr}_{NS}(e^{-\beta[(\Delta - \frac{c}{12}) - i\Omega J]} e^{2\pi i J p/q}), \quad \beta \ll 1 \quad (4.71)$$

we can use an $SL(2, \mathbb{Z})$ transform. In particular we would like to apply a modular transformation of the form

$$\begin{pmatrix} a & b \\ q & -p \end{pmatrix} \quad (4.72)$$

to (4.71). The result crucially depends on the parity of p, q . If $p + q$ is odd, then we can choose (4.72) to be in Γ_θ and map the partition function to the NS sector at low temperature. However, if $p + q$ is even, we map the partition function to the R sector at low temperature instead. We therefore get, for $\beta \ll 1$ and $0 \leq p/q < 2$:

$$\begin{aligned} \text{Tr}_{NS}(e^{-\beta[(\Delta - \frac{c}{12}) - i\Omega J]} e^{2\pi i J p/q}) &\sim e^{\frac{4\pi^2}{q^2\beta(1+\Omega^2)} \frac{c}{12}} & p + q \text{ odd, } \beta \ll 1, \\ \text{Tr}_{NS}(e^{-\beta[(\Delta - \frac{c}{12}) - i\Omega J]} e^{2\pi i J p/q}) &\sim N_{gs} e^{\frac{4\pi^2}{q^2\beta(1+\Omega^2)} \left(\frac{c}{12} - E_{gs}\right)} & p + q \text{ even, } \beta \ll 1. \end{aligned} \quad (4.73)$$

Equivalently we can always take $0 \leq \frac{p}{q} < 1$ with the insertion of a $(-1)^F$:

$$\begin{aligned} \text{Tr}_{NS}(e^{-\beta[(\Delta - \frac{c}{12}) - i\Omega J]} e^{2\pi i J p/q}) &\sim e^{\frac{4\pi^2}{q^2\beta(1+\Omega^2)} \frac{c}{12}} & p + q \text{ odd, } \beta \ll 1, \\ \text{Tr}_{NS}(e^{-\beta[(\Delta - \frac{c}{12}) - i\Omega J]} e^{2\pi i J p/q}) &\sim N_{gs} e^{\frac{4\pi^2}{q^2\beta(1+\Omega^2)} \left(\frac{c}{12} - E_{gs}\right)} & p + q \text{ even, } \beta \ll 1, \\ \text{Tr}_{NS}((-1)^F e^{-\beta[(\Delta - \frac{c}{12}) - i\Omega J]} e^{2\pi i J p/q}) &\sim e^{\frac{4\pi^2}{q^2\beta(1+\Omega^2)} \frac{c}{12}} & p \text{ odd, } \beta \ll 1, \\ \text{Tr}_{NS}((-1)^F e^{-\beta[(\Delta - \frac{c}{12}) - i\Omega J]} e^{2\pi i J p/q}) &\sim N_{gs} e^{\frac{4\pi^2}{q^2\beta(1+\Omega^2)} \left(\frac{c}{12} - E_{gs}\right)} & p \text{ even, } \beta \ll 1. \end{aligned} \quad (4.74)$$

We see that in (4.74), there are two real numbers that can determine the behavior of fermionic partition functions: the central charge c and the Ramond ground state

¹⁴For supersymmetric theories, $E_{gs} = \frac{c}{12}$, but for generic fermionic theories, E_{gs} can be above or below or equal to $\frac{c}{12}$.

energy E_{gs} . Moreover, which of the two high temperature behaviors we get ($\frac{c}{12}$ or $\frac{c}{12} - E_{gs}$ multiplying temperature in the free energy) depends on the parity of p and q . We will see this exact same behavior repeat itself for fermionic theories in higher dimensions in Section 4.4.

In 2D, we can also analyze the behavior of the partition function in the Ramond sector. This does not have a direct analog as far as we are aware in higher dimension, but we include it for completeness. By using the same modular transformation properties discussed earlier, we find

$$\begin{aligned} \text{Tr}_R(e^{-\beta[(\Delta-\frac{c}{12})-i\Omega J]} e^{2\pi i J p/q}) &\sim e^{\frac{4\pi^2}{q^2\beta(1+\Omega^2)}\frac{c}{12}} & q \text{ even, } \beta \ll 1, \\ \text{Tr}_R(e^{-\beta[(\Delta-\frac{c}{12})-i\Omega J]} e^{2\pi i J p/q}) &\sim N_{gs} e^{\frac{4\pi^2}{q^2\beta(1+\Omega^2)}(\frac{c}{12}-E_{gs})} & q \text{ odd, } \beta \ll 1, \\ \text{Tr}_R((-1)^F e^{-\beta[(\Delta-\frac{c}{12})-i\Omega J]} e^{2\pi i J p/q}) &\lesssim N_{gs} e^{\frac{4\pi^2}{q^2\beta(1+\Omega^2)}(\frac{c}{12}-E_{gs})} & \beta \ll 1. \end{aligned} \quad (4.75)$$

Because the final spin structure (where the fermion is periodic in both space and time directions) is invariant under the full modular group, it has the same universal behavior at high temperature regardless of the phase. In general this spin structure cannot be directly derived from the other three (although there are potentially powerful constraints coming from unitarity, and knowledge of $Z_{R,+}$ [23]). We write \lesssim rather than \sim in the last line of (4.75) due to possible cancellations between fermionic and bosonic Ramond ground states, which would effectively reduce N_{gs} (by an even number) for the final spin structure.

Higher d

Let us now consider fermionic CFTs in $d > 2$. For simplicity let us first consider turning on only a single spin and consider:

$$\text{Tr}[e^{-\beta(H-i\Omega J)} e^{2\pi i \frac{p}{q} J}], \quad (4.76)$$

with $\beta \ll 1$, $\Omega \sim O(1)$, $0 \leq p/q < 2$. As discussed before, this can be computed from a path integral of $S^{d-1} \times S^1_\beta$, where we insert a defect that rotates the sphere by $2\pi p/q$. Moreover, due to the fermions in the theory, we need to specify a spin structure on this geometry. In (4.76) we compute the path integral with anti-periodic boundary conditions for the fermion around the S^1_β . We now imagine the setup as in Figure 4.2 to reduce the setup into a geometry we can obtain a thermal EFT. In particular we need to stack q copies of the CFT, and perform a $2\pi p$ rotation in the spatial direction. The final geometry we get — in addition to the spatial sphere being modded by \mathbb{Z}_q and the thermal circle increasing by a factor of q — has different

periodicity for the fermions about the time circle depending on the parity of $p + q$. If $p + q$ is odd, the fermions remain antiperiodic, and we can use the original EFT description for fermionic CFTs on a long, thin cylinder. If $p + q$ is even, however, we need a *new* EFT, for fermionic CFTs with periodic boundary conditions on a long, thin cylinder.

We now see there are *two* different thermal EFTs we consider, depending on the periodicity of the fermions around S_β^1 . Each EFT comes with its own set of Wilson coefficients. We write them as

$$\begin{aligned} Z_{\text{CFT}}[S^{d-1} \times S_{\beta, \text{anti-periodic}}^1] &= Z_{\text{gapped}}[S^{d-1}] \sim e^{-S_{\text{th}}[g_{ij}, A_i, \phi]}, \\ Z_{\text{CFT}}[S^{d-1} \times S_{\beta, \text{periodic}}^1] &= \tilde{Z}_{\text{gapped}}[S^{d-1}] \sim e^{-\tilde{S}_{\text{th}}[g_{ij}, A_i, \phi]}. \end{aligned} \quad (4.77)$$

The two expressions $e^{-S_{\text{th}}}$ and $e^{-\tilde{S}_{\text{th}}}$ respectively compute the partition function with and without the insertion of $(-1)^F$:

$$\begin{aligned} \text{Tr} [e^{-\beta(H-i\Omega J)}] &\sim e^{-S_{\text{th}}}, \\ \text{Tr} [(-1)^F e^{-\beta(H-i\Omega J)}] &\sim e^{-\tilde{S}_{\text{th}}}. \end{aligned} \quad (4.78)$$

Let us write the two thermal actions as

$$\begin{aligned} S_{\text{th}} &= \int \frac{d^{d-1}\vec{x}}{\beta^{d-1}} \sqrt{\hat{g}} \left(-f + c_1 \beta^2 \hat{R} + c_2 \beta^2 F^2 + \dots \right) + S_{\text{anom}}, \\ \tilde{S}_{\text{th}} &= \int \frac{d^{d-1}\vec{x}}{\beta^{d-1}} \sqrt{\hat{g}} \left(-\tilde{f} + \tilde{c}_1 \beta^2 \hat{R} + \tilde{c}_2 \beta^2 F^2 + \dots \right) + S_{\text{anom}}. \end{aligned} \quad (4.79)$$

The most general leading term behavior of (4.76) then goes as

$$\log \left[\text{Tr}(e^{-\beta(H-i\Omega J)} e^{2\pi i \frac{p}{q} J}) \right] \sim \begin{cases} \frac{1}{q^d} \frac{f \text{ vol } S^{d-1}}{\beta^{d-1} (1+\Omega^2)} + \dots, & p+q \text{ odd}, \\ \frac{1}{q^d} \frac{\tilde{f} \text{ vol } S^{d-1}}{\beta^{d-1} (1+\Omega^2)} + \dots, & p+q \text{ even}. \end{cases} \quad (4.80)$$

Note that if we specialize (4.80) to $d = 2$, this is precisely the behavior we get for (4.73), if we identify

$$\begin{aligned} f &= \frac{2\pi c}{12}, \\ \tilde{f} &= 2\pi \left(\frac{c}{12} - E_{gs} \right). \end{aligned} \quad (4.81)$$

We can think of the difference between the two sets of Wilson coefficients in (4.79) as the higher-dimensional analog of the "Ramond ground state energy".

We can generalize (4.76) to turning on n spins and consider

$$\text{Tr} \left[e^{-\beta(H-i(\Omega_1 J_1 + \dots + \Omega_n J_n))} e^{2\pi i \frac{p_1}{q_1} J_1} \dots e^{2\pi i \frac{p_n}{q_n} J_n} \right] \quad (4.82)$$

for $\beta \ll 1$, $\Omega_i \sim O(1)$, $0 \leq \frac{p_i}{q_i} < 2$. If we define

$$q := \text{lcm}(q_1, \dots, q_n), \quad (4.83)$$

then in our EFT, we will go around the time circle q times and go around the spatial sphere $\sum_i \frac{p_i q}{q_i}$ times. Thus depending on if $q + \sum_i \frac{p_i q}{q_i}$ is odd or even, we get the thermal EFT described by S_{th} or \tilde{S}_{th} .

Finally, all of these results are consistent with (4.32) if we simply interpret $e^{i\beta\Omega \cdot J} R$ as an element of $\text{Spin}(d)$ and interpret Tr as imposing periodic boundary conditions for both bosonic and fermionic variable. With this understanding, (4.32) is the general recipe. If we instead interpret Tr as imposing periodic boundary conditions for bosons and antiperiodic boundary conditions for fermions, (4.32) should be modified to

$$-\log \text{Tr}[gR] \sim -\frac{1}{q} \log \text{Tr}\left[(-1)^{(q-1)F} g^q\right] + \text{topological} + \sum_{\mathfrak{D}_i} S_{\mathfrak{D}_i}. \quad (4.84)$$

We will see explicit examples of this in Section 4.5.

4.5 Free theories

We now present several examples involving free fields to show explicitly that (4.30) and (4.32) hold (along with their appropriate generalizations to fermionic theories). We begin in Section 4.5 by checking a *massive* quantum field theory, namely a massive free boson in 2D. We then consider free CFTs in 3D and 4D. Our main tool for computing partition functions in free CFTs is the *plethystic exponential*, which we review in Appendix 4.10 (see e.g. [88, 112, 165]).

In Section 4.5, we consider various examples involving free scalar fields and free fermions in 3 dimensions. In Section 4.5, we explore few more examples in 4 dimension. We present additional 4D and 6D examples in Appendix 4.10. Lastly, in Section 4.6, we consider 2D CFTs with a local gravitational anomaly. Such theories can include Chern-Simons term in their thermal effective action, which are not integrals of local gauge/coordinate invariant densities. These furnish examples of the "topological" terms in (4.30) and (4.32).

Massive free boson in 2D

As a first check on our formalism (and to illustrate that the basic ideas do not require conformal symmetry), let us study the partition function of a free scalar with mass m

in 2D. We begin by computing the partition function on a rectangular torus $S_L^1 \times S_\beta^1$:

$$\begin{aligned} \log Z &= -\frac{1}{2} \text{Tr} \log(m^2 + \Delta) - S_{\text{ct}} \\ &= -\frac{1}{2} \sum_{(r,s) \in \mathbb{Z}^2} \log \left(m^2 + \left(\frac{2\pi r}{L} \right)^2 + \left(\frac{2\pi s}{\beta} \right)^2 \right) - S_{\text{ct}} \\ &= -\sum_{r \in \mathbb{Z}} \log 2 \sinh \left(\frac{\beta \sqrt{m^2 + (\frac{2\pi r}{L})^2}}{2} \right) - S_{\text{ct}}, \end{aligned} \quad (4.85)$$

where S_{ct} is a cosmological constant counterterm, and in the third line we performed the sum over r and threw away a constant using the fact that $\sum_{s \in \mathbb{Z}} 1 = 0$ in ζ -function regularization.

Because the summand is slowly-varying in r , we can take the thermodynamic limit $L \rightarrow \infty$ by replacing the sum over r with an integral over momentum $k = \frac{2\pi r}{L}$:

$$\log Z \sim -\frac{L}{\pi} \int_0^\infty dk \left(\log \left(1 - e^{-\beta \sqrt{m^2 + k^2}} \right) - \frac{\beta \sqrt{m^2 + k^2}}{2} \right) - S_{\text{ct}} \quad (L \rightarrow \infty). \quad (4.86)$$

The second term in the integrand is UV-divergent, but proportional to $L\beta$. Hence, it takes the form of a cosmological constant and can be removed with an appropriate choice of S_{ct} . We will choose S_{ct} to simply subtract this contribution, which is equivalent to setting the free energy density to zero in flat \mathbb{R}^2 . We find

$$\log Z \sim \frac{L}{\beta} f(\beta m) \quad (L \rightarrow \infty), \quad (4.87)$$

where minus the effective free energy density is

$$f(y) = -\frac{y}{\pi} \int_0^\infty dx \log \left(1 - e^{-y\sqrt{1+x^2}} \right) \sim \begin{cases} \frac{\pi}{6} & y \ll 1, \\ \sqrt{\frac{y}{2\pi}} e^{-y} & y \gg 1. \end{cases} \quad (4.88)$$

Note that the limit of $f(y)$ as $y \rightarrow 0$ is consistent with $f = \frac{2\pi c}{12}$ with $c = 1$ for the massless free boson in 2D.

Before continuing to the twisted partition function, let us make two observations. Firstly, the partition function Z obeys a form of modular invariance. To formulate it, let us write $\mathbb{T}^2 = \mathbb{R}^2/\Lambda$, where the lattice Λ is spanned by basis vectors \vec{e}_1, \vec{e}_2 . We can arrange the basis vectors into a matrix $E \in \mathbb{R}^{2 \times 2}$ whose columns are \vec{e}_1 and \vec{e}_2 , and consider the partition function as a function of E . (Above, we studied

the case where $\vec{e}_1 = (L, 0)$ and $\vec{e}_2 = (0, \beta)$, and thus $E = \begin{pmatrix} L & 0 \\ 0 & \beta \end{pmatrix}$.) Rotational invariance implies that $Z(E)$ is invariant under left-multiplication by an orthogonal group element $g \in \mathrm{SO}(2)$. Modular invariance is the statement that $Z(E)$ is also invariant under an integer change of basis of the lattice Λ , which is equivalent to right-multiplication by $\gamma \in \mathrm{SL}(2, \mathbb{Z})$:

$$Z(E) = Z(gE\gamma). \quad (4.89)$$

In other words, Z is a function on the moduli space $\mathrm{SO}(2) \backslash \mathbb{R}^{2,2} / \mathrm{SL}(2, \mathbb{Z})$.

The second key observation is that in the thermodynamic limit, Z is unchanged under a small shift of the basis vector that grows as $L \rightarrow \infty$: $\vec{e}_1 \rightarrow \vec{e}_1 + \alpha \vec{e}_2$. To see why, note that the corresponding dual basis shifts by $\hat{e}_2 \rightarrow \hat{e}_2 - \alpha \hat{e}_1$ (with \hat{e}_1 unchanged). Thus, the sum (4.85) changes by shifting $r \rightarrow r - s\alpha$:

$$\begin{aligned} \log Z \left(\begin{pmatrix} L & 0 \\ \alpha\beta & \beta \end{pmatrix} \right) &= -\frac{1}{2} \sum_{(r,s) \in \mathbb{Z}^2} \log \left(m^2 + \left(\frac{2\pi(r-s\alpha)}{L} \right)^2 + \left(\frac{2\pi s}{\beta} \right)^2 \right) - S_{\mathrm{ct}} \\ &\sim \frac{L}{\beta} f(\beta m) \quad (L \rightarrow \infty). \end{aligned} \quad (4.90)$$

In the continuum limit, we can identify the momentum $k = \frac{2\pi(r-s\alpha)}{L}$ and rewrite the sum as an integral over k . The shift $r \rightarrow r - s\alpha$ becomes immaterial in this approximation.

Now let us finally consider the partition function with the insertion of a discrete rotation of the spatial circle S_L^1 by an angle $2\pi p/q$. This corresponds to the matrix

$$E' = \begin{pmatrix} L & \frac{pL}{q} \\ 0 & \beta \end{pmatrix} = \begin{pmatrix} \frac{L}{q} & 0 \\ (p^{-1})_q \beta & q\beta \end{pmatrix} \gamma', \quad \text{where} \quad \gamma' = \begin{pmatrix} q & p \\ -(p^{-1})_q & -b \end{pmatrix} \in \mathrm{SL}(2, \mathbb{Z}). \quad (4.91)$$

As before $(p^{-1})_q$ denotes the inverse of p modulo q , and b is chosen so that γ' has determinant 1. Applying modular invariance (4.89) and the result (4.90), we find

$$\log Z(E') = \log Z \left(\begin{pmatrix} \frac{L}{q} & 0 \\ (p^{-1})_q \beta & q\beta \end{pmatrix} \right) \sim \frac{L}{q^2 \beta} f(q\beta m) \quad (L \rightarrow \infty), \quad (4.92)$$

consistent with (4.32).

Using slightly fancier technology (see e.g. [79]), we can be more precise about what information is thrown away in the " \sim " in equation (4.92). We rewrite the partition function in terms of a spectral zeta function

$$\log Z(E) = \frac{1}{2} \zeta'_E(0) - S_{\mathrm{ct}}, \quad (4.93)$$

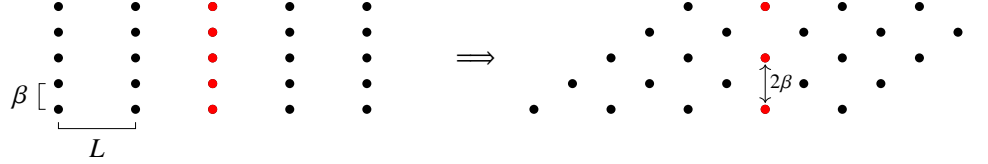


Figure 4.4: **Left:** the lattice Λ for a rectangular torus $S^1_L \times S^1_\beta$. In the thermodynamic limit $L \rightarrow \infty$, the sum (4.95) is dominated by $\lambda \in \Lambda_{\text{short}}$ (depicted in red), which are spaced apart by β . **Right:** the lattice after twisting by a spatial rotation by π . In the limit $L \rightarrow \infty$, the partition function is dominated by $\lambda \in \Lambda'_{\text{short}}$, which are now spaced apart by 2β .

where

$$\begin{aligned}
 \zeta_E(s) &= \text{Tr} \left[(m^2 + \Delta)^{-s} \right] = \frac{1}{\Gamma(s)} \int_0^\infty \frac{dt}{t} t^s \text{Tr} \left[e^{-t(m^2 + \Delta)} \right] \\
 &= \frac{1}{\Gamma(s)} \int_0^\infty \frac{dt}{t} t^s e^{-tm^2} \sum_{\vec{r} \in \mathbb{Z}^2} e^{-t(2\pi E^{-T} \vec{r})^2} \\
 &= \frac{1}{\Gamma(s)} \int_0^\infty \frac{dt}{t} t^s e^{-tm^2} \frac{\det E}{4\pi t} \sum_{\lambda \in \Lambda} e^{-\frac{\lambda^2}{4t}}. \tag{4.94}
 \end{aligned}$$

In the last line, we performed Poisson resummation to obtain a sum over lattice points $\lambda \in \Lambda$. (Recall that Λ is the lattice spanned by the columns of E .) We can now perform the integral over t and plug the result into (4.93). The term $\lambda = (0, 0)$ precisely cancels against S_{ct} , and we find

$$\log Z(E) = \frac{m \det E}{2\pi} \sum_{\lambda \in \Lambda - (0,0)} \frac{K_1(m|\lambda|)}{|\lambda|}, \tag{4.95}$$

where $K_1(x)$ is a modified Bessel function.

Now we can see clearly that in the thermodynamic limit, the lattice vectors $\lambda \in \Lambda$ that become longer give an exponentially suppressed contribution to $\log Z$ (since $K_1(r) \sim e^{-r}$ for large r). Indeed, we have

$$\log Z(E) = \frac{m \det E}{2\pi} \sum_{\lambda \in \Lambda_{\text{short}} - (0,0)} \frac{K_1(m|\lambda|)}{|\lambda|} + O(e^{-Lm}) \quad (L \rightarrow \infty), \tag{4.96}$$

where Λ_{short} are the lattice vectors that do not get longer in the thermodynamic limit $L \rightarrow \infty$; see Figure 4.4. Applying the result (4.96) to the rectangular torus $S^1_L \times S^1_\beta$, we find another expression for the effective free energy density:

$$f(y) = \frac{y}{\pi} \sum_{\ell=1}^{\infty} \frac{1}{\ell} K_1(y\ell), \tag{4.97}$$

which agrees with (4.88), as we can see by expanding $\log(1 - e^{-y\sqrt{1+x^2}}) = -\sum_\ell \frac{1}{\ell} e^{-\ell y\sqrt{1+x^2}}$ and integrating term-by-term. The result (4.96) also immediately implies (4.90). Combining this with modular invariance, we find that (4.92) holds up to exponential corrections of the form e^{-mL} . Note that this conclusion relies on finiteness of m in the thermodynamic limit. If instead we take $m \rightarrow 0$, then the thermal theory has a gapless sector, and we do not expect (4.32) to hold.

We can also understand (4.92) more directly from (4.96) as follows. When the partition function has a twist by a rational angle $\frac{2\pi p}{q}$, then a new Λ'_{short} emerges, as depicted in Figure 4.4. The emergent Λ'_{short} looks like Λ_{short} in the un-twisted case, but with the replacement $\beta \rightarrow q\beta$.

It is also straightforward to generalize this analysis to a massive free scalar in d dimensions. The torus partition function is¹⁵

$$\log Z(E) = \det E \left(\frac{m}{2\pi}\right)^{d/2} \sum_{\lambda \in \Lambda} \frac{K_{d/2}(m|\lambda|)}{|\lambda|^{d/2}}. \quad (4.98)$$

This is again consistent with (4.32) (with vanishing topological and defect contributions) through the mechanism depicted in Figure 4.4.

3D CFTs

- Free scalar

We now turn our attention to partition functions of higher dimensional CFTs on a spatial S^{d-1} . Let us begin by studying the partition function of a free scalar in 3D, with various discrete rotations inserted. The usual KK reduction of a free scalar on a circle possesses a zero mode. However, in order to apply thermal EFT, the KK reduced theory must be gapped. Thus, in order to avoid zero modes, we will study a *complex* scalar charged under a \mathbb{Z}_k flavor symmetry. We will turn on the \mathbb{Z}_k fugacity as appropriate to eliminate zero modes, and study the thermal EFT description of the resulting twisted partition functions. Note that in a generic interacting CFT (as opposed to a free theory) we would not expect to have zero modes, and it would not be necessary to consider flavor symmetry.

Let $R(\theta) \in \text{SO}(3)$ denote a rotation around the z -axis, and let Ψ denote a reflection in the z direction. We will consider insertions of $R(\theta, s) = R(\theta) \circ \Psi^s \in O(3)$, where $\theta = \frac{2\pi p}{q}$. Note that the reflection potential s takes values in $\{0, 1\}$, since $\Psi^2 = 1$.

¹⁵This is an example of an Epstein ζ -function; see e.g. [83].

The partition function is given by

$$\begin{aligned} & \log \text{Tr} \left[e^{-\beta(H-i\Omega J)} e^{\frac{2\pi i \ell Q}{k}} R(\theta, s) \right] \\ &= \sum_n \frac{1}{n} \left(e^{\frac{2\pi i \ell n}{k}} + e^{-\frac{2\pi i \ell n}{k}} \right) \frac{e^{-n\beta/2}(1-e^{-2n\beta})}{(1-(-1)^{ns}e^{-n\beta})(1-e^{-n\beta}x^n)(1-e^{-n\beta}x^{-n})}, \end{aligned} \quad (4.99)$$

where $x = e^{2\pi i p/q+i\beta\Omega}$, and Q is the charge of the scalar under $U(1)$ (of which \mathbb{Z}_k is a subgroup).

When we turn on a big rotation $R(\theta, s)$ with order q and include the global symmetry operator $V = e^{\frac{2\pi i \ell Q}{k}}$, a zero mode will be present on the EFT bundle whenever $V^q = 1$, since V wraps q times around the base of the EFT bundle — see the discussion around (4.30).

Let us consider the case $p/q = 1/2$, corresponding to a rotation by an angle π , which fixes the north and south poles of S^2 . If the flavor group were \mathbb{Z}_2 , then we would necessarily have a zero mode on the EFT bundle. Hence we instead consider \mathbb{Z}_3 flavor symmetry.

The thermal partition function of a free scalar field with non-zero \mathbb{Z}_3 flavor and small rotation-fugacity has the following high temperature expansion:

$$\begin{aligned} & \log \text{Tr} \left[e^{-\beta(H-i\Omega J)} e^{\frac{4\pi i Q}{3}} \right] \\ &= -\frac{16\zeta(3)}{9(1+\Omega^2)\beta^2} - \frac{(1+2\Omega^2)\log 3}{12(1+\Omega^2)} + \frac{(21+4\Omega^2-24\Omega^4)\beta^2}{4320(1+\Omega^2)} + O(\beta^4). \end{aligned} \quad (4.100)$$

Now we would like to turn on the fugacity for the big rotation with or without a reflection, leading to absence or presence of non trivial defect action, respectively.

Free action: without defect

Let us first consider an insertion of $R(\pi, 1) = R(\pi) \circ \Psi$. This is a parity transformation $\vec{n} \mapsto -\vec{n}$ on S^2 , and it does not have any fixed points. Thus, the thermal effective action will be free of defects. Concretely, we find

$$\begin{aligned} & \log \text{Tr} \left[e^{-\beta(H-i\Omega J)} e^{\frac{2\pi i Q}{3}} R(\pi, 1) \right] \\ &= -\frac{2\zeta(3)}{9(1+\Omega^2)\beta^2} - \frac{(1+2\Omega^2)\log 3}{24(1+\Omega^2)} + \frac{(21+4\Omega^2-24\Omega^4)\beta^2}{2160(1+\Omega^2)} + O(\beta^4). \end{aligned} \quad (4.101)$$

Comparing (4.100) with (4.101) we find

$$\log \text{Tr} \left[e^{-\beta(H-i\Omega J)} e^{\frac{2\pi i Q}{3}} R(\pi, 1) \right] \sim \frac{1}{2} \log \text{Tr} \left[e^{-2\beta(H-i\Omega J)} e^{\frac{4\pi i Q}{3}} \right], \quad (4.102)$$

so (4.30) holds.

Non-free action: defect

Without the reflection fugacity, the action of R has fixed points and thermal EFT predicts a non-trivial $S_{\mathfrak{D}}$ as in (4.32). We find

$$\begin{aligned} \log \text{Tr} \left[e^{-\beta(H-i\Omega J)} e^{\frac{4\pi i Q}{3}} R(\pi, 0) \right] \\ = -\frac{2\zeta(3)}{9(1+\Omega^2)\beta^2} - \frac{(7+8\Omega^2)\log 3}{24(1+\Omega^2)} + \frac{(-69+94\Omega^2+156\Omega^4)\beta^2}{2160(1+\Omega^2)} + O(\beta^4). \end{aligned} \quad (4.103)$$

Comparing with (4.100), we obtain

$$-\log \text{Tr} \left[e^{-\beta(H-i\Omega J)} e^{\frac{2\pi i Q}{3}} R(\pi, 0) \right] \sim -\frac{1}{2} \log \text{Tr} \left[e^{-2\beta(H-i\Omega J)} e^{\frac{4\pi i Q}{3}} \right] + S_{\mathfrak{D}}, \quad (4.104)$$

where the total defect action $S_{\mathfrak{D}}(\beta, \Omega)$ is given by

$$S_{\mathfrak{D}}(\beta, \Omega) = -\frac{\log 3}{4} + \frac{2\Omega^2 - 1}{24}\beta^2 + O(\beta^4). \quad (4.105)$$

Note that $S_{\mathfrak{D}}$ has precisely the form predicted in (4.61), with

$$a_{0,1/2} = -\frac{\log 3}{4}, \quad a_{2,1/2} = -\frac{1}{192}, \quad a_{3,1/2} = \frac{7}{384}. \quad (4.106)$$

Furthermore, the linear term in β vanishes because $a_{1,1/2} = a_{1,-1/2}$ in bosonic theories.

More generally, we can consider a rotation $R(\frac{2\pi p}{q}, 0)$, where p and q are coprime and q is not divisible by 3 (so that there is no zero mode upon dimensional reduction). The leading defect Wilson coefficients in this case satisfy:

$$\begin{aligned} a_{0,p/q} + a_{0,-p/q} = -\frac{1}{3} \sum_{k=1}^{q-1} \frac{1}{\sin(\frac{\pi kp}{3})^2} & \left[\cos\left(\frac{2\pi(k+q)}{3}\right) \left(\psi\left(\frac{k}{3q} + \frac{1}{3}\right) - \psi\left(\frac{k}{3q}\right) \right) \right. \\ & \left. + \cos\left(\frac{2\pi(k+2q)}{3}\right) \left(\psi\left(\frac{k}{3q} + \frac{2}{3}\right) - \psi\left(\frac{k}{3q}\right) \right) \right], \end{aligned} \quad (4.107)$$

$$a_{1,p/q} - a_{1,-p/q} = \frac{1}{6} \sum_{k=1}^{q-1} \frac{\cos(\frac{\pi kp}{3})}{\sin(\frac{\pi kp}{3})^3} \left[\cos\left(\frac{2\pi(k+q)}{3}\right) + 2 \cos\left(\frac{2\pi(k+2q)}{3}\right) \right], \quad (4.108)$$

where $\psi(z)$ is the digamma function.

- Free fermion

We can perform a similar exercise with free Dirac fermions. The partition function is given by

$$\begin{aligned} & \log \text{Tr} \left[e^{-\beta H} e^{\frac{2\pi i \ell Q}{k}} R(\theta, 0) (-1)^{F_W} \right] \\ &= \sum_n (-1)^{nw} \frac{(-1)^{n+1}}{n} \left(e^{\frac{2\pi i \ell n}{k}} + e^{-\frac{2\pi i \ell n}{k}} \right) \frac{e^{-n\beta} \left[\left((\sqrt{x})^n + \frac{1}{(\sqrt{x})^n} \right) - e^{-n\beta} \left((\sqrt{x})^n + \frac{1}{(\sqrt{x})^n} \right) \right]}{(1 - e^{-n\beta})(1 - e^{-n\beta}(\sqrt{x})^{2n})(1 - e^{-n\beta}(\sqrt{x})^{-2n})}. \end{aligned} \quad (4.109)$$

Fermions are antiperiodic in the time direction at finite temperature. Hence, when no fugacities corresponding to a big rotation or fermion number are turned on, there is no zero mode contribution to the thermal EFT description of the partition function. In this case, we have the following high temperature behavior:

$$\log \text{Tr} \left[e^{-\beta(H-i\Omega J)} \right] = \frac{3\zeta(3)}{(1+\Omega^2)\beta^2} - \frac{(2+\Omega^2)\log 2}{6(1+\Omega^2)} + \frac{(24-4\Omega^2-21\Omega^4)\beta^2}{5760(1+\Omega^2)} + O(\beta^4). \quad (4.110)$$

However, when $(-1)^F$ and big rotations are turned on, we must be careful about zero modes. If the big rotation is given by $e^{2\pi i p/q}$, then we have various cases depending on the parity of p, q and presence or absence of $(-1)^F$. We consider all possible cases in the Table 4.1.

Let us consider the case when q is even. We take $q = 2$ for simplicity. According to Table 4.1, we do not need a flavor twist to remove zero modes. We compute

$$\begin{aligned} & \log \text{Tr} \left[e^{-\beta(H-i\Omega J)} R(\pm\pi, 0) \right] \\ &= \frac{3\zeta(3)}{8(1+\Omega^2)\beta^2} - \frac{(2+\Omega^2)\log 2}{12(1+\Omega^2)} \mp \frac{\Omega\beta}{4} + \frac{(24-4\Omega^2-21\Omega^4)\beta^2}{2880(1+\Omega^2)} + O(\beta^3). \end{aligned} \quad (4.111)$$

Note that $\log \text{Tr} \left[e^{-\beta(H-i\Omega J)} (-1)^F R(\pi, 0) \right] = \log \text{Tr} \left[e^{-\beta(H-i\Omega J)} R(-\pi, 0) \right]$.

Comparing (4.110) and (4.111), we verify the appropriate generalizations of (4.32) to fermionic CFT. In particular, see (4.84) and note that as an element of spin group, we have $R^2(\pm\pi, 0) = (-1)^F$. We find

$$-\log \text{Tr} \left[e^{-\beta(H-i\Omega J)} R(\pm\pi, 0) \right] \sim -\frac{1}{2} \log \text{Tr} \left[e^{-2\beta(H-i\Omega J)} \right] + S_{\mathfrak{D}_{\pm}}, \quad (4.112)$$

where $S_{\mathfrak{D}_{\pm}}$ is given by

$$S_{\mathfrak{D}_{\pm}} = \mp \frac{\Omega\beta}{4} + O(\beta^3). \quad (4.113)$$

$(-1)^F$?	Rotation	Boundary Condition	Flavor?	Equation
	p/q	$(-1)^{q(w+1)}(-1)^p$		
No ($w = 0$)	1/2	$(-1)^2(-1)^1 = -1$	No	(4.111), (4.112)
Yes ($w = 1$)	1/2	$(-1)^4(-1)^1 = -1$	No	(4.111), (4.112)
No ($w = 0$)	1/3	$(-1)^3(-1)^1 = +1$	\mathbb{Z}_2	(4.115), (4.116)
Yes ($w = 1$)	1/3	$(-1)^6(-1)^1 = -1$	No	(4.115), (4.116)
No ($w = 0$)	2/3	$(-1)^3(-1)^2 = -1$	No	(4.118), (4.119)
Yes ($w = 1$)	2/3	$(-1)^6(-1)^2 = +1$	\mathbb{Z}_2	(4.118), (4.119)

Table 4.1: Turning on fugacities corresponding to flavor, rotation and fermionic number. $w = 0, 1$ refers to turning off and on the fugacity corresponding to $(-1)^F$ respectively. The fugacity corresponding to big rotation is $e^{2\pi i p/q}$. The third column lists the effective spin structure on the EFT bundle, ± 1 in this column refers to periodic and antiperiodic boundary condition respectively. The fourth column lists whether we need a flavor twist to make sure that there is no zero mode. Note that antiperiodic boundary condition rules out the presence of zero modes. The final column refers to relevant equations in the main text.

This has precisely the form predicted in (4.61), with

$$a_{1,1/2} - a_{1,-1/2} = \frac{1}{8}, \quad a_{0,1/2} + a_{0,-1/2} = 0. \quad (4.114)$$

Next we consider the case when q is odd. Now p can be either even or odd. For example, let us consider $q = 3$ and $p = 1$ or $p = 2$. We introduce a flavor twist according to Table 4.1. Note that, operationally the insertion of $(-1)^F$ is same as introducing a \mathbb{Z}_2 flavor twist. The insertion of both amounts to inserting nothing. In what follows, we choose to insert $(-1)^F$ to eliminate the zero mode.

For $p/q = 1/3$, we find that

$$\begin{aligned} & \log \text{Tr} [e^{-\beta(H-i\Omega J)} (-1)^F R(2\pi/3, 0)] \\ & \sim \frac{\zeta(3)}{9(1+\Omega^2)\beta^2} - \frac{(10+9\Omega^2)\log 2}{18(1+\Omega^2)} + \frac{5\Omega\beta}{3\sqrt{3}} + \frac{(-568+1028\Omega^2+1617\Omega^4)\beta^2}{5760(1+\Omega^2)} + O(\beta^3). \end{aligned} \quad (4.115)$$

Comparing (4.110) and (4.115) we find that

$$\log \text{Tr} [e^{-\beta(H-i\Omega J)} (-1)^F R(2\pi/3, 0)] \sim \frac{1}{3} \log \text{Tr} [e^{-3\beta(H-i\Omega J)}] + S_{\mathfrak{D}}(\beta, \Omega), \quad (4.116)$$

where the total defect action $S_{\mathfrak{D}}(\beta, \Omega)$ takes the form predicted in (4.61):

$$S_{\mathfrak{D}}(\beta, \Omega) \sim -\frac{4 \log 2}{9} + \frac{5\Omega\beta}{3\sqrt{3}} - \frac{(8 - 21\Omega^2)\beta^2}{72} + O(\beta^3). \quad (4.117)$$

The $p/q = 2/3$ case can be easily be done using the following identity

$$\log \text{Tr} [e^{-\beta(H-i\Omega J)} R(4\pi/3, 0)] = \log \text{Tr} [e^{-\beta(H+i\Omega J)} (-1)^F R(2\pi/3, 0)], \quad (4.118)$$

from which it follows that

$$\log \text{Tr} [e^{-\beta(H-i\Omega J)} R(4\pi/3, 0)] \sim \frac{1}{3} \log \text{Tr} [e^{-3\beta(H-i\Omega J)}] + S_{\mathfrak{D}}(\beta, -\Omega), \quad (4.119)$$

where $S_{\mathfrak{D}}(\beta, \Omega)$ is given by (4.117).

More examples with a defect action: 4d CFTs

In 4D, the rotation group has two Cartan generators, which we call J_1 and J_2 . Let us consider inserting $R = \exp(2\pi i \frac{p_1}{q_1} J_1 + 2\pi i \frac{p_2}{q_2} J_2)$ into the trace. When $q_1 = q_2$, the action of R is free and there will be no vortex defects. However, when $q_1 \neq q_2$, we will have two 1-dimensional vortex defects $\mathfrak{D}^{(1)}$ and $\mathfrak{D}^{(2)}$, whose combined action is given by (4.65).

As a concrete example, consider the free Dirac fermion in 4D. Using plethystic exponentials, we find

$$-\log \text{Tr} [e^{-\beta(H-i\vec{\Omega} \cdot \vec{J})} e^{2\pi i \frac{p_1}{q_1} J_1 + 2\pi i \frac{p_2}{q_2} J_2}] \sim -\frac{1}{q} \log \text{Tr} [e^{-q\beta(H-i\vec{\Omega} \cdot \vec{J})}] + S_{\mathfrak{D}}. \quad (4.120)$$

Here we impose that $q \left(1 + \frac{p_1}{q_1} + \frac{p_2}{q_2}\right)$ is odd. This ensures absence of the $(-1)^F$ insertion in the right hand side above. Thus the zero mode is absent and the thermal EFT applies.

Furthermore, $S_{\mathfrak{D}}$ has precisely the form predicted by (4.65) with the leading Wilson coefficients given by the following function of $(-1)^P$ and coprime integers P, Q :

$$a_{0,P/Q,(-1)^P} = \sum_{k=1}^{Q-1} \frac{(-1)^{pk} \cos(\pi k \frac{P}{Q})}{8\pi \sin^2(\pi k \frac{P}{Q})} \left(\psi' \left(\frac{1}{2} + \frac{k}{2Q} \right) - \psi' \left(\frac{k}{2Q} \right) \right), \quad (4.121)$$

where $\psi'(z)$ is the derivative of the digamma function. This is a highly nontrivial check of (4.65). Matching (4.65) requires not just reproducing the correct function of $\beta, \Omega_1, \Omega_2$, but also the fact that the Wilson coefficient of $\mathfrak{D}^{(1)}$ depends only on P_2/Q_2 and $(-1)^{p_1}$ (and analogously for $\mathfrak{D}^{(2)}$).

Note that when $q_1 = q_2$, we have $Q_1 = Q_2 = 1$, hence the sum is non-existent, leading to $a_{0,P_1/Q_1,(-1)^{p_2}} = a_{0,P_2/Q_2,(-1)^{p_1}} = 0$, which is consistent with the fact that the action of R becomes free and $S_{\mathfrak{D}}$ should vanish.

4.6 Topological terms: example in 2D CFT

So far, we have focused on cases where the thermal effective action can be written as the integral of a local gauge- and coordinate-invariant density. As discussed in Section 4.3, we can choose a gauge ("EFT gauge") where the background fields g, A, ϕ on the EFT bundle look locally the same as on $S^{d-1} \times S^1_\beta$ (possibly with "small" angular twists turned on). Curvature invariants built out of these fields are then also the same as on $S^{d-1} \times S^1_\beta$, and their integral is not sensitive to global properties of the EFT bundle.

By contrast, when d is even, the thermal effective action can also include Chern-Simons-type terms that are not integrals of local curvature invariants, and hence can be sensitive to global properties of the EFT bundle. The contributions of such terms were called "topological" in (4.30) and (4.32). The coefficients of such Chern-Simons terms can be determined systematically from the anomaly polynomial of the CFT [124–126, 153, 154, 171]. The simplest case is when $d = 2$, where the thermal effective action contains a 1d Chern Simons term whose coefficient is proportional to the local gravitational anomaly $c_L - c_R$.

In more detail, consider such a 2D CFT with a local gravitational anomaly, $c_L \neq c_R$. We assume that $c_L - c_R = 24k$ with $k \in \mathbb{Z}$. From modular invariance we have a high-temperature expansion of the partition function as¹⁶

$$\log \left(\text{Tr} \left[e^{-\beta(H-i\Omega J)} e^{2\pi i \frac{p}{q} J} \right] \right) \sim \frac{4\pi^2(c_L + c_R - 24ik\Omega)}{24q^2(1 + \Omega^2)\beta} - \frac{2\pi ik(p^{-1})_q}{q}, \quad (4.122)$$

where (4.122) is accurate to all orders in perturbation theory in β . This generalizes (4.19) to theories with $c_L \neq c_R$.

In the thermal effective action, we can reproduce the terms in (4.122) with a Chern-Simons term from the KK gauge field in the action. In particular, we add a term of the form

$$-\frac{2\pi ik}{q\beta} \oint A \quad (4.123)$$

to the thermal effective action. From (4.47), we see that (4.123) precisely reproduces the additional terms in (4.122). Note that (4.123) is properly quantized precisely when k is an integer, since A is a connection on a circle bundle where the fiber has circumference $q\beta$.

¹⁶To derive (4.122), we apply the modular transform (4.18) to the vacuum state $e^{-\frac{2\pi i \tau c_L - 2\pi i \bar{\tau} c_R}{24}}$ with $\tau = \frac{i\beta}{2\pi} + \frac{\beta\Omega}{2\pi} + \frac{p}{q}$ and expand in small β .

4.7 Holographic theories

In this section we consider CFTs dual to semiclassical Einstein gravity in AdS. The high temperature behavior of the thermal partition function, $\text{Tr}[e^{-\beta H+i\vec{\theta}\cdot\vec{J}}]$ around $\theta_i = 0$, of such holographic CFTs in d dimensions are captured by the thermodynamics of black hole solutions in AdS_{d+1} . We would like to understand the bulk solution that captures the high temperature behavior of $\text{Tr}[e^{-\beta H+i\vec{\theta}\cdot\vec{J}}]$ near $\theta_i = 2\pi p_i/q_i$, where at least one of the $p_i \neq 0$ and $q_i \geq 2$.

First, let us consider a $d = 2$ dimensional CFT in the context of $\text{AdS}_3/\text{CFT}_2$ duality. The relevant bulk solution is given by the rotating BTZ black hole with the metric

$$ds^2 = -f(r)dt^2 + \frac{dr^2}{f(r)} + r^2 \left(d\phi - \frac{r_+r_-}{r^2}dt \right)^2, \quad f(r) := \frac{(r^2 - r_+^2)(r^2 - r_-^2)}{r^2}, \quad (4.124)$$

where r_{\pm} are radius of outer and inner horizon respectively. The BH temperature β^{-1} and angular potential $\Omega = \theta/\beta$ are given by

$$\Omega = \frac{r_-}{r_+}, \quad \beta^{-1} = \frac{r_+^2 - r_-^2}{2\pi r_+}. \quad (4.125)$$

Asymptotically, the metric is Weyl equivalent to $-dt^2 + d\phi^2$. In Euclidean signature, $t_E = it$ and we have $(\phi, t_E) \sim (\phi - \beta\Omega, t_E + \beta)$. The Euclidean action evaluated on this bulk saddle reproduces the high temperature behavior of $\text{Tr}[e^{-\beta(H-i\Omega J)}]$.

Now let us compute $\text{Tr}[e^{-\beta(H-i\Omega J)+2\pi ip/qJ}]$ for a holographic 2D CFT. As explained in Section 4.2, this can be computed by doing a path integral over $M_{q\beta,\Omega}/\mathbb{Z}_q$,¹⁷ where the action of $\mathbb{Z}_q = \langle h \rangle$ is given by

$$h : (\phi, t_E) \mapsto (\phi + 2\pi p/q - \beta\Omega, t_E + \beta), \quad (4.126)$$

and $M_{q\beta,\Omega}$ is obtained from $S^1 \times \mathbb{R}$ by quotienting by $\langle h^q \rangle$.

Note that the action of \mathbb{Z}_q has a natural extension into the AdS bulk, where the radial direction goes along for the ride

$$h : (r, \phi, t_E) \mapsto (r, \phi + 2\pi p/q - \beta\Omega, t_E + \beta). \quad (4.127)$$

We can use this natural extension to build a bulk dual solution. We start with a BTZ black hole $\Sigma_{q\beta,\Omega}$ with parameters $\tilde{r}_{\pm} = r_{\pm}/q$, such that the black hole is at inverse temperature $\tilde{\beta} = q\beta$. The Euclidean metric is given by

$$ds^2 = \tilde{f}(r)dt_E^2 + \frac{dr^2}{\tilde{f}(r)} + r^2 \left(d\phi + i\frac{\tilde{r}_+\tilde{r}_-}{r^2}dt_E \right)^2, \quad \tilde{f}(r) := \frac{(r^2 - \tilde{r}_+^2)(r^2 - \tilde{r}_-^2)}{r^2}. \quad (4.128)$$

¹⁷In this section, we use the compressed notation $M_{\beta,e^{iJ\Omega}} \rightarrow M_{\beta,\Omega}$.

Note that $(\phi, t_E) \sim (\phi - q\beta\Omega, t_E + q\beta)$. We can then quotient $\Sigma_{q\beta,\Omega}$ by the action of $\mathbb{Z}_q = \langle h \rangle$, given by (4.127). The manifold $\Sigma_{q\beta,\Omega}/\mathbb{Z}_q$ is smooth because the action of h in the bulk (4.127) is free.

Recall that on the boundary, the quotient $M_{q\beta,\Omega}/\mathbb{Z}_q$ is a nontrivial bundle over S^1/\mathbb{Z}_q . The discussion in 4.3 applies here, with the radial direction of AdS going along for the ride. In short, we consider open sets in the total space and consider the bulk region that asymptotes to this set. Locally in this bulk region, the metric is precisely given by (4.128). However, there are non-trivial transition functions when we go from one open patch to a different one.

By construction, the quotient $\Sigma_{q\beta,\Omega}/\mathbb{Z}_q$ solves Einstein's equations with the appropriate asymptotic geometry. Compared to a rotating BTZ black hole at temperature $q\beta$, the above quotient geometry has its angular variable restricted to $0 < \phi < 2\pi/q$. (Note that this almost covers the full manifold except the locus $\phi = 0$. This locus is covered by another open patch and we have nontrivial transition function between these two patches.) Thus the evaluation of the bulk action amounts to an integral over the angular variable in the range $0 < \phi < 2\pi/q$ producing a factor of $1/q$, and a replacement $\beta \rightarrow q\beta$ which produces another factor of $1/q$ compared to the evaluation of Euclidean action on BTZ black hole at temperature β . Thus, the Euclidean action evaluated on the saddle $\Sigma_{q\beta,\Omega}/\mathbb{Z}_q$ reproduces

$$\begin{aligned} \log \text{Tr}[e^{-\beta(H-i\Omega J)+2\pi ip/qJ}] &\sim \log Z_{\text{grav}} [\Sigma_{q\beta,\Omega}/\mathbb{Z}_q] \\ &= \frac{1}{q} \log Z_{\text{grav}} [\Sigma_{q\beta,\Omega}] \sim \frac{1}{q} \log \text{Tr}[e^{-q\beta(H-i\Omega J)}], \end{aligned} \tag{4.129}$$

where $Z_{\text{grav}} [\Sigma]$ is the gravitational path integral evaluated on the saddle Σ .

Overall, we have a quotient of a BTZ black hole whose boundary has a temporal cycle of length $\beta_L = q\beta(1 - i\Omega)$ and a spatial cycle of length $L = \frac{2\pi}{q}$. This naively leads to the modular parameter

$$\tilde{\tau} \stackrel{?}{=} iL/\beta_L = \frac{2\pi i}{q^2\beta(1 - i\Omega)}. \tag{4.130}$$

The above is almost correct, but we must amend it by recalling the presence of nontrivial transition functions. This leads to the following identification:

$$\tilde{\tau} = \frac{2\pi i}{q^2\beta(1 - i\Omega)} - \frac{(p^{-1})_q}{q}, \quad \tilde{\bar{\tau}} = -\frac{2\pi i}{q^2\beta(1 + i\Omega)} - \frac{(p^{-1})_q}{q}, \tag{4.131}$$

which precisely matches the modular parameter $\tilde{\tau}$ obtained after applying a modular transformation, as explained around (4.17). Note that we have

$$\frac{1}{2} \left(\tilde{\tau} + \bar{\tilde{\tau}} \right) = -\frac{(p^{-1})_q}{q} - \frac{2\pi\Omega}{q^2\beta(1+\Omega^2)}, \quad (4.132)$$

which is consistent with the holonomy of A derived in (4.47). We conclude that $\Sigma_{q\beta,\Omega}/\mathbb{Z}_q$ is simply a modular transformation of the BTZ black hole geometry.

In dimensions greater than two, we follow the same prescription. Let $\Sigma_{\beta,\vec{\Omega}}$ be a black hole solution that captures the high temperature behavior of the thermal partition function with small angular fugacity, i.e. the AdS-Kerr black hole with inverse temperature β and angular velocities $i\vec{\Omega}$. We claim that the insertion of a big angular fugacity R with $R^q = 1$ is captured by the bulk manifold $\Sigma_{q\beta,\vec{\Omega}}/\mathbb{Z}_q$, where \mathbb{Z}_q is the natural extension of the boundary \mathbb{Z}_q into the bulk. To be precise, the AdS-Kerr solution possesses a time-translation isometry, which we parametrize by t_E . It furthermore possesses isometries under the Cartan subgroup of the rotation group, which we parametrize by ϕ_a . Then the $\mathbb{Z}_q = \langle h \rangle / \langle h^q \rangle$ group is generated by

$$h : (r, r_a, \phi_a, t_E) \mapsto (r, r_a, \phi_a + \frac{2\pi p_a}{q_a}, t_E + \beta), \quad (4.133)$$

where r_a and r are the remaining bulk coordinates.

When the bulk action of h is free, $\Sigma_{q\beta,\vec{\Omega}}/\mathbb{Z}_q$ is a smooth solution to Einstein's equations with the correct asymptotic geometry to describe the partition function with an insertion of R . At very high temperatures, the gravitational path integral on this geometry matches the field theory prediction (4.30) because the quotient by \mathbb{Z}_q just divides the semiclassical gravitational action by q . Thus we expect $\Sigma_{q\beta,\vec{\Omega}}/\mathbb{Z}_q$ is the dominant solution at high temperatures. As we move away from high temperatures, we conjecture that $\Sigma_{q\beta,\vec{\Omega}}/\mathbb{Z}_q$ remains the dominant solution down to a finite temperature.

Unlike in 2d, in higher dimensions it is possible for the bulk \mathbb{Z}_q action (4.133) to have a fixed locus. Such a fixed locus must occur at the horizon of the black hole (where the Euclidean time circle degenerates), and at a location on the sphere S^{d-1} where the boundary action of h has a fixed point as well. For example, consider a 3D CFT, with a four-dimensional bulk dual, and consider the case $p_1/q_1 = 1/2$. The bulk action of h rotates the ϕ circle by π , and also shifts $t_E \rightarrow t_E + \beta$ (which is equivalent to rotating the thermal circle by π). Fixed points of h occur at the north and south poles of the horizon S^2 . For example, near the north pole, we can choose

coordinates so that the metric locally takes the form

$$dr_1^2 + r_1^2 d\phi^2 + dy^2 + y^2 d\psi^2, \quad (4.134)$$

where $\psi = \frac{2\pi}{2\beta} t_E$, and $y \propto \sqrt{r - r_H}$ (with r_H the location of the horizon). In these coordinates, the \mathbb{Z}_2 action rotates both angles ϕ, ψ by π . Quotienting by this \mathbb{Z}_2 , we obtain an orbifold singularity of the form $\mathbb{C}^2/\mathbb{Z}_2$.

When $\Sigma_{q\beta, \vec{\Omega}}/\mathbb{Z}_q$ contains an orbifold singularity, it no longer furnishes a smooth solution to Einstein's equations. To understand the correct bulk dual of the R -twisted partition function, we must understand the fate of the orbifold singularity in the bulk theory. The physics of the singularity (or its resolution) essentially determines the defect action $S_{\mathfrak{D}}$ in holographic CFTs. Note that in a spacetime with vanishing cosmological constant, a $\mathbb{C}^2/\mathbb{Z}_2$ singularity can be resolved by the "gravitational instanton" described by the Eguchi-Hansen metric. Perhaps orbifold singularities occurring in the $\Sigma_{q\beta, \vec{\Omega}}/\mathbb{Z}_q$ can be resolved similarly. Or perhaps the orbifold singularity is resolved by stringy effects. We leave these questions to future work.

For fermionic theories dual to Einstein gravity (which all known examples are), there is another set of Wilson coefficients $\tilde{f}, \tilde{c}_1, \dots$ that can be defined (see (4.79)) coming from periodic boundary conditions for the fermion. The behavior of the partition function with $(-1)^F$ inserted was explored in [62], which found a black hole solution that lead to an exponentially subleading (in temperature) contribution in the large N limit. Since generically we expect \tilde{f} to be nonvanishing, this means the black hole solution found in [62] should not be the dominant contribution in the $T \gg N \gg 1$ limit. It would be interesting to explore further if there are universal results or constraints on the Wilson coefficients $\tilde{f}, \tilde{c}_1, \dots$ in (fermionic) holographic CFTs (for instance by looking at the theories studied in [31]).

Finally, let us note that our construction works also in the case when the boundary theory possesses a reflection symmetry and the group element R includes a reflection. In this case, the bulk dual solution $\Sigma_{q\beta, \vec{\Omega}}/\mathbb{Z}_q$ is non-orientable. This is allowed because the boundary reflection symmetry must be gauged in the bulk, which means we must include contributions from non-orientable geometries. It so happens that a non-orientable geometry dominates in this case.¹⁸

¹⁸See [101] for a recent discussion of gauging spacetime symmetries in the bulk.

4.8 Journey to $\beta = 0$

So far we have described the structure of CFT partition functions $Z(\beta, \vec{\theta})$ at high temperature near rational angles $\frac{\vec{\theta}}{2\pi} \in \mathbb{Q}^n$. In this section we will use these results to sketch the behavior of the partition function at high temperature around any (possibly irrational) angle. For simplicity let us consider turning on only one angle θ , and study the partition function

$$Z(\beta, \theta) = \text{Tr} [e^{-\beta H + i J \theta}] \quad (4.135)$$

at small β with θ fixed. Suppose the angle has the following continued fraction expansion:

$$\frac{\theta}{2\pi} = a_0 + \frac{1}{a_1 + \frac{1}{a_2 + \frac{1}{a_3 + \dots}}}, \quad (4.136)$$

where $a_i \in \mathbb{N}$. We also define the fractions $\frac{p_i}{q_i}$ as truncations of the continued fraction, i.e.

$$\frac{p_i}{q_i} := a_0 + \frac{1}{a_1 + \dots + \frac{1}{a_i}}. \quad (4.137)$$

For a generic angle, the probability of $a_i = n$ scales as $\frac{1}{n^2}$ for large n , which means that the distribution of a_i 's for a generic angle has infinite mean.¹⁹

Suppose we have an angle θ where $a_i \gg 1$ for some i . How does the partition function behave at high temperature? Since we assume $a_i \gg 1$, we have $q_i \approx a_i q_{i-1} \gg q_{i-1}$. So for

$$q_{i-1} \ll T \ll q_i, \quad (4.138)$$

we expect

$$\log Z(T) \sim \text{vol} S^{d-1} f T^{d-1} q_{i-1}^{-d}. \quad (4.139)$$

However, when

$$T \sim q_i \quad (4.140)$$

the constant or proportionality in (4.139) suddenly shrinks.

In Figure 4.5, we illustrate this explicitly for two example CFTs. We plot both the Klein invariant j function (which is the partition function of some 2D CFTs at central charge 24) and the 3D free boson partition function as a function of temperature, with chemical potential $\frac{\theta}{2\pi} = \frac{3-\pi}{7\pi-22}$. This has the continued fraction expansion:

$$\frac{\theta}{2\pi} = \frac{3-\pi}{7\pi-22} = 15 + \frac{1}{292 + \frac{1}{1+\dots}}. \quad (4.141)$$

¹⁹One way to see this scaling is, for a random real number between 0 and 1, the probability that $a_1 = n$ is roughly $\frac{1}{n} - \frac{1}{n+1} \sim \frac{1}{n^2}$.

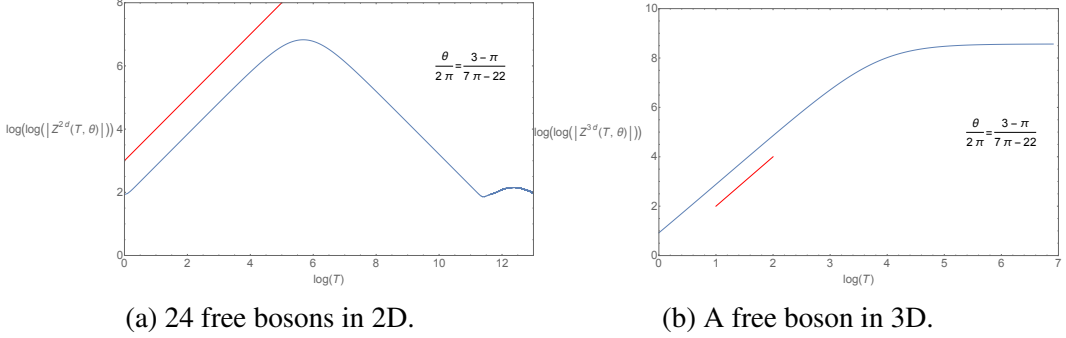


Figure 4.5: In blue, the log of the free energy of two CFTs evaluated at chemical potential $\frac{\theta}{2\pi} = \frac{3-\pi}{7\pi-22}$ vs. $\log T$. In red, a line with slope $d-1$. (a): $d=2$. (b): $d=3$. We see that at some temperature, there is a region where the slope matches $d-1$, meaning the effective field theory is a good description. If we continue this plot to higher and higher temperatures, there will be infinitely many times the slope matches $d-1$.

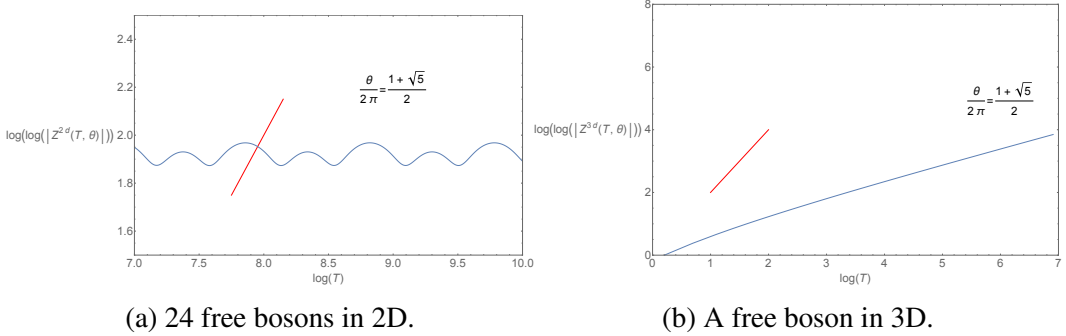


Figure 4.6: In blue, the log of the free energy of two CFTs evaluated at chemical potential $\frac{\theta}{2\pi} = \frac{1+\sqrt{5}}{2}$ vs. $\log T$. In red, a line with slope $d-1$. (a): $d=2$. (b): $d=3$. We see that at no temperature is there a region where the slope matches $d-1$, meaning the effective field theory is never a good description. Since we have fine-tuned the chemical potential to be a real number whose continued fraction has no large numbers in it, we do not guarantee any region in temperature where we have a good EFT description of our theory.

(Although any generic real number would serve to illustrate the partition function's behavior, we choose (4.141) for convenience because of the large 292 showing up immediately.) We see that there indeed is a region of T where the free energies scale as we predict from the effective field theory; but when we increase T further, the scaling breaks down. At large T for generic chemical potential, there will be an infinite number of times the plot in Figure 4.5 has slope $d-1$, which is when the continued fraction approximation is well-approximated by a rational number (i.e. whenever $a_i \gg a_{i-1}$ in the continued fraction).

Finally we note that if we fine-tune the angle θ so that none of the a_i 's ever become large, we can make there be no regime where the partition function obviously grows as T^{d-1} . For example, choosing the angle to be the golden ratio

$$\frac{\theta}{2\pi} = \frac{1 + \sqrt{5}}{2} = 1 + \frac{1}{1 + \frac{1}{1 + \dots}} \quad (4.142)$$

gives an angle where there's never a large enough regime in T trust our effective field theory. In Figure 4.6, we again plot the Klein invariant j function and the free boson partition functions as a function of temperature, but this time with the chemical potential set to $\frac{\theta}{2\pi} = \frac{1 + \sqrt{5}}{2}$. We see that the slope of $\log \log |Z|$ against $\log T$ never matches $d - 1$ in a large region, so there is no good EFT description of our system.

4.9 Nonperturbative corrections

In this section, we consider nonperturbative corrections to the thermodynamic limit $L \rightarrow \infty$ at finite β . For concreteness, we focus on a CFT_d and its dimensional reduction on S_β^1 to a $d-1$ -dimensional gapped theory. By conformal symmetry, the thermodynamic limit is equivalent to $\beta \rightarrow 0$ (with a fixed-size spatial manifold). For simplicity, we will not turn on "small" angular twists $\beta \vec{\Omega}$, though it would be straightforward to incorporate them.

The thermal effective action essentially captures the dynamics of the ground state of the $d-1$ dimensional gapped theory, while nonperturbative corrections come from particle excitations. On the geometry $\mathbb{R}^{d-1} \times S_\beta^1$, the excitations can be classified into irreps of the $d-1$ -dimensional Poincaré group and the Kaluza-Klein $U(1)$ that rotates the S_β^1 . Irreps of the Poincaré group are labeled by a mass and a little group representation — for simplicity, we will focus on scalars. Thus, each excitation of interest is labeled by a mass m_i and a KK charge $q_i \in \mathbb{Z}$. The lightest mass m_q for each KK charge q is sometimes called the " q -th screening mass", while the lightest nonzero mass overall is the "thermal mass" of the theory. Note that when $d = 2$, the spectrum of masses (m_i, q_i) are simply $(\frac{2\pi}{\beta} \Delta_i, \ell_i)$, where (Δ_i, ℓ_i) are scaling dimensions and spins of local operators. However, in higher dimensions, the masses m_i are not related in an obvious way to the local operator spectrum.

In the partition function $Z_{\text{CFT}}[\mathcal{M}_{d-1} \times S_\beta^1]$, the leading nonperturbative effects at small β are expected to come from "worldline instantons" associated with particles of mass m_i propagating along geodesics of \mathcal{M}_{d-1} , see e.g. [39, 79, 99, 109, 110].

Such contributions can be computed from the worldline path integral

$$\log Z \Big|_{\text{single-particle}} = \sum_{(m_i, \mathbf{q}_i)} \int Dx^\mu(\tau) \exp \left(-m_i \int d\tau \sqrt{\dot{x}_\mu \dot{x}^\mu} + \frac{2\pi i \mathbf{q}_i}{\beta} \oint A \right). \quad (4.143)$$

Here, for each particle, we have included a length term $-m_i \int ds$ proportional to the mass, along with a coupling $\frac{2\pi i \mathbf{q}_i}{\beta} \oint A$ to the background KK gauge field. (Note that we include a factor of $\frac{2\pi}{\beta}$ because in our conventions, A is a connection on a circle bundle where the fiber has circumference β , instead of the usual 2π .)

In Appendix 4.10, we compute the wordline path integral (4.143) on some geometries of interest. For example, by computing (4.143) on S^{d-1} , we find that the leading nonperturbative terms in the partition function $Z_{\text{CFT}}[S^{d-1} \times S_\beta^1]$ have the form

$$\log(\text{Tr}_{\mathcal{H}_{S^{d-1}}} [e^{-\beta H}]) \supset \sum_{m_i} e^{-2\pi m_i} \frac{(\pm i)^{d-2} m_i^{d-2}}{\Gamma(d-1)} \left(1 + O\left(\frac{1}{m_i}\right) \right). \quad (4.144)$$

Note that the effect of each particle is exponential in the mass $e^{-2\pi m_i}$, where 2π is the length of a great circle on S^{d-1} . By dimensional analysis, the masses are proportional to $1/\beta$, and hence these are indeed nonperturbative corrections in β . In addition to the exponential dependence, the worldline path integral makes an unambiguous prediction for the leading coefficient of the exponential, coming from a gaussian determinant. We immediately see that the interpretation of (4.144) is subtle because the coefficient becomes *imaginary* when d is odd (even when the partition function must be real). We discuss this phenomenon and its interpretation in Appendix 4.10.

Specializing to 4D, we can similarly compute leading nonperturbative corrections to a partition function on a lens space $L(q; 1)$, coming from a "short" geodesic of length $2\pi/q$:

$$\log(\text{Tr}_{\mathcal{H}_{L(q;1)}} [e^{-\beta H}]) \supset \begin{cases} \sum_{m_i} e^{-\frac{2\pi m_i}{q}} \frac{m_i}{2 \sin(\frac{2\pi}{q})} \left(1 + O\left(\frac{1}{m_i}\right) \right) & (q \neq 2), \\ \sum_{m_i} e^{-\pi m_i} \frac{m_i^2}{2} \left(1 + O\left(\frac{1}{m_i}\right) \right) & (q = 2). \end{cases} \quad (4.145)$$

By our discussion of the EFT bundle, this result is closely related to the partition function on S^3 , with a twist by a rational angle of order q . To obtain the latter, we must replace $\beta \rightarrow q\beta$, and account for the presence of a nontrivial holonomy for the

KK gauge field (since $S_{q\beta}^1$ is nontrivially fibered over $L(q; 1)$). We find

$$\log(\text{Tr}_{\mathcal{H}_{S^3}}[e^{-\beta H - \frac{2\pi i}{q} J_{12} - \frac{2\pi i}{q} J_{34}}]) \supset \begin{cases} \sum_{(m_i, q_i)} e^{-\frac{2\pi m_i}{q^2} + \frac{2\pi i q_i}{q}} \frac{m_i}{2q \sin(\frac{2\pi}{q})} \left(1 + O\left(\frac{1}{m_i}\right)\right) & (q \neq 2), \\ \sum_{(m_i, q_i)} e^{-\frac{\pi m_i}{2} + \pi i q_i} \frac{m_i^2}{8} \left(1 + O\left(\frac{1}{m_i}\right)\right) & (q = 2). \end{cases} \quad (4.146)$$

In particular, nonperturbative corrections to the twisted partition function go like $e^{-2\pi m_i/q^2}$, as opposed to $e^{-2\pi m_i}$ in the un-twisted case.

More generally, in any dimension d , when the quotient by \mathbb{Z}_q creates a short geodesic of length $\ell_{\text{short}} = 2\pi/q$, the leading nonperturbative corrections will behave like $e^{-(m_i/q)\ell_{\text{short}}} = e^{-2\pi m_i/q^2}$, where m_i/q comes from the replacement $\beta \rightarrow q\beta$. Note that this matches the result from modular invariance in 2D. In 2D, after applying a modular transformation, the twisted partition function becomes $\text{Tr} \left[e^{2\pi i \tilde{\tau} (L_0 - \frac{c}{24}) - 2\pi i \tilde{\tau} (\bar{L}_0 - \frac{c}{24})} \right]$, where $\tilde{\tau} = \text{const} + \frac{2\pi i}{q^2 \beta}$. Thus, the leading β -dependence of the contribution of excited states to the twisted partition function is $e^{-4\pi^2 \Delta_i/(q^2 \beta)} = e^{-2\pi m_i/q^2}$, where $m_i = \frac{2\pi \Delta_i}{\beta}$.

Note that the action (4.143) is only the leading approximation to the effective action of a worldline instanton in the small β limit. In particular, there can be power-law corrections in β coming from higher curvature terms. Thus, while the tree-level and 1-loop terms (4.144), (4.145), and (4.146) in the worldline path integral are universal, the subleading corrections in $1/m_i$ are not necessarily universal, since they get contributions both from (computable) loops and from higher curvature terms.²⁰

In Appendix 4.10, we derive (4.144), (4.145), and (4.146) by performing the worldline path integral explicitly. We also verify the universal leading terms in several examples from free field theory.

4.10 Discussion and future directions

In this work, we found that the high-temperature partition function, twisted by a finite-order discrete rotation R , is captured by the same thermal EFT as the un-twisted partition function. One consequence is that "spin-refined" densities of states (like the difference between the density of even-spin and odd-spin operators) are determined by the same Wilson coefficients as the usual density of states, up to

²⁰Furthermore, our choice of ζ -function regularization does not in general respect coordinate-invariance of the worldline path integral. To restore coordinate invariance one must add non-coordinate-invariant counterterms like $g^{\mu\nu} g^{\rho\tau} g_{\alpha\beta} \Gamma_{\mu\rho}^\alpha \Gamma_{\nu\tau}^\beta$ with the appropriate coefficients. See [16] for discussion.

subleading contributions from Kaluza-Klein vortices. Furthermore, the partition function $Z(\beta, \vec{\theta})$ itself has an intricate fractal-like structure as a function of angle at small β , with the same universal asymptotics controlling the neighborhood of every rational angle.

These results follow entirely from effective field theory, together with the assumption that generic CFTs develop a mass gap when dimensionally-reduced. It would be interesting to revisit this assumption and understand how our results are modified in the presence of potential gapless modes. It would also be interesting to investigate whether Kaluza-Klein vortex defects can support gapless excitations, contribute to Weyl anomalies, and/or have nontrivial topological terms in their effective action²¹.

Our central construction is simple: it is essentially the observation that it is useful to construct a mapping torus $M_{\beta,R} = (\mathcal{M}_L \times \mathbb{R})/\mathbb{Z}$ from two successive quotients: first quotienting by $q\mathbb{Z}$, and then by $\mathbb{Z}_q = \mathbb{Z}/q\mathbb{Z}$. This idea is applicable on other geometries besides $S^{d-1} \times \mathbb{R}$, and it would be interesting to explore its implications for other types of partition functions. For example, one could explore "spin-refined" statistics of OPE coefficients by studying the behavior of discrete spacetime symmetries on the "genus-2" geometry of [25], or spin-refined lens-space partition functions [182], or the interaction of discrete spacetime symmetries with other forms of higher-dimensional "modular invariance" [7, 156, 189, 190]. Supersymmetric partition functions have been studied on a wide variety of geometries; see e.g. [178]. It is an enduring challenge to understand observables of non-supersymmetric (potentially nonperturbative) theories on these geometries.

One can also consider applying thermal EFT to BCFTs to study the asymptotic spectra of boundary operators. In two dimensions, this boils down to studying the partition function on a finite cylinder in the $\beta \rightarrow 0$ limit and writing down an EFT on a finite interval with two end points. The end points will become point-like defects in the thermal effective action. In higher dimensions, by introducing defects one may break the $SO(d)$ invariance down to some subgroup H . We can imagine turning on a rotation belonging to H and applying thermal EFT ideas in this context.

So far, our main tool for computing partition functions has been thermal EFT, which is organized in an expansion in small β . This expansion is likely asymptotic in general. In fact we can see its asymptotic nature explicitly in odd-dimensional free theories. It is an important question whether one can obtain more precise results

²¹See e.g. [22, 65] for a study of similar vortex defects in the context of supersymmetric quantum field theories.

about high temperature partition functions, potentially including convergent expansions and/or numerical bounds (as is possible in 2D using the modular bootstrap [108]).

One possible approach is through a better understanding of resurgence in the small- β expansion. In particular, it would be nice to better understand the structure of nonperturbative terms beyond the worldline instantons discussed in Section 4.9. We expect that in an interacting theory, there should also be contributions from an infinite sum of "instanton graphs," representing massive particles propagating and interacting. An old example of instanton graphs are Lüscher corrections in field theories on torii [157, 158]. However, to our knowledge, the rules for general instanton graphs on general geometries in general massive QFTs have not been spelled out.

Relatedly, modular invariance in 2D CFTs constrains some of the nonperturbative behavior of the partition function. Given some input light spectra, modular invariance highly constrains the resulting spectra, which in effect forces the partition functions with any phase inserted to behave in a certain way. Techniques such as Poincare series and Rademacher series have been used to complete the light spectrum of a 2D CFT (see e.g. [5, 77, 132, 162]), which roughly take the form of a (convergent) sum over rational angles. It would be interesting if there were related techniques in higher dimensions, resumming all rational angle insertions in the partition function trace.

Another potential avenue to making the high-temperature expansion precise is using Tauberian techniques, which have been applied successfully to correlation functions [73, 173, 176, 180] and torus partition functions in 2D [168, 174, 175]. An essential ingredient in Tauberian methods is positivity,²² which has not yet played an important role in applications of thermal EFT.

²²See [163] where, even if OPE coefficient can become negative, Tauberian theorems were used along with some boundedness conditions from below, to predict asymptotics of OPE coefficient averaged over a large microcanonical window. However, it is not clear how to extend the result rigorously for an order one window. The same theorem is used in [172] as well.

Appendix A Qualitative picture of the 3D Ising partition function

In this appendix, we explain our procedure for producing Figure 4.1. Let $S_{p/q}$ denote the leading contribution to the thermal effective action around the angle $\frac{2\pi p}{q}$ in 3D:

$$-S_{p/q} = \frac{1}{q^3} \frac{f \text{vol } S^2}{\beta^2 + (\theta - \frac{2\pi p}{q})^2}. \quad (4.147)$$

We expect $-S_{p/q}$ to be a good estimate for the action when it is large. Thus, to patch together different EFT descriptions, we roughly want to choose the action $-S_{p/q}$ that is largest for each (β, θ) . This would lead to the approximation $-S \approx \max_{p,q} -S_{p/q}$, where p, q runs over co-prime pairs of integers. However, such an estimate would not be smooth, so we instead combine the different actions with a root-mean-square:

$$-S \approx \left(\sum_{p,q} (-S_{p/q})^2 \right)^{1/2}. \quad (4.148)$$

In Figure 4.1, we plot $\log \log Z = \log(-S)$, for S given in (4.148), with coprime pairs of integers up to denominator 15. We use the value of minus the free energy density $f \approx 0.153$ determined from Monte-Carlo simulations [144, 145, 198].

Note that the approximation (4.148) has some unrealistic features. Firstly, its expansion around each rational angle contains subleading corrections in β that do not conform with the expectation from thermal EFT (4.32). Secondly, it does not incorporate the nonperturbative effects discussed in Section 4.9. Our goal with this approximation is simply to give a qualitative picture of the partition function. It is interesting to ask whether there is a natural basis of functions for Z that naturally incorporates these constraints.

In principle, the qualitative features of Figure 4.1 can be checked. For instance, one can explicitly build the partition function of the 3D Ising model with a phase (e.g. $(-1)^J$) inserted, by simply using the operator scaling dimensions that have been estimated from the conformal bootstrap (or other methods). One can then plot it as a function of β, Ω , and check that, for instance, the leading Wilson coefficient is approximately $\frac{0.153}{8}$ (similar to what was done in Appendix A of [119] and Appendix D of [25]). An important technical obstacle we run into when attempting this is: when computing the partition function with the phase $(-1)^J$, the EFT is valid when $2\beta \ll 1$ (rather than $\beta \ll 1$), so in effect, one needs to keep more operators in the partition function to get a trustworthy estimate. It would be interesting if other techniques to estimate the scaling dimensions of the 3D Ising model know about enough high energy operators to see explicitly the qualitative features of Figure 4.1.

Appendix B Review of plethystic sums

In this appendix, we review some facts about the high temperature expansion of plethystic sums. Plethystic sums can be written as derivatives of various spectral zeta functions and to compute the high temperature expansion, one "resums" the zeta functions following a procedure very similar to (4.94). The same resummation technique is also used to compute the high temperature expansion of massive free field free energy, as we discussed in the Section 4.10.

Plethystic sums and spectral zeta functions We start with some general discussion. Let $f(\beta) = \sum_k d_k e^{-\beta \lambda_k}$ be a generating function. We define a few related quantities:

- Plethystic sum:

$$\log(\text{PE}[f]) := \sum_{n=1} \frac{1}{n} f(n\beta). \quad (4.149)$$

- Spectral zeta function:

$$\zeta(s; f) := \sum_{n \in \mathbb{Z}} \sum_k d_k \left[\left(\frac{2\pi n}{\beta} \right)^2 + \lambda_k^2 \right]^{-s}. \quad (4.150)$$

- Heat trace:

$$H(t; f) := \sum_k d_k e^{-t\lambda_k^2}. \quad (4.151)$$

The plethystic sum is related to the spectral zeta function in a simple way:

$$\log(\text{PE}[f]) - \frac{\beta}{2} \sum_k d_k \lambda_k = \frac{1}{2} \frac{d}{ds} \Big|_{s=0} \zeta(s; f), \quad (4.152)$$

where the second term on the left hand side is the zeta function regularized Casimir energy.²³

To derive (4.152), we start by using the Schwinger parametrization to obtain:

$$\begin{aligned} \zeta(s; f) &= \sum_{n \in \mathbb{Z}} \sum_k d_k \left[\left(\frac{2\pi n}{\beta} \right)^2 + \lambda_k^2 \right]^{-s} = \frac{1}{\Gamma(s)} \sum_{n \in \mathbb{Z}} \sum_k d_k \int_0^\infty \frac{dt}{t} t^s e^{-t(\frac{2\pi n}{\beta})^2 - t\lambda_k^2} \\ &= \frac{1}{\Gamma(s)} \frac{\beta}{2\sqrt{\pi}} \sum_{m \in \mathbb{Z}} \sum_k d_k \int_0^\infty \frac{dt}{t} t^{s-\frac{1}{2}} e^{\frac{m^2 \beta^2}{4t} - t\lambda_k^2}, \end{aligned} \quad (4.153)$$

²³Note that the Casimir energy computed using zeta function regularization is NOT the same as the Casimir energy included in Appendix 4.10. See Section 3.1 in [25] for a discussion of schemes and [113] for the difference with zeta function regularization.

where in the last line we've Poisson resummed with respect to n . Now we split the summation over m into an "excited part" with $m \neq 0$ and a "vacuum part" where $m = 0$:

$$\begin{aligned}\zeta_{\text{excited}}(s; f) &= \frac{1}{\Gamma(s)} \frac{\beta}{\sqrt{\pi}} \sum_{m=1}^{\infty} \sum_k d_k \int_0^{\infty} \frac{dt}{t} t^{s-\frac{1}{2}} e^{\frac{m^2 \beta^2}{4t} - t \lambda_k^2}, \\ \zeta_{\text{vacuum}}(s; f) &= \frac{1}{\Gamma(s)} \frac{\beta}{\sqrt{\pi}} \sum_k d_k \int_0^{\infty} \frac{dt}{t} t^{s-\frac{1}{2}} e^{-t \lambda_k^2}.\end{aligned}\quad (4.154)$$

Performing the integral over t , we get

$$\begin{aligned}\frac{d}{ds} \Big|_{s=0} \zeta_{\text{excited}}(s; f) &= \frac{\beta}{\sqrt{\pi}} \sum_{m=1}^{\infty} \sum_k d_k \int_0^{\infty} \frac{dt}{t} t^{-1/2} e^{-\frac{m^2 \beta^2}{4t} - t \lambda_k^2} \\ &= 2 \sum_{m=1}^{\infty} \frac{1}{m} \sum_k d_k e^{-\beta m \lambda_k} = 2 \log(\text{PE}[f]).\end{aligned}\quad (4.155)$$

For $\zeta_{\text{vacuum}}(s; f)$, we invert the Schwinger parametrization:

$$\frac{d}{ds} \Big|_{s=0} \zeta_{\text{vacuum}}(s; f) = \frac{\beta}{2\sqrt{\pi}} \Gamma(-1/2) \sum_k d_k \lambda_k = -\beta \sum_k d_k \lambda_k. \quad (4.156)$$

Putting everything together we arrive at (4.152).

To compute partition functions with flavor twists and rational angular fugacities we need to consider plethystic sums taking the following form:

$$\sum_{n=1}^{\infty} \frac{e^{-in\theta}}{n} F(n\beta, \omega_q^n), \quad \omega_q = \exp\left(\frac{2\pi i}{q}\right). \quad (4.157)$$

Some formal manipulation shows that when the "twisted generating function" $F(\beta, \omega_q)$ satisfies $F(\beta, \omega_q) = F(\beta, \omega_q^{-1})$, the following relation holds:

$$\begin{aligned}\sum_{n=1}^{\infty} \frac{e^{-in\theta}}{n} F(n\beta, \omega_q^n) + \sum_{n=1}^{\infty} \frac{e^{in\theta}}{n} F(n\beta, \omega_q^n) &= \frac{1}{q} \frac{d}{ds} \Big|_{s=0} \zeta[q\theta, s; F(q\beta, 1)] + \frac{\beta}{q} \sum_k d_k \lambda_k \\ &+ \frac{1}{2q} \sum_{\ell=1}^{q-1} \frac{d}{ds} \Big|_{s=0} \left[L\left(q\theta, \frac{\ell}{q}, s; F(q\beta, \omega_q^\ell)\right) + L\left(-q\theta, \frac{\ell}{q}, s; F(q\beta, \omega_q^\ell)\right) \right],\end{aligned}\quad (4.158)$$

where

- In the second sum on the right hand side, d_k and λ_k are supposed to be read from $F(q\beta, 1)$, that is, $F(q\beta, 1) = \sum_{k=0}^{\infty} d_k e^{-\beta \lambda_k}$

$$\zeta(\theta, s; f) = \sum_{n \in \mathbb{Z}} \sum_k d_k \left[\left(\frac{2\pi n}{\beta} + \frac{\theta}{\beta} \right)^2 + \lambda_k^2 \right]^{-s}, \quad \text{with } f(\beta) = \sum_{k=0} d_k e^{-\beta \lambda_k}. \quad (4.159)$$

$$L(\theta, a, s; f) = \sum_{n \in \mathbb{Z}} \sum_k d_k \frac{e^{2\pi i n a}}{\left[\left(\frac{2\pi n}{\beta} + \frac{\theta}{\beta} \right)^2 + \lambda_k^2 \right]^s}, \quad \text{with } f(\beta) = \sum_{k=0} d_k e^{-\beta \lambda_k}. \quad (4.160)$$

Now that we've related different plethystic sums to various spectral zeta functions, the high temperature expansion can be computed by "resumming" all these zeta functions. For concreteness, we look at some examples:

Example: free scalar on $S^1 \times S^3$ The relevant generating function is²⁴

$$f(\beta) = \frac{e^{-\beta}(1 - e^{-2\beta})}{(1 - e^{-\beta})^4} = \sum_{k=1} k^2 e^{-\beta k}. \quad (4.161)$$

The spectral zeta function is

$$\zeta(s; f) = \frac{1}{\Gamma(s)} \sum_{n \in \mathbb{Z}} \int_0^\infty \frac{dt}{t} t^s e^{-t(\frac{2\pi n}{\beta})^2} H(t; f) \quad (4.162)$$

with

$$H(t; f) = \sum_{k=1}^\infty k^2 e^{-tk^2} = \frac{\sqrt{\pi}}{4} t^{-3/2} + \sqrt{\pi} \sum_{\ell=1}^\infty e^{-\ell^2 \pi^2 / t} \left(\frac{1}{2} t^{-3/2} - \ell^2 \pi^2 t^{-5/2} \right).$$

Here we performed a Poisson resummation with respect to k and separated the piece with $\ell = 0$ from $\ell \neq 0$.

- The term with $n = 0$ in the sum (4.162) is the contribution of zero mode:

$$\zeta(s; f) \Big|_{n=0} = \sum_{k=1}^\infty d_k \lambda_k^{-s} = \sum_{k=1}^\infty k^{2-2s} = \zeta_R(2s-2). \quad (4.163)$$

²⁴This is the spectral generating function of the operator $\Delta + \frac{(d-2)}{4(d-1)} R$ with Δ being the Laplacian on S^3 and $d = 4$.

- Terms with $n \neq 0$ and $\ell = 0$ generate the perturbative series:

$$\begin{aligned}\zeta(s; f) \Big|_{n \neq 0, \ell=0} &= \frac{\sqrt{\pi}}{4\Gamma(s)} \sum_{n \in \mathbb{Z}, n \neq 0} \int_0^\infty \frac{dt}{t} t^s e^{-t(\frac{2\pi n}{\beta})^2} t^{-3/2} \\ &= \sqrt{\pi} \frac{\Gamma(s - \frac{3}{2})}{2\Gamma(s)} \left(\frac{2\pi}{\beta}\right)^{3-2s} \zeta_R(2s - 3).\end{aligned}\quad (4.164)$$

- Terms with $n \neq 0$ and $\ell \neq 0$ generate the non-perturbative corrections:

$$\zeta(s; f) \Big|_{n \neq 0, \ell \neq 0} = \frac{\sqrt{\pi}}{\Gamma(s)} \sum_{n=1}^\infty \sum_{\ell=1}^\infty \left[2^{\frac{5}{2}-s} \left(\frac{n}{\ell\beta}\right)^{\frac{3}{2}-s} K_{-\frac{3}{2}+s} \left(\frac{4\pi^2\ell n}{\beta}\right) - 2^{\frac{9}{2}-s} \pi^2 \ell^2 \left(\frac{n}{\ell\beta}\right)^{\frac{5}{2}-s} K_{-\frac{5}{2}+s} \left(\frac{4\pi^2\ell n}{\beta}\right) \right]. \quad (4.165)$$

Following (4.152), we find

$$\log(\text{PE}[f]) - \frac{\beta}{240} = \frac{\pi^4}{45\beta^3} - \frac{\zeta(3)}{4\pi^2} - \frac{1}{2\pi^2} \sum_{n=1}^\infty \sum_{\ell=1}^\infty e^{-\frac{4\pi^2 n \ell}{\beta}} \left(\frac{1}{\ell^3} + \frac{4n\pi^2}{\ell^2\beta} + \frac{8n^2\pi^4}{\ell\beta^2} \right). \quad (4.166)$$

With the same d_k and λ_k , we can construct a slightly different zeta function:

$$\zeta_m(s) = \sum_{k=0}^\infty \frac{d_k}{(\lambda_k^2 + m^2)^s} \quad (4.167)$$

this spectral zeta function satisfies

$$\frac{1}{2} \frac{d}{ds} \Big|_{s=0} \zeta_m(s) = \log(Z_{\text{massive}}[S^3]), \quad (4.168)$$

where $Z_{\text{massive}}[S^3]$ is given in eqn(4.216). Applying the same resummation procedure, we get (4.217). The lens space partition functions $Z_{\text{massive}}[L(q; 1)]$ can be computed in an almost identical way. One simply replace $d_k = k^2$ by [12]:

$$\begin{aligned}d_k &= \begin{cases} k \left[\frac{k}{q} \right], & k - q \left[\frac{k}{q} \right] \in 2\mathbb{Z}, \\ k \left(\left[\frac{k}{q} \right] + 1 \right), & k - q \left[\frac{k}{q} \right] \in 2\mathbb{Z} + 1, \end{cases} \quad (q \in 2\mathbb{Z} + 1), \\ d_k &= \begin{cases} 0, & k \in 2\mathbb{Z}, \\ k \left(2 \left[\frac{k}{q} \right] + 1 \right), & k \in 2\mathbb{Z} + 1, \end{cases} \quad (q \in 2\mathbb{Z}).\end{aligned}\quad (4.169)$$

which are the degeneracy for $\Delta + \frac{(d-2)}{4(d-1)} R$ with Δ being the Laplacian in $L(q; 1)$ and $d = 4$. The same calculations will yield (4.221) and (4.222).

Example: free scalar on $S^1 \times S^5$

The relevant generating function is

$$f(\beta) = \frac{q^2(1-q^2)}{(1-q)^6} = \sum_{k=1}^{\infty} \frac{k^2(k^2-1)}{12} e^{-\beta k}$$

and the heat trace is:

$$\begin{aligned} H(t; f) &= \frac{1}{24} \sum_{k \in \mathbb{Z}} k^2(k^2-1) e^{-tk^2} \\ &= \sqrt{\pi} \left(\frac{1}{32t^{5/2}} - \frac{1}{48t^{3/2}} \right) + \sqrt{\pi} \sum_{l=1}^{\infty} e^{-\frac{l^2\pi^2}{t}} \left[\frac{\pi^4 l^4}{12t^{9/2}} - \frac{\pi^2 l^2}{4t^{7/2}} + \frac{1}{t^{5/2}} \left(\frac{\pi^2 l^2}{12} + \frac{1}{16} \right) - \frac{1}{24t^{3/2}} \right]. \end{aligned} \quad (4.170)$$

Following the same procedure as in the example above, we obtain

$$\log(\text{PE}[f] - \frac{31}{60480} \beta) = \frac{2\pi^6}{945\beta^5} - \frac{\pi^4}{540\beta^3} + \frac{\zeta(5)}{16\pi^4} + \frac{\zeta(3)}{48\pi^2} \quad (4.171)$$

$$+ \sum_{n=1}^{\infty} \sum_{\ell=1}^{\infty} e^{-\frac{4\pi^2 n \ell}{\beta}} \left[\frac{4\pi^4 n^4}{3\beta^4 \ell} + \frac{4\pi^2 n^3}{3\beta \ell^2} + \frac{1}{\beta^2} \left(\frac{n^2}{\ell^3} + \frac{\pi^2 n^2}{3\ell} \right) + \frac{1}{\beta} \left(\frac{n}{2\pi^2 \ell^4} + \frac{n}{6\ell^2} \right) + \frac{1}{8\pi^4 \ell^5} + \frac{1}{24\pi^2 \ell^3} \right]. \quad (4.172)$$

If we replace $\zeta(s; f)$ by $\zeta_m(s)$, we reproduce (4.218).

Example: free scalar on $S^1 \times S^3$ with \mathbb{Z}_2 flavor twist

The plethystic sum in interest is

$$\sum_{n=1}^{\infty} \frac{(-1)^n}{n} f(n\beta), \quad f(\beta) = \frac{e^{-\beta}(1-e^{-2\beta})}{(1-e^{-\beta})^4} = \sum_{k=1}^{\infty} k^2 e^{-\beta k}. \quad (4.173)$$

Setting $q = 1$ and $\theta = \pi$ in (4.158), we find that

$$\sum_{n=1}^{\infty} \frac{(-1)^n}{n} f(n\beta) = \frac{1}{2} \frac{d}{ds} \Big|_{s=0} \zeta(\pi, s; f) + \frac{\beta}{2} \sum_k d_k \lambda_k. \quad (4.174)$$

where $\zeta(\pi, s; f)$ is defined in (4.159). After resumming the zeta function, we find

$$\sum_{n=1}^{\infty} \frac{(-1)^n}{n} f(n\beta) - \frac{\beta}{240} = -\frac{7\pi^4}{360\beta^3} - \sum_{n=1}^{\infty} \sum_{\ell=1}^{\infty} e^{-\frac{(4n-2)\ell\pi^2}{\beta}} \left(\frac{(2n-1)^2\pi^2}{\ell\beta^2} + \frac{2n-1}{\ell^2\beta} + \frac{1}{\ell^3\pi^2} \right). \quad (4.175)$$

Finally, we discuss twisted partition function with rational angular fugacity. These are the main objects of interest in this paper. Even though the techniques outlined

in this appendix can be very easily generalized to higher dimensions and to more complicated combinations of angles, we will focus on 4D scalar partition functions twisted by $e^{-\frac{2\pi i}{q}J_{12}-\frac{2\pi i}{q}J_{34}}$ for simplicity. As explained in Section 4.10, the subtle difference between the lens space partition function and the twisted partition function is related to the non-trivial topology of the EFT bundle.

Example: free scalar in $S^1 \times S^3$ with \mathbb{Z}_q rotation, q odd

We focus on the twisted partition function $\log \left(\text{Tr}[e^{-\beta H - \frac{2\pi i}{q}J_{12} - \frac{2\pi i}{q}J_{34}}] \right)$ and restrict to the case where q is odd. The plethystic sum in interest is

$$\sum_{n=1}^{\infty} \frac{1}{n} F(n\beta, \omega_q^n), \quad F(\beta, \omega_q) = \frac{e^{-\beta}(1 - e^{-2\beta})}{(1 - \omega_q e^{-\beta})^2 (1 - \omega_q^{-1} e^{-\beta})^2}. \quad (4.176)$$

It is easy to verify

$$F(q\beta, \omega_q^\ell) = \begin{cases} \sum_{k=1}^{\infty} k^2 e^{-q\beta k}, & \ell = 0 \\ \sum_{k=1}^{\infty} \frac{k \sin(\frac{2\pi k\ell}{q})}{\sin(\frac{2\pi\ell}{q})} e^{-q\beta k}, & \ell \neq 0 \end{cases} \quad (4.177)$$

Setting $\theta = 0$ in (4.158), we find

$$\begin{aligned} \sum_{n=1}^{\infty} \frac{1}{n} F(n\beta, \omega_q^n) &= \frac{1}{2q} \frac{d}{ds} \Big|_{s=0} \zeta[0, s; F(q\beta, 1)] + \frac{\beta}{q} \sum_k d_k \lambda_k \\ &\quad + \frac{1}{2q} \sum_{\ell=1}^{q-1} \frac{d}{ds} \Big|_{s=0} L\left(q\theta, \frac{\ell}{q}, s; F(q\beta, \omega_q^\ell)\right). \end{aligned} \quad (4.178)$$

where $d_k = k^2$, $\lambda_k = qk$ for the second sum on the right hand side. After resumming all the zeta functions, we find

$$\begin{aligned} \sum_{n=1}^{\infty} \frac{1}{n} \frac{e^{-n\beta}(1 - e^{-2n\beta})}{(1 - \omega_q^n e^{-n\beta})^2 (1 - \omega_q^{-n} e^{-n\beta})^2} &= \frac{\pi^4}{45\beta^3 q^4} + \frac{\beta}{240} - \frac{\zeta(3)}{4\pi^2 q} \\ &\quad - \frac{1}{q} \sum_{n=1}^{\infty} \sum_{\ell=1}^{\infty} e^{-\frac{4\pi^2 \ell n}{\beta q}} \left(\frac{1}{2\pi^2 \ell^3} + \frac{2n}{\beta \ell^2 q} + \frac{4\pi^2 n^2}{\beta^2 \ell q^2} \right) \\ &\quad + \sum_{n=1}^{\infty} \sum_{\substack{\ell=1 \\ \ell \notin q\mathbb{Z}}}^{\infty} \frac{\cos(\frac{2\pi n \ell}{q})}{\sin(\frac{2\pi \ell}{q})} e^{-\frac{4\pi^2 n \ell}{q^2 \beta}} \left(\frac{2\pi n}{\ell q \beta} + \frac{q}{2\ell^2 \pi} \right) \\ &\quad + \sum_{\substack{\ell=1 \\ \ell \notin q\mathbb{Z}}}^{\infty} \frac{1}{4\pi \ell^2} \frac{1}{\sin(\frac{2\pi \ell}{q})}. \end{aligned} \quad (4.179)$$

Example: free scalar in $S^1 \times S^3$ with \mathbb{Z}_q rotation and \mathbb{Z}_2 flavor twist, $q=\text{odd}$

The relevant plethystic sum is

$$\sum_{n=1}^{\infty} \frac{(-1)^n}{n} F(n\beta, \omega_q^n), \quad F(\beta, \omega_q) = \frac{e^{-\beta}(1 - e^{-2\beta})}{(1 - \omega_q e^{-\beta})^2(1 - \omega_q^{-1} e^{-\beta})^2}. \quad (4.180)$$

Setting $\theta = \pi$ in (4.158) and resum all the zeta functions, we get

$$\begin{aligned} \sum_{n=1}^{\infty} \frac{(-1)^n}{n} \frac{e^{-n\beta}(1 - e^{-2n\beta})}{(1 - \omega_q^n e^{-n\beta})^2(1 - \omega_q^{-n} e^{-n\beta})^2} &= -\frac{7\pi^4}{360\beta^3 q^4} + \frac{\beta}{240} \\ &- \sum_{n=1}^{\infty} \sum_{\ell=1}^{\infty} e^{-\frac{2\ell(2n-1)\pi^2}{q\beta}} \left(\frac{(2n-1)^2\pi^2}{\ell q^3 \beta^2} + \frac{2n-1}{\beta \ell^2 q^2} + \frac{1}{2\ell^3 q \pi^2} \right) \\ &+ \sum_{\substack{\ell=1 \\ \ell \notin q\mathbb{Z}}}^{\infty} \sum_{n=0}^{\infty} \frac{\cos\left(\frac{2\pi\ell}{q}\left(\frac{q-1}{2} - n\right)\right)}{\sin\left(\frac{2\pi\ell}{q}\right)} e^{-\frac{2\ell(2n+1)\pi^2}{q^2\beta}} \left(\frac{(2n+1)\pi}{\ell q \beta} + \frac{q}{2\ell^2 \pi} \right). \end{aligned} \quad (4.181)$$

Appendix C More examples for 4D and 6D CFTs

In this appendix, we compute a few more examples of the high temperature expansion of CFTs with a large rotation inserted. We will focus on insertions R without fixed points (so that $S_{\mathcal{D}}$ vanishes). In odd d , $SO(d)$ necessarily has a nontrivial fixed locus, so we focus on even d . In even d , if we insert $R = \exp\left(2\pi i \left(\frac{p_1}{q} J_1 + \dots + \frac{p_n}{q} J_n\right)\right)$ (namely all the denominators are equal, with $\gcd(p_i, q) = 1$), then R has no fixed points and there is no defect action. Previously in Section 4.5, we described 4d examples with a defect coming from $q_1 \neq q_2$; in this example we will consider the (simpler) case with no defect action.

We note that the formulas in this section are accurate to all orders in perturbation theory in β ; this is because the free energy of free theories in even dimensions truncates at $O(\beta)$. This is an accident of free theories in even dimensions and does not generalize.

Finally, we note that in even dimensions, the Hamiltonian $H = D + \varepsilon_0$ includes a contribution from the Casimir energy, which is not accounted for in the sum over characters using plethystic exponentials (see Section 3.1 of [25] for details on this scheme, [113] for a calculation of the Casimir energy, and e.g. [96] for values of the α anomaly). We have included this contribution to the final expression (although terms linear in β are invariant when acting on with (4.32)).

Example: 4D \mathbb{Z}_2 -twisted complex scalar

Here we consider a 4D free complex scalar. We insert a \mathbb{Z}_2 twist (which we denote as $e^{\pi i Q}$) where we identify the field ϕ with $-\phi$ as we go around the thermal circle, in order to remove the gapless sector. Without any insertion of a rotation R , we get the following free energy:

$$\begin{aligned} & \log \text{Tr} [e^{-\beta(H-i\Omega_1 J_1 - i\Omega_2 J_2)} e^{\pi i Q}] \\ & \sim \frac{1}{\prod_{i=1}^2 (1 + \Omega_i^2)} \left(-\frac{7\pi^4}{180\beta^3} - \frac{\pi^2 \sum_{i=1}^2 \Omega_i^2}{36\beta} + \frac{(3 + 6 \sum_{i=1}^2 \Omega_i^2 - 10\Omega_1^2 \Omega_2^2 + 6 \sum_{i=1}^2 \Omega_i^4)\beta}{720} \right). \end{aligned} \quad (4.182)$$

Now let us consider a rotation by $2\pi/3$ in each Cartan direction. As expected, when we insert the large rotation, we find

$$\log \text{Tr} \left[e^{-\beta(H-i\Omega_1 J_1 - i\Omega_2 J_2)} e^{\pi i Q} e^{2\pi i \left(\frac{J_1}{3} + \frac{J_2}{3} \right)} \right] \sim \frac{1}{3} \log \text{Tr} [e^{-3\beta(H-i\Omega_1 J_1 - i\Omega_2 J_2)} e^{3\pi i Q}]. \quad (4.183)$$

Example: 4D Dirac fermion

As discussed in Section 4.4, for fermionic theories we need to compute the partition function without and with a $(-1)^F$ insertion:

$$\begin{aligned} & \log \text{Tr} [e^{-\beta(H-i\Omega_1 J_1 - i\Omega_2 J_2)}] \\ & \sim \frac{1}{\prod_{i=1}^2 (1 + \Omega_i^2)} \left(\frac{7\pi^4}{90\beta^3} - \frac{\pi^2(3 + \sum_{i=1}^2 \Omega_i^2)}{36\beta} + \frac{(18 + 6 \sum_{i=1}^2 \Omega_i^2 + 10\Omega_1^2 \Omega_2^2 - 21 \sum_{i=1}^2 \Omega_i^4)\beta}{1440} \right) \end{aligned} \quad (4.184)$$

$$\begin{aligned} & \log \text{Tr} [(-1)^F e^{-\beta(H-i\Omega_1 J_1 - i\Omega_2 J_2)} e^{4\pi i Q/3}] \\ & \sim \frac{1}{\prod_{i=1}^2 (1 + \Omega_i^2)} \left(\frac{52\pi^4}{1215\beta^3} - \frac{\pi^2(3 + \sum_{i=1}^2 \Omega_i^2)}{54\beta} + \frac{(18 + 6 \sum_{i=1}^2 \Omega_i^2 + 10\Omega_1^2 \Omega_2^2 - 21 \sum_{i=1}^2 \Omega_i^4)\beta}{1440} \right). \end{aligned} \quad (4.185)$$

Fermions carry $U(1)$ charge. We use a convention where the particle carries charge $+1$ and anti-particle carries charge -1 . To make sure that the zero mode does not contribute in the thermal effective field theory description, we turned on the fugacity corresponding to $U(1)$ and set it to $e^{4\pi i/3}$, along with a $(-1)^F$ insertion. This amounted to turning on $\mathbb{Z}_3 \subset U(1)$ flavor symmetry for the partition function with a $(-1)^F$ insertion. After turning on a large rotation $e^{2\pi i J_1 p_1/q} e^{2\pi i J_2 p_2/q}$, we get

the following results (exactly as predicted in Section 4.4):

$$\log \text{Tr} \left[e^{-\beta(H-i\Omega_1 J_1 - i\Omega_2 J_2)} e^{2\pi i \left(\frac{J_1}{3} + \frac{J_2}{3} \right)} \right] \sim \frac{1}{3} \log \text{Tr} \left[e^{-3\beta(H-i\Omega_1 J_1 - i\Omega_2 J_2)} \right] \quad (4.186)$$

$$\log \text{Tr} \left[e^{-\beta(H-i\Omega_1 J_1 - i\Omega_2 J_2)} e^{2\pi i Q/3} e^{2\pi i \left(\frac{J_1}{2} + \frac{J_2}{2} \right)} \right] \sim \frac{1}{2} \log \text{Tr} \left[(-1)^F e^{-2\beta(H-i\Omega_1 J_1 - i\Omega_2 J_2)} e^{4\pi i Q/3} \right]. \quad (4.187)$$

Example: 6D twisted complex scalar

Here we consider a 6D free scalar with a \mathbb{Z}_2 twist:

$$\begin{aligned} & \log \text{Tr} \left[e^{-\beta(H-i\sum_{k=1}^3 \Omega_k J_k)} e^{\pi i Q} \right] \\ & \sim \frac{1}{\prod_{i=1}^3 (1 + \Omega_i^2)} \left(-\frac{31\pi^6}{7560\beta^5} + \frac{7\pi^4(1 - \sum_{i=1}^3 \Omega_i^2)}{2160\beta^3} + \frac{\pi^2(8\sum_{i=1}^3 \Omega_i^2 - 5\sum_{cyc} \Omega_1^2 \Omega_2^2 - 3\sum_{i=1}^3 \Omega_i^4)}{2160\beta} \right. \\ & \left. - \frac{(37 + 62\sum_{i=1}^3 \Omega_i^2 - 154\sum_{cyc} \Omega_1^2 \Omega_2^2 - 104\sum_{i=1}^3 \Omega_i^4 + 70\Omega_1^2 \Omega_2^2 \Omega_3^2 + 42\sum_{i=1}^3 \Omega_i^2 \sum_{i=1}^3 \Omega_i^4 - 22\sum_{i=1}^3 \Omega_i^6)\beta}{60480} \right). \end{aligned} \quad (4.188)$$

With the insertion of a large rotation, we get

$$\log \text{Tr} \left[e^{-\beta(H-i\sum_{k=1}^3 \Omega_k J_k)} e^{\pi i Q} e^{2\pi i \left(\frac{J_1}{3} + \frac{J_2}{3} + \frac{J_3}{3} \right)} \right] \sim \frac{1}{3} \log \text{Tr} \left[e^{-3\beta(H-i\sum_{k=1}^3 \Omega_k J_k)} e^{3\pi i Q} \right] \quad (4.189)$$

Example: 6D Dirac fermion

Finally we consider a 6D free Dirac fermion. We get

$$\begin{aligned} & \log \text{Tr} \left[e^{-\beta(H-i\sum_{k=1}^3 \Omega_k J_k)} \right] \\ & \sim \frac{1}{\prod_{i=1}^3 (1 + \Omega_i^2)} \left(\frac{31\pi^6}{1890\beta^5} - \frac{7\pi^4(5 + \sum_{i=1}^3 \Omega_i^2)}{1080\beta^3} + \frac{\pi^2(135 + 26\sum_{i=1}^3 \Omega_i^2 + 10\sum_{cyc} \Omega_1^2 \Omega_2^2 - 21\sum_{i=1}^3 \Omega_i^4)}{4320\beta} \right. \\ & \left. + \frac{(-880 + 55\sum_{i=1}^3 \Omega_i^2 - 14\sum_{cyc} \Omega_1^2 \Omega_2^2 - 743\sum_{i=1}^3 \Omega_i^4 - 70\Omega_1^2 \Omega_2^2 \Omega_3^2 + 147\sum_{i=1}^3 \Omega_i^2 \sum_{i=1}^3 \Omega_i^4 - 302\sum_{i=1}^3 \Omega_i^6)\beta}{120960} \right). \end{aligned} \quad (4.190)$$

With an insertion of a rotation R , we get the following:

$$\log \text{Tr} \left[e^{-\beta(H-i\sum_{k=1}^3 \Omega_k J_k)} e^{2\pi i \left(\frac{J_1}{2} + \frac{J_2}{2} + \frac{J_3}{2} \right)} \right] \sim \frac{1}{2} \log \text{Tr} \left[e^{-2\beta(H-i\sum_{k=1}^3 \Omega_k J_k)} \right] \quad (4.191)$$

Appendix D More on nonperturbative terms

In this appendix, we discuss more details on the nonperturbative parts of the partition function outlined in Section 4.9. In Appendix 4.10, we derive equations (4.144), (4.145) and (4.146) by performing the worldline path integral. In appendices 4.10,

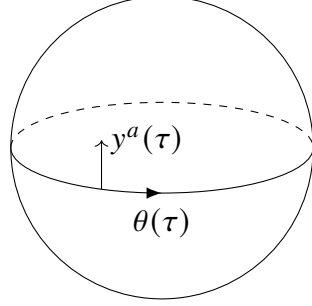


Figure 4.7: Coordinates on S^{d-1} . The classical path is $\theta(\tau) = 2\pi\tau$ and perpendicular fluctuations $y^a(\tau)$ are integrated over.

4.10, and 4.10, we verify the universal leading terms in several examples from free field theory.

Worldline path integral

- Worldline path integral on the sphere

Let us begin by computing the worldline path integral on S^{d-1} . Let θ denote a coordinate along a great circle and let y^i ($i = 1, \dots, d-2$) parametrize the perpendicular directions, see Figure 4.7. The metric on S^{d-1} takes the form:

$$ds^2 = dy^2 + \cos^2 |y| d\theta^2. \quad (4.192)$$

In the absence of a background gauge field, a single worldline instanton contribution is given by

$$\begin{aligned} \int Dx^\mu(\tau) e^{-m_i \int ds} &= \int Dy^i(\tau) \exp \left[-m_i \int_0^1 d\tau \sqrt{\cos^2 |y| \left(\frac{d\theta}{d\tau} \right)^2 + \left(\frac{dy}{d\tau} \right)^2} \right] \\ &\sim e^{-2\pi m_i} \int Dy^i(\tau) \exp \left[-m_i \int_0^1 d\tau \left(\frac{\dot{y}^2}{4\pi} - \pi y^2 \right) \right], \end{aligned} \quad (4.193)$$

where in the last line we Taylor-expanded the square root in fluctuations around the great circle.²⁵ We also used reparameterization invariance of the Nambu-Goto action to set $\theta(\tau) = 2\pi\tau$. In the path integral, we sum over periodic paths $y^i(\tau)$ satisfying $y^i(0) = y^i(1)$, with the following mode expansion:

$$y^i(\tau) = \sum_{n=1}^{\infty} a_n^i \sin(2\pi n\tau) + \sum_{n=1}^{\infty} b_n^i \cos(2\pi n\tau) + \frac{b_0^i}{\sqrt{2}}. \quad (4.194)$$

²⁵This approximation is allowed as long as the thermal wavelength $\sqrt{2\pi/m}$ is much smaller than the size of the sphere.

In writing this mode expansion, we have defined the mode numbers and coefficients a_n^i, b_n^i so that the measure on the moduli space of geodesics is locally $\prod_i da_1^i db_1^i$. We furthermore imposed that each mode should be unit-normalized under the inner product $\langle y, y \rangle = 2 \int d\tau |y|^2$. The path integral can then be reduced to a product of ordinary integrals over a_n^i, b_n^i :²⁶

$$\begin{aligned} & \int Dy^i(\tau) \exp \left[-m_i \int_0^1 d\tau \left(\frac{\dot{y}^2}{4\pi} - \pi y^2 \right) \right] \\ &= \prod_{i=1}^{d-2} \left\{ \prod_{n=1}^{\infty} \int da_n^i db_n^i \exp \left[-\frac{m_i \pi}{2} (n^2 - 1) ((a_n^i)^2 + (b_n^i)^2) \right] \times \int db_0^i \exp \left[\frac{m_i \pi}{2} (b_0^i)^2 \right] \right\}. \end{aligned} \quad (4.195)$$

Modes with $n > 1$ are massive and correspond to oscillations around the geodesic. The modes with $n = 0$ are tachyonic. After adding these tachyonic fluctuations, the trajectory of the particle will deviate from the great circle and shrink towards a point, reducing its length (see e.g. Figure 4 and the surrounding discussions in [79]). Consequently, the classical trajectory we are expanding around is an *unstable* saddle point of the Nambu-Goto action. To define the integral over the tachyonic directions, we need to make sense of integral of the form $\int_{-\infty}^{\infty} dx e^{\alpha^2 x^2}$ where $\text{Re}(\alpha^2) > 0$. We do so by analytically continuing from the region where $\text{Re}(\alpha^2) < 0$ and defining:

$$\int_{-\infty}^{\infty} dx e^{\alpha^2 x^2} := (\pm i) \frac{\sqrt{\pi}}{|\alpha|}, \quad \text{Re } \alpha^2 > 0. \quad (4.196)$$

Furthermore, we make the same choice of sign in (4.196) for integrals over all such tachyonic modes. This prescription, however, does not remove all ambiguities. Since there are $d - 2$ perpendicular directions and each of them contributes a single tachyonic mode, the overall phase factor is $(\pm i)^{(d-2)}$. When d is even, both choices of sign give the same result. But when d is odd, the ambiguity remains. As we will see in Appendix 4.10, this remaining two-fold ambiguity is related to a contour ambiguity in performing a Borel resummation.

The zero modes with $n = 1$ represent rotations of the great circle. The corresponding mode coefficients a_1^i, b_1^i are local coordinates on the moduli space of geodesics.

²⁶The path integral measure $Dy(\tau)$ is induced from a choice of inner product. This inner product must be local — i.e. an integral over τ — in order for the path integral to satisfy proper cutting and gluing rules. However, the overall coefficient of the inner product does not matter because $\det(\text{const}) = \prod_{n \in \mathbb{Z}} \text{const} = 1$ in ζ -function regularization. As long as the modes are all normalized the same way with respect to the inner product, the measure factorizes into an integral over each mode coefficient $Dy = \prod_i db_0^i \prod_{n,i} da_n^i db_n^i$.

Every geodesic on S^{d-1} is an intersection of S^{d-1} with a 2-plane in \mathbb{R}^d containing the origin, so this moduli space is the same as the Grassmannian $\text{Gr}(2, \mathbb{R}^d)$. Hence, the zero mode integral is the volume of this Grassmannian:

$$\prod_{i=1}^{d-2} \int da_1^i db_1^i = \text{vol}(\text{Gr}(2, \mathbb{R}^d)) = \frac{\text{vol}(O(d))}{\text{vol}(O(2)) \times \text{vol}(O(d-2))} = \frac{\text{vol}(S^{d-1}) \times \text{vol}(S^{d-2})}{2\text{vol}(S^1)}. \quad (4.197)$$

We can finally explicitly calculate the path-integral over $y^i(\tau)$:

$$\begin{aligned} & \int Dy^i(\tau) \exp \left[-m_i \int_0^1 d\tau \left(\frac{\dot{y}^2}{4\pi} - \pi y^2 \right) \right] \\ &= \text{vol}(\text{Gr}(2, \mathbb{R}^d)) \prod_{i=1}^{d-2} \left[(\pm i) \sqrt{\frac{2}{m_i}} \times \prod_{n=1}^{\infty} \frac{2}{m_i} \prod_{n=1}^{\infty} \frac{1}{n^2 - 1} \right] \\ &= \frac{(\pm i)^{d-2} m_i^{d-2}}{\Gamma(d-1)}, \end{aligned} \quad (4.198)$$

where \prod_n' means we skip the mode $n = 1$. We computed the infinite product above using zeta function regularization [8]. In particular, the following formulas are useful for such computations:

$$\prod_{n=1}^{\infty} n = \sqrt{2\pi}, \quad \text{and} \quad \prod_{n=1}^{\infty} a = a^{-1/2} \quad (a > 0). \quad (4.199)$$

Putting everything together, we obtain (4.144).

- Worldline path integral on lens space

Three dimensional homogeneous lens space $L(q; 1)$ can be defined as the quotient of the three sphere $S^3 = \{(z_1, z_2) \in \mathbb{C}^2 \mid |z_1|^2 + |z_2|^2 = 1\}$ by the equivalence relation $(z_1, z_2) \sim (e^{2\pi i/q} z_1, e^{2\pi i/q} z_2)$. Geodesics in $L(q; 1)$ comes in two types: the contractable "long geodesics" with length 2π , and the non-contractable "short geodesics" with length $2\pi/q$. If $q \neq 2$, each short geodesic is an intersection of a complex line $\alpha z_1 + \beta z_2 = 0$ with S^3 , so the corresponding moduli space is $\text{Gr}(1, \mathbb{C}^2)$. When $q = 2$, every real two-plane $\alpha z_1 + \beta z_2 + \gamma \bar{z}_1 + \delta \bar{z}_2$ in \mathbb{R}^4 intersects S^3 at a short geodesic, so the corresponding moduli space is $\text{Gr}(2, \mathbb{R}^4)$.

To compute worldline instanton contributions to the lens space partition function, we choose the classical trajectory $\theta(\tau)$ to wind around a short geodesic and integrate over perpendicular fluctuations obeying a slightly different boundary condition:

$$\begin{pmatrix} y^1(1) \\ y^2(1) \end{pmatrix} = \begin{pmatrix} \cos(\frac{2\pi}{q}) & -\sin(\frac{2\pi}{q}) \\ \sin(\frac{2\pi}{q}) & \cos(\frac{2\pi}{q}) \end{pmatrix} \begin{pmatrix} y^1(0) \\ y^2(0) \end{pmatrix}. \quad (4.200)$$

Introducing the complex variable $z(\tau) = y^1(\tau) + iy^2(\tau)$, we have the following mode expansion:

$$z(\tau) = \sum_{n \in \mathbb{Z}} c_n e^{2\pi i(n+1/q)\tau}. \quad (4.201)$$

Plugging in $\theta(\tau) = \frac{2\pi\tau}{q}$, we find the worldline path integral

$$\begin{aligned} & \int Dz(\tau) \exp \left[-m_i \int_0^1 d\tau \sqrt{(1 - |z|^2) \left(\frac{d\theta}{d\tau} \right)^2 + \left| \frac{dz}{d\tau} \right|^2} \right] \\ &= e^{-\frac{2m_i\pi}{q}} \prod_{n \in \mathbb{Z}} \int dc_n d\bar{c}_n \exp \left[-m_i \pi (n^2 q + 2n) |c_n|^2 \right]. \end{aligned} \quad (4.202)$$

When $q \neq 2$, the only zero mode is $c_0 e^{(2\pi i/q)\tau}$. In this case, following the treatment of zero modes outlined above, we find

$$\prod_{n \in \mathbb{Z}} \int dc_n d\bar{c}_n \exp \left[-m_i \pi (n^2 q + 2n) |c_n|^2 \right] = \text{vol}(\text{Gr}(1, \mathbb{C}^2)) \prod_{n \in \mathbb{Z}_{\neq 0}} \frac{1}{m_i} \frac{1}{n (2 + nq)} = \frac{m_i}{2 \sin(\frac{2\pi}{q})}, \quad (4.203)$$

where we've used

$$\text{vol}(\text{Gr}(k, \mathbb{C}^d)) = \frac{\text{vol}(U(d))}{\text{vol}(U(k)) \times \text{vol}(U(d-k))} = \frac{\pi^{k(d-k)} G(k+1) G(d-k+1)}{G(d+1)}, \quad (4.204)$$

where $G(z)$ is the Barnes G-function.

When $q = 2$, there are two zero modes $c_0 e^{\pi i \tau}$ and $c_{-1} e^{-\pi i \tau}$. Thus,

$$\prod_{n \in \mathbb{Z}} \int dc_n d\bar{c}_n \exp \left[-m_i \pi (2n^2 + 2n) |c_n|^2 \right] = \int dc_0 d\bar{c}_0 dc_{-1} d\bar{c}_{-1} \prod_{n \in \mathbb{Z}_{\neq 0, -1}} \frac{1}{2m_i} \frac{1}{n (1+n)}. \quad (4.205)$$

The integral over zero mode coefficients c_0 and c_{-1} is not exactly the same as the volume of $\text{Gr}(2, \mathbb{R}^4)$: the correct local coordinates on $\text{Gr}(2, \mathbb{R}^4)$ should be the coefficient in front of $\cos(\pi\tau)$, $i \cos(\pi\tau) \sin(\pi\tau)$ and $i \sin(\pi\tau)$, therefore

$$d\text{Vol}(\text{Gr}(2, \mathbb{R}^4)) = 4 dc_0 d\bar{c}_0 dc_{-1} d\bar{c}_{-1}. \quad (4.206)$$

Combining zero modes with massive modes, we get

$$\prod_{n \in \mathbb{Z}} \int dc_n d\bar{c}_n \exp \left[-m_i \pi (2n^2 + 2n) |c_n|^2 \right] = \frac{m_i^2}{2}. \quad (4.207)$$

Notice that tachyonic modes never appeared in the computations above. This is consistent with the fact that short geodesics are non-contractable!

- World line contribution to spin-refined partition function in 4D

We would like to compute single-particle non-perturbative corrections for a spin-refined sphere partition function in 4D. As explained in Section 4.2, the corresponding EFT bundle is non-trivial. By winding around the fundamental cycle in $L(q; 1)$, one also advances by β along the thermal circle whose total length is $q\beta$. Thus, after Kaluza-Klein reduction, we have a flat connection on an $S^1_{q\beta}$ bundle over $L(q; 1)$ whose holonomy along a short geodesic is given by $\oint A = \beta$. The corresponding phase in the worldline action is thus $\exp(\frac{2\pi i q_i}{q\beta} \beta) = \exp(\frac{2\pi i q_i}{q})$. Since the connection is flat, the classical equations of motion will not be affected, and we can compute the "Nambu-Goto part" of the worldline path integral in exactly the same way as for the lens space partition function. Putting everything together, we arrive at (4.146).

A closer look at free field theory

In this subsection, we discuss non-perturbative corrections in free field partition functions. In particular, we will show that they indeed have the structure predicted in Section 4.9. Actually, thanks to the Fock space structure of the Hilbert space, we can easily predict the leading terms in all non-perturbative corrections to free theory partition functions using worldline instantons. The "free-theory upgraded predictions" in (4.211), (4.213), and (4.214) can also be checked explicitly, as we will do in Section 4.10.

In the language of Section 4.10, there is a worldline instanton correction for each Poincaré irrep in the $d-1$ dimensional massive theory on \mathbb{R}^{d-1} . In a free theory, the Hilbert space furthermore has the structure of a Fock space, so that for any symmetry generator g , we have

$$\text{Tr}_{\mathcal{H}}[g] = \sum_{n=1}^{\infty} \text{Tr}_{\mathcal{H}_n}[g] = \sum_{n=1}^{\infty} \text{Tr}_{\text{Sym}^n(\mathcal{H}_1)}[g] = \exp\left(\sum_{\ell=1}^{\infty} \frac{1}{\ell} \text{Tr}_{\mathcal{H}_1}[g^\ell]\right), \quad (4.208)$$

where \mathcal{H}_1 is the single-particle Hilbert space.

We can apply this result to a free massive theory on S^{d-1} as follows. Consider the sphere S^{d-1} in "angular" quantization, where we choose an angle $\phi \in [0, 2\pi)$ and slice the path integral on slices of constant ϕ . Each spatial slice is a $d-2$ -dimensional hemisphere, with some boundary conditions at the equator of the hemisphere. (Our arguments will be heuristic because we will be vague about the nature of these boundary conditions, see [4] for a recent discussion.) Let the

corresponding Hamiltonian be H . The sphere partition function is then

$$\text{Tr}_{\mathcal{H}}(e^{-2\pi H}) = \exp\left(\sum_{\ell=1}^{\infty} \frac{1}{\ell} \text{Tr}_{\mathcal{H}_1}[e^{-2\pi\ell H}]\right). \quad (4.209)$$

Each single-particle worldline instanton discussed in Section 4.10 computes the leading contribution to $\text{Tr}_{\mathcal{H}_1}[e^{-2\pi H}]$. To instead compute $\text{Tr}_{\mathcal{H}_1}[e^{-2\pi\ell H}]$, we should expand around a classical trajectory $\theta(\tau) = 2\pi\ell\tau$ that winds ℓ times around the great circle. Expanding the worldline path integral around this trajectory, we find:

$$\text{Tr}_{\mathcal{H}_1}[e^{-2\pi\ell H}] = \sum_m e^{-2\pi\ell m} \frac{(\pm i)^{(d-2)(2\ell-1)} m^{d-2}}{\Gamma(d-1)} \left(1 + O\left(\frac{1}{m}\right)\right). \quad (4.210)$$

For a free scalar CFT on $S^{d-1} \times S^1_\beta$, the single-particle states are KK modes, so that we expect

$$\log(Z_{\text{free}}[S^{d-1} \times S^1_\beta]) \sim \sum_m \sum_{\ell=1}^{\infty} \frac{1}{\ell} \text{Tr}_{\mathcal{H}_1} e^{-2\pi\ell H}, \quad (4.211)$$

where each $\text{Tr}_{\mathcal{H}_1} e^{-2\pi\ell H}$ is given by (4.210), and m runs over the spectrum of KK masses. Here, " \sim " means that the right-hand side displays the nonperturbative terms in the left-hand side.

We can derive similar results for a free massive theory on the lens space $L(q; 1)$. If we consider an instanton on the locus $|z_1| = 1$, wrapping ℓ times around the "short geodesic," then the lens space worldline path integral evaluates $\text{Tr}_{\mathcal{H}_1}[e^{-\frac{2\pi\ell}{q}H - \frac{2\pi\ell i}{q}J}]$, where J generates a rotation in the z_2 plane. Hence for the free scalar on $L(q; 1) \times S^1_\beta$, when q is odd:

$$\begin{aligned} \log(Z_{\text{free}}[L(q; 1) \times S^1_\beta]) &= \sum_m \sum_{\ell=1}^{\infty} \frac{1}{\ell} \text{Tr}_{\mathcal{H}_1}[e^{-\frac{2\pi\ell}{q}H - \frac{2\pi\ell i}{q}J}] \\ &= \sum_m \sum_{\ell=1}^{\infty} \frac{1}{q\ell} \text{Tr}_{\mathcal{H}_1}[e^{-2\pi\ell H}] + \sum_m \sum_{\ell \notin q\mathbb{Z}} \frac{1}{\ell} \text{Tr}_{\mathcal{H}_1}[e^{-\frac{2\pi\ell}{q}H - \frac{2\pi\ell i}{q}J}]. \end{aligned} \quad (4.212)$$

In the last line, we singled out terms where $\ell \in q\mathbb{Z}$. Up to a $1/q$ factor, the first sum is exactly the same as the nonperturbative terms in $\log(Z_{\text{free}}[S^{d-1} \times S^1_\beta])$. Indeed, since the short geodesic generates $\pi_1(L(q; 1)) \simeq \mathbb{Z}_q$, after winding around q times, the loop becomes contractable. Notice that each contractable long geodesic in $L(q; 1)$ will be lifted to q different geodesics in S^3 , so the moduli space of a long geodesic

in $L(q; 1)$ should have $1/q$ -th the volume of $\text{Gr}(2, \mathbb{R}^4)$ and this is the origin of the $1/q$ factor.

Combining everything, the leading order terms are

$$\log(Z_{\text{free}}[L(q; 1) \times S_\beta^1]) \sim \sum_m \left(-\frac{1}{q} \sum_{\ell=1}^{\infty} e^{-2\pi\ell m} \frac{m^2}{2\ell} + \sum_{\substack{\ell=1 \\ \ell \notin q\mathbb{Z}}}^{\infty} e^{-\frac{2\pi\ell m}{q}} \frac{m}{2\ell \sin(\frac{2\pi\ell}{q})} \right) \quad (\text{odd } q),$$

(4.213)

where " \sim " means we show nonperturbative corrections. Similarly when q is even, we find

$$\begin{aligned} & \log(Z_{\text{free}}[L(q; 1) \times S_\beta^1]) \\ & \sim \sum_m \left(-\frac{1}{q} \sum_{\ell=1}^{\infty} e^{-2\pi\ell m} \frac{m^2}{2\ell} + \sum_{\substack{\ell=1 \\ \ell \notin (q/2)\mathbb{Z}}}^{\infty} e^{-\frac{2\pi\ell m}{q}} \frac{m}{2\ell \sin(\frac{2\pi\ell}{q})} + \frac{1}{q} \sum_{\ell=1}^{\infty} e^{-\pi(2\ell-1)m} \frac{m^2}{2\ell-1} \right) \quad (\text{even } q). \end{aligned}$$

(4.214)

Partition function from functional determinants

In this section, we use the methods of [12] to compute the partition function of free scalar theories by explicitly summing over the Laplacian spectrum. We will find agreement with (4.211), (4.213), and (4.214). In particular, this will verify the general predictions of Section 4.10 for free theories.

Consider a massive scalar field on S^{d-1} with the action

$$S_{\text{free}} = \frac{1}{2} \int d^{d-1}x \sqrt{g} \left[g_{\mu\nu} \partial^\mu \phi \partial^\nu \phi + m^2 \phi^2 + \frac{1}{4} \frac{(d-2)}{(d-1)} R \phi^2 \right],$$

(4.215)

with $R = (d-1)(d-2)$. Here, we have chosen the curvature coupling $\frac{1}{2}\xi R\phi^2$ to have the form appropriate for a conformally-coupled scalar in d -dimensions, dimensionally reduced to $d-1$ dimensions. However, this coupling will not affect the leading form of nonperturbative corrections that are our main focus. The partition function is the functional determinant

$$Z_{\text{massive}}[S^{d-1}] = \det \left[\Delta + m^2 + \frac{(d-2)^2}{4} \right]^{-1/2},$$

(4.216)

where Δ is the Laplace operator on S^{d-1} , which has eigenvalues $\lambda_k = k(k+d-2)$ with degeneracies $d_k = \frac{(d-3+k)!(d-2+2k)}{k!(d-2)!}$. Let us focus on $d = 4$ and $d = 6$, i.e the sphere partition function of a massive theory on S^3 and S^5 .

Using zeta function regularization, we find

$$\log(Z_{\text{massive}}[S^3]) = \frac{\pi m^3}{6} - \sum_{\ell=1}^{\infty} \frac{e^{-2\pi\ell m}}{2\ell} \left(m^2 + \frac{m}{\pi\ell^2} + \frac{1}{2\pi^2\ell^3} \right), \quad (4.217)$$

$$\begin{aligned} \log(Z_{\text{massive}}[S^5]) = & -\frac{\pi}{120}m^5 - \frac{\pi}{72}m^3 + \sum_{\ell=1}^{\infty} \frac{e^{-2\pi\ell m}}{24\ell} \left(m^4 + \frac{2m^3}{\pi\ell} + m^2 \left(1 + \frac{3}{\pi^2\ell^2} \right) \right. \\ & \left. + m \left(\frac{1}{\pi\ell} + \frac{3}{\pi^2\ell^2} + \frac{3}{2\pi^4\ell^4} + \frac{1}{2\pi^2\ell^2} \right) \right). \end{aligned} \quad (4.218)$$

We now need to sum over the KK masses to obtain $Z_{\text{free}}[S^{d-1} \times S^1_{\beta}]$. Let us consider \mathbb{Z}_2 -twisted free scalar fields as an example, where the \mathbb{Z}_2 twist is introduced to remove a zero mode upon dimensional reduction. The KK mass spectrum is $m = |(2n-1)/\beta|$ for $n \in \mathbb{Z}$. Thus, the free energy in $d = 4$ and $d = 6$ is

$$\log(Z_{\text{free}}[S^3 \times S^1_{\beta}]) \sim - \sum_{n=1}^{\infty} \sum_{\ell=1}^{\infty} e^{-\frac{2\pi^2(2n-1)\ell}{\beta}} \frac{1}{\ell} \left(\frac{(2n-1)^2\pi^2}{\beta^2} + \frac{2n-1}{\beta\ell^2} + \frac{1}{2\pi^2\ell^3} \right), \quad (4.219)$$

$$\begin{aligned} \log(Z_{\text{free}}[S^5 \times S^1_{\beta}]) \sim & \sum_{n=1}^{\infty} \sum_{\ell=1}^{\infty} \frac{e^{-2\pi^2(2n-1)\ell/\beta}}{12\ell} \left(\frac{\pi^4(2n-1)^4}{\beta^4} + \frac{2\pi^2(2n-1)^3}{\ell\beta^3} \right. \\ & \left. + \frac{\pi^2(2n-1)^2}{\beta^2} \left(1 + \frac{3}{\pi^2\ell^2} \right) + \frac{\pi(2n-1)}{\beta} \left(\frac{1}{\pi\ell} + \frac{3}{\pi^2\ell^2} + \frac{3}{2\pi^4\ell^4} + \frac{1}{2\pi^2\ell^2} \right) \right), \end{aligned} \quad (4.220)$$

where " \sim " means we only show non-perturbative corrections. These results are in agreement with the general form (4.211) predicted from worldline instantons, together with the Fock-space structure of the free theory.

The same approach can be generalized to compute a lens space partition function in 4D. We display the result here for a more direct comparison with the twisted partition function:

$$\begin{aligned} \log(Z_{\text{massive}}[L(q; 1)]) = & \frac{\pi m^3}{6q} - \frac{1}{q} \sum_{\ell=1}^{\infty} \frac{e^{-2\pi\ell m}}{2\ell} \left(m^2 + \frac{m}{\pi\ell} + \frac{1}{2\pi^2\ell^2} \right) \\ & + \sum_{\substack{\ell=1 \\ \ell \notin q\mathbb{Z}}}^{\infty} \frac{e^{-\frac{2\pi\ell m}{q}}}{\sin\left(\frac{2\pi\ell}{q}\right)} \left(\frac{m}{2\ell} + \frac{q}{4\pi\ell^2} \right) \quad (q \in 2\mathbb{Z} + 1), \end{aligned} \quad (4.221)$$

$$\begin{aligned}
\log(Z_{\text{massive}}[L(q; 1)]) = & \frac{\pi m^3}{6q} - \frac{1}{q} \sum_{\ell}^{\infty} \frac{e^{-2\pi\ell m}}{2\ell} \left(m^2 + \frac{m}{\pi\ell} + \frac{1}{2\pi^2\ell^2} \right) \\
& + \frac{1}{q} \sum_{\ell}^{\infty} \frac{e^{-\pi(2\ell-1)m}}{2\ell-1} \left(m^2 + \frac{2m}{\pi(2\ell-1)} + \frac{2}{\pi^2(2\ell-1)^2} \right) \\
& + \sum_{\substack{\ell=1 \\ \ell \notin \frac{q}{2}\mathbb{Z}}}^{\infty} \frac{e^{-\frac{2\pi\ell m}{q}}}{\sin\left(\frac{2\pi\ell}{q}\right)} \left(\frac{m}{2\ell} + \frac{q}{4\pi\ell^2} \right) \quad (q \in 2\mathbb{Z}). \quad (4.222)
\end{aligned}$$

In Appendix 4.10, we computed the high temperature expansion of a free scalar twisted by $e^{-\frac{2\pi i}{q}J_{12}-\frac{2\pi i}{q}J_{34}}$. Restricting to odd q and inserting a \mathbb{Z}_2 twist to remove the zero mode, we find

$$\begin{aligned}
& \log \left(\text{Tr} \left[e^{-\beta H - \frac{2\pi i}{q}J_{12} - \frac{2\pi i}{q}J_{34}} (-1)^N \right] \right) \\
& \sim - \sum_{n=1}^{\infty} \sum_{\ell=1}^{\infty} e^{-\frac{2\ell(2n-1)\pi^2}{q\beta}} \left(\frac{(2n-1)^2\pi^2}{\ell q^3\beta^2} + \frac{2n-1}{\beta\ell^2q^2} + \frac{1}{2\ell^3q\pi^2} \right) \\
& \quad + \sum_{\substack{\ell=1 \\ \ell \notin q\mathbb{Z}}}^{\infty} \sum_{n=0}^{\infty} \frac{\cos\left(\frac{2\pi\ell}{q}\left(\frac{q-1}{2}-n\right)\right)}{\sin\left(\frac{2\pi\ell}{q}\right)} e^{-\frac{2\ell(2n+1)\pi^2}{q^2\beta}} \left(\frac{(2n+1)\pi}{\ell q\beta} + \frac{q}{2\ell^2\pi} \right), \quad (4.223)
\end{aligned}$$

where " \sim " means we only show non-perturbative corrections and N is the ϕ -number operator, so that $(-1)^N$ implements the \mathbb{Z}_2 twist. Note that this is not quite identical to the lens space partition function (4.221) summed over the mass spectrum $m = \frac{|2n+1|\pi}{q\beta}$. To obtain the twisted partition function (4.223), we must additionally modify the lens space result to account for the nontrivial background gauge field. To do so, we multiply each term in the summation over short geodesics by a phase $\exp\left(\frac{2\pi i\ell q_i}{q}\right)$. For a \mathbb{Z}_2 twisted free scalar field, the KK charge spectrum is $q = n + \frac{1}{2} + \frac{q}{2}$. After putting in all the phases, we recover (4.223). Finally, note that this result is consistent with the general prediction (4.146) from worldline instantons.

Free theories in odd dimension

The examples presented in Section 4.10 were all in even d . In odd d , we face the puzzle that the contribution of a worldline instanton (4.144) is imaginary (even when the partition function should be real), and furthermore its phase depends on how we choose the integration contours for tachyonic modes. The proper interpretation of these kinds of contributions is explained for example in [79]. They can be understood as characterizing singularities in the Borel plane when computing the partition function via Borel resummation.

In this appendix, we provide a quick summary of the discussion from [79] in the example of a massive free scalar on S^2 . (We can think of this theory as the contribution of a single KK mode to the partition function of the 3D free scalar on $S^2 \times S_\beta^1$.) We can compute the partition function in terms of the heat trace, following Appendix 4.10. The heat trace on S^2 is

$$\begin{aligned} \text{Tr} \left[e^{-t(\Delta + (\frac{d-2}{2})^2)} \right] &= \sum_{k=0}^{\infty} (2k+1) e^{-t(k+\frac{1}{2})^2} = \sum_{k \in \mathbb{Z}} |k + \frac{1}{2}| e^{-t(k+\frac{1}{2})^2} \\ &= \sum_{\ell \in \mathbb{Z}} \left(\frac{1}{t} - \frac{2\pi\ell}{t^{3/2}} F \left(\frac{\pi\ell}{\sqrt{t}} \right) \right), \end{aligned} \quad (4.224)$$

where $F(z)$ is Dawson's function which admits the following asymptotic expansion near $z = \infty$:

$$F(z) \sim \sum_{n=0}^{\infty} \frac{(2n-1)!!}{2^{n+1}} \left(\frac{1}{z} \right)^{2n+1}. \quad (4.225)$$

The heat trace therefore has the following expansion near $t = 0$:

$$\text{Tr} \left[e^{-t(\Delta + (\frac{d-2}{2})^2)} \right] \sim \sum_{n=0}^{\infty} a_n t^{n-1}, \quad a_n = \frac{(-1)^{n+1} (1 - 2^{1-2n})}{n!} B_{2n}, \quad (4.226)$$

where B_{2n} are the Bernoulli numbers.

Let us now perform a Borel resummation of the series $\Phi \equiv \sum_{n=0}^{\infty} a_n t^n$:

$$\mathcal{S}[\Phi](t) = \frac{2}{\sqrt{t}} \int_0^\infty d\zeta e^{-\zeta^2/t} \mathcal{B}\Phi(\zeta), \quad (4.227)$$

where the Borel transformed series $\mathcal{B}\Phi(\zeta)$ is

$$\mathcal{B}\Phi(\zeta) = \sum_{n=0}^{\infty} \frac{a_n}{\Gamma(n + \frac{1}{2})} \zeta^{2n} = \frac{1}{\sqrt{\pi}} \frac{\zeta}{\sin(\zeta)}. \quad (4.228)$$

With this expression for $\mathcal{B}\Phi$, the integral in (4.227) is apparently ill-defined since there are poles located at $\zeta = \ell\pi$, $\ell \in \mathbb{Z}$ on the positive real axis. A contour prescription is needed to define the integral.

One natural option is to deform the integration contour to pass over (we will refer to the corresponding contour as C_+) or under (we will refer to the corresponding contour as C_-) the poles. However, these two choices are not equivalent. Their difference is the sum of residues at the poles:

$$\frac{2}{\sqrt{t}} \int_{C_+ - C_-} d\zeta e^{-\zeta^2/t} \mathcal{B}\Phi(\zeta) = 2it \left(\frac{\pi}{t} \right)^{3/2} \sum_{\ell \neq 0} (-1)^{\ell+1} |\ell| e^{-\ell^2 \pi^2/t}. \quad (4.229)$$

The ambiguity in integration contour leads to an ambiguity in the Borel-resummed heat trace:

$$\text{Tr} \left[e^{-t(\Delta + (\frac{d-2}{2})^2)} \right] = \frac{2}{\sqrt{\pi} t^{3/2}} \int_{C_\pm} d\zeta \frac{\zeta e^{-\zeta^2/t}}{\sin \zeta} + 2i \left(\frac{\pi}{t} \right)^{3/2} \sum_{\ell \neq 0} \sigma_\ell^\pm (-1)^{\ell+1} |\ell| e^{-\frac{\ell^2 \pi^2}{t}}, \quad (4.230)$$

where σ_ℓ^\pm are arbitrary coefficients which jump as we switch from C_+ to C_- . If we require the heat trace to be real when $t \in \mathbb{R}_+$, then the σ_ℓ^\pm are fixed to be $\pm \frac{1}{2}$. This is equivalent to a principal value prescription for the Borel integral:

$$\text{Tr} \left[e^{-t(\Delta + (\frac{d-2}{2})^2)} \right] = \frac{2}{\sqrt{\pi} t^{3/2}} \int_0^\infty d\zeta \mathcal{P} \left[\frac{\zeta e^{-\zeta^2/t}}{\sin \zeta} \right]. \quad (4.231)$$

To compute $\log Z$, we must supply a factor of e^{-tm^2} and integrate $\int dt/t$. If we start with (4.231), we get a valid integral representation for the partition function. However, if we start with (4.230) and perform the t -integral term by term, we obtain the series of nonperturbative corrections

$$\log(Z_{\text{free}}[S^2]) \Big|_{\text{non-perturbative}} = \pm i \sum_{\ell=1}^{\infty} \frac{(-1)^\ell e^{-2\pi m\ell}}{\ell} \left(m + \frac{1}{2\pi\ell} \right), \quad (4.232)$$

whose leading terms in m agree precisely with the worldline instanton predictions (4.210) and (4.211) when $d = 3$.

To summarize, worldline instantons encode residues of certain singularities in the Borel plane. We conjecture that this remains true in interacting theories. In general, the thermal effective action gives an asymptotic expansion in β . When we Borel-resum this expansion, we encounter singularities in the Borel plane coming from worldline instantons (together with other nonperturbative effects like instanton graphs).

BIBLIOGRAPHY

- [1] Larry F Abbott and Stanley Deser. “Stability of gravity with a cosmological constant”. In: *Nuclear Physics B* 195.1 (1982), pp. 76–96.
- [2] Allan Adams et al. “Causality, analyticity and an IR obstruction to UV completion”. In: *JHEP* 0610 (2006), p. 014. doi: [10.1088/1126-6708/2006/10/014](https://doi.org/10.1088/1126-6708/2006/10/014). arXiv: [hep-th/0602178](https://arxiv.org/abs/hep-th/0602178) [hep-th].
- [3] Nima Afkhami-Jeddi et al. “Einstein gravity 3-point functions from conformal field theory”. In: *JHEP* 12 (2017), p. 049. doi: [10.1007/JHEP12\(2017\)049](https://doi.org/10.1007/JHEP12(2017)049). arXiv: [1610.09378](https://arxiv.org/abs/1610.09378) [hep-th].
- [4] Nicholas Agia and Daniel L. Jafferis. “Angular Quantization in CFT”. In: (Apr. 2022). arXiv: [2204.11872](https://arxiv.org/abs/2204.11872) [hep-th].
- [5] Luis F. Alday and Jin-Beom Bae. “Rademacher Expansions and the Spectrum of 2d CFT”. In: *JHEP* 11 (2020), p. 134. doi: [10.1007/JHEP11\(2020\)134](https://doi.org/10.1007/JHEP11(2020)134). arXiv: [2001.00022](https://arxiv.org/abs/2001.00022) [hep-th].
- [6] Luis F. Alday and Juan Martin Maldacena. “Comments on operators with large spin”. In: *JHEP* 11 (2007), p. 019. doi: [10.1088/1126-6708/2007/11/019](https://doi.org/10.1088/1126-6708/2007/11/019). arXiv: [0708.0672](https://arxiv.org/abs/0708.0672) [hep-th].
- [7] Kurosh Allameh and Edgar Shaghoulian. “Modular invariance and thermal effective field theory in CFT”. In: (Feb. 2024). arXiv: [2402.13337](https://arxiv.org/abs/2402.13337) [hep-th].
- [8] Jean-Paul Allouche. “Zeta-regularization of arithmetic sequences”. In: *European Physical Journal Web of Conferences*. Vol. 244. European Physical Journal Web of Conferences. Jan. 2020, 01008, p. 01008. doi: [10.1051/epjconf/202024401008](https://doi.org/10.1051/epjconf/202024401008).
- [9] Tarek Anous et al. “OPE statistics from higher-point crossing”. In: *JHEP* 06 (2022), p. 102. doi: [10.1007/JHEP06\(2022\)102](https://doi.org/10.1007/JHEP06(2022)102). arXiv: [2112.09143](https://arxiv.org/abs/2112.09143) [hep-th].
- [10] Arash Arabi Ardehali and Sameer Murthy. “The 4d superconformal index near roots of unity and 3d Chern-Simons theory”. In: *JHEP* 10 (2021), p. 207. doi: [10.1007/JHEP10\(2021\)207](https://doi.org/10.1007/JHEP10(2021)207). arXiv: [2104.02051](https://arxiv.org/abs/2104.02051) [hep-th].
- [11] Richard Arnowitt, Stanley Deser, and Charles W Misner. “Dynamical structure and definition of energy in general relativity”. In: *Physical Review* 116.5 (1959), p. 1322.
- [12] M. Asorey et al. “Thermodynamics of conformal fields in topologically non-trivial space-time backgrounds”. In: *JHEP* 04 (2013), p. 068. doi: [10.1007/JHEP04\(2013\)068](https://doi.org/10.1007/JHEP04(2013)068). arXiv: [1212.6220](https://arxiv.org/abs/1212.6220) [hep-th].

- [13] Benjamin Assel et al. “The Casimir Energy in Curved Space and its Supersymmetric Counterpart”. In: *JHEP* 07 (2015), p. 043. doi: [10.1007/JHEP07\(2015\)043](https://doi.org/10.1007/JHEP07(2015)043). arXiv: [1503.05537](https://arxiv.org/abs/1503.05537) [hep-th].
- [14] Nabamita Banerjee et al. “Constraints on Fluid Dynamics from Equilibrium Partition Functions”. In: *JHEP* 09 (2012), p. 046. doi: [10.1007/JHEP09\(2012\)046](https://doi.org/10.1007/JHEP09(2012)046). arXiv: [1203.3544](https://arxiv.org/abs/1203.3544) [hep-th].
- [15] F. Bastianelli, S. Frolov, and Arkady A. Tseytlin. “Conformal anomaly of (2,0) tensor multiplet in six-dimensions and AdS / CFT correspondence”. In: *JHEP* 02 (2000), p. 013. doi: [10.1088/1126-6708/2000/02/013](https://doi.org/10.1088/1126-6708/2000/02/013). arXiv: [hep-th/0001041](https://arxiv.org/abs/hep-th/0001041).
- [16] Fiorenzo Bastianelli and Peter van Nieuwenhuizen. “Path integrals for quantum mechanics in curved space”. In: *Path Integrals and Anomalies in Curved Space*. Cambridge Monographs on Mathematical Physics. Cambridge University Press, 2006, pp. 1–2.
- [17] Alexandre Belin, Jan de Boer, and Diego Liska. “Non-Gaussianities in the statistical distribution of heavy OPE coefficients and wormholes”. In: *JHEP* 06 (2022), p. 116. doi: [10.1007/JHEP06\(2022\)116](https://doi.org/10.1007/JHEP06(2022)116). arXiv: [2110.14649](https://arxiv.org/abs/2110.14649) [hep-th].
- [18] Alexandre Belin, Jan De Boer, and Jorrit Kruthoff. “Comments on a state-operator correspondence for the torus”. In: *SciPost Phys.* 5.6 (2018), p. 060. doi: [10.21468/SciPostPhys.5.6.060](https://doi.org/10.21468/SciPostPhys.5.6.060). arXiv: [1802.00006](https://arxiv.org/abs/1802.00006) [hep-th].
- [19] Alexandre Belin, Diego M. Hofman, and Gregoire Mathys. “Einstein gravity from ANEC correlators”. In: (2019). arXiv: [1904.05892](https://arxiv.org/abs/1904.05892) [hep-th].
- [20] Alexandre Belin et al. “Generalized spectral form factors and the statistics of heavy operators”. In: *JHEP* 11 (2022), p. 145. doi: [10.1007/JHEP11\(2022\)145](https://doi.org/10.1007/JHEP11(2022)145). arXiv: [2111.06373](https://arxiv.org/abs/2111.06373) [hep-th].
- [21] Alexandre Belin et al. “Universality of sparse $d > 2$ conformal field theory at large N ”. In: *JHEP* 03 (2017), p. 067. doi: [10.1007/JHEP03\(2017\)067](https://doi.org/10.1007/JHEP03(2017)067). arXiv: [1610.06186](https://arxiv.org/abs/1610.06186) [hep-th].
- [22] Francesco Benini and Stefano Cremonesi. “Partition Functions of $\mathcal{N} = (2, 2)$ Gauge Theories on S^2 and Vortices”. In: *Commun. Math. Phys.* 334.3 (2015), pp. 1483–1527. doi: [10.1007/s00220-014-2112-z](https://doi.org/10.1007/s00220-014-2112-z). arXiv: [1206.2356](https://arxiv.org/abs/1206.2356) [hep-th].
- [23] Nathan Benjamin and Ying-Hsuan Lin. “Lessons from the Ramond sector”. In: *SciPost Phys.* 9.5 (2020), p. 065. doi: [10.21468/SciPostPhys.9.5.065](https://doi.org/10.21468/SciPostPhys.9.5.065). arXiv: [2005.02394](https://arxiv.org/abs/2005.02394) [hep-th].
- [24] Nathan Benjamin et al. “Light-cone modular bootstrap and pure gravity”. In: *Phys. Rev. D* 100.6 (2019), p. 066029. doi: [10.1103/PhysRevD.100.066029](https://doi.org/10.1103/PhysRevD.100.066029). arXiv: [1906.04184](https://arxiv.org/abs/1906.04184) [hep-th].

- [25] Nathan Benjamin et al. “Universal asymptotics for high energy CFT data”. In: *JHEP* 03 (2024), p. 115. doi: [10.1007/JHEP03\(2024\)115](https://doi.org/10.1007/JHEP03(2024)115). arXiv: [2306.08031](https://arxiv.org/abs/2306.08031) [hep-th].
- [26] Sayantani Bhattacharyya. “Entropy current and equilibrium partition function in fluid dynamics”. In: *JHEP* 08 (2014), p. 165. doi: [10.1007/JHEP08\(2014\)165](https://doi.org/10.1007/JHEP08(2014)165). arXiv: [1312.0220](https://arxiv.org/abs/1312.0220) [hep-th].
- [27] Sayantani Bhattacharyya et al. “Large rotating AdS black holes from fluid mechanics”. In: *JHEP* 09 (2008), p. 054. doi: [10.1088/1126-6708/2008/09/054](https://doi.org/10.1088/1126-6708/2008/09/054). arXiv: [0708.1770](https://arxiv.org/abs/0708.1770) [hep-th].
- [28] Jeff Bjaraker and Yutaka Hosotani. “Monopoles, dyons and black holes in the four-dimensional Einstein-Yang-Mills theory”. In: *Phys. Rev. D* 62 (2000), p. 043513. doi: [10.1103/PhysRevD.62.043513](https://doi.org/10.1103/PhysRevD.62.043513). arXiv: [hep-th/0002098](https://arxiv.org/abs/hep-th/0002098).
- [29] Jefferson Bjaraker and Yutaka Hosotani. “Stable monopole and dyon solutions in the Einstein-Yang-Mills theory in asymptotically Anti-de Sitter space”. In: *Phys. Rev. Lett.* 84 (2000), p. 1853. doi: [10.1103/PhysRevLett.84.1853](https://doi.org/10.1103/PhysRevLett.84.1853). arXiv: [gr-qc/9906091](https://arxiv.org/abs/gr-qc/9906091).
- [30] Matthias Blau and George Thompson. “Quantum Yang-Mills theory on arbitrary surfaces”. In: *Int. J. Mod. Phys. A* 7 (1992), pp. 3781–3806. doi: [10.1142/S0217751X9200168X](https://doi.org/10.1142/S0217751X9200168X).
- [31] Nikolay Bobev, Junho Hong, and Valentin Reys. “Holographic thermal observables and M2-branes”. In: *JHEP* 12 (2023), p. 054. doi: [10.1007/JHEP12\(2023\)054](https://doi.org/10.1007/JHEP12(2023)054). arXiv: [2309.06469](https://arxiv.org/abs/2309.06469) [hep-th].
- [32] Jan de Boer et al. “Black hole bound states in AdS(3) x S**2”. In: *JHEP* 11 (2008), p. 050. doi: [10.1088/1126-6708/2008/11/050](https://doi.org/10.1088/1126-6708/2008/11/050). arXiv: [0802.2257](https://arxiv.org/abs/0802.2257) [hep-th].
- [33] L Bonora, P Pasti, and M Bregola. “Weyl cocycles”. In: *Classical and Quantum Gravity* 3.4 (1986), p. 635. doi: [10.1088/0264-9381/3/4/018](https://doi.org/10.1088/0264-9381/3/4/018). URL: <https://dx.doi.org/10.1088/0264-9381/3/4/018>.
- [34] Nicolas Boulanger. “General solutions of the Wess-Zumino consistency condition for the Weyl anomalies”. In: *JHEP* 07 (2007), p. 069. doi: [10.1088/1126-6708/2007/07/069](https://doi.org/10.1088/1126-6708/2007/07/069). arXiv: [0704.2472](https://arxiv.org/abs/0704.2472) [hep-th].
- [35] Tomas Brauner et al. “Snowmass White Paper: Effective Field Theories for Condensed Matter Systems”. In: *Snowmass 2021*. Mar. 2022. arXiv: [2203.10110](https://arxiv.org/abs/2203.10110) [hep-th].
- [36] Enrico M. Brehm, Diptarka Das, and Shouvik Datta. “Probing thermality beyond the diagonal”. In: *Phys. Rev. D* 98.12 (2018), p. 126015. doi: [10.1103/PhysRevD.98.126015](https://doi.org/10.1103/PhysRevD.98.126015). arXiv: [1804.07924](https://arxiv.org/abs/1804.07924) [hep-th].

- [37] Tara Brendle, Nathan Broaddus, and Andrew Putman. “The mapping class group of connect sums of $S^2 \times S^1$ ”. In: *Trans. Amer. Math. Soc.* 376 (2023), pp. 2557–2572. doi: [10.1090/tran/8758](https://doi.org/10.1090/tran/8758). arXiv: [2012.01529](https://arxiv.org/abs/2012.01529) [math.GT].
- [38] J. David Brown and M. Henneaux. “Central Charges in the Canonical Realization of Asymptotic Symmetries: An Example from Three-Dimensional Gravity”. In: *Commun. Math. Phys.* 104 (1986), pp. 207–226. doi: [10.1007/BF01211590](https://doi.org/10.1007/BF01211590).
- [39] Joao Caetano, Shota Komatsu, and Yifan Wang. “Large charge ’t Hooft limit of $\mathcal{N} = 4$ super-Yang-Mills”. In: *JHEP* 02 (2024), p. 047. doi: [10.1007/JHEP02\(2024\)047](https://doi.org/10.1007/JHEP02(2024)047). arXiv: [2306.00929](https://arxiv.org/abs/2306.00929) [hep-th].
- [40] Roberto Camporesi and Atsushi Higuchi. “On the eigenfunctions of the Dirac operator on spheres and real hyperbolic spaces”. In: *J. Geom. Phys.* 20 (1996), pp. 1–18. doi: [10.1016/0393-0440\(95\)00042-9](https://doi.org/10.1016/0393-0440(95)00042-9). arXiv: [gr-qc/9505009](https://arxiv.org/abs/gr-qc/9505009).
- [41] P. Candelas and J. S. Dowker. “Field theories on conformally related space-times: Some global considerations”. In: *Phys. Rev. D* 19 (1979), p. 2902. doi: [10.1103/PhysRevD.19.2902](https://doi.org/10.1103/PhysRevD.19.2902).
- [42] Weiguang Cao, Tom Melia, and Sridip Pal. “Universal fine grained asymptotics of weakly coupled Quantum Field Theory”. In: (Nov. 2021). arXiv: [2111.04725](https://arxiv.org/abs/2111.04725) [hep-th].
- [43] Vitor Cardoso and Oscar J. C. Dias. “Small Kerr-anti-de Sitter black holes are unstable”. In: *Phys. Rev. D* 70 (2004), p. 084011. doi: [10.1103/PhysRevD.70.084011](https://doi.org/10.1103/PhysRevD.70.084011). arXiv: [hep-th/0405006](https://arxiv.org/abs/hep-th/0405006).
- [44] John Cardy, Alexander Maloney, and Henry Maxfield. “A new handle on three-point coefficients: OPE asymptotics from genus two modular invariance”. In: *JHEP* 10 (2017), p. 136. doi: [10.1007/JHEP10\(2017\)136](https://doi.org/10.1007/JHEP10(2017)136). arXiv: [1705.05855](https://arxiv.org/abs/1705.05855) [hep-th].
- [45] John L. Cardy. “Operator content and modular properties of higher dimensional conformal field theories”. In: *Nucl. Phys. B* 366 (1991), pp. 403–419. doi: [10.1016/0550-3213\(91\)90024-R](https://doi.org/10.1016/0550-3213(91)90024-R).
- [46] John L. Cardy. “Operator Content of Two-Dimensional Conformally Invariant Theories”. In: *Nucl. Phys. B* 270 (1986), pp. 186–204. doi: [10.1016/0550-3213\(86\)90552-3](https://doi.org/10.1016/0550-3213(86)90552-3).
- [47] Steven Carlip. “Logarithmic corrections to black hole entropy from the Cardy formula”. In: *Class. Quant. Grav.* 17 (2000), pp. 4175–4186. doi: [10.1088/0264-9381/17/20/302](https://doi.org/10.1088/0264-9381/17/20/302). arXiv: [gr-qc/0005017](https://arxiv.org/abs/gr-qc/0005017).
- [48] Simon Caron-Huot. “Analyticity in Spin in Conformal Theories”. In: *JHEP* 09 (2017), p. 078. doi: [10.1007/JHEP09\(2017\)078](https://doi.org/10.1007/JHEP09(2017)078). arXiv: [1703.00278](https://arxiv.org/abs/1703.00278) [hep-th].

- [49] Simon Caron-Huot. “Holographic cameras: an eye for the bulk”. In: *JHEP* 03 (2023), p. 047. doi: [10.1007/JHEP03\(2023\)047](https://doi.org/10.1007/JHEP03(2023)047). arXiv: [2211.11791](https://arxiv.org/abs/2211.11791) [hep-th].
- [50] Simon Caron-Huot and Vincent Van Duong. “Extremal Effective Field Theories”. In: *JHEP* 05 (2021), p. 280. doi: [10.1007/JHEP05\(2021\)280](https://doi.org/10.1007/JHEP05(2021)280). arXiv: [2011.02957](https://arxiv.org/abs/2011.02957) [hep-th].
- [51] Simon Caron-Huot et al. “AdS bulk locality from sharp CFT bounds”. In: *JHEP* 11 (2021), p. 164. doi: [10.1007/JHEP11\(2021\)164](https://doi.org/10.1007/JHEP11(2021)164). arXiv: [2106.10274](https://arxiv.org/abs/2106.10274) [hep-th].
- [52] Simon Caron-Huot et al. “Sharp boundaries for the swampland”. In: *JHEP* 07 (2021), p. 110. doi: [10.1007/JHEP07\(2021\)110](https://doi.org/10.1007/JHEP07(2021)110). arXiv: [2102.08951](https://arxiv.org/abs/2102.08951) [hep-th].
- [53] Horacio Casini et al. “Entanglement entropy and superselection sectors. Part I. Global symmetries”. In: *JHEP* 02 (2020), p. 014. arXiv: [1905.10487](https://arxiv.org/abs/1905.10487) [hep-th].
- [54] Horacio Casini et al. “Entropic order parameters for the phases of QFT”. In: *JHEP* 04 (2021), p. 277. doi: [10.1007/JHEP04\(2021\)277](https://doi.org/10.1007/JHEP04(2021)277). arXiv: [2008.11748](https://arxiv.org/abs/2008.11748) [hep-th].
- [55] Noam Chai et al. “Thermal Order in Conformal Theories”. In: *Phys. Rev. D* 102.6 (2020), p. 065014. doi: [10.1103/PhysRevD.102.065014](https://doi.org/10.1103/PhysRevD.102.065014). arXiv: [2005.03676](https://arxiv.org/abs/2005.03676) [hep-th].
- [56] Andrew Chamblin et al. “Charged AdS black holes and catastrophic holography”. In: *Phys. Rev. D* 60 (1999), p. 064018. doi: [10.1103/PhysRevD.60.064018](https://doi.org/10.1103/PhysRevD.60.064018). arXiv: [hep-th/9902170](https://arxiv.org/abs/hep-th/9902170).
- [57] Andrew Chamblin et al. “Holography, thermodynamics and fluctuations of charged AdS black holes”. In: *Phys. Rev. D* 60 (1999), p. 104026. doi: [10.1103/PhysRevD.60.104026](https://doi.org/10.1103/PhysRevD.60.104026). arXiv: [hep-th/9904197](https://arxiv.org/abs/hep-th/9904197).
- [58] Jeevan Chandra et al. “Semiclassical 3D gravity as an average of large-c CFTs”. In: *JHEP* 12 (2022), p. 069. doi: [10.1007/JHEP12\(2022\)069](https://doi.org/10.1007/JHEP12(2022)069). arXiv: [2203.06511](https://arxiv.org/abs/2203.06511) [hep-th].
- [59] Chi-Ming Chang et al. “Proving the 6d Cardy Formula and Matching Global Gravitational Anomalies”. In: *SciPost Phys.* 11.2 (2021), p. 036. doi: [10.21468/SciPostPhys.11.2.036](https://doi.org/10.21468/SciPostPhys.11.2.036). arXiv: [1910.10151](https://arxiv.org/abs/1910.10151) [hep-th].
- [60] Cyuan-Han Chang et al. “Bootstrapping the 3d Ising stress tensor”. In: *JHEP* 03 (2025), p. 136. doi: [10.1007/JHEP03\(2025\)136](https://doi.org/10.1007/JHEP03(2025)136). arXiv: [2411.15300](https://arxiv.org/abs/2411.15300) [hep-th].
- [61] Peter Chang and J. S. Dowker. “Vacuum energy on orbifold factors of spheres”. In: *Nucl. Phys. B* 395 (1993), pp. 407–432. doi: [10.1016/0550-3213\(93\)90223-C](https://doi.org/10.1016/0550-3213(93)90223-C). arXiv: [hep-th/9210013](https://arxiv.org/abs/hep-th/9210013).

- [62] Yiming Chen and Gustavo J. Turiaci. “Spin-statistics for black hole microstates”. In: *JHEP* 04 (2024), p. 135. doi: [10.1007/JHEP04\(2024\)135](https://doi.org/10.1007/JHEP04(2024)135). arXiv: [2309.03478](https://arxiv.org/abs/2309.03478) [hep-th].
- [63] Shai M. Chester et al. “Carving out OPE space and precise $O(2)$ model critical exponents”. In: *JHEP* 06 (2020), p. 142. doi: [10.1007/JHEP06\(2020\)142](https://doi.org/10.1007/JHEP06(2020)142). arXiv: [1912.03324](https://arxiv.org/abs/1912.03324) [hep-th].
- [64] Minjae Cho, Scott Collier, and Xi Yin. “Genus Two Modular Bootstrap”. In: *JHEP* 04 (2019), p. 022. doi: [10.1007/JHEP04\(2019\)022](https://doi.org/10.1007/JHEP04(2019)022). arXiv: [1705.05865](https://arxiv.org/abs/1705.05865) [hep-th].
- [65] Cyril Closset, Heeyeon Kim, and Brian Willett. “Seifert fiberings operators in 3d $\mathcal{N} = 2$ theories”. In: *JHEP* 11 (2018), p. 004. doi: [10.1007/JHEP11\(2018\)004](https://doi.org/10.1007/JHEP11(2018)004). arXiv: [1807.02328](https://arxiv.org/abs/1807.02328) [hep-th].
- [66] Sidney R. Coleman, John Preskill, and Frank Wilczek. “Quantum hair on black holes”. In: *Nucl. Phys. B* 378 (1992), pp. 175–246. doi: [10.1016/0550-3213\(92\)90008-Y](https://doi.org/10.1016/0550-3213(92)90008-Y). arXiv: [hep-th/9201059](https://arxiv.org/abs/hep-th/9201059).
- [67] Scott Collier et al. “Universal dynamics of heavy operators in CFT_2 ”. In: *JHEP* 07 (2020), p. 074. doi: [10.1007/JHEP07\(2020\)074](https://doi.org/10.1007/JHEP07(2020)074). arXiv: [1912.00222](https://arxiv.org/abs/1912.00222) [hep-th].
- [68] Miguel S. Costa and Tobias Hansen. “Conformal correlators of mixed-symmetry tensors”. In: *JHEP* 02 (2015), p. 151. doi: [10.1007/JHEP02\(2015\)151](https://doi.org/10.1007/JHEP02(2015)151). arXiv: [1411.7351](https://arxiv.org/abs/1411.7351) [hep-th].
- [69] Miguel S. Costa et al. “Spinning Conformal Correlators”. In: *JHEP* 11 (2011), p. 071. doi: [10.1007/JHEP11\(2011\)071](https://doi.org/10.1007/JHEP11(2011)071). arXiv: [1107.3554](https://arxiv.org/abs/1107.3554) [hep-th].
- [70] Paolo Creminelli, Oliver Janssen, and Leonardo Senatore. “Positivity bounds on effective field theories with spontaneously broken Lorentz invariance”. In: *JHEP* 09 (2022), p. 201. doi: [10.1007/JHEP09\(2022\)201](https://doi.org/10.1007/JHEP09(2022)201). arXiv: [2207.14224](https://arxiv.org/abs/2207.14224) [hep-th].
- [71] Michael Crossley, Paolo Glorioso, and Hong Liu. “Effective field theory of dissipative fluids”. In: *JHEP* 09 (2017), p. 095. doi: [10.1007/JHEP09\(2017\)095](https://doi.org/10.1007/JHEP09(2017)095). arXiv: [1511.03646](https://arxiv.org/abs/1511.03646) [hep-th].
- [72] Diptarka Das, Shouvik Datta, and Sridip Pal. “Universal asymptotics of three-point coefficients from elliptic representation of Virasoro blocks”. In: *Phys. Rev. D* 98.10 (2018), p. 101901. doi: [10.1103/PhysRevD.98.101901](https://doi.org/10.1103/PhysRevD.98.101901). arXiv: [1712.01842](https://arxiv.org/abs/1712.01842) [hep-th].
- [73] Diptarka Das, Yuya Kusuki, and Sridip Pal. “Universality in asymptotic bounds and its saturation in 2D CFT”. In: *JHEP* 04 (2021), p. 288. doi: [10.1007/JHEP04\(2021\)288](https://doi.org/10.1007/JHEP04(2021)288). arXiv: [2011.02482](https://arxiv.org/abs/2011.02482) [hep-th].

- [74] Luca V. Delacretaz. “Heavy Operators and Hydrodynamic Tails”. In: *SciPost Phys.* 9.3 (2020), p. 034. doi: [10.21468/SciPostPhys.9.3.034](https://doi.org/10.21468/SciPostPhys.9.3.034). arXiv: [2006.01139](https://arxiv.org/abs/2006.01139) [hep-th].
- [75] Lorenzo Di Pietro and Zohar Komargodski. “Cardy formulae for SUSY theories in $d = 4$ and $d = 6$ ”. In: *JHEP* 12 (2014), p. 031. doi: [10.1007/JHEP12\(2014\)031](https://doi.org/10.1007/JHEP12(2014)031). arXiv: [1407.6061](https://arxiv.org/abs/1407.6061) [hep-th].
- [76] Óscar J. C. Dias, Jorge E. Santos, and Benson Way. “Lattice Black Branes: Sphere Packing in General Relativity”. In: *JHEP* 05 (2018), p. 111. doi: [10.1007/JHEP05\(2018\)111](https://doi.org/10.1007/JHEP05(2018)111). arXiv: [1712.07663](https://arxiv.org/abs/1712.07663) [hep-th].
- [77] Robbert Dijkgraaf et al. “A Black hole Farey tail”. In: (May 2000). arXiv: [hep-th/0005003](https://arxiv.org/abs/hep-th/0005003).
- [78] F. A. Dolan and H. Osborn. “Conformal four point functions and the operator product expansion”. In: *Nucl. Phys.* B599 (2001), pp. 459–496. doi: [10.1016/S0550-3213\(01\)00013-X](https://doi.org/10.1016/S0550-3213(01)00013-X). arXiv: [hep-th/0011040](https://arxiv.org/abs/hep-th/0011040) [hep-th].
- [79] Nicola Dondi et al. “Resurgence of the large-charge expansion”. In: *JHEP* 05 (2021), p. 035. doi: [10.1007/JHEP05\(2021\)035](https://doi.org/10.1007/JHEP05(2021)035). arXiv: [2102.12488](https://arxiv.org/abs/2102.12488) [hep-th].
- [80] J. S. Dowker. “Remarks on spherical monodromy defects for free scalar fields”. In: (Apr. 2021). arXiv: [2104.09419](https://arxiv.org/abs/2104.09419) [hep-th].
- [81] J. S. Dowker and Gerard Kennedy. “Finite Temperature and Boundary Effects in Static Space-Times”. In: *J. Phys. A* 11 (1978), p. 895. doi: [10.1088/0305-4470/11/5/020](https://doi.org/10.1088/0305-4470/11/5/020).
- [82] M. J. Duff. “Twenty years of the Weyl anomaly”. In: *Class. Quant. Grav.* 11 (1994), pp. 1387–1404. doi: [10.1088/0264-9381/11/6/004](https://doi.org/10.1088/0264-9381/11/6/004). arXiv: [hep-th/9308075](https://arxiv.org/abs/hep-th/9308075).
- [83] Gerald V. Dunne. “Functional determinants in quantum field theory”. In: *J. Phys. A* 41 (2008). Ed. by Manuel Gadella et al., p. 304006. doi: [10.1088/1751-8113/41/30/304006](https://doi.org/10.1088/1751-8113/41/30/304006). arXiv: [0711.1178](https://arxiv.org/abs/0711.1178) [hep-th].
- [84] Anatoly Dymarsky et al. “The 3d Stress-Tensor Bootstrap”. In: *JHEP* 02 (2018). [,343(2017)], p. 164. doi: [10.1007/JHEP02\(2018\)164](https://doi.org/10.1007/JHEP02(2018)164). arXiv: [1708.05718](https://arxiv.org/abs/1708.05718) [hep-th].
- [85] Christopher Eling et al. “Conformal Anomalies in Hydrodynamics”. In: *JHEP* 05 (2013), p. 037. doi: [10.1007/JHEP05\(2013\)037](https://doi.org/10.1007/JHEP05(2013)037). arXiv: [1301.3170](https://arxiv.org/abs/1301.3170) [hep-th].
- [86] Rajeev S. Erramilli, Luca V. Iliesiu, and Petr Kravchuk. “Recursion relation for general 3d blocks”. In: *Journal of High Energy Physics* 2019.12 (2019), p. 116. doi: [10.1007/JHEP12\(2019\)116](https://doi.org/10.1007/JHEP12(2019)116). URL: [https://doi.org/10.1007/JHEP12\(2019\)116](https://doi.org/10.1007/JHEP12(2019)116).

[87] Rajeev S. Erramilli et al. “The Gross-Neveu-Yukawa archipelago”. In: *JHEP* 02 (2023), p. 036. doi: [10.1007/JHEP02\(2023\)036](https://doi.org/10.1007/JHEP02(2023)036). arXiv: [2210.02492](https://arxiv.org/abs/2210.02492) [hep-th].

[88] Bo Feng, Amihay Hanany, and Yang-Hui He. “Counting gauge invariants: The Plethystic program”. In: *JHEP* 03 (2007), p. 090. doi: [10.1088/1126-6708/2007/03/090](https://doi.org/10.1088/1126-6708/2007/03/090). arXiv: [hep-th/0701063](https://arxiv.org/abs/hep-th/0701063).

[89] S. Ferrara et al. “The shadow operator formalism for conformal algebra. Vacuum expectation values and operator products”. In: *Lettere al Nuovo Cimento (1971-1985)* 4.4 (May 1972), pp. 115–120. issn: 1827-613X. doi: [10.1007/BF02907130](https://doi.org/10.1007/BF02907130). url: <https://doi.org/10.1007/BF02907130>.

[90] D. S. Fine. “Quantum Yang-Mills on the two-sphere”. In: *Commun. Math. Phys.* 134 (1990), pp. 273–292. doi: [10.1007/BF02097703](https://doi.org/10.1007/BF02097703).

[91] A. Liam Fitzpatrick et al. “Eikonalization of Conformal Blocks”. In: (2015). arXiv: [1504.01737](https://arxiv.org/abs/1504.01737) [hep-th].

[92] A. Liam Fitzpatrick et al. “The Analytic Bootstrap and AdS Superhorizon Locality”. In: *JHEP* 1312 (2013), p. 004. doi: [10.1007/JHEP12\(2013\)004](https://doi.org/10.1007/JHEP12(2013)004). arXiv: [1212.3616](https://arxiv.org/abs/1212.3616) [hep-th].

[93] Kenji Fukushima and Tetsuo Hatsuda. “The phase diagram of dense QCD”. In: *Rept. Prog. Phys.* 74 (2011), p. 014001. doi: [10.1088/0034-4885/74/1/014001](https://doi.org/10.1088/0034-4885/74/1/014001). arXiv: [1005.4814](https://arxiv.org/abs/1005.4814) [hep-ph].

[94] Shouvik Ganguly and Sridip Pal. “Bounds on the density of states and the spectral gap in CFT_2 ”. In: *Phys. Rev. D* 101.10 (2020), p. 106022. doi: [10.1103/PhysRevD.101.106022](https://doi.org/10.1103/PhysRevD.101.106022). arXiv: [1905.12636](https://arxiv.org/abs/1905.12636) [hep-th].

[95] G. W. Gibbons, M. J. Perry, and C. N. Pope. “The first law of thermodynamics for Kerr-anti-de Sitter black holes”. In: *Class. Quant. Grav.* 22 (2005), pp. 1503–1526. doi: [10.1088/0264-9381/22/9/002](https://doi.org/10.1088/0264-9381/22/9/002). arXiv: [hep-th/0408217](https://arxiv.org/abs/hep-th/0408217).

[96] Simone Giombi and Igor R. Klebanov. “Interpolating between a and F ”. In: *JHEP* 03 (2015), p. 117. doi: [10.1007/JHEP03\(2015\)117](https://doi.org/10.1007/JHEP03(2015)117). arXiv: [1409.1937](https://arxiv.org/abs/1409.1937) [hep-th].

[97] Simone Giombi et al. “AdS Description of Induced Higher-Spin Gauge Theory”. In: *JHEP* 10 (2013), p. 016. doi: [10.1007/JHEP10\(2013\)016](https://doi.org/10.1007/JHEP10(2013)016). arXiv: [1306.5242](https://arxiv.org/abs/1306.5242) [hep-th].

[98] Siavash Golkar and Savdeep Sethi. “Global Anomalies and Effective Field Theory”. In: *JHEP* 05 (2016), p. 105. doi: [10.1007/JHEP05\(2016\)105](https://doi.org/10.1007/JHEP05(2016)105). arXiv: [1512.02607](https://arxiv.org/abs/1512.02607) [hep-th].

[99] Alba Grassi, Zohar Komargodski, and Luigi Tizzano. “Extremal correlators and random matrix theory”. In: *JHEP* 04 (2021), p. 214. doi: [10.1007/JHEP04\(2021\)214](https://doi.org/10.1007/JHEP04(2021)214). arXiv: [1908.10306](https://arxiv.org/abs/1908.10306) [hep-th].

- [100] Bertrand I. Halperin. “On the Hohenberg–Mermin–Wagner Theorem and Its Limitations”. In: *Journal of Statistical Physics* 175.3-4 (2018), pp. 521–529. doi: [10.1007/s10955-018-2202-y](https://doi.org/10.1007/s10955-018-2202-y). arXiv: 1812.00220 [cond-mat.stat-mech].
- [101] Daniel Harlow and Tokiro Numasawa. “Gauging spacetime inversions in quantum gravity”. In: (Nov. 2023). arXiv: 2311.09978 [hep-th].
- [102] Daniel Harlow and Hirosi Ooguri. “A universal formula for the density of states in theories with finite-group symmetry”. In: *Class. Quant. Grav.* 39.13 (2022), p. 134003. doi: [10.1088/1361-6382/ac5db2](https://doi.org/10.1088/1361-6382/ac5db2). arXiv: 2109.03838 [hep-th].
- [103] Thomas Hartman, Sachin Jain, and Sandipan Kundu. “Causality Constraints in Conformal Field Theory”. In: *JHEP* 05 (2016), p. 099. doi: [10.1007/JHEP05\(2016\)099](https://doi.org/10.1007/JHEP05(2016)099). arXiv: 1509.00014 [hep-th].
- [104] Thomas Hartman, Christoph A. Keller, and Bogdan Stoica. “Universal Spectrum of 2d Conformal Field Theory in the Large c Limit”. In: *JHEP* 09 (2014), p. 118. doi: [10.1007/JHEP09\(2014\)118](https://doi.org/10.1007/JHEP09(2014)118). arXiv: 1405.5137 [hep-th].
- [105] Thomas Hartman, Dalimil Mazáč, and Leonardo Rastelli. “Sphere Packing and Quantum Gravity”. In: *JHEP* 12 (2019), p. 048. doi: [10.1007/JHEP12\(2019\)048](https://doi.org/10.1007/JHEP12(2019)048). arXiv: 1905.01319 [hep-th].
- [106] Stephen W Hawking and Gary T Horowitz. “The gravitational Hamiltonian, action, entropy and surface terms”. In: *Classical and Quantum Gravity* 13.6 (1996), p. 1487.
- [107] Idse Heemskerk et al. “Holography from Conformal Field Theory”. In: *JHEP* 0910 (2009), p. 079. doi: [10.1088/1126-6708/2009/10/079](https://doi.org/10.1088/1126-6708/2009/10/079). arXiv: 0907.0151 [hep-th].
- [108] Simeon Hellerman. “A Universal Inequality for CFT and Quantum Gravity”. In: *JHEP* 08 (2011), p. 130. doi: [10.1007/JHEP08\(2011\)130](https://doi.org/10.1007/JHEP08(2011)130). arXiv: 0902.2790 [hep-th].
- [109] Simeon Hellerman. “On the exponentially small corrections to $\mathcal{N} = 2$ superconformal correlators at large R-charge”. In: (Mar. 2021). arXiv: 2103.09312 [hep-th].
- [110] Simeon Hellerman and Domenico Orlando. “Large R-charge EFT correlators in $N=2$ SQCD”. In: (Mar. 2021). arXiv: 2103.05642 [hep-th].
- [111] Simeon Hellerman et al. “On the CFT Operator Spectrum at Large Global Charge”. In: *JHEP* 12 (2015), p. 071. doi: [10.1007/JHEP12\(2015\)071](https://doi.org/10.1007/JHEP12(2015)071). arXiv: 1505.01537 [hep-th].
- [112] Brian Henning et al. “Operator bases, S -matrices, and their partition functions”. In: *JHEP* 10 (2017), p. 199. doi: [10.1007/JHEP10\(2017\)199](https://doi.org/10.1007/JHEP10(2017)199). arXiv: 1706.08520 [hep-th].

- [113] Christopher P. Herzog and Kuo-Wei Huang. “Stress Tensors from Trace Anomalies in Conformal Field Theories”. In: *Phys. Rev. D* 87 (2013), p. 081901. doi: [10.1103/PhysRevD.87.081901](https://doi.org/10.1103/PhysRevD.87.081901). arXiv: [1301.5002](https://arxiv.org/abs/1301.5002) [hep-th].
- [114] Eliot Hijano et al. “Witten Diagrams Revisited: The AdS Geometry of Conformal Blocks”. In: *JHEP* 01 (2016), p. 146. doi: [10.1007/JHEP01\(2016\)146](https://doi.org/10.1007/JHEP01(2016)146). arXiv: [1508.00501](https://arxiv.org/abs/1508.00501) [hep-th].
- [115] Yasuaki Hikida, Yuya Kusuki, and Tadashi Takayanagi. “Eigenstate thermalization hypothesis and modular invariance of two-dimensional conformal field theories”. In: *Phys. Rev. D* 98.2 (2018), p. 026003. doi: [10.1103/PhysRevD.98.026003](https://doi.org/10.1103/PhysRevD.98.026003). arXiv: [1804.09658](https://arxiv.org/abs/1804.09658) [hep-th].
- [116] Gary T. Horowitz and Edgar Shaghoulian. “Detachable circles and temperature-inversion dualities for CFT_d ”. In: *JHEP* 01 (2018), p. 135. doi: [10.1007/JHEP01\(2018\)135](https://doi.org/10.1007/JHEP01(2018)135). arXiv: [1709.06084](https://arxiv.org/abs/1709.06084) [hep-th].
- [117] Liangdong Hu, Yin-Chen He, and W. Zhu. “Operator Product Expansion Coefficients of the 3D Ising Criticality via Quantum Fuzzy Sphere”. In: (Mar. 2023). arXiv: [2303.08844](https://arxiv.org/abs/2303.08844) [cond-mat.stat-mech].
- [118] Luca Iliesiu, Murat Koloğlu, and David Simmons-Duffin. “Bootstrapping the 3d Ising model at finite temperature”. In: *JHEP* 12 (2019), p. 072. doi: [10.1007/JHEP12\(2019\)072](https://doi.org/10.1007/JHEP12(2019)072). arXiv: [1811.05451](https://arxiv.org/abs/1811.05451) [hep-th].
- [119] Luca Iliesiu et al. “The Conformal Bootstrap at Finite Temperature”. In: *JHEP* 10 (2018), p. 070. doi: [10.1007/JHEP10\(2018\)070](https://doi.org/10.1007/JHEP10(2018)070). arXiv: [1802.10266](https://arxiv.org/abs/1802.10266) [hep-th].
- [120] Mikhail Isachenkov and Volker Schomerus. “Integrability of conformal blocks. Part I. Calogero-Sutherland scattering theory”. In: *JHEP* 07 (2018), p. 180. doi: [10.1007/JHEP07\(2018\)180](https://doi.org/10.1007/JHEP07(2018)180). arXiv: [1711.06609](https://arxiv.org/abs/1711.06609) [hep-th].
- [121] Daniel Jafferis, Baur Mukhametzhanov, and Alexander Zhiboedov. “Conformal Bootstrap At Large Charge”. In: *JHEP* 05 (2018), p. 043. doi: [10.1007/JHEP05\(2018\)043](https://doi.org/10.1007/JHEP05(2018)043). arXiv: [1710.11161](https://arxiv.org/abs/1710.11161) [hep-th].
- [122] Daniel Louis Jafferis et al. “Matrix models for eigenstate thermalization”. In: (Sept. 2022). arXiv: [2209.02130](https://arxiv.org/abs/2209.02130) [hep-th].
- [123] Kristan Jensen. “Triangle Anomalies, Thermodynamics, and Hydrodynamics”. In: *Phys. Rev. D* 85 (2012), p. 125017. doi: [10.1103/PhysRevD.85.125017](https://doi.org/10.1103/PhysRevD.85.125017). arXiv: [1203.3599](https://arxiv.org/abs/1203.3599) [hep-th].
- [124] Kristan Jensen, R. Loganayagam, and Amos Yarom. “Anomaly inflow and thermal equilibrium”. In: *JHEP* 05 (2014), p. 134. doi: [10.1007/JHEP05\(2014\)134](https://doi.org/10.1007/JHEP05(2014)134). arXiv: [1310.7024](https://arxiv.org/abs/1310.7024) [hep-th].
- [125] Kristan Jensen, R. Loganayagam, and Amos Yarom. “Chern-Simons terms from thermal circles and anomalies”. In: *JHEP* 05 (2014), p. 110. doi: [10.1007/JHEP05\(2014\)110](https://doi.org/10.1007/JHEP05(2014)110). arXiv: [1311.2935](https://arxiv.org/abs/1311.2935) [hep-th].

- [126] Kristan Jensen, R. Loganayagam, and Amos Yarom. “Thermodynamics, gravitational anomalies and cones”. In: *JHEP* 02 (2013), p. 088. doi: [10.1007/JHEP02\(2013\)088](https://doi.org/10.1007/JHEP02(2013)088). arXiv: [1207.5824](https://arxiv.org/abs/1207.5824) [hep-th].
- [127] Kristan Jensen et al. “Towards hydrodynamics without an entropy current”. In: *Phys. Rev. Lett.* 109 (2012), p. 101601. doi: [10.1103/PhysRevLett.109.101601](https://doi.org/10.1103/PhysRevLett.109.101601). arXiv: [1203.3556](https://arxiv.org/abs/1203.3556) [hep-th].
- [128] Monica Jinwoo Kang, Jaeha Lee, and Hirosi Ooguri. “Universal formula for the density of states with continuous symmetry”. In: *Phys. Rev. D* 107.2 (2023), p. 026021. doi: [10.1103/PhysRevD.107.026021](https://doi.org/10.1103/PhysRevD.107.026021). arXiv: [2206.14814](https://arxiv.org/abs/2206.14814) [hep-th].
- [129] Daniel Kapec, Raghu Mahajan, and Douglas Stanford. “Matrix ensembles with global symmetries and ’t Hooft anomalies from 2d gauge theory”. In: *JHEP* 04 (2020), p. 186. arXiv: [1912.12285](https://arxiv.org/abs/1912.12285) [hep-th].
- [130] Denis Karateev, Petr Kravchuk, and David Simmons-Duffin. “Harmonic Analysis and Mean Field Theory”. In: *JHEP* 10 (2019), p. 217. doi: [10.1007/JHEP10\(2019\)217](https://doi.org/10.1007/JHEP10(2019)217). arXiv: [1809.05111](https://arxiv.org/abs/1809.05111) [hep-th].
- [131] Robin Karlsson et al. “Thermal stress tensor correlators, OPE and holography”. In: *JHEP* 09 (2022), p. 234. doi: [10.1007/JHEP09\(2022\)234](https://doi.org/10.1007/JHEP09(2022)234). arXiv: [2206.05544](https://arxiv.org/abs/2206.05544) [hep-th].
- [132] Christoph A. Keller and Alexander Maloney. “Poincare Series, 3D Gravity and CFT Spectroscopy”. In: *JHEP* 02 (2015), p. 080. doi: [10.1007/JHEP02\(2015\)080](https://doi.org/10.1007/JHEP02(2015)080). arXiv: [1407.6008](https://arxiv.org/abs/1407.6008) [hep-th].
- [133] Seok Kim et al. “‘Grey Galaxies’ as an endpoint of the Kerr-AdS superradiant instability”. In: (May 2023). arXiv: [2305.08922](https://arxiv.org/abs/2305.08922) [hep-th].
- [134] Igor R. Klebanov, Silviu S. Pufu, and Benjamin R. Safdi. “F-Theorem without Supersymmetry”. In: *JHEP* 10 (2011), p. 038. doi: [10.1007/JHEP10\(2011\)038](https://doi.org/10.1007/JHEP10(2011)038). arXiv: [1105.4598](https://arxiv.org/abs/1105.4598) [hep-th].
- [135] Murat Kologlu et al. “Shocks, Superconvergence, and a Stringy Equivalence Principle”. In: *JHEP* 11 (2020), p. 096. doi: [10.1007/JHEP11\(2020\)096](https://doi.org/10.1007/JHEP11(2020)096). arXiv: [1904.05905](https://arxiv.org/abs/1904.05905) [hep-th].
- [136] Murat Kologlu et al. “The light-ray OPE and conformal colliders”. In: *JHEP* 01 (2021), p. 128. doi: [10.1007/JHEP01\(2021\)128](https://doi.org/10.1007/JHEP01(2021)128). arXiv: [1905.01311](https://arxiv.org/abs/1905.01311) [hep-th].
- [137] Zohar Komargodski and Adam Schwimmer. “On Renormalization Group Flows in Four Dimensions”. In: *JHEP* 12 (2011), p. 099. doi: [10.1007/JHEP12\(2011\)099](https://doi.org/10.1007/JHEP12(2011)099). arXiv: [1107.3987](https://arxiv.org/abs/1107.3987) [hep-th].
- [138] Zohar Komargodski and Alexander Zhiboedov. “Convexity and Liberation at Large Spin”. In: *JHEP* 1311 (2013), p. 140. doi: [10.1007/JHEP11\(2013\)140](https://doi.org/10.1007/JHEP11(2013)140). arXiv: [1212.4103](https://arxiv.org/abs/1212.4103) [hep-th].

- [139] Filip Kos, David Poland, and David Simmons-Duffin. “Bootstrapping Mixed Correlators in the 3D Ising Model”. In: *JHEP* 11 (2014), p. 109. doi: [10.1007/JHEP11\(2014\)109](https://doi.org/10.1007/JHEP11(2014)109). arXiv: [1406.4858](https://arxiv.org/abs/1406.4858) [hep-th].
- [140] Filip Kos, David Poland, and David Simmons-Duffin. “Bootstrapping the $O(N)$ vector models”. In: *JHEP* 1406 (2014), p. 091. doi: [10.1007/JHEP06\(2014\)091](https://doi.org/10.1007/JHEP06(2014)091). arXiv: [1307.6856](https://arxiv.org/abs/1307.6856) [hep-th].
- [141] Per Kraus and Alexander Maloney. “A cardy formula for three-point coefficients or how the black hole got its spots”. In: *JHEP* 05 (2017), p. 160. doi: [10.1007/JHEP05\(2017\)160](https://doi.org/10.1007/JHEP05(2017)160). arXiv: [1608.03284](https://arxiv.org/abs/1608.03284) [hep-th].
- [142] Petr Kravchuk and David Simmons-Duffin. “Counting Conformal Correlators”. In: *JHEP* 02 (2018), p. 096. doi: [10.1007/JHEP02\(2018\)096](https://doi.org/10.1007/JHEP02(2018)096). arXiv: [1612.08987](https://arxiv.org/abs/1612.08987) [hep-th].
- [143] M. Krech and D. P. Landau. “Casimir effect in critical systems: A Monte Carlo simulation”. In: *Phys. Rev. E* 53 (5 1996), pp. 4414–4423. doi: [10.1103/PhysRevE.53.4414](https://doi.org/10.1103/PhysRevE.53.4414).
- [144] M. Krech and D. P. Landau. “Casimir effect in critical systems: A Monte Carlo simulation”. In: *Phys. Rev. E* 53 (5 1996), pp. 4414–4423. doi: [10.1103/PhysRevE.53.4414](https://doi.org/10.1103/PhysRevE.53.4414). url: <https://link.aps.org/doi/10.1103/PhysRevE.53.4414>.
- [145] Michael Krech. “Casimir forces in binary liquid mixtures”. In: *Phys. Rev. E* 56 (2 1997), pp. 1642–1659. doi: [10.1103/PhysRevE.56.1642](https://doi.org/10.1103/PhysRevE.56.1642). arXiv: [cond-mat/9703093](https://arxiv.org/abs/cond-mat/9703093) [cond-mat.soft]. url: <https://link.aps.org/doi/10.1103/PhysRevE.56.1642>.
- [146] Yuya Kusuki. “Modern Approach to 2D Conformal Field Theory”. In: (Dec. 2024). arXiv: [2412.18307](https://arxiv.org/abs/2412.18307) [hep-th].
- [147] David Kutasov and Finn Larsen. “Partition sums and entropy bounds in weakly coupled CFT”. In: *JHEP* 01 (2001), p. 001. doi: [10.1088/1126-6708/2001/01/001](https://doi.org/10.1088/1126-6708/2001/01/001). arXiv: [hep-th/0009244](https://arxiv.org/abs/hep-th/0009244).
- [148] Pedro Liendo, Leonardo Rastelli, and Balt C. van Rees. “The Bootstrap Program for Boundary CFT_d”. In: *JHEP* 07 (2013), p. 113. doi: [10.1007/JHEP07\(2013\)113](https://doi.org/10.1007/JHEP07(2013)113). arXiv: [1210.4258](https://arxiv.org/abs/1210.4258) [hep-th].
- [149] Aike Liu et al. “Skydiving to Bootstrap Islands”. In: (July 2023). arXiv: [2307.13046](https://arxiv.org/abs/2307.13046) [hep-th].
- [150] Hong Liu and Paolo Glorioso. “Lectures on non-equilibrium effective field theories and fluctuating hydrodynamics”. In: *PoSTASI2017* (2018), p. 008. doi: [10.22323/1.305.0008](https://doi.org/10.22323/1.305.0008). arXiv: [1805.09331](https://arxiv.org/abs/1805.09331) [hep-th].
- [151] Junyu Liu et al. “ d -dimensional SYK, AdS Loops, and $6j$ Symbols”. In: *JHEP* 03 (2019), p. 052. doi: [10.1007/JHEP03\(2019\)052](https://doi.org/10.1007/JHEP03(2019)052). arXiv: [1808.00612](https://arxiv.org/abs/1808.00612) [hep-th].

- [152] Junyu Liu et al. “The Lorentzian inversion formula and the spectrum of the 3d $O(2)$ CFT”. In: *JHEP* 09 (2020). [Erratum: *JHEP* 01, 206 (2021)], p. 115. doi: [10.1007/JHEP09\(2020\)115](https://doi.org/10.1007/JHEP09(2020)115). arXiv: [2007.07914](https://arxiv.org/abs/2007.07914) [hep-th].
- [153] R. Loganayagam. “Anomalies and the Helicity of the Thermal State”. In: *JHEP* 11 (2013), p. 205. doi: [10.1007/JHEP11\(2013\)205](https://doi.org/10.1007/JHEP11(2013)205). arXiv: [1211.3850](https://arxiv.org/abs/1211.3850) [hep-th].
- [154] R. Loganayagam and Piotr Surówka. “Anomaly/Transport in an Ideal Weyl gas”. In: *JHEP* 04 (2012), p. 097. doi: [10.1007/JHEP04\(2012\)097](https://doi.org/10.1007/JHEP04(2012)097). arXiv: [1201.2812](https://arxiv.org/abs/1201.2812) [hep-th].
- [155] LAJ London. “Arbitrary dimensional cosmological multi-black holes”. In: *Nuclear Physics B* 434.3 (1995), pp. 709–735.
- [156] Conghuan Luo and Yifan Wang. “Casimir energy and modularity in higher-dimensional conformal field theories”. In: *JHEP* 07 (2023), p. 028. doi: [10.1007/JHEP07\(2023\)028](https://doi.org/10.1007/JHEP07(2023)028). arXiv: [2212.14866](https://arxiv.org/abs/2212.14866) [hep-th].
- [157] M. Lüscher. “Volume Dependence of the Energy Spectrum in Massive Quantum Field Theories. 1. Stable Particle States”. In: *Commun. Math. Phys.* 104 (1986), p. 177. doi: [10.1007/BF01211589](https://doi.org/10.1007/BF01211589).
- [158] M. Lüscher. “Volume Dependence of the Energy Spectrum in Massive Quantum Field Theories. 2. Scattering States”. In: *Commun. Math. Phys.* 105 (1986), pp. 153–188. doi: [10.1007/BF01211097](https://doi.org/10.1007/BF01211097).
- [159] M. Lüscher. “Volume dependence of the energy spectrum in massive quantum field theories”. In: *Communications in Mathematical Physics* 104.2 (June 1986), pp. 177–206. ISSN: 1432-0916. doi: [10.1007/BF01211589](https://doi.org/10.1007/BF01211589). URL: <https://doi.org/10.1007/BF01211589>.
- [160] Javier M. Magan. “Proof of the universal density of charged states in QFT”. In: *JHEP* 12 (2021), p. 100. doi: [10.1007/JHEP12\(2021\)100](https://doi.org/10.1007/JHEP12(2021)100). arXiv: [2111.02418](https://arxiv.org/abs/2111.02418) [hep-th].
- [161] Juan Maldacena, David Simmons-Duffin, and Alexander Zhiboedov. “Looking for a bulk point”. In: *JHEP* 01 (2017), p. 013. doi: [10.1007/JHEP01\(2017\)013](https://doi.org/10.1007/JHEP01(2017)013). arXiv: [1509.03612](https://arxiv.org/abs/1509.03612) [hep-th].
- [162] Alexander Maloney and Edward Witten. “Quantum Gravity Partition Functions in Three Dimensions”. In: *JHEP* 02 (2010), p. 029. doi: [10.1007/JHEP02\(2010\)029](https://doi.org/10.1007/JHEP02(2010)029). arXiv: [0712.0155](https://arxiv.org/abs/0712.0155) [hep-th].
- [163] Enrico Marchetto, Alessio Micsioscia, and Elli Pomoni. “Sum rules & Tauberian theorems at finite temperature”. In: (Dec. 2023). arXiv: [2312.13030](https://arxiv.org/abs/2312.13030) [hep-th].
- [164] Eric Mefford, Edgar Shaghoulian, and Milind Shyani. “Sparseness bounds on local operators in holographic CFT_d ”. In: *JHEP* 07 (2018), p. 051. doi: [10.1007/JHEP07\(2018\)051](https://doi.org/10.1007/JHEP07(2018)051). arXiv: [1711.03122](https://arxiv.org/abs/1711.03122) [hep-th].

- [165] Tom Melia and Sridip Pal. “EFT Asymptotics: the Growth of Operator Degeneracy”. In: *SciPost Phys.* 10.5 (2021), p. 104. doi: [10.21468/SciPostPhys.10.5.104](https://doi.org/10.21468/SciPostPhys.10.5.104). arXiv: [2010.08560](https://arxiv.org/abs/2010.08560) [hep-th].
- [166] Alexander A. Migdal. “Recursion Equations in Gauge Theories”. In: *Sov. Phys. JETP* 42 (1975). Ed. by I. M. Khalatnikov and V. P. Mineev, p. 413.
- [167] Alexander Monin et al. “Semiclassics, Goldstone Bosons and CFT data”. In: *JHEP* 06 (2017), p. 011. doi: [10.1007/JHEP06\(2017\)011](https://doi.org/10.1007/JHEP06(2017)011). arXiv: [1611.02912](https://arxiv.org/abs/1611.02912) [hep-th].
- [168] Baur Mukhametzhanov and Sridip Pal. “Beurling-Selberg Extremization and Modular Bootstrap at High Energies”. In: *SciPost Phys.* 8.6 (2020), p. 088. doi: [10.21468/SciPostPhys.8.6.088](https://doi.org/10.21468/SciPostPhys.8.6.088). arXiv: [2003.14316](https://arxiv.org/abs/2003.14316) [hep-th].
- [169] Baur Mukhametzhanov and Alexander Zhiboedov. “Analytic Euclidean Bootstrap”. In: *JHEP* 10 (2019), p. 270. doi: [10.1007/JHEP10\(2019\)270](https://doi.org/10.1007/JHEP10(2019)270). arXiv: [1808.03212](https://arxiv.org/abs/1808.03212) [hep-th].
- [170] Baur Mukhametzhanov and Alexander Zhiboedov. “Modular invariance, tauberian theorems and microcanonical entropy”. In: *JHEP* 10 (2019), p. 261. doi: [10.1007/JHEP10\(2019\)261](https://doi.org/10.1007/JHEP10(2019)261). arXiv: [1904.06359](https://arxiv.org/abs/1904.06359) [hep-th].
- [171] Gim Seng Ng and Piotr Surówka. “One-loop effective actions and 2D hydrodynamics with anomalies”. In: *Phys. Lett. B* 746 (2015), pp. 281–284. doi: [10.1016/j.physletb.2015.05.011](https://doi.org/10.1016/j.physletb.2015.05.011). arXiv: [1411.7989](https://arxiv.org/abs/1411.7989) [hep-th].
- [172] Sridip Pal. “Bound on asymptotics of magnitude of three point coefficients in 2D CFT”. In: *JHEP* 01 (2020), p. 023. doi: [10.1007/JHEP01\(2020\)023](https://doi.org/10.1007/JHEP01(2020)023). arXiv: [1906.11223](https://arxiv.org/abs/1906.11223) [hep-th].
- [173] Sridip Pal, Jiaxin Qiao, and Slava Rychkov. “Twist Accumulation in Conformal Field Theory: A Rigorous Approach to the Lightcone Bootstrap”. In: *Commun. Math. Phys.* 402.3 (2023), pp. 2169–2214. doi: [10.1007/s00220-023-04767-w](https://doi.org/10.1007/s00220-023-04767-w). arXiv: [2212.04893](https://arxiv.org/abs/2212.04893) [hep-th].
- [174] Sridip Pal and Zhengdi Sun. “High Energy Modular Bootstrap, Global Symmetries and Defects”. In: *JHEP* 08 (2020), p. 064. doi: [10.1007/JHEP08\(2020\)064](https://doi.org/10.1007/JHEP08(2020)064). arXiv: [2004.12557](https://arxiv.org/abs/2004.12557) [hep-th].
- [175] Sridip Pal and Zhengdi Sun. “Tauberian-Cardy formula with spin”. In: *JHEP* 01 (2020), p. 135. doi: [10.1007/JHEP01\(2020\)135](https://doi.org/10.1007/JHEP01(2020)135). arXiv: [1910.07727](https://arxiv.org/abs/1910.07727) [hep-th].
- [176] Duccio Pappadopulo et al. “OPE Convergence in Conformal Field Theory”. In: *Phys. Rev. D* 86 (2012), p. 105043. doi: [10.1103/PhysRevD.86.105043](https://doi.org/10.1103/PhysRevD.86.105043). arXiv: [1208.6449](https://arxiv.org/abs/1208.6449) [hep-th].
- [177] João Penedones, Emilio Trevisani, and Masahito Yamazaki. “Recursion Relations for Conformal Blocks”. In: *JHEP* 09 (2016), p. 070. doi: [10.1007/JHEP09\(2016\)070](https://doi.org/10.1007/JHEP09(2016)070). arXiv: [1509.00428](https://arxiv.org/abs/1509.00428) [hep-th].

- [178] Vasily Pestun et al. “Localization techniques in quantum field theories”. In: *J. Phys. A* 50.44 (2017), p. 440301. doi: [10.1088/1751-8121/aa63c1](https://doi.org/10.1088/1751-8121/aa63c1). arXiv: [1608.02952](https://arxiv.org/abs/1608.02952) [hep-th].
- [179] A. M. Polyakov. “Nonhamiltonian approach to conformal quantum field theory”. In: *Zh. Eksp. Teor. Fiz.* 66 (1974), pp. 23–42.
- [180] Jiaxin Qiao and Slava Rychkov. “A tauberian theorem for the conformal bootstrap”. In: *JHEP* 12 (2017), p. 119. doi: [10.1007/JHEP12\(2017\)119](https://doi.org/10.1007/JHEP12(2017)119). arXiv: [1709.00008](https://arxiv.org/abs/1709.00008) [hep-th].
- [181] Riccardo Rattazzi et al. “Bounding scalar operator dimensions in 4D CFT”. In: *JHEP* 12 (2008), p. 031. doi: [10.1088/1126-6708/2008/12/031](https://doi.org/10.1088/1126-6708/2008/12/031). arXiv: [0807.0004](https://arxiv.org/abs/0807.0004) [hep-th].
- [182] Shlomo S. Razamat and Brian Willett. “Global Properties of Supersymmetric Theories and the Lens Space”. In: *Commun. Math. Phys.* 334.2 (2015), pp. 661–696. doi: [10.1007/s00220-014-2111-0](https://doi.org/10.1007/s00220-014-2111-0). arXiv: [1307.4381](https://arxiv.org/abs/1307.4381) [hep-th].
- [183] L. J. Romans. “Supersymmetric, cold and lukewarm black holes in cosmological Einstein-Maxwell theory”. In: *Nucl. Phys. B* 383 (1992), pp. 395–415. doi: [10.1016/0550-3213\(92\)90684-4](https://doi.org/10.1016/0550-3213(92)90684-4). arXiv: [hep-th/9203018](https://arxiv.org/abs/hep-th/9203018).
- [184] B. E. Rusakov. “Loop averages and partition functions in U(N) gauge theory on two-dimensional manifolds”. In: *Mod. Phys. Lett. A* 5 (1990), pp. 693–703.
- [185] Slava Rychkov and Pierre Yvernay. “Remarks on the Convergence Properties of the Conformal Block Expansion”. In: *Phys. Lett. B* 753 (2016), pp. 682–686. doi: [10.1016/j.physletb.2016.01.004](https://doi.org/10.1016/j.physletb.2016.01.004). arXiv: [1510.08486](https://arxiv.org/abs/1510.08486) [hep-th].
- [186] Subir Sachdev. “Polylogarithm identities in a conformal field theory in three-dimensions”. In: *Phys. Lett. B* 309 (1993), pp. 285–288. doi: [10.1016/0370-2693\(93\)90935-B](https://doi.org/10.1016/0370-2693(93)90935-B). arXiv: [hep-th/9305131](https://arxiv.org/abs/hep-th/9305131).
- [187] A. Schwimmer and S. Theisen. “Spontaneous Breaking of Conformal Invariance and Trace Anomaly Matching”. In: *Nucl. Phys. B* 847 (2011), pp. 590–611. doi: [10.1016/j.nuclphysb.2011.02.003](https://doi.org/10.1016/j.nuclphysb.2011.02.003). arXiv: [1011.0696](https://arxiv.org/abs/1011.0696) [hep-th].
- [188] Edgar Shaghoulian. “Black hole microstates in AdS”. In: *Phys. Rev. D* 94.10 (2016), p. 104044. doi: [10.1103/PhysRevD.94.104044](https://doi.org/10.1103/PhysRevD.94.104044). arXiv: [1512.06855](https://arxiv.org/abs/1512.06855) [hep-th].
- [189] Edgar Shaghoulian. “Modular forms and a generalized Cardy formula in higher dimensions”. In: *Phys. Rev. D* 93.12 (2016), p. 126005. doi: [10.1103/PhysRevD.93.126005](https://doi.org/10.1103/PhysRevD.93.126005). arXiv: [1508.02728](https://arxiv.org/abs/1508.02728) [hep-th].

- [190] Edgar Shaghoulian. “Modular Invariance of Conformal Field Theory on $S^1 S^3$ and Circle Fibrations”. In: *Phys. Rev. Lett.* 119.13 (2017), p. 131601. doi: [10.1103/PhysRevLett.119.131601](https://doi.org/10.1103/PhysRevLett.119.131601). arXiv: [1612.05257](https://arxiv.org/abs/1612.05257) [hep-th].
- [191] Ben L. Shepherd and Elizabeth Winstanley. “Dyons and dyonic black holes in SU(N) Einstein-Yang-Mills theory in anti de Sitter spacetime”. In: *Physical Review D* 93.6 (Mar. 2016). doi: [10.1103/physrevd.93.064064](https://doi.org/10.1103/physrevd.93.064064). URL: <https://doi.org/10.1103%2Fphysrevd.93.064064>.
- [192] David Simmons-Duffin. *PH230A: Quantum Field Theory Notes*. 2023. URL: <https://gitlab.com/davidsd/ph230a-notes> (visited on 01/09/2025).
- [193] David Simmons-Duffin. “Projectors, Shadows, and Conformal Blocks”. In: *JHEP* 04 (2014), p. 146. doi: [10.1007/JHEP04\(2014\)146](https://doi.org/10.1007/JHEP04(2014)146). arXiv: [1204.3894](https://arxiv.org/abs/1204.3894) [hep-th].
- [194] David Simmons-Duffin. “The Conformal Bootstrap”. In: *Proceedings, Theoretical Advanced Study Institute in Elementary Particle Physics: New Frontiers in Fields and Strings (TASI 2015): Boulder, CO, USA, June 1-26, 2015*. 2017, pp. 1–74. doi: [10.1142/9789813149441_0001](https://doi.org/10.1142/9789813149441_0001). arXiv: [1602.07982](https://arxiv.org/abs/1602.07982) [hep-th]. URL: <http://inspirehep.net/record/1424282/files/arXiv:1602.07982.pdf>.
- [195] David Simmons-Duffin. “The Lightcone Bootstrap and the Spectrum of the 3d Ising CFT”. In: *JHEP* 03 (2017), p. 086. doi: [10.1007/JHEP03\(2017\)086](https://doi.org/10.1007/JHEP03(2017)086). arXiv: [1612.08471](https://arxiv.org/abs/1612.08471) [hep-th].
- [196] Robert Southey. “The Story of the Three Bears”. In: *The Doctor & C.* Longman, Rees, Orme, Brown, Green and Longman, 1837, pp. 318–326.
- [197] Andrew Strominger. “Black hole entropy from near horizon microstates”. In: *JHEP* 02 (1998), p. 009. doi: [10.1088/1126-6708/1998/02/009](https://doi.org/10.1088/1126-6708/1998/02/009). arXiv: [hep-th/9712251](https://arxiv.org/abs/hep-th/9712251).
- [198] O. Vasilyev et al. “Universal scaling functions of critical Casimir forces obtained by Monte Carlo simulations”. In: *Phys. Rev. E* 79 (4 2009), p. 041142. doi: [10.1103/PhysRevE.79.041142](https://doi.org/10.1103/PhysRevE.79.041142). arXiv: [0812.0750](https://arxiv.org/abs/0812.0750) [cond-mat.stat-mech].
- [199] Erik P. Verlinde. “On the holographic principle in a radiation dominated universe”. In: (Aug. 2000). arXiv: [hep-th/0008140](https://arxiv.org/abs/hep-th/0008140).
- [200] M.S Volkov et al. “The number of sphaleron instabilities of the Bartnik-McKinnon solitons and non-Abelian black holes”. In: *Physics Letters B* 349.4 (Apr. 1995), pp. 438–442. doi: [10.1016/0370-2693\(95\)00293-t](https://doi.org/10.1016/0370-2693(95)00293-t). URL: <https://doi.org/10.1016%2F0370-2693%2895%2900293-t>.

- [201] Mikhail S. Volkov. “Hairy black holes in the XX-th and XXI-st centuries”. In: *14th Marcel Grossmann Meeting on Recent Developments in Theoretical and Experimental General Relativity, Astrophysics, and Relativistic Field Theories*. Vol. 2. 2017, pp. 1779–1798. doi: [10.1142/9789813226609_0184](https://doi.org/10.1142/9789813226609_0184). arXiv: [1601.08230](https://arxiv.org/abs/1601.08230) [gr-qc].
- [202] Mikhail S. Volkov and Dmitri V. Gal’tsov. “Gravitating nonAbelian solitons and black holes with Yang-Mills fields”. In: *Phys. Rept.* 319 (1999), pp. 1–83. doi: [10.1016/S0370-1573\(99\)00010-1](https://doi.org/10.1016/S0370-1573(99)00010-1). arXiv: [hep-th/9810070](https://arxiv.org/abs/hep-th/9810070).
- [203] Elizabeth Winstanley. “A menagerie of hairy black holes”. In: *Springer Proc. Phys.* 208 (2018). Ed. by Piero Nicolini et al., pp. 39–46. doi: [10.1007/978-3-319-94256-8_3](https://doi.org/10.1007/978-3-319-94256-8_3). arXiv: [1510.01669](https://arxiv.org/abs/1510.01669) [gr-qc].
- [204] Elizabeth Winstanley. “Classical Yang-Mills black hole hair in anti-de Sitter space”. In: *Lect. Notes Phys.* 769 (2009). Ed. by Eleftherios Papantonopoulos, pp. 49–87. arXiv: [0801.0527](https://arxiv.org/abs/0801.0527) [gr-qc].
- [205] Edward Witten. “Two-dimensional gauge theories revisited”. In: *J. Geom. Phys.* 9 (1992), pp. 303–368. arXiv: [hep-th/9204083](https://arxiv.org/abs/hep-th/9204083).
- [206] Al.B Zamolodchikov. “Conformal symmetry in two-dimensional space: Recursion representation of conformal block”. English. In: *Theoretical and Mathematical Physics* 73.1 (1987), pp. 1088–1093. ISSN: 0040-5779. doi: [10.1007/BF01022967](https://doi.org/10.1007/BF01022967).
- [207] Wei Zhu et al. “Uncovering Conformal Symmetry in the 3D Ising Transition: State-Operator Correspondence from a Quantum Fuzzy Sphere Regularization”. In: *Phys. Rev. X* 13.2 (2023), p. 021009. doi: [10.1103/PhysRevX.13.021009](https://doi.org/10.1103/PhysRevX.13.021009). arXiv: [2210.13482](https://arxiv.org/abs/2210.13482) [cond-mat.stat-mech].